Sensing the rainbow: genetic and physiological responses to light quality in *Ostreococcus*, an ecologically important picoeukaryote phytoplankton

Betty Sands

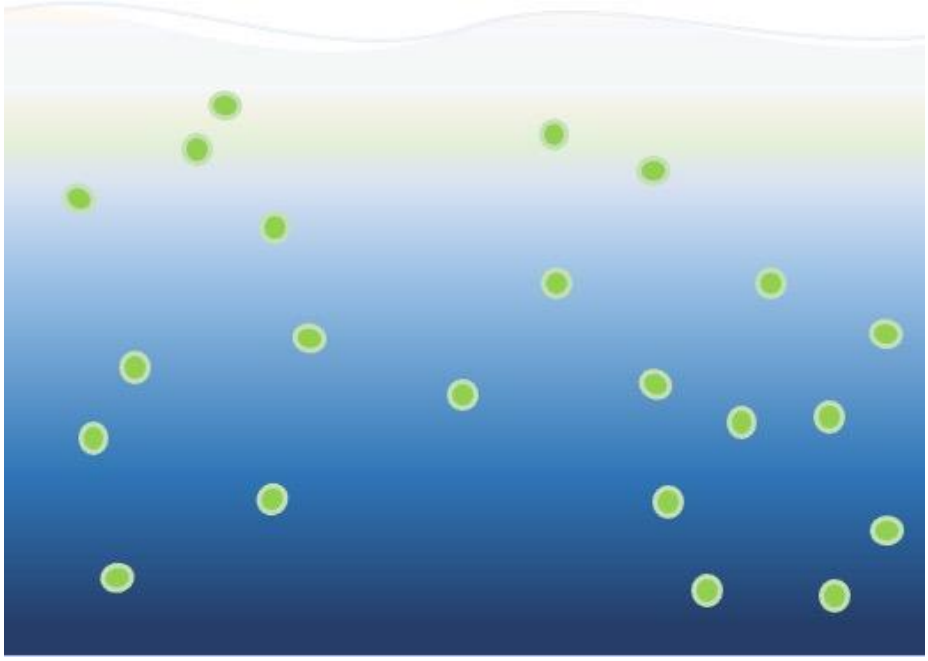

A thesis submitted for the degree of Doctor of Philosophy
School of Life Sciences, University of Warwick

August 2021

1.1 Contents

Acknowledgements

I am enormously grateful for the support I have been given during the journey of this PhD. Thank you to NERC CENTA for funding this research, for the training, and for supporting my placement with the kind and welcoming people of Devon Wildlife Trust at Seaton Jurassic.

Thank you to all of the Bouget group in the Banyuls LOMIC for hosting my visit and for sharing cultures and culture with me.

Thank you also to my advisors Dr Joseph Christie-Oleza, Dr Steve Jackson and Dr Rich Puxty for generously sharing their time, expertise, and thoughtful advice.

I thank my supervisors, Professor Isabelle Carré and Professor David Scanlan for their wisdom and encouragement which left me walking away from every meeting with renewed enthusiasm and which helped me to transform Mount Doom into Hobbiton Hills.

I thank my parents, who cheerfully point out that without them I wouldn't exist, for their patience, calm, and for the buckets of tea. Thanks to my family, I like going south, somehow it will always feel like going downhill.

I am grateful for all the company of the lab, the fellowship of the coffee break, and particularly for the support of Dr Amy Newman, Dr Ellis Monaghan, Holly Shropshire, Helen Scorgie, Snedith Achatina, and everyone else who kept me merry and sane during a socially distanced write-up, even when I felt like a fool of a Took.

Thank you to Rachel Stirrup, Ranger of the North, for invaluable breaks in the forests of Middle Earth, and for teaching me valuable foraging skills.

I wouldn't have got far without Emma Murphy and Dr Séverine Rangama, my Samwise and ma lumière d'Eärendil, thank you for the great craic and the bon courage.

Thank you Lizzie Mawdsley for the tireless cheerleading, my fiercest supporter, my Shelob because I'm running out of characters and because I think she'd enjoy being a giant, man eating spider.

I dedicate this work to Abbie Barr who sailed West too soon and will not be forgotten.

Declaration

This thesis is submitted to the University of Warwick in support of my application for the degree of Doctor of Philosophy. It has been composed by myself and has not been submitted in any previous application for any degree.

The work presented (including data generated and data analysis) was carried out by the author except in the cases outlined below:

- Preparation, extraction, and sequencing of RNA for RNASeq was carried out by Dr Sian Davies
- Identification and quantification of pigments using HPLC was carried out by DHI Group

Abstract

The photosynthetic activity of phytoplankton is vital, not only as primary production in the ocean, or for carbon sequestration, but also as a source of almost half the oxygen in our atmosphere. This project is an investigation of the genetic and physiological consequences of light responses in *Ostreococcus*, a genus of eukaryotic picophytoplankton. The light quality responses of two different ecotypes of *Ostreococcus* are compared: the coastal and lagoon associated OTH95, and the ocean associated RCC809. It is known that *Ostreococcus* ecotypes can adapt to high or low intensities of light, however their responses to light of different wavelengths are unknown.

It was hypothesised that *Ostreococcus* ecotypes possess distinct light quality niches, to address this, differential gene expression was determined under monochromatic red, green, and blue light conditions, and functional annotation used to describe the likely physiological effects of the transcriptional responses. These transcriptional light quality responses were ecotype-specific and were tested by measuring physiological photosynthetic parameters using pulse-amplitude modulation fluorometry analysis (PhytoPAM) technology, and relative pigment contents using high performance liquid chromatography (HPLC). These responses represent likely adaptations to the spectral conditions in the ecotypes' light quality environments.

Finally, potential mechanisms controlling the light quality responses were identified by locating candidate regulatory sequence motifs in the promoters of responsive genes and comparing these to transcription factor DNA binding sites. This allowed prospective markers for light quality responses to be identified and enables future investigations of phytoplankton communities in an environmental context.

This work provides evidence of distinct light quality responses in *Ostreococcus* ecotypes and demonstrates the importance of light quality for the adaptation of eukaryotic phytoplankton to ecological niches in the marine environment.

List of Abbreviations

ANOVA Analysis of variance
ASW Artificial seawater
BAM Binary alignment map
BLAST Basic local alignment search tool
bZIP Basic and leucine zipper domain
C2H2 Cysteine2-histidine2
CCA1 Circadian clock associated 1
CCT CONSTANS, CO-like, and TOC1
Chl Chlorophyll
DCM Deep chlorophyll maximum
DEGs Differentially expressed genes
DOM Dissolved organic matter
DPS Depoxidation state
FC Fold change
FDR False discovery rate
FIMO Find individual motif occurrences
Fm Maximal fluorescence
FMN Flavin mononucleotide
Fo Background fluorescence level
FPKM Fragments per kilobase of exon per million reads mapped
Fv Variable fluorescence
GO Gene ontology
HTH Helix-turn-helix
ITS Internal transcribed spacer
JGI Joint genome institute
LHC Light harvesting complex
LOV-HK Light and oxygen voltage histidine kinase
LYC Lycopene synthase
MCM Mini-chromosome maintenance
MEME Multiple Em for motif elicitation
MgDVP Mg-2,4-divinyl pheoporphyrin a5 monomethylester
Myb Myeloblastosis domain gene
NPQ Non-photochemical quenching
OD Optical density
OtCDK *Ostreococcus* cyclin-dependant kinase
OtPhot *Ostreococcus* phototropin
PAM Pulse-amplitude modulation
PAR Photosynthetically active/available radiation
PCA Principal component analysis
PCR Polymerase chain reaction
PS Photosystem
rETR Relative electron transport rate
Rhod-HK Rhodopsin histidine kinase
RNASeq Ribonucleic acid sequencing
RuBisCO Ribulose 1,5-bisphosphate carboxylase-oxygenase
SMART Simple modular architecture research tool

List of Tables

List of Figures

List of Appendices

Chapter 1: Introduction

1.1 The importance of picoeukaryotic phytoplankton for global marine ecosystems

Phytoplankton are a vital part of the marine ecosystem; as primary producers, they not only provide a source of energy for the food web, but also cycle nutrients, form a sink for carbon, and are responsible for roughly half the oxygen released to the atmosphere globally. The role of picoeukaryotic phytoplankton (varyingly defined as either <3µm or < 2µm in diameter,) in global CO_2 fixation is vital as these species are responsible for a considerable amount of carbon capture in the oceans through photosynthesis (Mullin, 2001, Kirkham et al., 2013, Jardillier et al., 2010, Rii et al., 2016). This is partly due to their high rates of growth and cell-specific CO_2 fixation which increase their impact in comparison to the relatively higher biomasses of prokaryotic picophytoplankton, such as the cyanobacterial species *Prochlorococcus* and *Synechococcus* (Jardillier et al., 2010). Thus, at a sample site near Southern California photosynthetic picoeukaryotes contributed 79% of the total carbon consumption by picoplankton despite only making up between 7-20% of the total biomass, the rest being mainly cyanobacteria (Worden et al., 2004). Similarly, a study in the south-east Pacific Ocean found that picophytoplankton were responsible for over 60% of the primary production, around half of which was contributed by picoeukaryotes, with the prasinophyte green algae genus *Ostreococcus* dominant in this size class in upwelling waters (Rii et al., 2016). Prasinophytes are a diverse group of photosynthetic picoeukaryotes, comprising chlorophyte green algae which are dominant in coastal areas with high nutrient availability (Lopes dos Santos et al., 2017). The genus *Ostreococcus*, like other chlorophyte algae in the order Mamiellales and the family Bathycoccaceae, is found in oceans across the world and most frequently in tropical or temperate environments (Rii et al., 2016, Limardo et al., 2017). The distribution of *Ostreococcus* species is delineated by environmental adaptation with discrete clades occupying specific waters (see section 1.7) (Leconte et al., 2020, Guillou et al., 2004). A meta-analysis of picophytoplankton biomass data encompassing studies across the globe estimates a greater contribution by photosynthetic picoeukaryotes (approximately 50-70%) compared to cyanobacterial genera, although this did include larger cells up to 3µm in diameter (Buitenhuis et al., 2012). Many factors can cause variation in picophytoplankton biomass and community composition including seasonal effects, position within the water column, nutrient availability, and dramatic

changes during massive transient blooms so that estimates often vary accordingly (Bolaños et al., 2021, O'Kelly et al., 2003, Choi et al., 2016, Hernández-Ruiz et al., 2018, Kirkham et al., 2013, Cloern et al., 2014). However, these studies show the enormous potential of picoeukaryotes to impact ecosystems.

1.2 Phytoplankton: current and future climate effects

Alteration of the environment due to climate change demands clarification of the effects on the dynamics of marine picophytoplankton communities. It is generally accepted that rising temperatures are increasing stratification which reduces mixing of nutrients, prolongs exposure to radiation in the surface layer, and causes expanding oxygen minimum zones in the oceans (Li et al., 2020, Schmidtko et al., 2017, Gao et al., 2018, Polovina et al., 2008). Increased dissolved CO_2 driven by rising atmospheric concentrations is also causing ocean acidification and carbon uptake by phytoplankton is the main mechanism for mitigating this effect (Humphreys, 2016, Gao et al., 2018, Bates et al., 2014, Landschützer et al., 2018). It is important, but challenging, to accurately determine the effect of these global trends of change on phytoplankton activity and diversity, and effects will vary with optimum conditions for certain taxa, existing adaptations, and geographic location. Ocean acidification is expected to change phytoplankton community structure and biodiversity as some species will cope better with this change. Attempts have been made to characterise this effect on phytoplankton communities, although contradictory results are seen when acidification is investigated in combination with other factors such as light intensity so that communities in diverse coastal and open ocean environments are likely to show different responses (Gao et al., 2018). Rising temperatures and changing currents may favour smaller species including picophytoplankton and drive temperate phytoplankton populations towards the poles as has been noted already in coccolithophores and zooplankton such as foraminifera and krill (Morán et al., 2010, Oziel et al., 2020). Rising temperatures have led to a reduction in sea ice in the Arctic and enabled longer growing seasons for phytoplankton resulting in increased net primary production (Arrigo and van Dijken, 2015). Increased thermal tolerance was seen in successive generations of *Ostreococcus* exposed to temperatures of 33ºC in a laboratory setting, showing the potential for these photosynthetic picoeukaryotes to adapt to rising ocean temperatures (Barton et al., 2020). Predictions of global phytoplankton community shifts with climate change suggest an increased importance

of picoeukaryotes due to their tolerance to nutrient limitation, warming, fluctuating light intensity, and increased acidification through dissolved CO_2 (Seifert et al., 2020, Flombaum et al., 2020, Hoppe et al., 2018, Schulz et al., 2017, Hyun et al., 2020, Benner et al., 2020).

The light quality environment of the oceans as determined by the contribution to spectral scattering and absorption by phytoplankton is also expected to alter as a consequence of community shifts due to climate change (Lain and Bernard, 2018). This is due to the different light harvesting pigments and photoprotective mechanisms that different functional groups of phytoplankton are able to synthesise and employ. Fluorescence from chlorophyll *a* (chl-*a*) is frequently used to remotely estimate phytoplankton biomass and productivity on large spatial and temporal scales across oceans and seasons, and ocean colour across a broader spectrum is increasingly being considered as an important metric for assessing phytoplankton community health as well as determining taxa-specific contributions to light absorption from other light harvesting photopigments such as carotenoids and biliproteins (Blondeau-Patissier et al., 2014, Groom et al., 2019, Markager and Vincent, 2001, Bracher and Tilzer, 2001). A recent model of remote chl-*a* estimations found that the colour of surface ocean water is likely to become more dominantly blue due to a shift in phytoplankton community structure and bleaching of coloured dissolved organic matter (DOM) (Dutkiewicz et al., 2019). Blue light presents a competitive advantage for eukaryotic picophytoplankton which utilise chlorophyll and carotenoid complexes to harvest light for photosynthesis and are able to absorb blue wavelengths more efficiently than some cyanobacteria which also utilise phycobilisome antennae to harvest light (Luimstra et al., 2020b). This may mean that feedback occurs as phytoplankton communities shift in the response to the oceans' light environment causing further changes and resulting in drastic ecological effects.

1.3 Light quality in the environment, land plants

Visible light within the range 400-700nm is known as photosynthetically active radiation (PAR) and is used for photosynthesis (Hader et al., 1998). On land, the light environment is broadly composed of light across the visible spectrum, while an increased ratio of far-red light to red light is caused by shading by leaves compared to direct light. Responding to the spectral light environment allows photosynthetic organisms to maximise the efficiency of light capture, for example by altering the

composition of light harvesting photopigments, by increasing energy storage, or by increasing growth to avoid shade; these responses are known as photomorphogenesis (Murchie and Horton, 1997). Plants possess photoreceptors which allow them to sense and respond to the light environment as well as to regulate their development accordingly. In general terms, plant photoreceptors contain photosensory domains such as a light-oxygen-voltage (LOV) domain in phototropins, which contain a chromophore binding domain such as the blue light absorbing flavin adenine dinucleotide (FAD) binding domain in response to the absorption of light photons at UV or PAR wavelength (Möglich et al., 2010). Photoreceptors also possess a receiver domain such as a serine/threonine kinase which transduces the light signal by phosphorylating a response regulator or binding DNA, proteins, or membranes, initiating a cascade of downstream responses. Red and blue light wavelengths are most efficiently absorbed by chlorophylls *a* and *b* for photosynthesis and plants are able to sense and respond to these light qualities using specific photoreceptors (Figure 1.1a) (Lichtenthaler, 1987, Kume et al., 2018). A combination of these photoreceptors allows some of the composition of available light spectra to be sensed so that cells are able to respond in a specialised way to their environment. These photoreceptors may therefore be used to control circadian entrainment and photomorphogenic responses for more efficient light capture (Möglich et al., 2010). For example, in shade-avoiding higher plants, the photoreceptors which sense red light, known as phytochromes, are able to sense and avoid areas of leafy shade by detecting the higher proportion of far-red light to red light and respond by inducing stem extension; a growth strategy known as etiolation (Devlin, 2016, Yang et al., 2016b, Yang et al., 2016a, Murchie and Horton, 1997). Understanding the effects of the relative contents of blue, red, and far-red light wavelengths for the indoor growth of plants in crop production can be used to optimise growth strategy, such as increased flower content in red light (Darko et al., 2014, Rabara et al., 2017). Green light has been found to induce responses in plants which are similar to physiological responses to low light intensities and while the exact mechanism driving the green light response is unknown, the responses are suggested to be adaptive to the increased proportional presence of green light wavelengths in shaded areas (Wang et al., 2009, Battle et al., 2020, Mawphlang and Kharshiing, 2017).

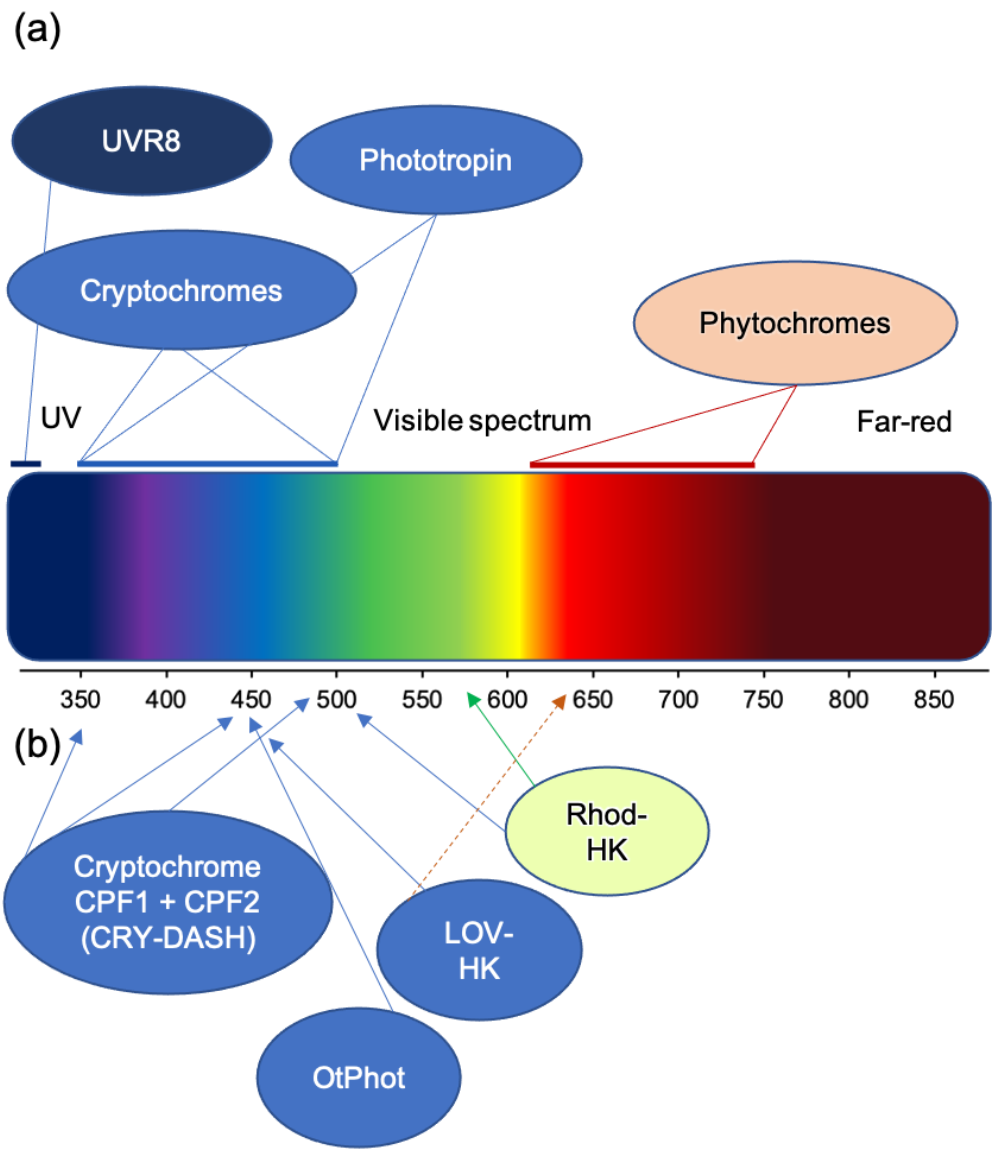

Figure 1.1 Approximate absorbencies or responses to the light spectrum for common photoreceptors
(a) land plants and (b) *Ostreococcus.* Solid arrows indicate peaks in measured absorbencies. Dashed arrows represent wavelengths to which responses in these photoreceptors have been hypothesized. Photoreceptor abbreviations: UV resistance locus 8 (UVR8), *Drosophila*, *Arabidopsis*, *Synechocystis*, human (DASH)-type cryptochromes, Rhodopsin histidine kinase (RhodHK), Light-oxygen-voltage histidine kinase (LOV-HK), *Ostreococcus* phototropin (OtPhot), Cryptochrome photolyase family (CPF). (Casal, 2013, Ouzounis et al., 2015, Luck et al., 2019, Thommen et al., 2015, Sullivan et al., 2016).

1.4 Light quality in the environment, marine systems

Visible light in the PAR range reaches a maximum depth of around 200m depending on sunlight intensity and water clarity. This forms the oceans' euphotic zone. Most PAR present in deeper waters is composed of blue light as it is made up of shorter wavelengths with higher energy and so it penetrates further through the water. Red, far-red and (to a lesser extent) green light wavelengths attenuate more quickly and are only present in shallower waters (Bouman et al., 2000). This underwater light

environment as caused by absorbance and scattering of wavelengths by water is illustrated by Figure 1.2. Coastal waters also tend to contain more green light as blue and red wavelengths are primarily absorbed by chlorophylls in phytoplankton (Lichtenthaler, 1987, Kume et al., 2018, Schubert et al., 2001).

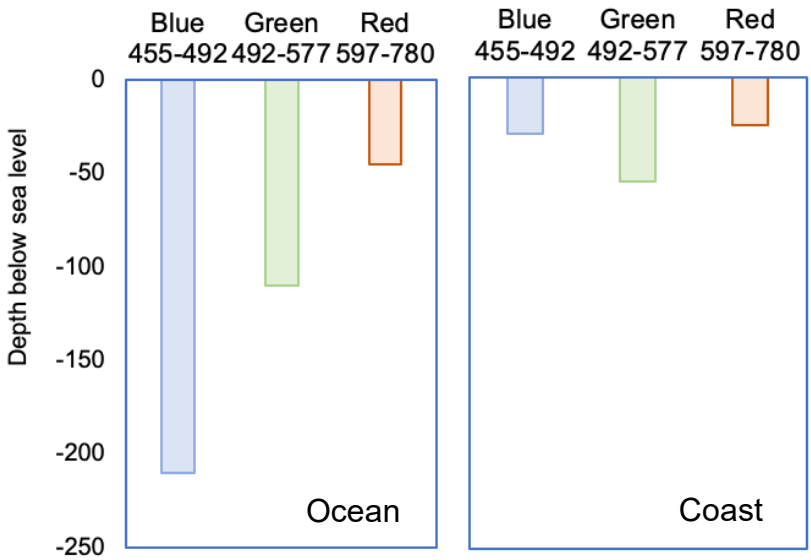

Figure 1.2 The underwater light environment.
Bars represent the penetration depth of light qualities in the visible spectrum and are coloured according to their visual appearance. Adapted from NOAA 2016.

These variations in light quality may be accompanied by other environmental factors. Oligotrophic ocean waters are characterised by having consistently low levels of nutrients and chlorophyll. While the ocean euphotic zone changes both by latitude and season, the depth of the euphotic zone also varies depending on water clarity. This latter feature differs the most between open-ocean and coastal regions, dependent on the amount of particulate material in the water column (V-Balogh et al., 2009). In coastal waters, light absorbance and scattering by dissolved organic matter and run-off from rivers cause a proportional increase in yellow wavelengths (Erga et al., 2012). These changes in the spectrum of PAR in water describe the light field penetrating downwards through the water, the downwelling irradiance, and further effects can be seen in light reflected back upwards, the upwelling irradiance spectrum, particularly in coastal waters as reflectance from phytoplankton causes higher levels of green wavelengths (Schubert et al., 2001, Sun et al., 2010, Tilzer et al., 1995).

Phytoplankton blooms characteristically reduce light intensity and narrow the PAR spectrum of marine waters (Churilova et al., 2020, Bracher and Tilzer, 2001). Diatoms and dinoflagellates in coastal environments have been shown to primarily absorb

shorter wavelengths during a bloom leading to a predominantly green and red spectral downwelling irradiance when compared to ambient levels at the same optical depths. This effect of a bloom on the downwelling irradiance has also been observed in laboratory conditions in cyanobacteria (Soja-Woźniak et al., 2018). Blooms favour small, low light adapted phytoplankton which are tolerant of self-shading as this allows survival during competition (Lewandowska et al., 2015).

Light quality sensing in phytoplankton species may therefore be used to distinguish deep water environments indicated by the prevalence of blue wavelengths, from surface environments indicated by a signature of a broader visible spectrum, or to detect the presence of particulate matter and of other phytoplankton.

Light quality can also vary according to the time of the day. In a North Sea study of shallow waters down to 3.5m, blue and far-red light wavelengths were increased in relation to red light at dawn and dusk. Corresponding changes in pigment production were noted in green macroalgae on a diurnal scale, in response to these spectral changes (López-Figueroa, 1992).

Light quality responses have been extensively described in cyanobacteria. Some *Synechococcus* strains are able to alter the composition and quantity of light harvesting pigments, the red/orange wavelength absorbing phycocyanin and green absorbing phycoerythrin, in order to absorb light optimally in a varied light environment; this is known as complementary chromatic adaptation (Six et al., 2007, Palenik, 2001, Kehoe and Grossman, 1994). However other cyanobacteria in the *Synechococcus* genus constitutively produce different ratios of these pigments allowing them to occupy environmental niches corresponding to different spectral qualities, and this allows the prediction of their environmental distribution (Stomp et al., 2004, Grébert et al., 2018). Cyanobacteria also exhibit a photoadaptive response to damaging UV light. This includes the production of photoprotective compounds such as scytonemin which are used in biotechnology for the production of protective suncreams (Rastogi et al., 2015).

1.5 Light quality responses in picophytoplankton

As with land plants, phytoplankton use photoreceptors to sense different wavelengths of light. Though their responses and signalling effects have been less well described, different light qualities have been noted to prompt changes in gene expression in some

species of photosynthetic plankton (Luimstra et al., 2020a, Meng et al., 2019). For example, the chlorophyte green alga *Chlamydomonas reinhardtii* responds to red, green, and blue light distinctly showing changes in gene expression (Beel et al., 2012). In addition to a plant-like cryptochrome, it possesses an animal-like cryptochrome (aCRY) which is able to sense red light (at 633nm) and yellow light (at 585nm), but not far-red light. The responses of *C. reinhardtii* to red and blue light in terms of gene expression were found to be more similar to each other than to the green light response (Beel et al., 2012). For example, transcription of chlorophyll synthesis genes increased as a response to both red and blue light compared to green light (Beel et al., 2012, Forbes-Stovall et al., 2014). In the diatom *Phaeodactylum tricornutum*, perception of red and far-red light via phytochromes induces changes in expression of around 200 gene. This species also exhibits distinct transcriptional responses to red, green, and blue light (Fortunato et al., 2016, Valle et al., 2014). The red algae *Cyanidioschyzon merolae*, also displays distinct transcriptional responses to blue and red wavelengths of light (Tardu et al., 2016). Genes involved in DNA repair and photosynthesis are induced under red light, while increased expression of protein synthesis genes is seen under blue light. These examples demonstrate a precedent for light quality responses as initiated by photoreceptors in phytoplankton which suggests that the ability to discern and respond to specific wavelengths in the underwater environment is advantageous.

1.6 An introduction to *Ostreococcus*

First discovered using flow cytometry measurements of chlorophyll fluorescence in 1994, *Ostreococcus* is the smallest free-living eukaryote identified to date (Demir-Hilton et al., 2011, Chretiennot-Dinet et al., 1995, Courties et al., 1994). The *Ostreococcus* cell features a single chloroplast, single mitochondrion, no flagella or cell wall, and a cell size of around 0.6-2.8μm in diameter (Derelle et al., 2002, Guillou et al., 2004). The existence of several adapted ecotypes, which are considered distinct species, makes this genus an ideal target for study of ecological adaptations (Derelle et al., 2006). *Ostreococcus* species are generally morphologically indistinguishable, although electron microscopy has revealed an outer membrane covered with protruding bumps in *O.* RCC809 which was not noted in the smooth membrane of *O. lucimarinus* (Limardo et al., 2017). Its small size, and its compact haploid genome (12.56Mbp in the ecotype OTH95 and 13.3Mbp in RCC809,) with minimal introns

and little duplication, presents a simple model to understand its photosynthetic function. *Ostreococcus* is also readily transformable which allows precise studies of gene function, as well as the potential for use in biotechnology. For example, its use as a biosensor for contamination in water has been investigated in the strain *Ostreococcus tauri* (hereafter referred to as OTH95) (Lozano et al., 2014, Henríquez-Castillo et al., 2018, Sanchez et al., 2019, van Ooijen et al., 2012, Thomy et al., 2021). Transgene overexpression and gene knockdown via antisense have been used successfully to demonstrate the effects of clock genes in the regulation of circadian control of gene expression in OTH95 (Corellou et al., 2009).

The genome of OTH95 has a GC content of 59%, with notable exceptions being chromosomes 2 and 19 which possess a lower GC content, a higher incidence of transposons, and evidence of horizontal transfer of some genes with a bacterial origin (Grimsley et al., 2010, Blanc-Mathieu et al., 2017). A study of *Ostreococcus* strains in 2005 found variation in the total chromosome number, from 15-20, with chromosome sizes of 0.15-1.5Mbp (Rodríguez et al., 2005). This study separated the strains into four clades (A-D) using variability in the internal transcribed spacer (ITS) DNA and 18S rRNA gene. Strains within these clades are sufficiently varied to be considered distinct species (Subirana et al., 2013, Palenik et al., 2007). Clade B is associated with temperate and tropical oligotrophic waters and adaptation to low light intensities, while clades A and C are both associated with higher light intensities, A with colder water, and C with surface coastal waters. Clade D may be limited to brackish waters (Demir-Hilton et al., 2011). A fifth clade (E) associated with temperate coastal waters has been isolated in the Mediterranean sea (Tragin and Vaulot, 2019). The species are likely to be sexually incompatible due to the presence of two or more hypervariable chromosomes (such as chromosome 2 in OTH95) which are characterised by a lower percentage GC content and feature transposons and evidence of horizontal transfer. The variability of these chromosomes would prevent pairing between species and prevent offspring being viable (Palenik et al., 2007). Sexual reproduction has also not been observed within *Ostreococcus* species to date, although evidence of rare meiosis is seen by chromosomal recombination events in OTH95 (Blanc-Mathieu et al., 2017). The inability to interbreed may explain why multiple species can be maintained in the same areas although they rarely co-occur and are primarily separated by their differential survival depending on light intensity. Thus, the low light and warmer water

associated oligotrophic *Ostreococcus* clade B are only found alongside the colder water and coastal associated mesotrophic clades A or C at transition slope waters where dynamic mixing occurs (Demir-Hilton et al., 2011, Six et al., 2008, Cardol et al., 2008, Limardo et al., 2017, Simmons et al., 2016).

1.7 Light sensing in *Ostreococcus*

A photosynthetic organism like *Ostreococcus* needs to be able to sense, respond, and adapt to changes in its light environment to efficiently regulate its photosynthetic machinery. *Ostreococcus* species are able to capture light across the visible spectrum for use in photosynthesis, and they achieve this using chlorophylls *a* and *b* which mainly absorb blue and red wavelengths. *Ostreococcus* also utilise a variety of accessory photopigments which broaden the spectrum absorbed, as each absorb light maximally at specific wavelengths, and provide photoprotection of the chlorophylls by dissipating excess light energy (Jagannathan and Golbeck, 2009, Six et al., 2009, Six et al., 2005). The relative contents of these chlorophylls and accessory photopigments are adjusted in response to light intensity changes in *Ostreococcus* and the magnitude of these responses differ between the low light adapted ecotype RCC809, and the higher light adapted OTH95 (Six et al., 2008). Some species including the RCC809 ecotype also contain an extra photopigment: Chl CS-170 which absorbs blue/green light and may be an adaptation to low light intensity environments (Rodríguez et al., 2005).

Responses to light may result from detection of metabolites produced through photosynthesis; this mechanism of indirectly sensing light using protein kinases to detect sugars is, for example, used to reset circadian rhythms in *Arabidopsis* plants (Frank et al., 2018). Photoreceptor-independent light sensing was also described in plants, in the cyanobacterium *Calothrix*, and in the green alga *Dunaliella salina,* where electron transport initiated by light absorption within the photosystems triggers responses in the regulation of the light harvesting complexes of its photosynthetic machinery (Maxwell et al., 1995, Pfannschmidt et al., 2001, Campbell et al., 1993). However, light quality-specific responses are mediated by dedicated light-sensing molecules also known as photoreceptors.

Five photoreceptors have been identified in *Ostreococcus:* two histidine kinases (LOV-HK and Rhod-HK), two cryptochromes (CPF1 and CPF2), and a phototropin. The light sensing and resultant signalling functions of these photoreceptors in

Ostreococcus are not yet fully understood and the exact wavelengths of light *Ostreococcus* is able to detect have not yet been fully described. Figure 1.1a gives an overview and approximate light wavelength absorbance of the common photoreceptors found in land plants, compared to those which have been described in *Ostreococcus* (Figure 1.1b), note the lack of a phytochrome photoreceptor in *Ostreococcus*. *Ostreococcus*, *Micromonas*, and *Bathycoccus* belong to the order Mamiellales within the green algal class Prasinophyceae. *Ostreococcus* and *Bathycoccus* are in the family of Bathycoccaceae and do not possess phytochrome photoreceptors (Duanmu et al., 2014). This means that the Bathycoccaceae family are not able to distinguish red from far-red (>680nm) light wavelengths.

The *Ostreococcus* light, oxygen, and voltage sensing histidine kinase (LOV-HK) photoreceptor, which senses blue light maximally at 450nm, may also play a role in responses to red light. Overexpression or antisense inhibition of its transcription altered the rhythmic expression of circadian clock genes under constant red light (Djouani-Tahri et al., 2011, Thommen et al., 2015). On the other hand, the other *Ostreococcus* histidine kinase photoreceptor, rhodopsin-HK (Rhod-HK) may respond to longer wavelengths, as this fits a model of circadian entrainment involving both blue and red light (Thommen et al., 2015). Rhod-HK in OTH95 absorbs green-orange light at 462 and 521nm and may act as a molecular switch in response to light quality conditions specific to dusk (Luck et al., 2019).

The two *Ostreococcus* cryptochrome photoreceptors, the CPF1 and CPF2 DASH, sense blue light and regulate circadian rhythms (Beel et al., 2013, Thommen et al., 2015). The phototropin photoreceptor (known in *Ostreococcus* OTH95 as Otphot) also senses blue light, with maximal absorbance at 449nm. However, it did not restore phototropism responses in transgenic *Arabidopsis* plants suggesting that it may be distinct from plant phototropins and may have reduced or different functions (Sullivan et al., 2016).

The findings to date on the peak absorbencies of *Ostreococcus* photoreceptors show that its blue light sensing is likely to be more sensitive compared to that of land plants Figure 1. This is explained in the context of the underwater environment in which red and green wavelengths are scattered and absorbed by water compared to the broader spectrum of light available in the atmosphere on land. Although the findings on these photoreceptors show some indication of the light sensing capabilities of *Ostreococcus*,

little is known about their downstream signalling pathways and resultant effects on cellular processes and physiology.

1.8 Environmental adaptations in *Ostreococcus*

O*streococcus* cells are not motile and must be able to adjust to changes in the environment to survive rather than by utilising responses through movement such as phototaxis. This lack of motility may have contributed to the formation of distinct *Ostreococcus* ecotypes adapted to high light and low light environments. It may also have driven adaptation of their photosystems to other abiotic factors, such as nutrient availability. For example, some ecotypes such as RCC809 are able to cope with reduced levels of iron while maintaining efficient photosynthesis (Six et al., 2009, Botebol et al., 2017, Rodríguez et al., 2005).

The variable magnitude of increased cell size and photosynthesis rates of 16 *Ostreococcus* ecotypes in response to CO_2 enrichment demonstrates their divergence in adaptations (Schaum et al., 2013). Smaller magnitudes of changes in response to the CO_2 enrichment were seen in strains isolated in deeper water than those isolated from surface waters, and it was concluded that surface ecotypes are likely to be more plastic in response to environmental change. Following this, it was found that the smaller magnitude of these responses of the deeper water ecotypes to variations in CO_2 was an adaptive response beneficial to longer term survival in variable conditions (Schaum and Collins, 2014).

Light intensity is thought to be the primary abiotic factor which determines clade distribution (Demir-Hilton et al., 2011). The OTH95 ecotype belongs to clade C and is found in shallow lagoon and coastal water, whereas the RCC809 ecotype belongs to clade B and was sourced from the open ocean at a depth of 105 meters. RCC809 was also found to have a higher light harvesting capacity than OTH95, a likely adaptation to limitation from lower light intensities, whereas the OTH95 samples were adapted for photoprotection (Six et al., 2005, Six et al., 2009, Demir-Hilton et al., 2011, Cardol et al., 2008). This project is focussed on these two ecotypes of *Ostreococcus*: OTH95 (from Thau Lagoon in the South of France), and RCC809 (sampled at a depth of 105m in the Atlantic Ocean) (Table 1.1). These ecotypes are distinct species which show adaptation to the environments from which they were derived, and are considered to be in separate clades (Rodríguez et al., 2005). The lagoon sourced OTH95 (clade C within the coastal associated OI) and RCC809 (clade B within the OII clade often

found to peak in abundance at the deep chlorophyll maximum (DCM) at depths around 100m) are considered to be the two most disparate *Ostreococcus* species in terms of their light intensity responses (Demir-Hilton et al., 2011, Limardo et al., 2017). However, variation in responses to light of different wavelengths has not been investigated.

Table 1.1 A comparison of genomic and physiological features for the ecotypes RCC809 and OTH95

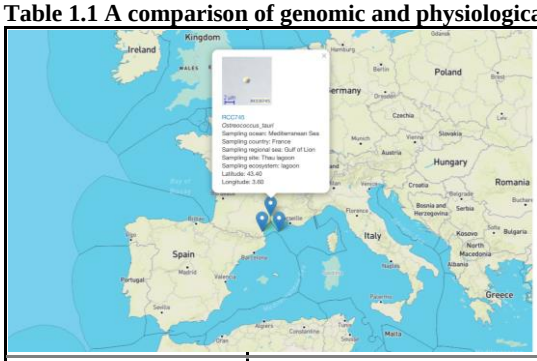

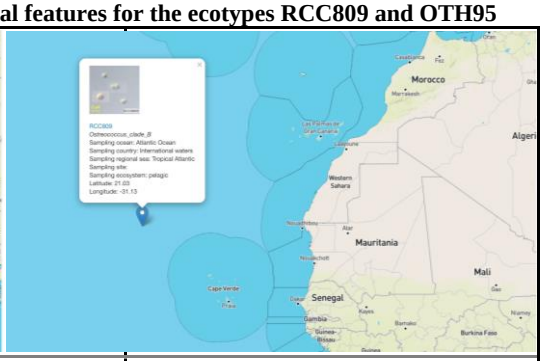

	OTH95 (also known as *Ostreococcus tauri, strain OTTH 0595* RCC745)	**RCC809 (a clone of the lost strain RCC141, also known as Eum16BBL_clonal, NIES-2674)**
Source (1)	Coastal sites including the Thau Lagoon, South France which has a mean depth: 4.5m max depth: 10m	105m deep Tropical Atlantic Ocean
Both possess the same light harvesting pigments and photoreceptors (2)	Lower ratio of chl-*b* to chl-*a* than RCC809 (0.65 ± 0.05)	Around a 50% higher ratio of chl-*b* to chl-*a* than OTH95 (1.01 ± 0.08) Also contains Chl CS-170 which may allow capture of low levels of blue/green light (7)
Genome (3) GC content (4)	7586 genes, 20 chromosomes (6650 homologues ~90%) 59% with lower GC in outlier chromosomes 2 and 19 which may be due to TEs	7536 genes, 20 chromosomes (6650 homologues ~90%) 60% with lower GC in outlier chromosomes 2, 7 and 20 which may be due to TEs

Differential survival under high light intensities (5)	Adapted for photoprotection Faster PSII repair cycle Higher PSI content than RCC809 Grows optimally at the higher light intensity of 100μE m^{-2} s^{-1}	Higher PSII light harvesting capacity compared to PSI, may be an adaptation to Fe limitation PSII antenna ~1.5 times larger Sensitivity to prolonged exposure to higher light intensities (cells deactivated after 8 to 10 days at 100μE m^{-2} s^{-1}) Grows more optimally at the lower light intensity of 10μE m^{-2} s^{-1}
Clade (6)	C within OI	B within OII

1) Location maps sourced from Roscoff collection (http://roscoff-culture-collection.org/)
2) (Cardol et al., 2008)
3) Determined using reciprocal BLAST
4) (Derelle et al., 2006, Blanc-Mathieu et al., 2017)
5) (Six et al., 2005, Six et al., 2009, Cardol et al., 2008, Demir-Hilton et al., 2011)
6) (van Baren et al., 2016)
7) (Rodríguez et al., 2005)

1.9 Aims and objectives

As phytoplankton community composition alters with a changing climate, the marine light environment will also shift. Understanding the adaptive potential of important primary producers is key to understanding the effects of climate change on oceans. However, little is known about light quality responses in picoeukaryote phytoplankton. The aim of this project is to determine whether *Ostreococcus*, a photosynthetic picoeukaryote, is able to respond distinctly to different light qualities, and to obtain evidence for the adaptive significance of light quality responses. To test the hypothesis that different *Ostreococcus* ecotypes have adapted to distinct light quality niches, and that responses to light quality contribute to fitness in the natural environment, light-quality responses were compared in two ecotypes sourced from distinct light quality environments. The deep ocean ecotype RCC809 is present in regions of the euphotic zone where mostly blue light is able to propagate, whereas the lagoon and coastal ecotype OTH95 is exposed to a wider spectrum of red, green and blue light.

To obtain initial clues to the effects of light quality on cell physiology, gene expression changes are investigated following acclimation to different light qualities, revealing extensive differences in the responsiveness of the two ecotypes. Chapter 3.

The consequences of these gene expression changes on pigment content and photosynthetic parameters are subsequently examined, giving insight into adaptive significance of light quality responses. Chapter 4.

Mechanisms involved in regulation of these light quality responses are investigated through identification of potential regulatory elements in light quality-responsive genes, and candidate transcription factors binding these elements. Prospective genetic markers for light quality responsiveness are identified by a comparison of the ecotypes. Chapter 5.

Chapter 2: Methods

2.1 Strain sources

Ostreococcus strains were obtained from the Roscoff Culture Collection (http://roscoff-culture-collection.org)

- OTH95 (also known as RCC745, RCC4221, OTTH 0595, and *tauri*). Sourced from the shallow Thau Lagoon, France (Chretiennot-Dinet et al., 1995).
- RCC809 (also known as Eum16BBL_clonal and NIES-2674). RCC809 is a clone of the lost strain RCC141 which was sourced at a depth of 105m in the Tropical Atlantic

2.2 Culture conditions

Cells were grown in Keller medium supplemented with vitamins B12 (3.69×10^{-10} M), thiamine (2.96×10^{-7} M), and biotin (2.05×10^{-9} M), and the antibiotics penicillin (25µg ml^{-1}), neomycin (20µg ml^{-1}), and kanamycin (25µg ml^{-1}) (Keller et al., 1987, Farinas et al., 2006). 20ml cultures were grown in 50ml Falcon cell culture flasks with vented caps. Batch cultures were incubated at 21ºC under 12h light 12h dark cycles using fluorescent white light at 20µmol photons m^{-2} s^{-1} and refreshed on a fortnightly basis. All handling of stocks was carried out under laminar flow hoods.

2.3 Determination of cell titre

Cell numbers of cultures were initially determined using a Beckman Coulter CytoFlex flow cytometer and results were correlated with those of OD_{550nm} using a Thermo Fisher NanoDrop 2000 spectrophotometer (the cells absorb minimal light at this wavelength). OD_{550nm} was then used as an approximation for cell titre using the equation Cell titre (cells ml^{-1}) = 2×10^9 OD.

2.4 DNA extraction and genotyping

For extraction of genomic DNA, 200ml cultures in early stationary phase (30-40 million cells ml^{-1}) were centrifuged at 4000rpm for 10 minutes at 4ºC. The supernatant was removed, leaving about 1ml behind. The pellet was resuspended and transferred to a microfuge tube. This was then centrifuged at 8000rpm 4ºC for a further 10 minutes. The supernatant was removed, and the pellet was frozen using liquid nitrogen. DNA was extracted using a modified version of a plant DNA extraction method (Dellaporta et al., 1983). 300µl extraction buffer (100mM Tris, 50mM EDTA, 500mM

NaCl, and 10mM b-Mercaptoethanol) and two metal beads were added to frozen cell pellets, and samples were shaken using a pre-cooled QIAGEN tissue lyser for 2 minutes at 30Hz. 1/10th volume of 10% SDS was added to lysates, and samples were incubated at 65°C for 10 minutes. 1/4th volume of 5M potassium acetate was then added, and samples were incubated at 4°C for 10 minutes before centrifugation at 13000rpm for 10 minutes to remove particulate material. The supernatant was transferred to a fresh tube, combined with half volume of isopropanol and 2µl glycogen (20mg/ml), and incubated at -20°C for 30 minutes before centrifugation at 13000rpm for 15 minutes at 4°C. The pellet was then drained and resuspended in 400µl TE (50mM Tris, 10mM EDTA, pH8) and centrifuged again for 10 minutes at 13000rpm to remove debris. The supernatant was incubated at 37°C for 30 minutes with 1µl of RNAse A. 1/10th volume of 5M NaCl and 2 volumes of EtOH were added before a final centrifugation was carried out at 13000rpm for 10 minutes at 4°C. The pellet was rinsed with 1ml 70% (v/v) ethanol, dried, and re-dissolved in TE. The DNA was then quantified using a Thermo Fisher NanoDrop 2000 spectrophotometer.

2.5 Genotyping

Ostreococcus strains were genotyped as described previously (Demir-Hilton et al., 2011, Clayton et al., 2017, Moon-van der Staay et al., 2001), by sequencing the 18S rRNA gene. Primers used for amplification of the sequence were:

EUKf: 5′-ACCTGGTTGATCCTGCCAG-3′

EUKr: 5′-TGATCCTTYGCAGGTTCAC-3′

PCR reactions were performed on genomic DNA using the Thermo Scientific™ DreamTaq green PCR master mix according to the standard protocol. Amplification was carried out on 30-80ng of genomic DNA template for 35 amplification cycles at an annealing temperature of 55°C. PCR products were purified using the QIAGEN QIAquick PCR purification kit according to the standard protocol. The fragments were sequenced by Eurofins Genomics GATC LightRun service using the internal primer:

EUK502f: 5′-GGAGGGCAAGTCTGGT-3′

2.6 Monochromatic light sources

Red and blue light was provided by LED arrays, and green light was provided by cool-white fluorescent bulbs covered with one layer of green filter (Lee filter 139). Light

intensity was 4µmol photons m^{-2} s^{-1}, as measured using a LI-COR photometer light meter (model LI-189) with a quantum sensor. The specific wavelengths of the monochromatic lights were determined using a Stellanet epc2000 spectroradiometer with a fibre lead as described in Figure 2.1.

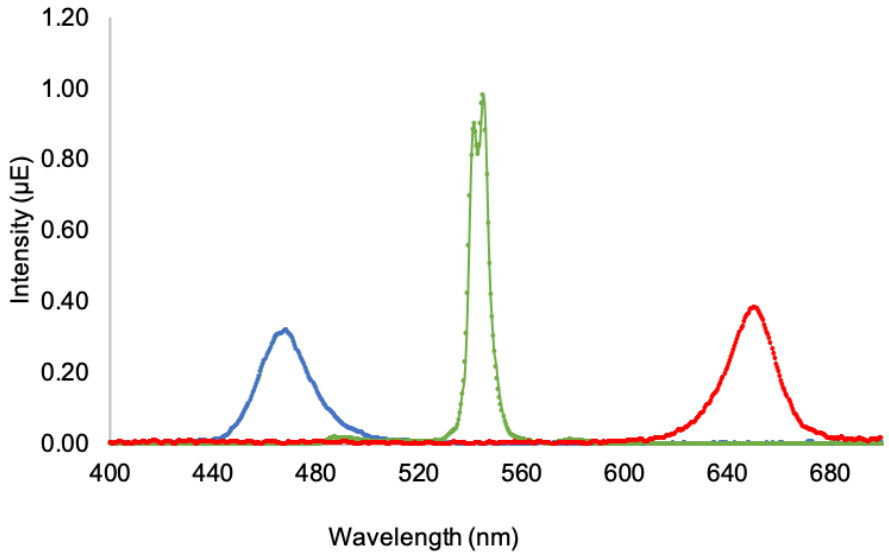

Figure 2.1 Spectroradiometer measurements of the three light treatments.
Peak wavelengths were: 650.5nm for red light, 545nm for green light, and 467.5nm for blue light.

2.7 RNA extraction and sequencing

For each sample, 200ml culture was harvested, at about 40 million cells per ml. Cells were spun down, pooled into 1ml cold PBS, transferred to a microfuge tube, then spun again at 13,000rpm to pellet the cells and eliminate the supernatant. Cells were then frozen in liquid nitrogen. To break down the cells for RNA extraction, samples were treated with 1ml of the guanidinium thiocyanate and phenol reagent TRIzol, then thawed out at room temperature and two sterile glass beads were added before shaking for 3 minutes using a Tissue Lyser (QIAGEN) at maximum speed. 200µl chloroform was added and mixed in by shaking for 15 seconds before incubating at room temperature for 3 minutes then spinning down at 12,000g at 4ºC for 15 minutes. The aqueous phase was transferred to a new tube, combined with 0.5ml isopropanol and 5µl glycogen (20mg/ml), incubated for 10 minutes at room temperature then spun down at 12,000g at 4ºC for 15 minutes. The supernatant was removed, and the pellet was washed twice with 1ml 70% (v/v) ethanol before resuspension in 50µl RNAse free water. To eliminate contaminating genomic DNA, the RNA was treated with RNAse-free DNAse (SIGMA) according to the manufacturer's instructions before

purification using the Spectrum Plant Total RNA Kit from Sigma-Aldrich. RNA quality was verified using a Bioanalyser before preparation of RNA-seq libraries using the Illumina Tru-Seq RNA library preparation kit, which enriches for mRNAs using Oligo-dT beads to capture polyA tails before cDNA synthesis. This method does not capture chloroplastic RNA. 100bp paired-end (PE) sequencing was carried out on an Illumina HiSeq at the Wellcome Trust. This provided the raw data at the start of this project.

2.8 RNASeq Downstream analysis

Reference genome sequence (fasta) files and annotation (gff3) files for each ecotype were sourced from the Online Resource for Community Annotation of Eukaryotes (ORCAE) database (http://bioinformatics.psb.ugent.be/orcae/ accessed March 2017). Genomes used were the ORCAE V2 OTH95 Genome, (Palenik et al., 2007, Derelle et al., 2006, Blanc-Mathieu et al., 2014) and the RCC809 genome V2.0 2009, project number 16233, annotated by the Joint Genome Institute (JGI) (Grigoriev et al., 2012). (https://mycocosm.jgi.doe.gov/OstRCC809_2/OstRCC809_2.info.html)

RNA-seq data were processed and analysed within the Discovery Environment in Cyverse (https://www.cyverse.org). Downstream analysis is summarised in Figure 2.2.

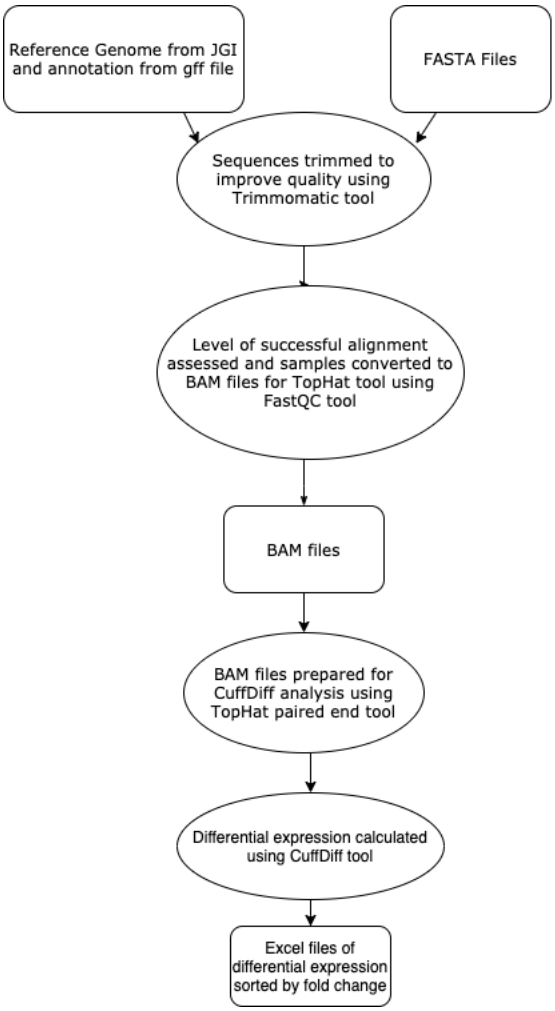

Figure 2.2 Pipeline for RNASeq downstream analysis

Read alignment was assessed using the Fastqc tool version 0.2 (Andrews, 2015). Two samples showed less than 80% alignment, suggesting contamination. Another gave about 120,000 reads compared to around 10 million reads for the other samples. These samples were discarded from further analyses.

Sequences were then trimmed using Trimmomatic version 0.36.0 in paired end mode, to improve read quality (Bolger et al., 2014). A Phred quality score of +33 was used, with a minimum read length of 50 bases and a minimum quality of 3 at both the leading and trailing ends of the read. Fastqc analysis showed improvement in read quality, i.e., a greater number of mapped reads and a higher percentage of sequence alignment.

The output files from Fastqc (fastq files) were then prepared for the differential expression analysis using the paired end tool TopHat version 2 which maps reads to a reference genome using Bowtie 2, identifies slice junctions, and then aligns these reads to the junctions (Kim et al., 2013, Langmead and Salzberg, 2012). The output of these

tools, BAM files, are binary formatted sequence alignment map (SAM) files which contain the paired read alignment coordinates.

These BAM files were then analysed using the CuffDiff tool (version 2.2.1a) , which calculates differential expression values for each gene (Trapnell et al., 2013). Sequences with less than 10 reads per-locus were discarded. Read counts were normalised by transcript length and by the total number of fragments using the geometric fragments per kilobase of transcript per million fragments mapped (FPKM) method. Differentially expressed genes were identified using q-values and a false discovery rate (FDR) less than 0.05.

Gene expression patterns were visualised using the CummeRbund package (Goff et al., 2020) in R (R Core Team, 2020) and the heatmaps produced were refined using the pheatmap package (Kolde, 2019).

2.9 Gene Ontology (GO) enrichment

OTH95 genes were annotated by compiling existing gene descriptions and GO terms from ORCAE and the Universal Protein knowledgebase (UniProt).

Annotation of RCC809 genes was carried out using a genome wide basic local alignment search tool (BLAST) to non-redundant databases using the sensitive diamond BLASTx command line tool: ‘translated Query-Protein Subject BLAST 2.2.31+’ (E value 1.00E-03) in July 2018 (Altschul et al., 1990, Altschul et al., 1997, Camacho et al., 2009). GO terms were then added to the BLAST result from the National Centre for Biotechnology Information (NCBI) using BLAST2GO software (Götz et al., 2008, Ashburner et al., 2000, The Gene Ontology Consortium, 2019). These annotations were compared to and merged with those available from the ORCAE and Interpro databases and with annotations from OTH95 homologues, identified by reciprocal BLAST. These were found to be consistent and, in some instances, more detailed than the existing annotations.

GO-term over-representation analysis of differentially expressed genes was carried out using the BiNGO 3.0.3 app in Cytoscape (Maere et al., 2005). Multiple testing correction was carried out using Benjamini & Hochberg False Discovery Rate (FDR) correction with a significance cut-off at 0.05. The enrichment tests were carried out for each set of light responsive genes relative to the whole genome, for the ontology categories of Biological process, Molecular function, and Cellular component.

Differentially expressed genes that were described as enzymes were mapped to pathways by highlighting relevant sections of maps downloaded from the Kyoto Encyclopedia of Genes and Genomes (KEGG) database (Kanehisa and Goto, 2000). As RCC809 was not described on KEGG at this time, homologues of the genes in OTH95 were identified and used in these maps.

2.10 Promoter motif identification

Analysis of the RCC809 genome's intergenic region length distribution (Figure 2.3) showed a peak around 200bp. This informed the selection of the region 250 bases upstream of the start codon for each gene for promoter analyses.

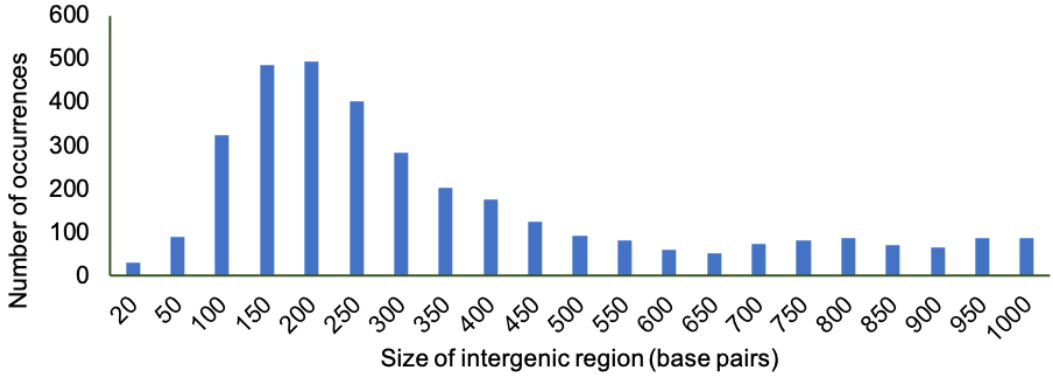

Figure 2.3 Intergenic region size across RCC809 genome used to derive estimation of promoter region

Coordinates of these regions were collected in bed files, listing the genomic coordinates for these promoter sequences. Fasta sequence files were then generated from the bed files using the GetFastaBed tool in Galaxy (usegalaxy.org) (Quinlan and Hall, 2010, Gruening, 2014). Short motifs that were over-represented in the promoters of light-responsive genes compared to a background of promoters genome-wide were identified using the Dreme 5.0.4 tool in the Meme suite (http://meme-suite.org) (Bailey, 2011). Following this, the Meme suite tool FIMO 5.0.4 was used to locate the positions of these motifs in the promoters of the light responsive genes (Grant et al., 2011).

Identified motifs were submitted to TOMTOM to find matches in either orientation to binding sites of experimentally determined transcription factors (Gupta et al., 2007, Lis and Walther, 2016). Databases used were: JASPAR (non-redundant) DNA database/JASPAR Core (2018) plants and *Arabidopsis* DNA Plant (motifs in these databases are determined using two methods: DNA affinity purification (DAP-seq) or protein-binding microarray (PBM) (O'Malley et al., 2016, Fornes et al., 2020).

Similarity of motifs to binding sites in sequences of published *Ostreococcus* transcription factors was also assessed visually (Weirauch et al., 2014).

2.11 PhytoPAM analyses

Cell cultures were grown and acclimated to low level (4μmol photons m^{-2} s^{-1}) monochromatic light for 72 hours under the same conditions and to the same densities as those of the original RNASeq experiment to allow comparison. Each sample was removed from monochromatic light just before measurement so that no sample was kept in darkness for more than 5 minutes prior to the pulse-amplitude modulation (PhytoPAM) measurements. Cultures were diluted 5-fold before analysis to avoid saturation of the signal.

A Walz Phytoplankton Analyzer PhytoPAM fluorometer was used to analyse photosynthetic parameters. In order to determine the maximum quantum yield of photosystem II (PSII) photochemistry (F_v/F_m), samples were kept in darkness in the cuvette for 5 minutes, so that the primary electron acceptor would be fully oxidised and a basal fluorescence level (F_0) could be measured. Then, a saturating pulse at maximum intensity was applied with 5 second intervals and maximum fluorescence (F_m) was measured.

To determine the effective quantum yield of PSII photochemistry (Φ_{PSII}), samples were subjected to increasing levels of photosynthetically active radiation (PAR) at 0, 3, 6, 36, 94, 124, 184, 213, 270, and 298μmol quanta m^{-2} s^{-1} at 120s intervals so that the Ft (the fluorescence steady state also known as Fs) could stabilise. Φ_{PSII} was calculated as (F_m'-F_t/F_m') using the Phyto-Win software (V 2.13). The Phyto-Win software also calculated the relative electron transport rate (rETR) as Yield x PAR x 0.5 x 0.84 μmol electrons $m^{-2}s^{-1}$, where the 0.5 coefficient assumes that only half the PAR is distributed to PSII, and the 0.84 coefficient accounts for relative absorptivity of incident light. These constants are the same as those used for higher plants and don't represent absolute ETR but allow comparison of measurements taken using the same methods.

Phyto-Win uses the Platt curve fitting model to provide alpha values and IK values from the light curve data (Platt et al., 1980). The alpha value describes the efficiency of light absorption as represented by the maximal PSII quantum yield. Alpha is taken as the initial slope of the light response curve (rETR vs PAR). The IK value describes the irradiance level at the onset of light saturation (alpha/rETR max).

2.12 Pigment analysis

10ml of each cell culture was then harvested onto GF/F Glass Microfiber filters using a vacuum pump. The filters were immediately flash frozen in cryovials in liquid nitrogen and stored at -80°C until they were shipped on dry ice for analysis.

The samples were sent to the Danish Hydraulic Institute (DHI) Group laboratory in Denmark, where analysis was carried out by high performance liquid chromatography (HPLC) as described by (Van Heukelem and Thomas, 2001, Hooker and Center, 2005), using pigments with known absorption spectra and relative retention times as standards to correct for errors such as those introduced by variations in solvent evaporation. The following pigments were quantified using pigment standards: chlorophyllide b, MgDVP (Mg-2,4-divinyl pheoporphyrin a5 monomethylester), chlorophyllide a, neoxanthin, prasinoxanthin, violaxanthin, antheraxanthin, zeaxanthin, lutein, chlorophyll b (chl-b), chlorophyll a (chl-a), pheophytin a, α-carotene, and β-carotene. Pigment standards were not available for uriolide, micromonal, dihydrolutein, and the unknown carotenoid previously described in Ostreococcus, so these were tentatively determined using the response factor of β-carotene. Two chlorophyll b-like pigments were also detected in the RCC809 ecotype. Their abundance was calculated using the chlorophyll b response factor. These chlorophyll b-like pigments were not detected in OTH95.

The depoxidation state was calculated as (Z + 0.5A)/(V + A + Z), where Z is zeaxanthin, A is antheraxanthin and V is violaxanthin according to (Munné-Bosch and Cela, 2006). The xanthophyll to chl a ratio was calculated as Z+A+V/chl a.

2.13 Measurement of cell size

Samples of each culture were diluted to around 1 million cells ml^{-1}. Pluronic acid (0.1% final) was added to reduce cell clumping, and samples were mixed by vortexing. Samples were analysed by flow cytometry immediately after harvest, so that fixation was not necessary. Fluoresbrite Multifluorescent beads with an average diameter of 0.5μm were used as reference in order to obtain comparative cell size estimates. A Beckman Coulter CytoFlex flow cytometer was used to determine cell size as the size of the FSC-A (forward scatter area) plotted against SSC-A (side scatter area) and compared to the size of reference beads (gated singlet population). Measurements were taken before and after the addition of the size reference beads and blank Keller medium

was also used for comparison. Samples were run through the flow cytometer at a ‘slow’ rate to reduce the likelihood of aggregate cells being recorded as a single ‘event’. CytExpert software version 2.4 was used to visualise the data.

Chapter 3: Transcriptomic responses to light quality

3.1 Introduction

Light is a source of energy for photosynthetic algae and the ability to sense and respond to its parameters such as intensity and wavelength provides adaptive advantages, such as the ability to increase photoprotection on exposure to high light intensities or increasing light capture in light limiting environments (Fortunato et al., 2016, Tardu et al., 2016, Demir-Hilton et al., 2011, Beel et al., 2012, Forbes-Stovall et al., 2014). Responses to monochromatic light qualities in terms of growth rate, cell size, and gene transcription were investigated in the coastal and lagoon associated *Ostreococcus* OTH95 and the ocean associated *Ostreococcus* RCC809 sourced from deep (105m) water. *Ostreococcus* ecotypes have been described in terms of their growth responses to light intensity, but responses to specific light qualities in terms of growth, gene expression, and physiological changes had not previously been examined (Demir-Hilton et al., 2011). Transcriptional analyses have previously been used for OTH95 to investigate responses to iron limitation and light dark cycles, demonstrating rhythmic expression of circadian clock genes (Lelandais et al., 2016, Monnier et al., 2010). Light quality responses have been investigated in other phytoplankton; for example, measurements of cell composition in the diatom *Thalassiosira rotula* and the green alga *Dunaliella tertiolecta*, after acclimation to blue or red light, demonstrated changes in protein, lipid, and carbon metabolism in response to light quality and that these changes were complex and dependant on species. However, changes in growth rate or cell size were not seen (Rivkin, 1989). This study's author cautions against directly comparing studies of light quality responses due to minor differences in wavelengths applied; they also adjusted the intensity of the light treatments according to the relative ability of each species to absorb those wavelengths. Despite this, the study does show a precedent for light quality induced metabolic changes in photosynthetic algae. The analyses in this chapter demonstrate distinct light quality responses in *Ostreococcus* which differ between the two ecotypes. The functional analysis of genes which showed light quality responsive changes in transcription allowed an overview of light quality induced changes in metabolism.

The aim of the work in this chapter was to test whether *Ostreococcus* exhibits responses to light quality, and whether there are differences in response between shallow and deep water associated ecotypes.

This was addressed through the following objectives:

- To test the effects of light quality on growth rate and cell size
- To investigate the effects of light quality on the cell transcriptome and analyse light quality responsive genes in terms of function
- To compare light quality responses of the RCC809 and OTH95 ecotypes

3.2 Methods

3.2.1 Growth rates

To compare the ability of the two *Ostreococcus* ecotypes, OTH95 and RCC809, to grow under different monochromatic light qualities, a growth rate experiment was carried out. *Ostreococcus* ecotypes were grown as described previously (section 2.2) until cell densities reached 4 x 10^6 cells ml^{-1} at which point they were transferred to 4μmol photons m^{-2} s^{-1} of monochromatic red, green, or blue light treatments and growth (change in cell number as approximated by optical density) followed for two weeks thereafter.

3.2.2 Cell size

To determine whether the measured differences in growth rate under monochromatic light were associated with changes with cell size, flow cytometry measurements of forward scatter signal height (FSC-H) were carried out. Full details in section 2.13. FSC-H has been shown to positively correlate with cell size, although this relationship is not necessarily directly proportional, and chlorophyll *a* fluorescence as detected by forward scatter has previously been used as a cell growth and biomass measure in OTH95 (Mullaney et al., 1969, Model, 2018, Chretiennot-Dinet et al., 1995). Fluoresbrite Multifluorescent beads with an average diameter of 0.5μm were used as calibration to allow comparison of relative cell size between light conditions and strains. Measurements of cell size were taken after 72 hours acclimation to the monochromatic light treatments.

All measurements were taken in triplicate. Significance was determined using an ANOVA and subsequent student's t-tests and the level of significance was assessed as $p=<0.05$.

3.2.3 GO annotation

To enable a GO enrichment analysis, existing genome annotations for both ecotypes were supplemented on the basis of sequence homology. A genome wide basic local alignment search (BLAST) was carried out to identify homologues in other organisms. The GO annotations from these homologues were combined with GO terms and descriptions for *Ostreococcus* genes from the InterPro database using the BLAST2GO program, then compared with existing annotations for the OTH95 v2 genome and the RCC809 v2 genome, (Blanc-Mathieu et al., 2014, Palenik et al., 2007, Derelle et al., 2006). Manual BLAST searches were carried out to investigate gene function further where there were discrepancies. Genome-wide, 85% of OTH95 genes and 83% of RCC809 genes were assigned GO terms. Further details on the methods of the genome annotations are given in section 2.8.

3.3 Results

3.3.1 Effects of light quality on growth rates and cell size

It was expected that RCC809 would have a higher growth rate and yield under blue light, the predominant light quality in its open ocean source environment, while OTH95 was not expected to differ greatly in its light responses as the light quality in its shallow source environment is less variable with depth. Both RCC809 and OTH95 showed growth in the three light treatments (Figure 3.1). As expected, the growth of RCC809 in blue light was significantly faster than under red and green light. In contrast, OTH95 showed a similar growth rate in all light treatments, although this was slightly slower under red light (Table 1.1). These data present evidence for light quality responses in *Ostreococcus*. The different growth rates of RCC809 under monochromatic light demonstrates the ability of this ecotype to respond to different light qualities, and that the blue light response is distinctive from red and green responses. The lack of significantly different growth rates in OTH95 also shows that the two ecotypes differ in terms of their light quality responses.

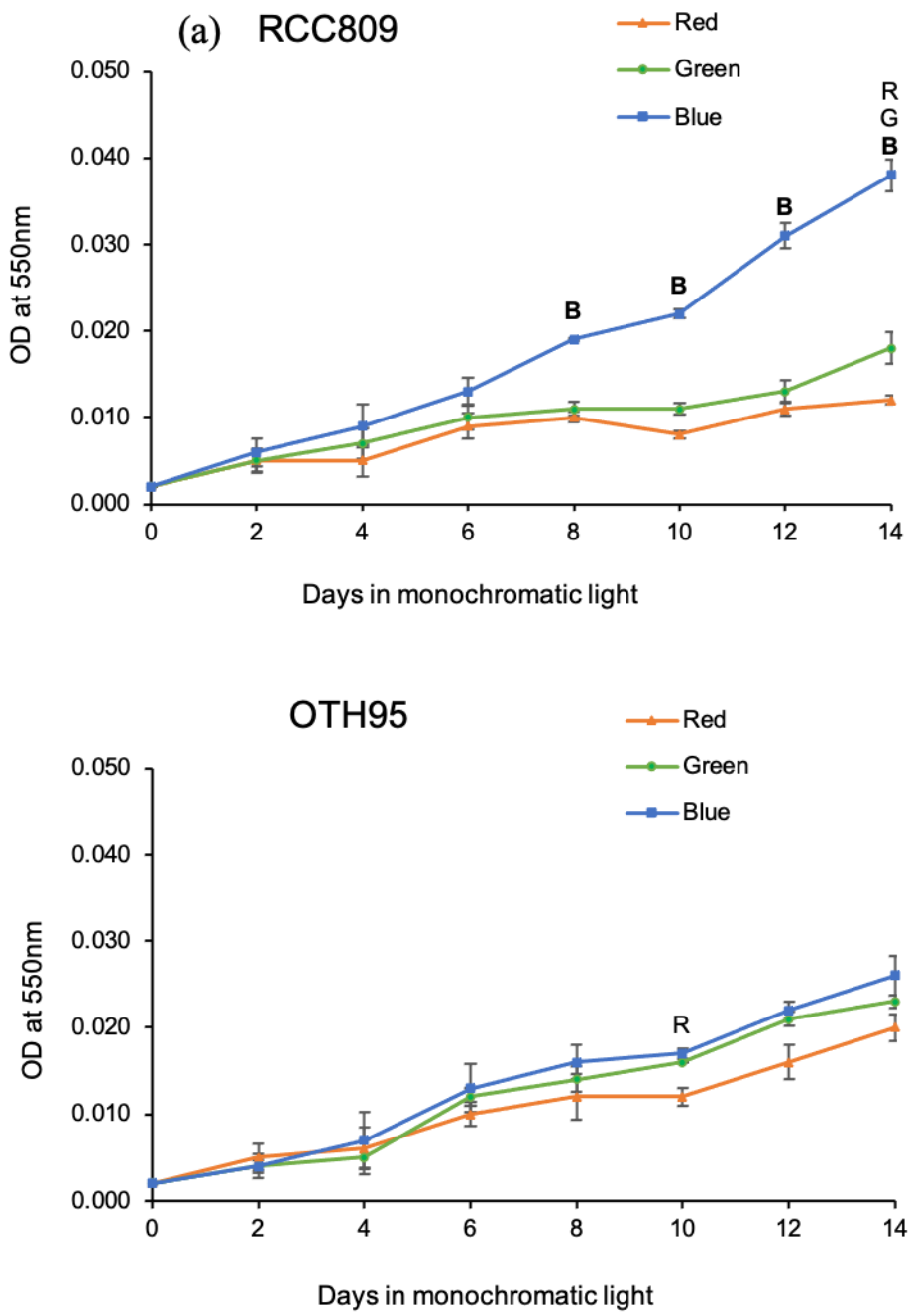

Figure 3.1 Comparative growth under constant monochromatic light (4µmols^{-1}m^{-2}).
(a) RCC809 (b) OTH95 Letters indicate significant ($p < 0.05$) comparisons based on ANOVA and student's t-tests between light responses R red, G green, and B blue. Letters in bold if $p < 0.01$.

Table 3.1 Growth rate and numbers yielded by light quality condition

Growth rate over 14 days $OD^{550nm} d^{-1}$		
	Ecotype	
Light treatment	RCC809	OTH95
Red	73.8 ± 6.30 x 10^{-5} P < 0.04 vs green	126 ± 18.9 x 10^{-5}
Green	116 ± 22.5 x 10^{-5}	147 ± 9.01 x 10^{-5}
Blue	**237** ± 20.8 x 10^{-5} p < 0.0025 vs red p < 0.0025 vs green	169 ± 27.4 x 10^{-5}
Cell numbers ml^{-1} yielded after 14 days approximated by OD		
Red	24.7 ± 1.02 x 10^{6}	39.3 ± 3.05 x 10^{6}
Green	36.4 ± 3.64 x 10^{6}	45.1 ± 1.46 x 10^{6}
Blue	76.2 ± 3.58 x 10^{6}	51.3 ± 4.44 x 10^{6}

Previous studies of the cell size of *Ostreococcus* species showed that RCC809 has a smaller cell volume (approximately 2.45 μm^3) than OTH95 (approximately 2.72 μm^3) (Botebol et al., 2017). Cell size differences between ecotypes in these light quality experiments were consistent with those described in previous studies. No significant changes in cell size as a response to light quality were found in either OTH95 or RCC809 (Figure 3.2).

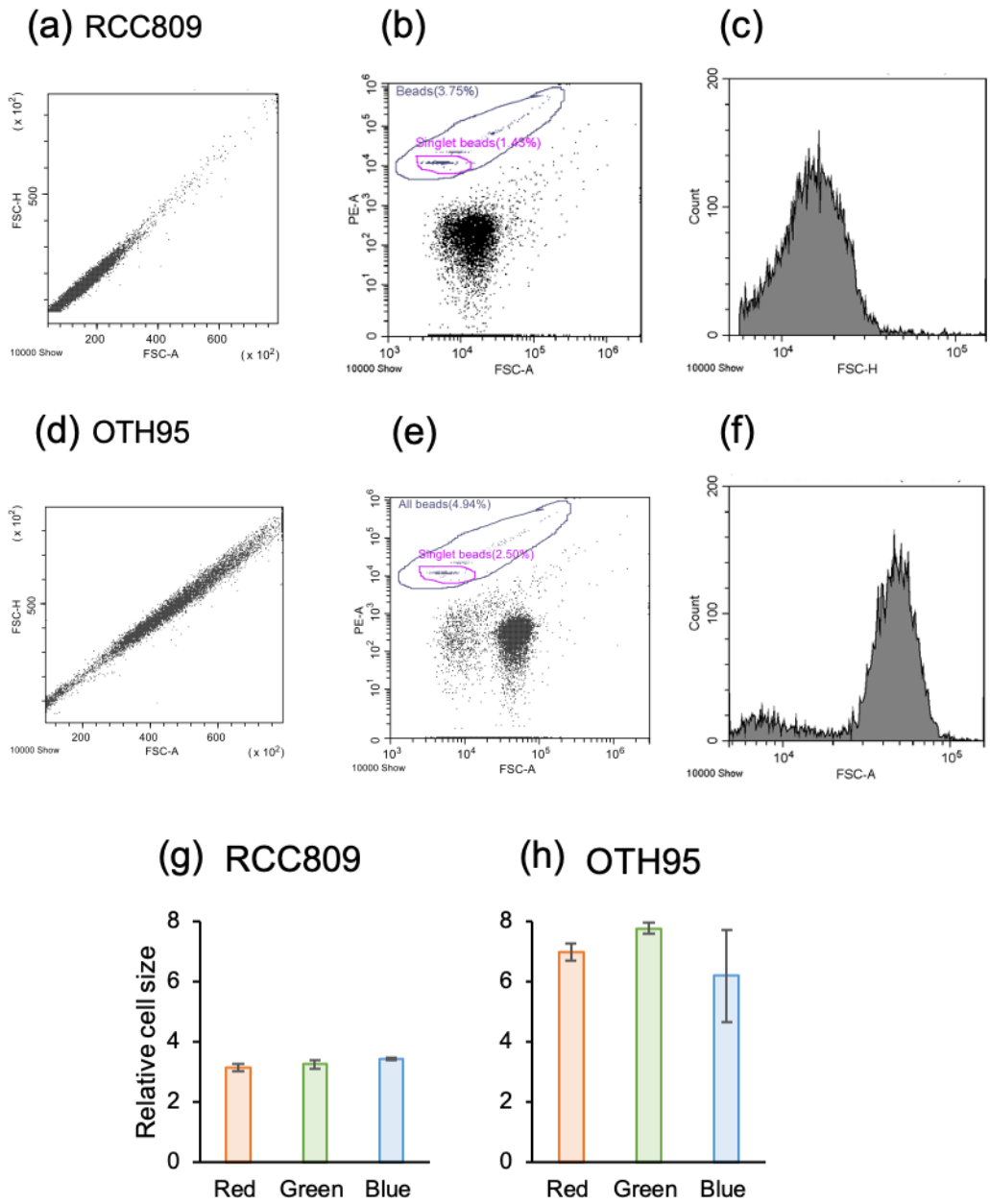

Figure 3.2 Cell size determination using flow cytometry.
These are examples of single replicates representative of samples measured. Forward scatter height (FS-H) vs area (FS-A) is used to discriminate doublets in (a) RCC809 and (d) OTH95. The phycoerythrin area channel (PE-A) which detects yellow fluorescence vs forward scatter area effectively separated the singlet bead populations from the larger values of aggregate calibration beads in (b) RCC809 and (e) OTH95 and singlet beads. Histogram of forward scatter height shows a representative distribution of individual cells in the sample in (c) RCC809 and (f) OTH95. Cell sizes as estimated using mean cell FSC-H / mean singlet bead FSC-H. The light responses seen did not differ significantly within the ecotypes but (g) RCC809 is much smaller than (h) OTH95

The generally smaller cell size of RCC809 is likely due to nutrient limitation experienced in the oligotrophic ocean environment as compared to the nutrient rich Thau Lagoon from which this OTH95 strain was isolated. In previous work OTH95, and to a lesser extent RCC809, were shown to reduce cell volumes in response to iron

limitation (Botebol et al., 2017). Thus, light quality does not appear to affect the cell size of either *Ostreococcus* ecotype analysed here. Instead, at least in the OTH95 ecotype, cell size is likely predominantly controlled by nutrient availability.

3.3.2 Transcriptomic analyses of the light quality response

To assess whether *Ostreococcus* responds to changes in light quality through changes in gene expression, and also to compare the potentially different responses of RCC809 and OTH95 ecotypes, responses to monochromatic red, green, and blue light exposure were analysed using RNA sequencing (RNASeq). An overview of the experimental conditions under which these data were obtained is shown in Figure 3.3 and full details can be found in sections 2.5-2.6. Briefly, cells were grown under 12-hour light/dark cycles of white light until they reached mid to late log phase. At this point they were transferred to constant red, green, or blue monochromatic light as applied during the growth and cell size experiments. After 72 hours exposure to monochromatic light the cultures were harvested, RNA was extracted and used for RNASeq analysis. This work was completed by Sian Davies. Downstream analyses were carried out by myself. Two samples, one from each ecotype, showed less than 80% alignment to the reference genomes, suggesting contamination. Another in RCC809 gave a low number of reads, approximately 120,000 compared to around 10 million reads for the other samples. These samples were discarded from further analyses.

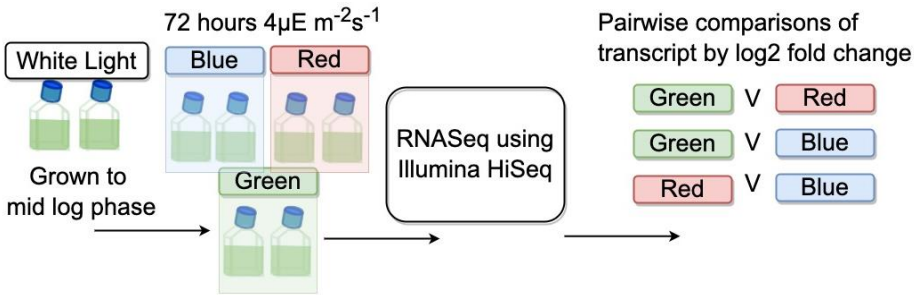

Figure 3.3 RNASeq differential expression analysis from culture growth conditions to data gathered

To generate pairwise comparisons of gene expression for the RNASeq data, downstream processing was carried out as described in section 2.7 using the Fastqc, Trimmomatic, TopHat, and CuffDiff tools in the Tuxedo suite. These pairwise comparisons were in the form of expression levels sorted by log2 fold change between each pair of light conditions. The pairs were: red versus blue light, green versus blue light, and red versus green light.

3.3.3 Transcriptional responses of RCC809

In the deep ocean associated RCC809 ecotype, 1997 genes were found to be significantly differentially expressed between red, green, and blue light conditions, based on q values less than 0.05 and a log2 fold change greater than 0.5. These genes and their expression values are described in Appendix 1. RCC809 showed a specific transcriptional response to each of the light conditions, as illustrated by the principal component analysis (PCA) of the significantly differentially expressed genes in each sample and replicate (Figure 3.4a), which clusters the replicate samples by the major components of variation, demonstrating the response to blue light as the most distinct and the responses to red and green light as more similar. The specificity of these responses is further illustrated in terms of numbers of differentially expressed genes in pairwise comparisons between light conditions (Figure 3.4b). The largest numbers of differentially expressed genes were seen in comparisons of blue light to the other conditions. Here the numbers are genes which were more highly expressed in: blue versus red (1368), and blue versus green (1553). Comparison between red and green light conditions yielded fewer differentially expressed genes (350) (Appendix 2). There is some overlap as some of the light responsive genes appear in more than one pairwise comparison which explains why the sum of these numbers of genes is larger than the total.

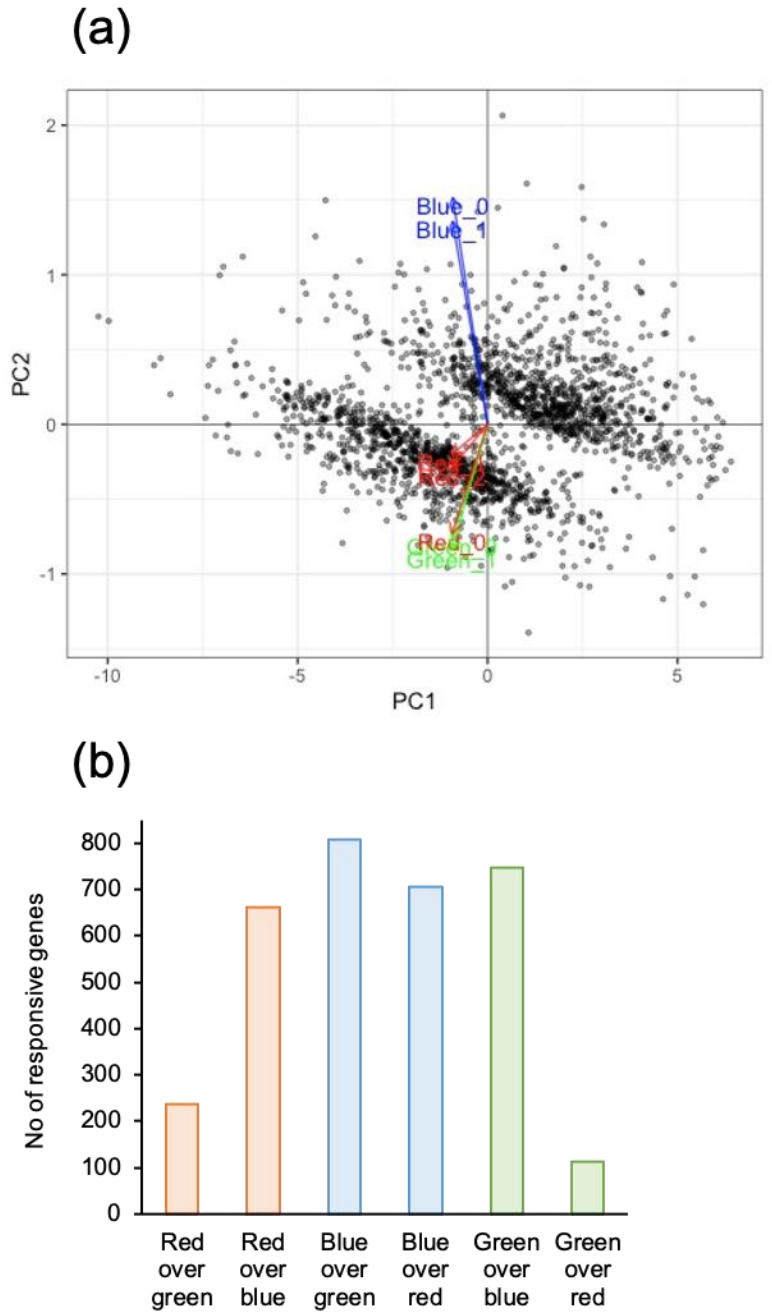

Figure 3.4 RCC809 visualisation of differentially expressed genes

. (a) Principal component analysis of expression data for each replicate, data for significantly differentially expressed genes shown only. (b) Total numbers of significantly differentially expressed genes identified as induced when compared pairwise between light quality treatments.

To identify responses specific to each light quality, genes which were significantly induced or repressed in that condition relative to both other light qualities were identified. For example, the expression level of genes identified as induced by blue light (‘up in blue’) showed positive fold-change values in both the ‘blue versus red’ and the ‘blue versus green’ lists of differentially expressed genes. Figure 3.5a-f shows how this was achieved for RCC809 using Venn diagrams in which the responses to specific wavelengths of light were identified as those genes present in the Venn intersections. Figure 3.5g shows the resultant numbers of responsive genes in RCC809.

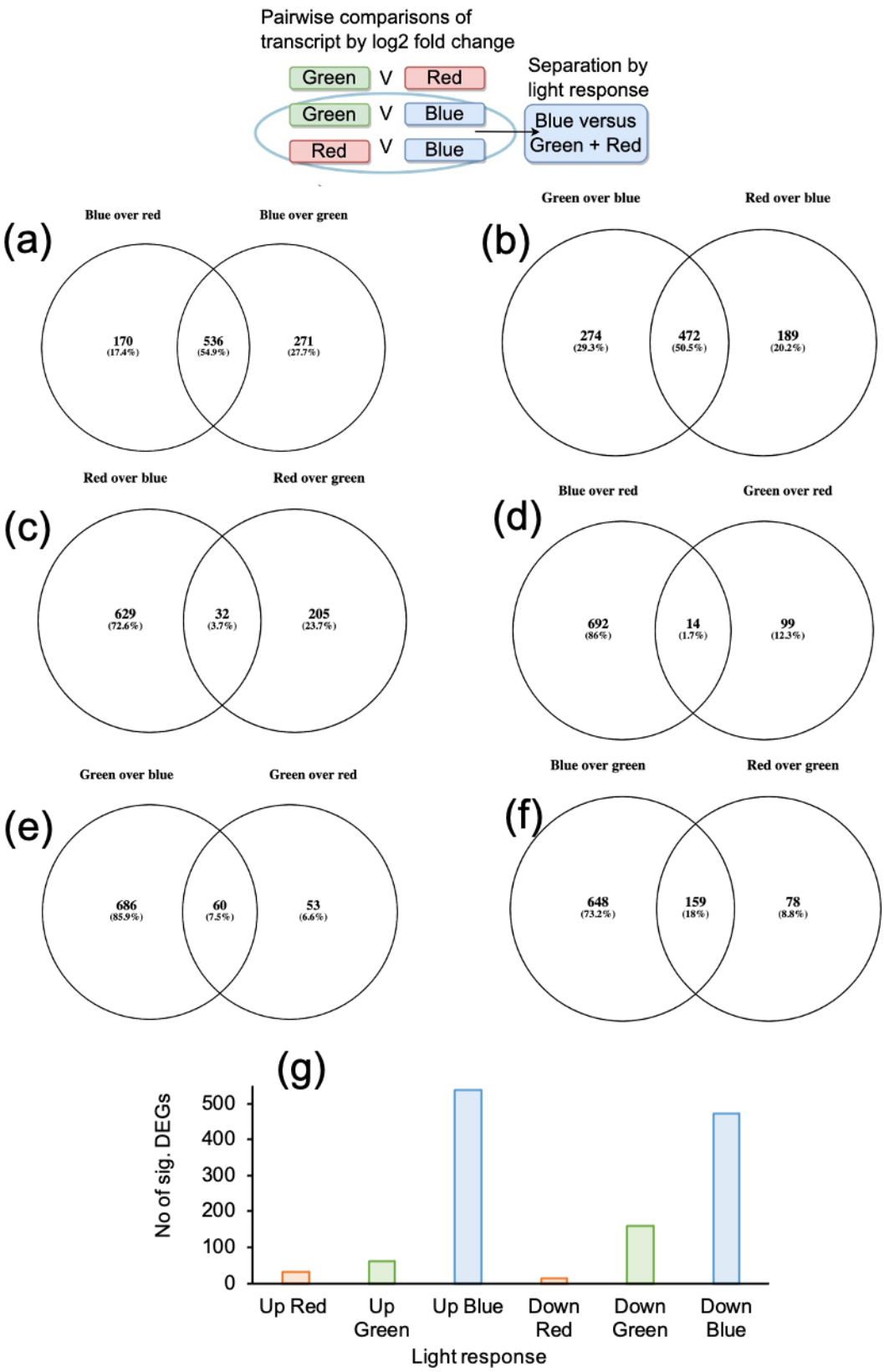

Figure 3.5 Separation of differentially expressed gene sets in RCC809 by light condition.
Pairwise comparisons were separated using Venn diagrams. The Venn diagrams are the derivations of the specific RCC809 responses to: (a) Up in blue light. (b) Down in blue light. (c) Up in red light. (d) Down in red light. (e) Up in green light. (f) Down in green light. Venn diagrams were generated using the Venny tool (Oliveras, 2015). (g) Total numbers of significantly differentially expressed genes (DEGs) in RCC809 after separation by light response.

For RCC809, the largest numbers of light responsive genes identified were those specific to the blue light response (536 induced and 472 repressed by blue light, relative to red and green). The fewest light responsive genes were found in response to red light (32 induced, and 14 repressed by red light relative to blue and green). The green light response was intermediate in terms of the number of light responsive genes (60 induced, and 159 repressed under green light relative to blue and red) Appendix 2. The specificity of these responses is illustrated by the heatmap in Figure 3.6. This indicates the size of the fold change for each significantly differentially expressed gene and each sample, compared to a mean of all conditions and replicates. The heatmap further illustrates that gene expression is most dissimilar between blue and green light conditions, and that the red and green responses are the most similar.

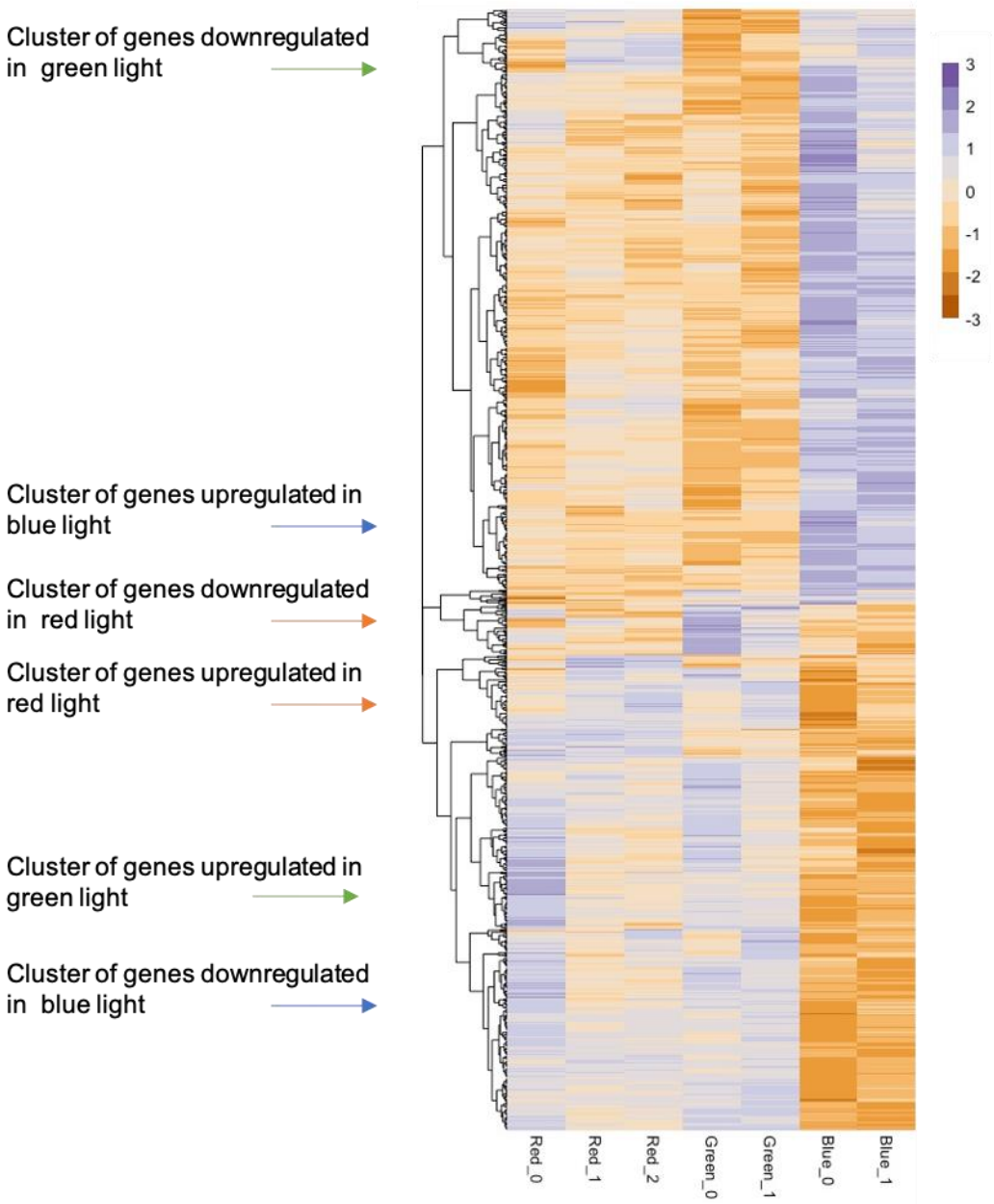

Figure 3.6 Heatmap of significantly differentially expressed light quality responsive genes in RCC809. Heatmap generated by log FPKM compared between light condition and replicates. Rows are clustered by Jensen-Shannon distance. Blue areas indicate a positive fold change resulting from higher expression compared to the negative fold change indicated by the yellow areas.

3.3.4 Functional interpretation of the RCC809 transcriptomic light response

To gain an insight into physiological responses that may be triggered by different light qualities, the differentially expressed genes identified by the RNASeq analysis were then investigated according to their functional annotations. To determine whether specific functional categories were overrepresented within a set of light-responsive genes compared to the genome as a whole, a gene ontology (GO) enrichment analysis

was carried out. This allowed an objective overview of the likely functional consequences to the cells of the light quality specific changes in gene expression.

The most significantly overrepresented GO terms within the umbrella category of 'biological processes' in the RCC809 light quality-responsive genes are summarised in Tables 3.2 to 3.4, and the full tables are reproduced in Appendix 3. There was some overlap across categories as many genes are annotated with multiple GO terms.

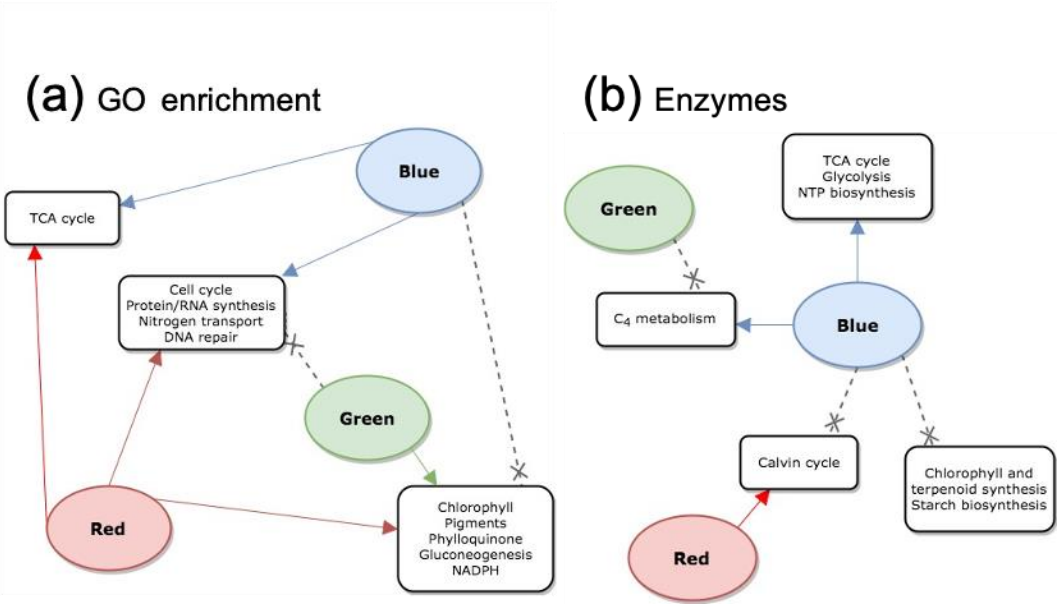

Figure 3.7 Summary of main functions in light quality responsive transcriptional changes in RCC809 identified by (a) GO enrichment. (b) mapping differentially expressed enzymes homologous to OTH95 metabolic pathways on KEGG (Kanehisa et al, 2000).

These analyses indicated biological processes affected by light quality as summarised in Figure 3.7a. The description of the functional changes resulting from gene expression was limited by the depth of GO annotation available for the genes. To elucidate some of these functions in RCC809, the results were compared to those found when marking all the differentially expressed genes which code for enzymes onto KEGG metabolic pathway maps (Kanehisa and Goto, 2000). Pathway mapping using KEGG was carried out by searching for the homologues of the RCC809 enzymes in OTH95 as RCC809 is not yet listed on KEGG. These homologues were determined using a reciprocal genome-wide BLAST between the ecotypes and assessed on the basis of homology with a minimum of 50% identity between genes. A summary of the functional changes suggested by these differentially expressed enzymes in RCC809 shows the same light responses as those in the GO enrichment with some added clarification (Figure 3.7b). Selected KEGG pathway maps showing key light quality responses have been reproduced here; the enzymes within these pathways which have

been identified in *Ostreococcus* are shaded in greyscale. Enzymes which have been noted as differentially expressed have been highlighted and annotations for these genes are also listed (Figures 3.11-3.20). These pathway maps will be discussed individually in the following pages.

This combined approach to the functional analysis was particularly useful for investigating the changes in glycolysis/gluconeogenesis in blue light, indicating that glycolysis increased in blue light while starch biosynthesis decreased in blue light compared to red and green light. The expression of genes related to DNA replication, chromosome organisation, and nitrogen transport decreased under green light and increased under blue light. Genes related to the TCA cycle also increased under blue light. Other key genes associated with macromolecular synthesis were downregulated after blue light exposure compared to red and green, including those related to synthesis of chlorophyll and some accessory pigments. Genes related to lipid synthesis and phylloquinone biosynthesis also decreased under blue light.

Table 3.2 Selected significantly overrepresented functional categories in RCC809 green light responsive genes

Functional Categories: Biological Process	Corrected p-value	Number of genes in this category in set	Number of genes in this category in genome	Total genes in test set	Total Bio Process genes in Genome
Downregulated in green light					
DNA replication	5.75E-10	18	89	101	4247
DNA duplex unwinding	1.08E-02	5	24	101	4247
Nitrate transport	1.84E-02	2	2	101	4247

Table 3.3 Selected significantly overrepresented functional categories in RCC809 red light responsive genes

Functional Categories: Biological Process	Corrected p-value	Number of genes in this category in set	Number of genes in this category in genome	Total genes in test set	Total Bio Process genes in Genome
Upregulated in red light					
NADPH regeneration	2.56E-03	4	29	25	4247
Nicotinamide nucleotide metabolic process	4.02E-03	4	41	25	4247
Glycolysis	1.29E-02	3	33	25	4247
Gluconeogenesis	1.45E-02	3	37	25	4247

Table 3.4 Selected significantly overrepresented functional categories in RCC809 blue light responsive genes

Functional Categories: Biological Process	Corrected p-value	Number of genes in this category in set	Number of genes in this category in genome	Total genes in test set	Total Bio Process genes in Genome
Upregulated in blue light					
Cellular response to stress	7.30E-03	29	204	262	4247
DNA-dependent DNA replication	7.81E-03	11	42	262	4247
Chromosome segregation	1.95E-02	7	21	262	4247
Tricarboxylic acid cycle	2.20E-02	9	37	262	4247
Downregulated in blue light					
Pigment biosynthetic process	1.56E-07	18	47	273	4247
Chlorophyll biosynthetic process	9.29E-07	11	19	273	4247
Glycolysis	3.89E-03	9	33	273	4247
Gluconeogenesis	7.91E-03	9	37	273	4247
Carotenoid (tetraterpenoid) biosynthetic process	1.04E-02	5	12	273	4247
Nicotinamide nucleotide metabolic process	1.49E-02	9	41	273	4247
Lipid biosynthetic process	1.58E-02	18	126	273	4247
Photosynthesis	2.45E-02	15	101	273	4247
Glucan biosynthetic process	4.67E-02	4	11	273	4247
Reductive pentose-phosphate cycle	4.67E-02	2	2	273	4247
Endosome organization	4.67E-02	2	2	273	4247
Phylloquinone biosynthetic process	4.67E-02	2	2	273	4247

3.3.5 Cell cycle genes increase in blue light

Functional categories related to the cell cycle which were induced under blue light and repressed under red and green light, including DNA replication, DNA repair and chromosome segregation (Table 3.5). Cell cycle genes including those related to DNA replication were also repressed under green light compared to red and blue light. This suggested that blue light may induce cell division, green light may inhibit it, and red light may have an intermediate effect.

Of particular note is the cyclin-dependent kinase B gene (Od14g01080) which is key in the regulation of mitotic cell division. Expression of this gene increased in blue light and decreased under green light, with intermediate levels seen under red light (Figure 3.8a). Transcription of the cyclin-dependant kinase B gene in OTH95 (OtCDKB) is induced during cell division in OTH95, peaking during the DNA synthesis S phase (Farinas et al., 2006, Corellou et al., 2005). The increased expression of this gene in blue light is consistent with the faster growth rate observed in blue light, relative to red and green light. The OTH95 cyclin-dependent kinase A gene (OtCDKA) has also been described and it was shown that expression of this gene did not vary across cell cycle stages (Farinas et al., 2006, Corellou et al., 2005). As could then be expected, its proposed homologue in RCC809 (Od04g05410) showed no expression changes in response to light quality.

Two Rad51 homologues (Od08g01730 Figure 3.8c, and Od06g06460), encoding recombinases involved in double strand repair during DNA replication, also increased expression under blue light. In yeast, homologous recombination is suppressed during the growth phase G1 and Rad51 is activated during S phase, through phosphorylation by a cyclin-dependant kinase (Lim et al., 2020). The upregulation of Rad51 under blue light is again consistent with the observation that cell division is induced in blue light compared to the red and green light conditions.

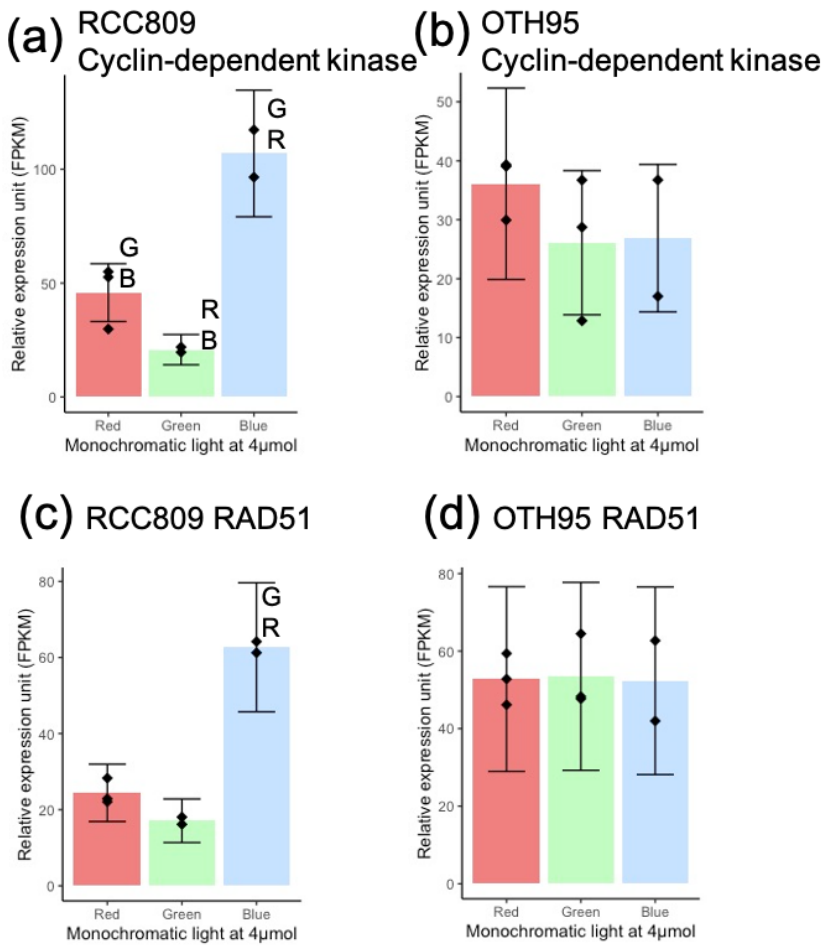

Figure 3.8 Cell cycle gene expression.
Cyclin-dependent kinase: (a) RCC809 Od14g01080 showing significant rise in blue light. Log2 fold change between blue and green is 2.36. (b) OTH95 homologue ostta15g00670 showing no significant light response. RAD51 DNA recombination: (c) RCC809 Od08g01730 showing significant rise in blue light. Log2 fold change between blue and green is 1.87 (d) OTH95 homologue ostta08g01800 showing no significant light response. Letters indicate significant (p=<0.05) differences after false discovery rate correction with either red (R) red, green (G), and blue (B) conditions

Table 3.5 Light quality responsive genes related to the cell cycle

Light response	Genes	Number of genes referencing cell cycle related terms
Down blue	6	1 DNA replication 4 Cell cycle 2 Cell division
Up blue	37	19 DNA replication 16 Cell cycle 5 Chromosome 7 Cell division 5 Repair
Down green	19	18 DNA replication 6 Cell cycle 1 Chromosome
Up red	2	1 DNA replication 1 Cell cycle

Table 3.5 summarises the individual annotations of light responsive genes related to the cell cycle within the parent categories highlighted in the enrichment analysis. As this table shows, some cell cycle related genes also decreased in expression under blue light. Further investigation is required to determine the effects of these changes on cell division.

Table 3.6 Annotations of key light responsive cell cycle related genes

Light response	**Gene**	**Description**
Down in blue	Od01g01520	Single-stranded DNA-binding protein, DNA replication
Down in blue	Od05g01780	DNA replication licensing factor, protein ubiquitination
Down in blue	Od07g01730	Lysine-specific demethylase 8, protein binding
Down in blue	Od07g02050	Predicted, GTPase activity, chloroplast fission, cell division
Down in blue	Od07g04740	Cell division FtsY homolog, chloroplastic, GTP binding
Down in blue	Od10g01360	Resistance-nodulation-cell division superfamily
Down in green	Od01g04460	DNA replication licensing factor Mcm6, helicase

Down in green	Od02g01320	DNA replication licensing factor Mcm7 helicase
Down in green	Od02g01330	DNA replication licensing factor Mcm7 helicase
Down in green	Od02g02310	DNA replication licensing factor Mcm3 helicase
Down in green	Od05g00150	Replication factor C subunit 3 DNA replication
Down in green	Od10g01480	ATP-dependent helicase/nuclease DNA2 isoform X1, 5'-flap DNA replication, Okazaki fragment processing
Down in green	Od17g03020	P4 family, helicase activity, ATP binding, DNA replication
Up in blue	Od01g02860	Histone H3, nucleosomal DNA binding, meiotic chromosome separation
Up in blue	Od02g03320	Predicted, peptide dephosphorylation, positive regulation of cell cycle, G2/M phase transition
Up in blue	Od02g03690	Serine/threonine-protein kinase 24, regulation of cell cycle
Up in blue	Od02g03890	Condensin complex component, non-smc subunit, mitotic chromosome condensation, cell division
Up in blue	Od03g01380	Predicted, replication, recombination, 3'-5' helicase activity
Up in blue	Od04g04750	Group J -like protein, DNA helicase, replication fork
Up in blue	Od06g00290	Predicted protein, binding, cell division
Up in blue	Od06g04320	Predicted protein, DNA binding, replication
Up in blue	Od08g00520	DNA replication, cell death, regulation of cell cycle
Up in blue	Od08g01730	RAD51 homolog, regulation of transcription, double-strand break repair, recombination-dependent replication fork
Up in blue	Od09g01440	Predicted protein, mitotic cell cycle, centromeric region
Up in blue	Od09g03260	Predicted protein, regulation of cell cycle
Up in blue	Od12g01680	Probable DNA helicase MCM8, DNA replication initiation
Up in blue	Od12g02990	Ribonuclease HII, RNA-DNA hybrid activity, mismatch repair, removal of RNA primer
Up in blue	Od20g01820	Predicted, heterochromatin assembly involved in chromatin silencing, mitotic DNA replication
Up in blue Down green	Od04g00830	Predicted, DNA replication initiation
Up in blue Down green	Od04g04360	Predicted, DNA replication initiation, cell division
Up in blue Down green	Od06g02850	Leading strand elongation, mismatch repair, DNA pol
Up in blue Down green	Od07g02890	Predicted, anaphase-promoting complex, regulation of mitotic metaphase/anaphase transition, cell division
Up in blue Down green	Od08g00650	DNA pol catalytic subunit, synthesis of RNA primer; DNA replication initiation, lagging strand elongation, transcription

Up in blue Down green	Od11g01890	Probable DNA primase large subunit, DNA replication, transcription
Up in blue Down green	Od11g02480	DNA polymerase alpha subunit B, DNA replication
Up in blue Down green	Od12g02680	DNA topoisomerase 1 beta, DNA replication, chromatin remodelling, chromosome segregation, replication fork
Up in blue Down green	Od13g01180	DNA primase small subunit isoform X2, DNA replication, transcription, DNA-templated
Up in blue Down green	Od14g01080	Predicted, G1/S mitotic cell cycle, cyclin-dependent kinase activity, regulation of G2/M mitotic cell cycle
Up in blue Down green	Od17g01560	Replication protein A 70 kDa DNA-binding subunit B, DNA repair; DNA recombination
Up in blue Down green	Od20g01140	Predicted, DNA helicase, DNA replication initiation, MCM complex, cell division
Up in red	Od04g04480	Predicted, histone methyltransferase (H3-K79 specific), regulation of cell cycle
Up in red	Od10g02070	DNA replication, helicase, nucleoside-triphosphatase

Table 3.6 lists key individual genes which were included in the light responsive cell cycle categories and also gives a summary of the available gene annotations. The level of depth of annotation for each gene's function is much more specific in some cases than others. It was necessary to take this into account when drawing conclusions on the likely functional changes in response to light. For example, gene Od07g04740 was listed as a cell division gene which was downregulated in blue light but is annotated as a 'chloroplastic FtsY precursor' and, according to UniProt, this protein is more likely to be involved in thylakoid binding in the chloroplast than in cell division (The UniProt Consortium, 2020). Table 3.6 also shows that the genes in the cell cycle categories which were downregulated in green light are of a similar nature, being mostly DNA replication licensing factor mini-chromosome maintenance (MCM) helicases. These proteins are required to license chromatin for replication before the S phase of DNA synthesis can begin, and they are activated by cyclin-dependant kinases (Tuteja et al., 2011). Of the 9 genes annotated as MCM in RCC809, 4 were downregulated in green light: MCM3, MCM6, and two consecutive MCM7 genes. MCM7 in particular has been shown to be essential for replication in *Arabidopsis* (Springer et al., 2000). One further gene annotated as a probable MCM8 was upregulated in blue light. The MCM complex of MCM2-7 controls the initiation of 'once per cell cycle' DNA replication (Moyer et al., 2006, Evrin et al., 2009, Remus et al., 2009). The functions of all MCM proteins have not been fully characterised in

plants (Tuteja et al., 2011). MCM gene expression during the cell cycle in OTH95 has been investigated and it was found that MCM2-7 all showed maximal expression levels during the S phase (Moulager et al., 2007). The light quality responses of MCMs 3, 6,7, and 8 seen here strengthen the suggestion of decreased cell cycle activity as a response to green light when compared to both red and blue conditions. The cell cycle has been found to be regulated in *Ostreococcus* according to the photoperiod length; a minimum of 6 hours of light was required before division initiated in OTH95 (Monnier et al., 2010, Farinas et al., 2006). This shows that light parameters can drive changes in the cell cycle. It can be concluded that blue light induces increased cell division in RCC809, an intermediate response is possible in red light, and cell division is reduced on exposure to green light. When comparing these changes in expression to the growth rate data, the increased level of cell division correlates with the observed faster growth in cell numbers in blue light (Figure 3.1a).

3.3.6 Photosystem related gene transcription changes in response to blue light

Both of the RCC809 genes annotated as enzymes involved in the synthesis of phylloquinone (vitamin K1) precursors were downregulated under blue light. These are Od07g04840 and Od20g02670. Phylloquinone is a photopigment which acts as a cofactor in Photosystem I (PSI). Changes in photosystem II (PSII) were also indicated; 8 genes predicted to encode PSII assembly proteins were found to be light quality responsive and of these the expression of 6 increased in blue light while the expression of 1 decreased in blue (Table 3.7). The relative importance of these 8 genes in PSII assembly is unknown although overall this suggests an increase in PSII content in blue light.

Table 3.7 RCC809 PSII-related light quality responsive genes

Light response	Gene	Description
Up blue	Od04g05310	Predicted protein, photosystem II assembly
Up blue	Od07g00100	Photosystem II 22 kDa protein, chloroplastic
Up blue	Od02g04230	Putative photosystem II 22 kDa protein, high light induced
Up blue versus red	Od06g01970	Photosystem II S4 domain protein
Up blue versus red	Od02g00750	PsbP domain 7, photosystem II oxygen evolving complex
Up blue versus green	Od11g00160	Photosystem II reaction centre PSB28, 13kD Protein
Down blue	Od14g01690	Predicted, Mog1/PsbP, photosystem II oxygen evolving complex

3.3.7 Chlorophyll and pigment synthesis decrease in blue light

It is clear that numerous pathways involved in chlorophyll and pigment synthesis are responsive to light quality in RCC809, these responses are most apparent when comparing blue light to red and green. The transcriptional changes annotated on the 'porphyrin and chlorophyll metabolism' KEGG map indicate that synthesis of chlorophyll and porphyrin precursors are reduced under blue light in favour of catabolism to allow iron redistribution as ferritin (Figure 3.9). Ferritin expression peaks at night in *Ostreococcus* and the role of ferritin in the circadian control of iron homeostasis has been described as regulatory rather than as longer term iron storage as seen in similar species (Botebol et al., 2015, Lelandais et al., 2016).

Seven genes in the terpenoid backbone biosynthesis pathway reduced expression levels under blue light, and one reduced expression in green (Figure 3.10). These genes encode enzymes involved in the conversion of glyceraldehyde to various precursors of pigment synthesis. These expression changes mapped onto the terpenoid and chlorophyll synthesis pathways together show that synthesis of photopigments in RCC809 is generally reduced in blue light as these pathways are upstream of the more specific pigment synthesis pathways.

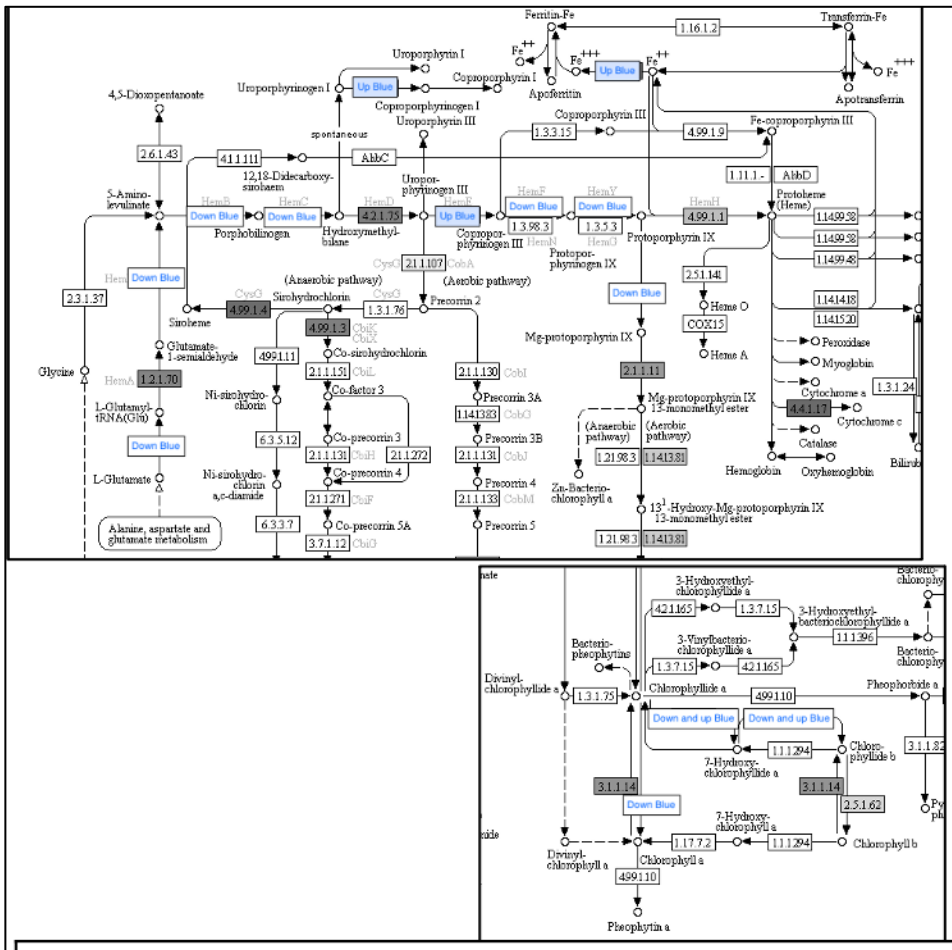

OTH95	RCC809	Response	Function
ostta08g01100	Od08g01040	Down blue	Chlorophyll synthase
ostta10g02720	Od09g01000	Down blue	Chlorophyllide a oxygenase
ostta06g03370	Od06g03440	Down blue	Protoporphyrinogen oxidase
ostta01g02390	Od01g04650	Down blue	Porphobilinogen synthase
ostta12g02460	Od12g03120	Down blue	Uroporphyrinogen decarboxylase
ostta17g00130	Od16g02600	Down blue	Uroporphyrinogen decarboxylase
ostta03g03160	Od06g04640	Down blue	Coproporphyrinogen oxidase
ostta13g01560	Od13g01670	Down blue	Tetrahydrofolate synthase
ostta01g05690	Od01g01020	Down blue	Magnesium chelatase
ostta05g04960	Od05g05120	Down blue	Magnesium chelatase
ostta04g02090	Od04g03220	Down blue	Magnesium chelatase
ostta02g02390	Od02g02530	Down blue	Magnesium chelatase
ostta01g04150	Od06g03340	Down blue	Glutamate--tRNA ligase
ostta02g03400	Od02g03670	Up blue	Ferroxidase, ferritin-like superfamily
ostta12g02470	Od12g03130	Up blue	Uroporphyrinogen decarboxylase
ostta15g00330	Od14g00700	Up blue	Chlorophyllide a oxygenase
ostta05g01070	Od05g01200	Down green	Uroporphyrinogen decarboxylase

Figure 3.9 Porphyrin and chlorophyll metabolism pathway
adapted from KEGG to show the transcriptional changes in response to light (Kanehisa and Goto, 2000).

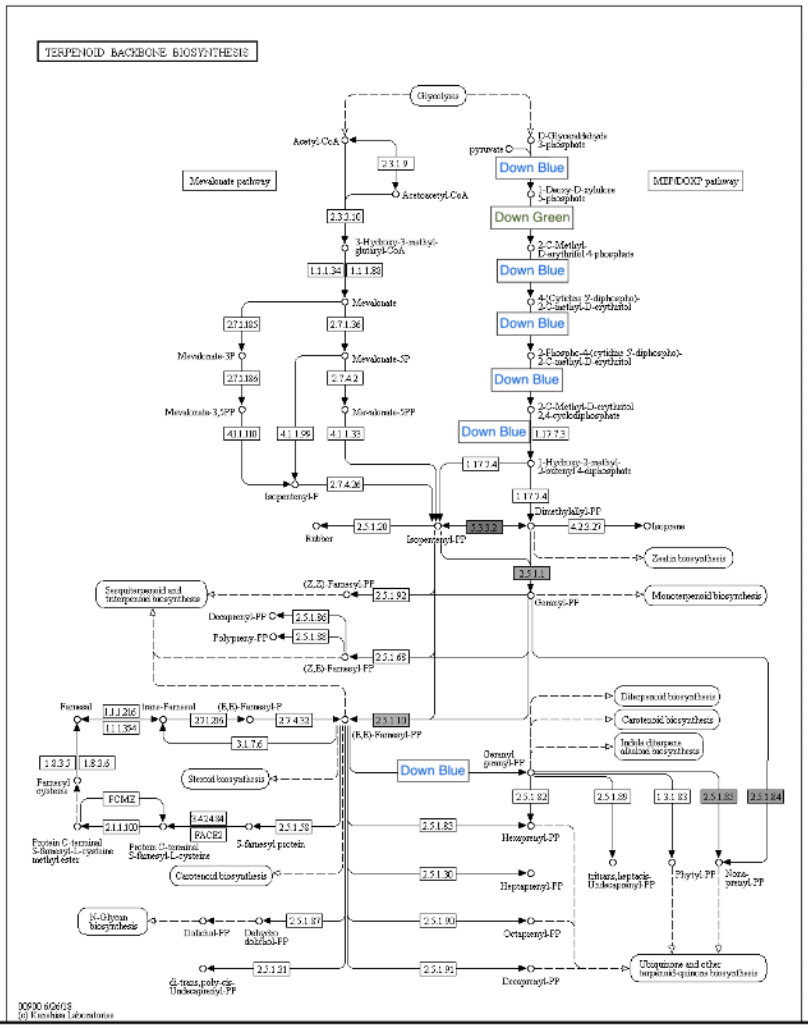

OTH95 homologue	RCC809 gene	Response	Function
ostta02g01730	Od02g01640	Down blue	1-deoxy-D-xylulose-5-phosphate synthase
ostta07g03570	Od07g03920	Down blue	2-C-methyl-D-erythritol 4-phosphate cytidylyltransferase
ostta08g01180	Od08g01130	Down blue	Ferredoxin
ostta09g00960	Od09g05360	Down blue	Ferredoxin
ostta11g00050	Od11g00960	Down blue	2-C-methyl-D-erythritol 2,4-cyclodiphosphate synthase
ostta12g01280	Od12g01950	Down blue	Geranylgeranyl diphosphate synthase
ostta16g01910	Od15g01050	Down blue	4-(cytidine 5'-diphospho)-2-C-methyl-D-erythritol kinase
ostta04g03270	Od04g02130	Down green	1-deoxy-D-xylulose-5-phosphate reductoisomerase

Figure 3.10 Terpenoid backbone biosynthesis pathway adapted from KEGG
to show the transcriptional changes in response to light (Kanehisa and Goto, 2000).

More specific pigment changes in response to light quality are indicated by the ‘carotenoid biosynthesis’ pathway KEGG map. This map also shows the position of the cytochrome P450 Od09g03950 homologue in OTH95 (ostta09g02540) in which it is annotated as the cytochrome CYP97C1 (Figure 3.11). CYP97C1 is in the CYP97 carotene hydroxylase family which is responsible for the conversion of carotenes to lutein (Cui et al., 2013). The expression of this enzyme was lower in response to blue light than to red, and it is interesting to note that the green light response is an intermediate (Figure 3.12e-f). This suggests that lutein content would decrease in blue light relative to carotenes.

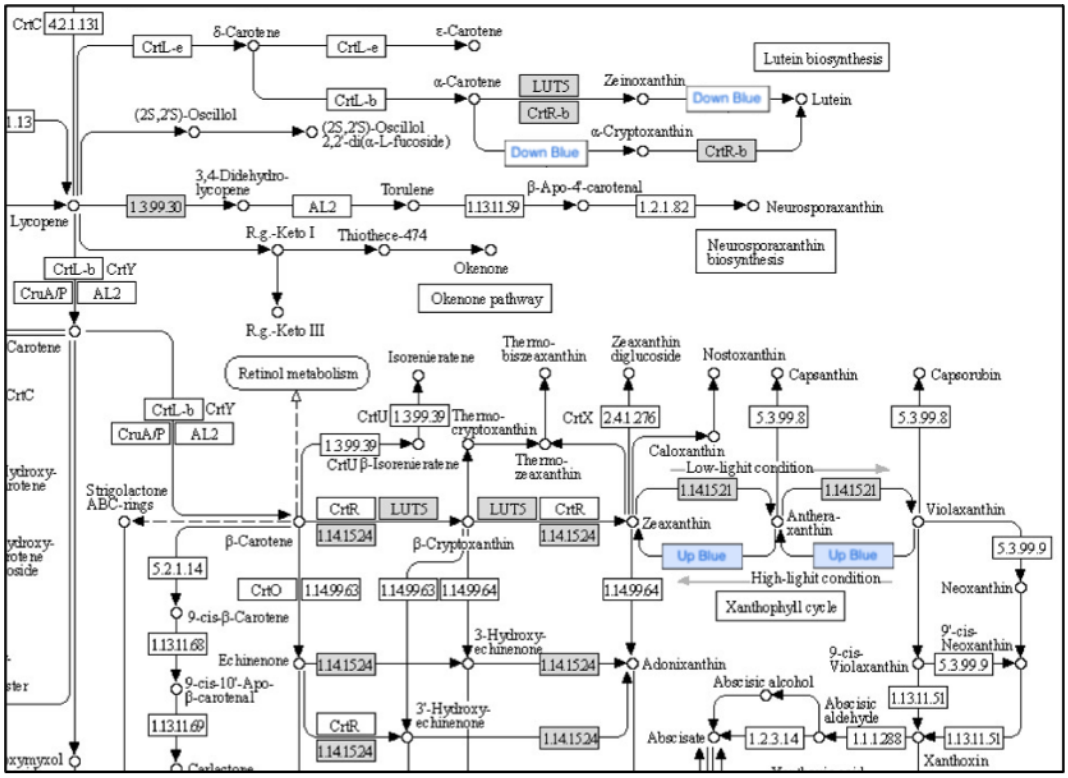

OTH95 homologue	RCC809 gene	Response	Function
ostta16g00660	Od11g00170	Up blue	Violaxanthin de-epoxidase
ostta09g02540	Od09g03950	Down blue	Cytochrome P450, LUT1, CYP97C1

Figure 3.11 Carotenoid biosynthesis pathway adapted from KEGG
to show the transcriptional changes in response to light (Kanehisa and Goto, 2000).

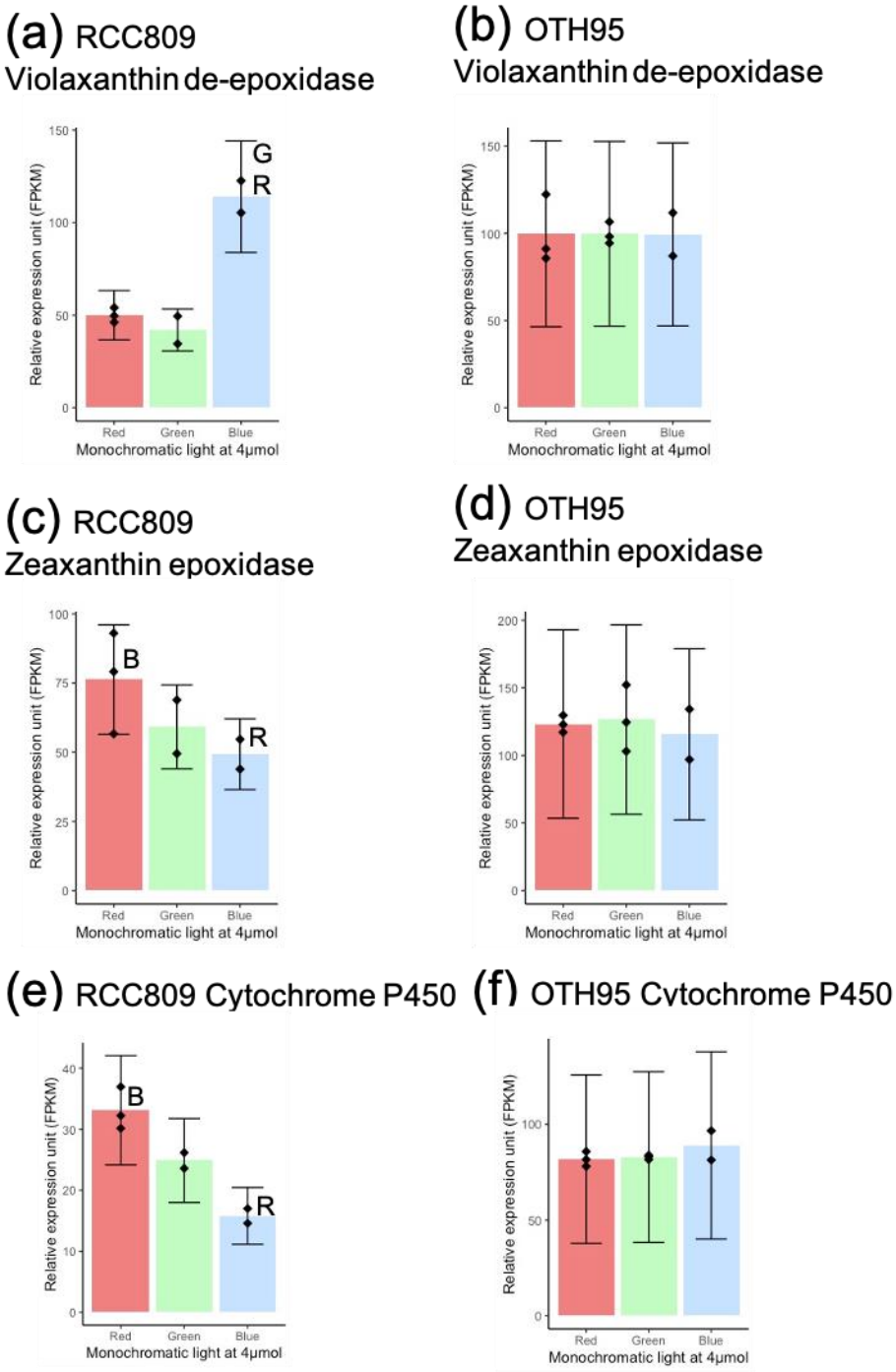

Figure 3.12 Carotenoid biosynthesis gene expression.
Violaxanthin de-epoxidase in (a) RCC809 Od11g00170 showing significant rise in blue light (b) OTH95 ostta16g00660 showing no light quality response. Zeaxanthin epoxidase in (c) RCC809 Od02g02570 showing rise in red light versus blue light (d) OTH95 ostta02g02500 showing no light quality response. Cytochrome P450, LUT1, CYP97C1, catalysing conversion of carotene to lutein (e) RCC809 Od09g03950 showing rise in red light versus blue light (f) OTH95 ostta09g02540 showing no response to light quality. Letters indicate significant (p=<0.05) differences after false discovery rate correction with either red (R) red, green (G), and blue (B) conditions.

A violaxanthin de-epoxidase gene (Od11g00170) increased under blue light compared to both red and green light (Figure 3.12a-b). This enzyme catalyses the conversion of violaxanthin to zeaxanthin in the xanthophyll cycle. Violaxanthin is converted to zeaxanthin in high light stressed plants to induce photoprotection using non-photochemical quenching (NPQ). A gene annotated as coding for the zeaxanthin epoxidase enzyme was also found to increase in red light when compared to blue. Zeaxanthin epoxidase catalyses the reverse reaction; the conversion of zeaxanthin to violaxanthin (Figure 3.12c-d). These transcriptional changes suggest that the relative content of xanthophylls is affected by light quality in RCC809; an increase in zeaxanthin in response to blue light, an increase of violaxanthin in red light, and an intermediate xanthophyll balance in green light.

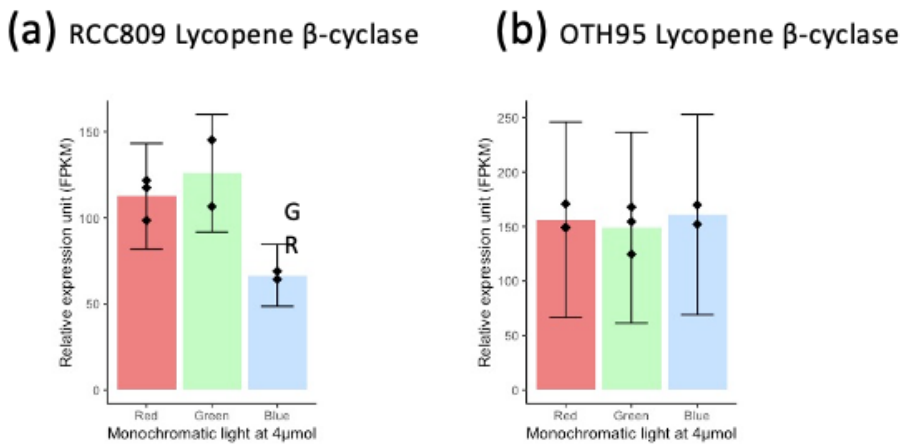

Figure 3.13 Lycopene β-cyclase (LCYB) gene expression.
(a) RCC809 Od20g00760 showing significant reduction in blue light (b) OTH95 ostta14g00700 showing no light quality response. Letters indicate significant (p=<0.05) differences after false discovery rate correction with either red (R) red, green (G), and blue (B) conditions.

The lycopene beta cyclase enzyme has not been assigned to a KEGG pathway, however this gene (Od20g00760) involved in carotenoid synthesis was found to decrease in blue light in RCC809 (Figure 3.13). Lycopene beta synthase (LYCB) appears to be encoded in the same gene as lycopene epsilon synthase (LYCE) in OTH95 and RCC809. These two synthases are also both encoded by a single gene in *Ostreococcus lucimarinus* which encodes a fused protein involved in the synthesis of alpha and beta carotenes, its overexpression increases the cellular content of both alpha and beta carotenes in tandem (Blatt et al., 2015). Due to this fusion of proteins involved in the synthesis of alpha and beta carotenes, it is not clear how the ratio of these two

carotene forms will be affected by decreased transcription although, as the study of *O. lucimarinus* showed, the general carotenoid content in the cell would likely be reduced after blue light acclimation as a result.

These results suggest that synthesis of chlorophyll and some accessory pigments is reduced under blue light. Comparing the pathways shows that the light quality responsive synthesis of these photopigments is controlled at various stages of the metabolic pathways.

3.3.8 Carbon metabolism changes in response to blue light

The 'carbon fixation' KEGG pathway map highlights expression changes in three consecutive genes which encode the same protein sequence for the small subunit of RuBisCO (Figure 3.14). Two of these genes were downregulated in blue light compared to both red and green light treatments (Od17g01990 and Od17g02000), and the third gene was upregulated in red light when compared to green and blue (Od17g02010) (Figure 3.15a). This suggests that RuBisCO content increases in RCC809 in red light and is at its lowest in blue light with green light being an intermediate. The genes encoding the large RuBisCO subunit are part of the chloroplast genome which was not obtained due to the method of RNA extraction (Section 2.7). The gene encoding RuBisCO activase (Od04g02820) showed increased expression in red light when compared to blue light only. RuBisCO content has been found to increase in response to blue light when compared to red in higher plants including common bean and soy and to also increase in blue compared to both red and green in cucumber (Wang et al., 2009, Eskins et al., 1991, Sawbridge et al., 1993). The changes seen here in *Ostreococcus* RCC809 RuBisCO and in expression of other genes shown by the 'carbon fixation' pathway map show that carbon fixation is increased in response to red light, decreased in blue light, and that the green light response is an intermediate (Figure 3.14). Interestingly, a previous study of RCC809 and OTH95 showed that RuBisCO protein content did not vary significantly in response to light intensity (Six et al., 2008). The RuBisCO activase gene (Od04g02820) was also significantly less expressed in blue light in RCC809 and not significantly differently expressed in OTH95 (Ostta04g02510) (Figure 3.15b-c). RuBisCO activase enhances the activity of RuBisCO by the removal of competitive inhibitors from the RuBisCO active site (Portis, 2003).

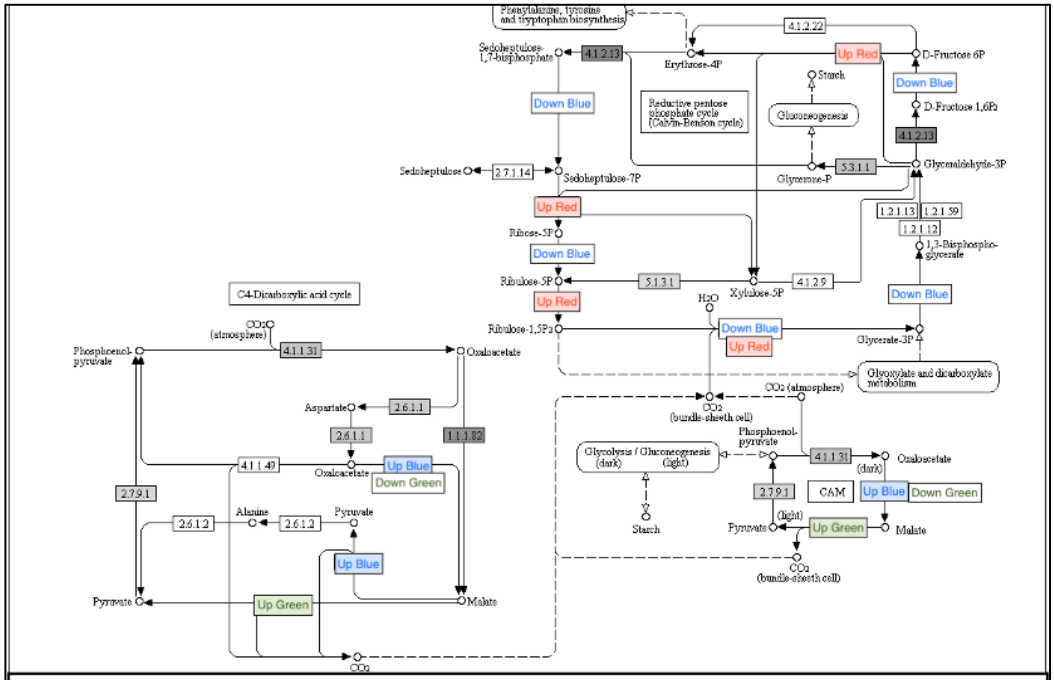

OTH95	RCC809	Response	Function
ostta18g01880	Od17g02010	Up red	Ribulose-bisphosphate carboxylase, small subunit
ostta04g02740	Od04g02610	Up red	Uridine kinase; phosphoribulokinase, carbon metabolism
ostta07g04370	Od07g04720	Up red	Transketolase, biosynthesis of amino acids
ostta05g01810	Od03g00550	Up green	Malate dehydrogenase, regulator of ribonuclease activity A
ostta18g01880	Od17g02000	Down blue	Ribulose-bisphosphate carboxylase, small subunit
ostta18g01880	Od17g01990	Down blue	Ribulose-bisphosphate carboxylase, small subunit
ostta05g04130	Od05g04230	Down blue	Ribose-5-phosphate isomerase, fructose 6P => ribose 5P
ostta09g00160	Od09g06250	Down blue	Fructose-bisphosphatase, photosynthesis in plants and cyanobacteria
ostta03g00350	Od03g02850	Down blue	Fructose-bisphosphatase, photosynthesis in plants and cyanobacteria
ostta03g05500	Od06g06980	Down blue	Fructose-bisphosphatase, glyceraldehyde-3P => ribulose-5P
ostta06g00700	Od06g00660	Down blue	Phosphoglycerate kinase, glycolysis
ostta06g03750	Od06g03790	Down blue	Malate dehydrogenase
ostta07g01040	Od07g01440	Down blue	Malate dehydrogenase
ostta06g01760	Od06g01710	Up blue	Ribulose-phosphate 3-epimerase, biosynthesis of amino acids
ostta01g00040	Od01g06980	Up blue	Malate dehydrogenase
ostta08g00050	Od08g00070	Up blue	Malate dehydrogenase
ostta06g02270	Od06g02230	Up blue	Malate dehydrogenase
ostta04g03550	Od04g01850	Up blue	Malate dehydrogenase
ostta03g00180	Od03g03160	Up blue, down green	Malate dehydrogenase

Figure 3.14 Carbon fixation pathway adapted from KEGG
to show the transcriptional changes in response to light (Kanehisa and Goto, 2000).

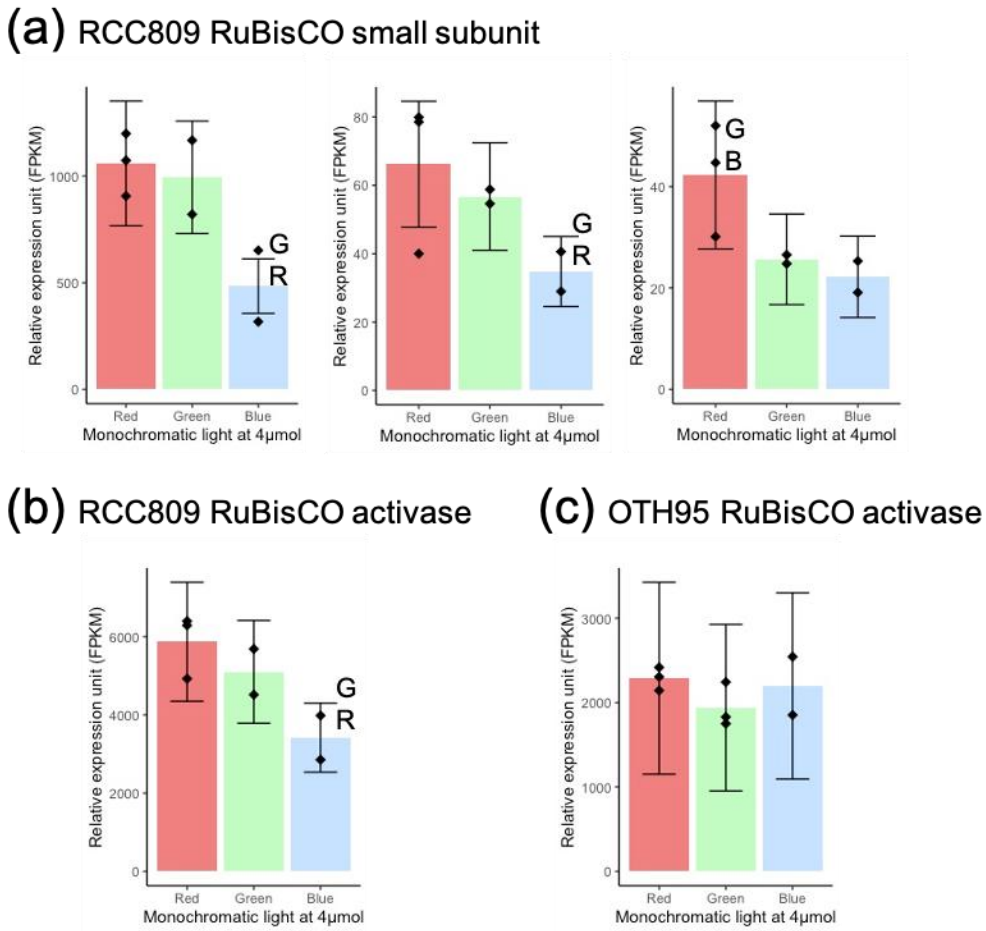

Figure 3.15 Expression of RuBisCO small subunit and RuBisCO activase.
(a) RCC809 RuBisCO small subunit genes Od17g01990 and Od17g02000 which decreased expression in blue light and Od17g02010 which increased expression in red light (b) RCC809 RuBisCO activase Od04g02820 showing a significant reduction in blue light and (c) OTH95 RuBisCO activase ostta04g02510 showing no significant response to light quality. . Letters indicate significant (p=<0.05) differences after false discovery rate correction with either red (R) red, green (G), and blue (B) conditions.

It is unclear from the 'glycolysis/gluconeogenesis' KEGG pathway mapping whether the changes listed in the GO enrichment test category as 'glucose metabolism' under blue light were most likely to specifically represent an increase in glycolysis or gluconeogenesis (Figure 3.16). The fructose-bisphosphatase gene (Od06g06980) which was downregulated in blue light, catalyses the conversion of fructose 1,6 bisphosphate to fructose-6-phosphate, suggesting that these expression changes represent decreased gluconeogenesis in response to blue light. This conclusion is compounded by the response illustrated by the differentially expressed genes marked on the 'starch and sucrose metabolism' map which shows glycogen synthesis genes downregulated in blue light (Figure 3.17). These analyses suggest that energy storage

in the form of both starch and glucose is decreased in blue light in RCC809, which may be connected to the induction of cell division seen in this light quality.

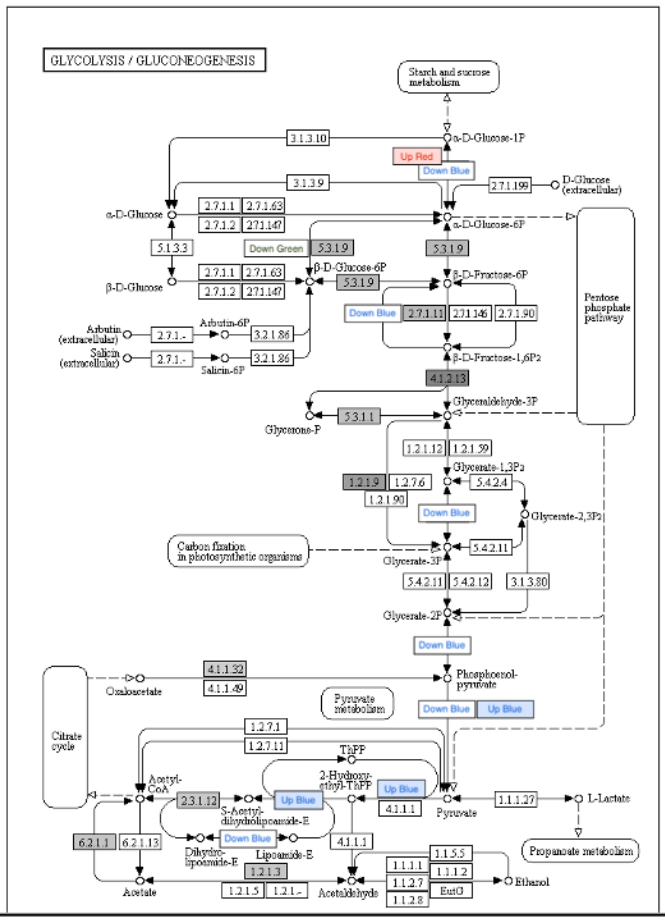

OTH95	RCC809	Response	Function
ostta15g02520	Od14g02940	Up red, down blue	Phosphoglucomutase
ostta03g00350	Od03g02850	Down blue	Fructose-bisphosphatase
ostta14g01010	Od20g01100	Down blue	Fructose-bisphosphatase
ostta06g00700	Od06g00660	Down blue	Phosphoglycerate kinase
ostta01g01500	Od01g05480	Down blue	Phosphopyruvate hydratase; Ubiquitinyl hydrolase 1
ostta06g00700	Od06g00660	Down blue	Phosphoglycerate kinase
ostta16g00480	Od14g00300	Down blue	Pyruvate kinase
ostta03g05500	Od06g06980	Down blue	Fructose-bisphosphatase, glyceraldehyde-3P => ribulose-5P
ostta04g04830	Od04g00660	Down blue	Dihydrolipoyl dehydrogenase
ostta01g05560	Od01g01190	Up blue	Pyruvate dehydrogenase
ostta16g00550	Od14g00390	Up blue	Pyruvate kinase
ostta01g05290	Od01g01440	Down green	Glucose-6-phosphate 1-epimerase

Figure 3.16 Glycolysis / gluconeogenesis pathway adapted from KEGG
to show the transcriptional changes in response to light (Kanehisa and Goto, 2000).

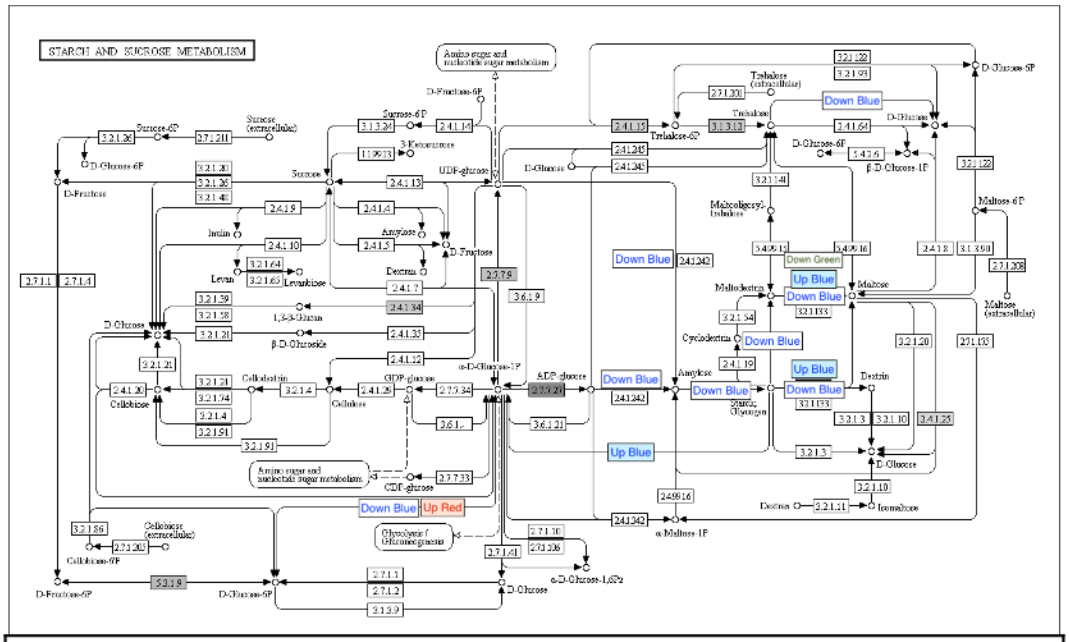

OTH95	RCC809	Response	Function
ostta15g02520	Od14g02940	Up red, down blue	Phosphoglucomutase (alpha-D-glucose-1,6-bisphosphate-dependent)
ostta13g01180	Od13g02060	Down blue	Glycogen biosynthesis, glucose-1P => glycogen/starch
ostta03g00870	Od03g02200	Down blue	Glycogen biosynthesis, glucose-1P => glycogen/starch
ostta14g02180	Od20g02470	Down blue	1,4-alpha-glucan branching enzyme, isoamylase, glycosyl hydrolase
ostta05g04330	Od05g04450	Down blue	Alpha-trehalase, glycosidase
ostta03g03180	Od06g04660	Down blue	Beta-amylase
ostta14g00250	Od20g00290	Up blue	Trehalose-phosphatase,
ostta11g00960	Od11g01910	Up blue	Glycogen phosphorylase
ostta07g03070	Od07g03500	Up blue	Glucose-1-phosphate adenylyltransferase, nucleotidyl transferase
ostta16g00910	Od11g00400	Up blue	Diacylglycerol O-acyltransferase, glycerolipid metabolism
ostta07g01950	Od07g02550	Up blue	Alpha-amylase, glycosyl hydrolase
ostta07g01950	Od07g02560	Up blue, down green	Alpha-amylase, glycosyl hydrolase

Figure 3.17 Starch and sucrose metabolism pathway adapted from KEGG

Differentially expressed enzymes map upstream of the 'TCA cycle' pathway which implicate an increase under blue light of the synthesis and subsequent catabolism of pyruvate (Figure 3.18). Although multiple blue light responsive enzymes map on to the TCA cycle pathway, the effects of this are unclear. Some of these enzymes are involved in multiple pathways and further investigation would be necessary to fully understand the physiological effects of these changes. For example, these pyruvate

metabolism enzymes also map to the C4-dicarboxylic acid cycle (Figure 3.14). It is not yet known if *Ostreococcus* performs C4 photosynthesis although it does possess the necessary genes (Derelle et al., 2006). As CO_2 increases with depth, and C4 photosynthesis is more efficient in low CO_2 environments, C4 photosynthesis might be downregulated under blue light as a signal of the higher CO_2 levels associated with depth.

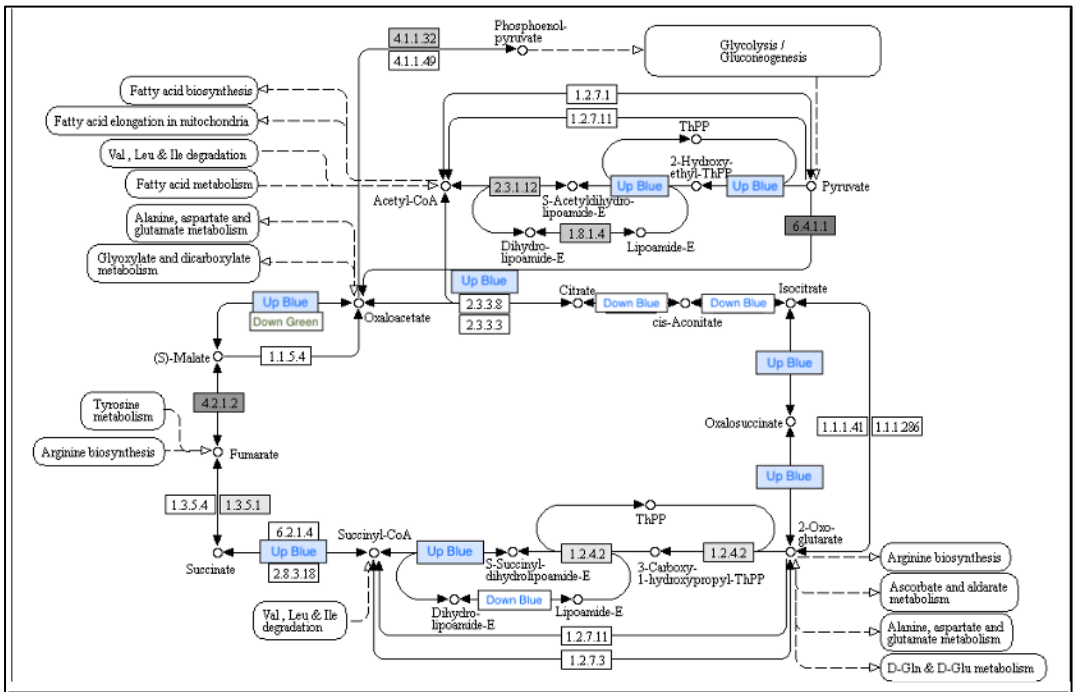

OTH95	RCC809	Response	Function
ostta01g05560	Od01g01190	Up blue	Pyruvate dehydrogenase, glycolysis
ostta02g04820	Od02g03200	Up blue	Succinyltransferase, amino acid metabolism
ostta03g00180	Od03g03160	Up blue, down green	Malate dehydrogenase, cysteine and methionine metabolism
ostta06g02270	Od06g02230	Up blue	Malate dehydrogenase, cysteine and methionine metabolism
ostta08g00050	Od08g00070	Up blue	Malate dehydrogenase
ostta05g01760	Od05g01850	Up blue	Citrate (Si)-synthase
ostta03g05920	Od06g07420	Up blue	Succinate--CoA ligase (ADP-forming)
ostta04g04830	Od04g00660	Down blue	Dihydrolipoyl dehydrogenase, glycolysis

Figure 3.18 Citrate cycle (TCA cycle) pathway adapted from KEGG
to show the transcriptional changes in response to light (Kanehisa and Goto, 2000).

3.3.9 Fatty acid synthesis decreases in blue light

Several other KEGG pathway maps show related changes in metabolic pathways. The 'fatty acid biosynthesis' map (Figure 3.19) shows how a decrease of four genes encoding enzymes under blue light (and one gene which increased under red light) may be responsible for a decrease in the synthesis of a number of fatty acids in this pathway. The green light response is intermediate between the red and blue light responses. As with the reduction in energy storage in the form of starch and glucose in blue light in RCC809, this reduction in fatty acid synthesis may be connected to the induction of cell division seen in this light quality.

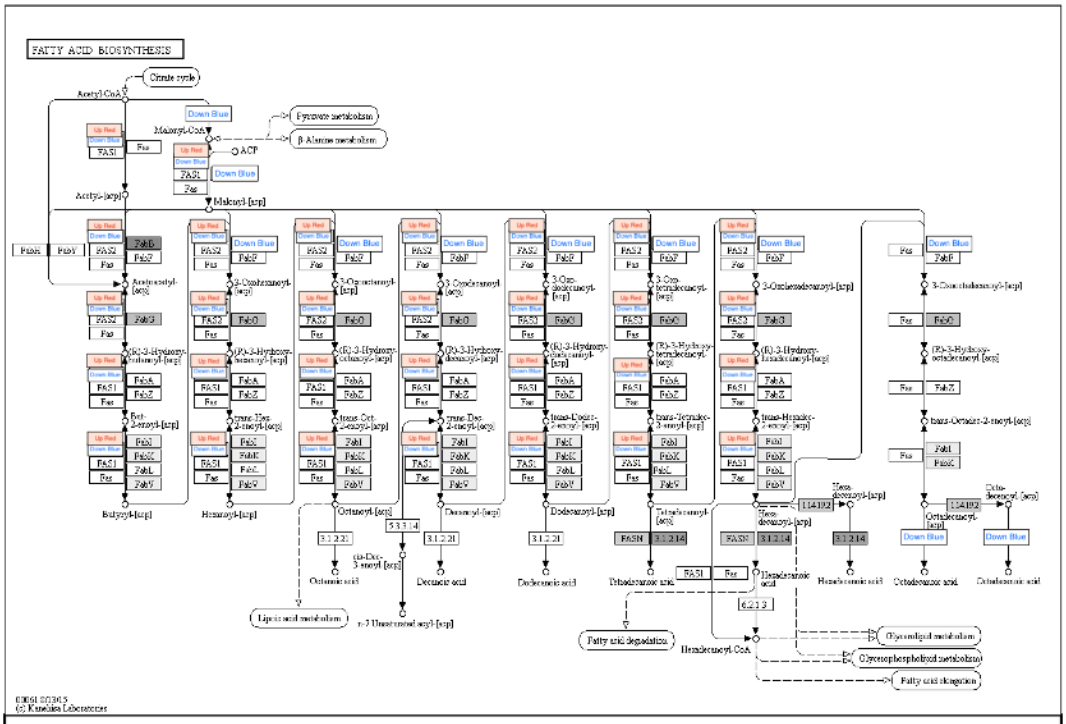

OTH95	RCC809	Response	Function
ostta07g03880	Od07g04250	Up red	Fatty-acid synthase; Enoyl-[acyl-carrier-protein] reductase (NADH)
ostta09g03060	Od09g03480	Down blue	Fatty-acid synthase; [Acyl-carrier-protein] S-malonyltransferase
ostta01g03280	Od01g03440	Down blue	Acetyl-CoA carboxylase
ostta04g03510	Od04g01890	Down blue	Stearoyl-[acyl-carrier-protein] 9-desaturase
ostta15g01470	Od14g01920	Down blue	Fatty-acid synthase; Beta-ketoacyl-[acyl-carrier-protein] synthase I

Figure 3.19 Fatty acid biosynthesis pathway adapted from KEGG
to show the transcriptional changes in response to light (Kanehisa and Goto, 2000).

3.3.10 Amino acid synthesis decreases in blue light

Changes in expression levels of enzymes involved in the synthesis of various amino acids were also noted in RCC809 (Appendix 4). In general, the trend is of a decrease under blue light in the expression of genes encoding enzymes involved in amino acid biosynthesis. Under blue light there was a decrease in expression of genes related to the synthesis of the following amino acids: aspartate, valine, tryptophan, leucine, and lysine. Genes related to the synthesis of serine and asparagine increased expression in blue light. Together, these enzymes indicate that, as with fatty acid synthesis, protein synthesis is likely to be reduced in a blue light acclimated RCC809 culture. The 'pyrimidine metabolism' KEGG pathway map also shows how enzymes upregulated under blue light are responsible for the synthesis of RNA and DNA (Figure 3.20). The increase in DNA synthesis in blue light is expected as an increase in cell division was indicated in this light quality by the GO enrichment analysis. This may also explain the reduction in energy storage and fat and protein synthesis as this is arrested in favour of cell division in blue light.

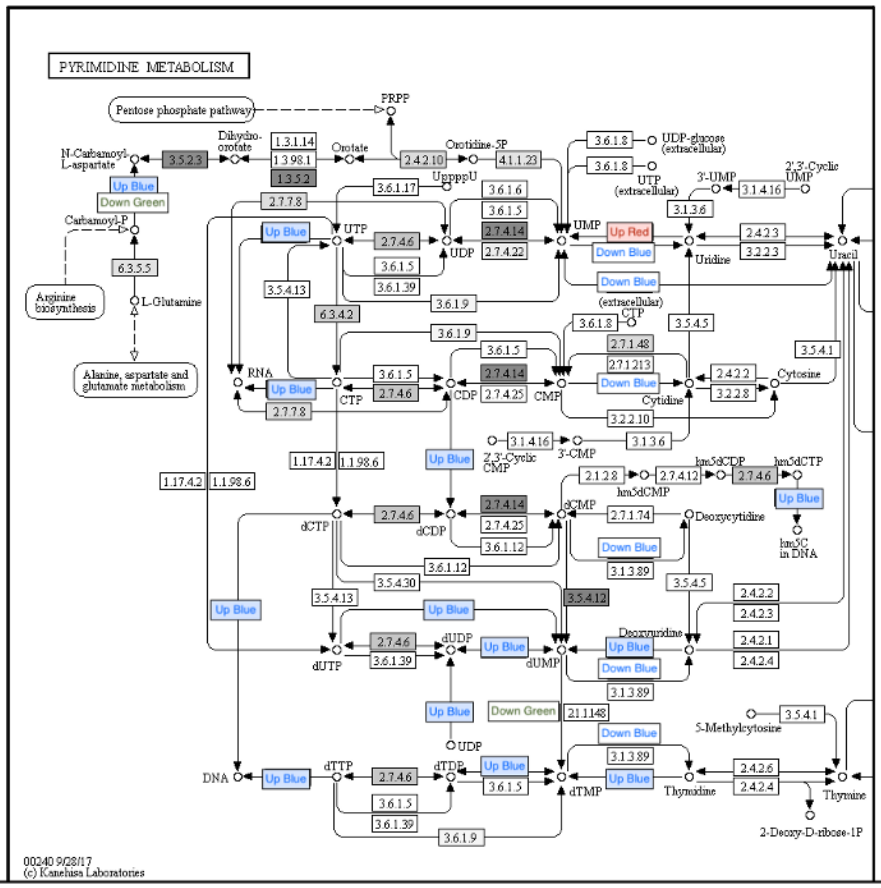

OTH95	RCC809	Response	Function
ostta15g00060	Od11g00060	Down green, up blue	Aspartate carbamoyltransferase
ostta07g03490	Od07g03910	Down blue	Uracil phosphoribosyltransferase
ostta01g05920	Od05g02890	Down green	Thymidylate synthase, dihydrofolate reductase
ostta01g04510	Od01g02300	Up blue	Deoxynucleoside kinase, thymidine kinase
ostta08g00560	Od08g00520	Up blue	Ribonucleoside-diphosphate reductase
ostta07g01340	Od07g01740	Up blue	Nucleoside-phosphate kinase, dTMP kinase
ostta17g02305	Od16g00170	Up blue	dUTP diphosphatase

Figure 3.20 Pyrimidine metabolism pathway adapted from KEGG
to show the transcriptional changes in response to light (Kanehisa and Goto, 2000).

3.2.4 Transcriptomic analyses of the OTH95 light quality response

The PCA of the OTH95 expression data shows a considerable overlap between red and blue light responses but some segregation from the green response (Figure 3.21b). When comparing the responses of replicates, this lack of distinction between the red and blue light responses appears to be due to two particularly similar samples, one from each light treatment. On further investigation, as illustrated by the heatmap in Figure 3.22, the differences within the red and blue replicate samples were greater than

between the conditions and therefore it cannot be concluded that OTH95 responds differently to red or blue light quality treatments. The heatmap also shows how the maximum magnitude of the changes in gene expression between the light treatments is around twofold, smaller than the maximum of threefold changes seen for RCC809 (Figure 3.22). A small number of genes (149) were identified by the differential expression analysis using CuffDiff as significantly repressed in green light compared to red and blue light, although it is unclear whether this due to variation in the red and blue light samples and it could not be concluded that these genes were part of a green light response.

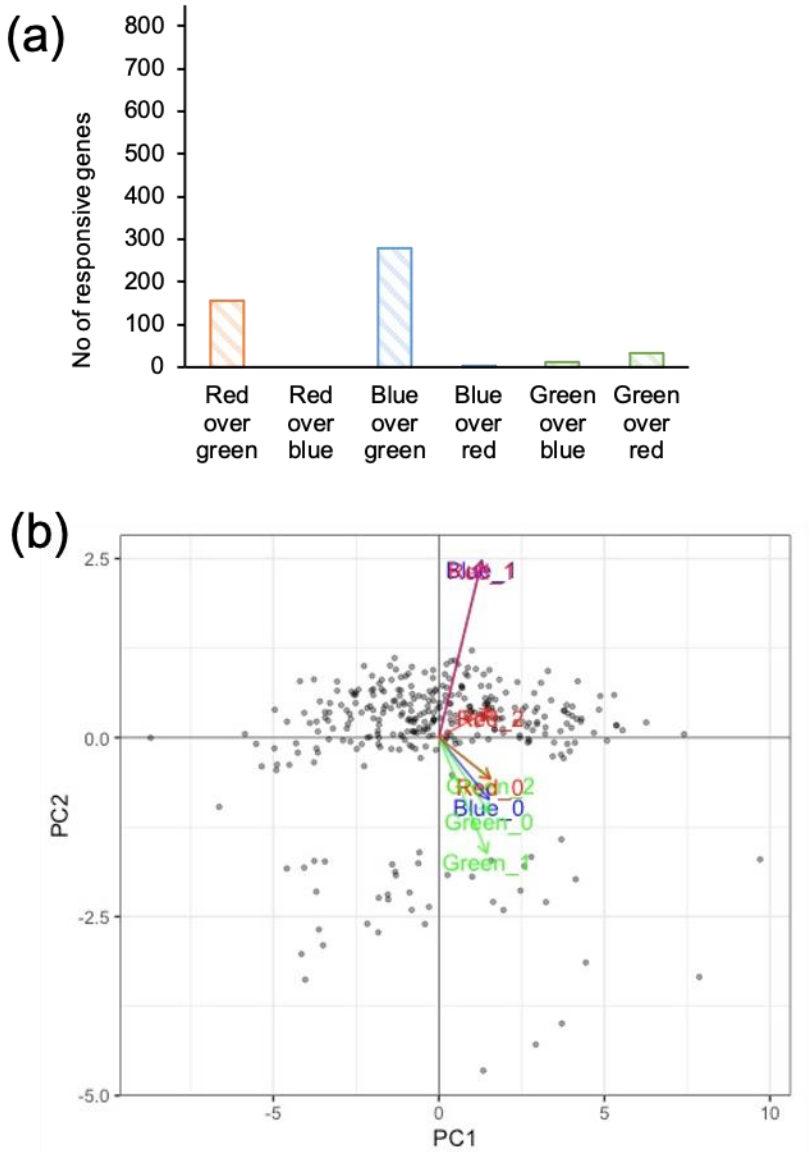

Figure 3.21 OTH95 visualisation of differentially expressed genes.
(a) Total numbers of significantly differentially expressed genes identified as induced when compared pairwise between light quality treatments. (b) Principal component analysis of expression data for each replicate, data for significantly differentially expressed genes shown only.

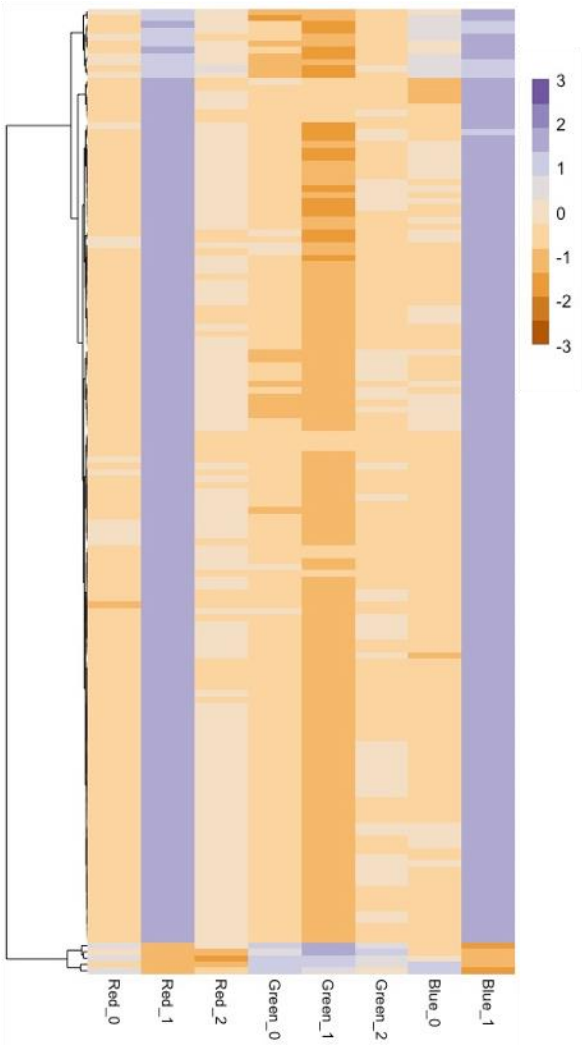

Figure 3.22 Heatmap of significantly differentially expressed genes in OTH95.
Heatmap generated by log FPKM compared between light condition and replicates. Blue areas indicate a positive fold change resulting from higher expression compared to the negative fold change indicated by the yellow areas. Rows are clustered by Jensen-Shannon distance.

3.4 Discussion

The transcriptional analysis of RCC809 allowed a functional profile to be described for the light quality responses seen in this ocean ecotype. This included a cell cycle gene set which increased expression in blue light and explains the faster growth rates due to increased cell division also seen in blue light. Light quality responsive genes associated with many of the functions highlighted by the transcriptional data have also been shown to change expression levels in response to other environmental parameters in similar studies, such as the changes suggested in phylloquinone and photosystem content. A decrease in the PSI to PSII ratio and phylloquinone content were both shown here to be associated with blue light acclimation in RCC809. A reduction in the PSI to PSII ratio has also been noted in *Ostreococcus* in response to iron limitation (Botebol et al., 2015, Botebol et al., 2017). RCC809 has a constitutively higher relative content of PSII to PSI than OTH95 and this has been indicated as an adaptation to iron limitation in the RCC809 deeper ocean source environment (Cardol et al., 2008). A decrease in phylloquinone is also shown to be accompanied by a reduction in PSI activity, this may represent a shift under blue light to PSII and the absorbance of shorter wavelengths (Gross et al., 2006). Phylloquinone also degrades in sunlight and so its synthesis may be expected to increase in surface waters where both the light intensity and the proportion of red and green light wavelengths are higher. This may not be the case for all phytoplankton species as some studies hypothesise that growth of algae in shorter wavelength light qualities would increase PSI content and thus increase phylloquinone yield (Tarento et al., 2019). Understanding how light quality can affect phylloquinone synthesis would allow optimisation of this biotechnological process. These results suggest that the relationship between phylloquinone production and light quality in algae depends on the species and also on the adaptation of that species to the light quality of its source environment.

Many of the light quality responsive genes identified in RCC809 in this chapter which are involved in pigment synthesis have also been investigated in green algae in terms of their light intensity responses. For example, the cytochrome carotene hydroxylase CYP97 gene (responsible for the conversion of carotenes to lutein) which decreased in RCC809 in blue light relative to red light is induced in high light in *Chlamydomonas reinhardtii*, and in *Haematococcus pluvialis* in which CYP97C also showed greater

induction of expression in high blue light than in high white light (Cui et al., 2013, Couso et al., 2012). Genes related to the increased synthesis of zeaxanthin were induced in blue light in RCC809; zeaxanthin is a xanthophyll pigment which is involved in photoprotection through nonphotochemical quenching (NPQ) and has also been indicated as a blue light photoreceptor in plant guard cells (Frechilla et al., 1999, Zeiger and Zhu, 1998). The reduction of lutein synthesis gene expression in blue light in contrast with the increase in zeaxanthin is interesting as lutein is also involved in NPQ and the two together would suggest a photoprotective response induced by high light intensities. Levels of violaxanthin, zeaxanthin, and lutein (in terms of percentages of total carotenoids) have all been found to increase in RCC809 with increases in light intensity from 150 μmol quanta $m^{-2} \cdot s^{-1}$ to 1200 μmol quanta $m^{-2} \cdot s^{-1}$ (Guyon et al., 2018). Lutein and zeaxanthin were not separated in the study by Guyon et al and so it is possible that a decrease in one carotenoid was compensated for by an increase in the other. It has been demonstrated that carotene content also decreases in response to high light in RCC809 in particular when compared to OTH95 and *O. lucimarinus*, although the specific composition of these carotenes was not analysed (Six et al., 2009). The same study found that lutein levels in RCC809 increased with light intensity, this is interesting as this expression analysis shows that lutein synthesis likely decreases in blue light.

3.5 Conclusions

RCC809 showed specific light quality responses in terms of increased growth in blue light, and distinct sets of gene expression for the red, green, and blue light treatments, while OTH95 showed no change in growth rates and repression in transcription of only a small set of genes in response to green light compared to red and blue light. These light quality responses were different between the two ecotypes. The response of RCC809 was most distinct in blue light (Figure 3.4), and the response of OTH95 only differed in green light, compared to the other light quality treatments (Figure 3.21). The ecotypes also showed no overlap in functions of the light quality responsive genes identified (examples in Figures 3.8-10).

3.5.1 RCC809 conclusion

RCC809 showed a distinct transcriptional response to each of the light qualities although, as the PCA (Figure 3.4b) demonstrates, its responses to red and green light were more similar when compared to the blue light response. Analysis of the differentially expressed genes in RCC809 suggests that blue light induces physiological changes involving an induced cell cycle, reduced chlorophyll and pigment synthesis, reduced amino acid, lipid, and starch synthesis, and reduced carbon fixation. The growth rate measurements confirmed that the mitotic cell cycle was accelerated in blue light, leading to increased cell division. These responses may be understood in the context of the RCC809 source environment. Often described as a 'deep water ecotype', RCC809 was taken at a depth of 105m in the Atlantic Ocean but, as *Ostreococcus* cells are not motile, this ecotype will be subject to variation in its environment as it is moved with upwellings and other changes in the water column and currents. An increase in the prevalence of blue light in the water occurs with depth as the other light wavelengths are scattered more easily. This suggests that occurrence of red or green light in the light environment for RCC809 should prompt physiological changes in the ecotype compared to its blue light response both to maximise efficient light capture and to respond to the changes in its environment that come with a move to surface waters. This complex series of metabolic changes in response to light quality in RCC809 reveals evidence that this phototroph is able to respond to changes in light quality which may translate to increased survival in a variable spectral marine environment.

3.5.2 OTH95 conclusion

OTH95 does not respond with distinct transcriptional changes after a 72-hour exposure to red, green, or blue light. This lack of a specific response may reflect the source environment for this strain of the coastal and lagoon associated OTH95; a relatively shallow lagoon is most likely to have a more stable light environment in terms of spectral quality. This is reflected in the transcriptional data for OTH95 which showed no evidence of a clear pattern of gene expression under any of the light qualities. It appears that light quality responses in OTH95 are not regulated by changes in the

expression levels of genes in metabolic pathways. It is possible that this ecotype does respond to light quality and that these responses are instead controlled by post-transcriptional processes such as methylation.

The physiological analyses detailed in Chapter 4 are intended to demonstrate how the light quality responsive changes in gene expression identified here translate to functional changes affecting cell physiology.

Chapter 4: Physiological responses to light quality

4.1 Introduction

As described in detail in Chapter 1, the spectral quality of light in the oceans is expected to be affected by ongoing climate change due to shifts in phytoplankton community structure and changes in reflectance from particulate matter. Analyses of light quality responses will allow predictions of how *Ostreococcus* may respond to the challenges of climate change and the environmental factors that are signalled by specific spectral qualities.

The transcriptional analysis described in Chapter 3 revealed changes in *Ostreococcus* gene expression in response to light quality. These transcriptional responses suggest specific effects on the cells' physiology. In RCC809, an ocean ecotype sourced from deep water, the transcriptomic analysis indicated reduced expression of several genes in the pathways for pigment synthesis after acclimation to blue light compared to red and green light. For example, expression of lycopene beta cyclase (Od20g00760), a key enzyme in β-carotene synthesis (Figure 4.1a), was significantly downregulated in blue light. Expression of the violaxanthin depoxidase gene (Od11g00170), which catalyses the conversion of violaxanthin to antheraxanthin in the xanthophyll cycle, increased significantly in blue light, whereas expression of the gene which catalyses the reverse reaction, the violaxanthin epoxidase gene (Od02g02570), decreased. Expression of the cytochrome P450 gene (Od09g03950) in the CYP97 family, involved in the conversion of carotenes to lutein, was downregulated, suggesting a reduction in lutein-derived accessory pigment content in blue light.

These data suggested changes in the levels of specific accessory pigments in the RCC809 ecotype in response to changes in light quality. These changes, affecting both light harvesting and photoprotection through the xanthophyll cycle, may translate into changes in photosynthetic efficiency. In contrast, no such changes were observed in OTH95, the lagoon ecotype, suggesting the absence of light quality acclimation in this ecotype.

Most of the light energy for photosynthesis by *Ostreococcus* is absorbed by two chlorophylls, *a* and *b*, which maximally absorb red and blue wavelengths (Kume et al., 2018, Lichtenthaler, 1987, Bouman et al., 2018). Metabolites of chlorophyll present in *Ostreococcus*, such as Mg-2,4-divinyl pheoporphyrin a5 monomethylester (MgDVP) and pheophytin, are also involved in light harvesting.

Ostreococcus also contains various accessory pigments which maximally absorb light at different wavelengths. In photosynthetic organisms, the relative contents of these pigments can be dynamically adjusted to efficiently capture light of different qualities (Jagannathan and Golbeck, 2009). Light quality can induce changes in carotenoid content in green algae, for example the chlorophyte *Haematococcus pluvialis* which accumulates more carotenoid in response to blue light than red light (Kobayashi et al., 1992). Complementary chromatic adaptation through changes in light absorbing pigments has also been demonstrated in photosynthetic algae. The ratio of the light harvesting pigment protein complexes phycocyanin and phycoerythrin is altered in some species of red algae and cyanobacteria to maximise light capture by complementing the ratio of red to green wavelengths present in the environment (Stowe et al., 2011, Wu, 2016, Borlongan et al., 2020, Stomp et al., 2004). Complementary chromatic adaptation cannot solely be assessed by comparing available radiation to the pigment absorption spectrums. The pigment absorption peaks are often found to be 'offset' from the spectral bands for which the incident light is most intense so that fluctuations in light intensity are less disruptive or damaging. This offset in absorbance was demonstrated by successful predictions of pigment responses in plants and aquatic green sulphur bacteria from the spectrum of incident light using modelling (Arp et al., 2020).

The accessory pigments also serve a secondary role, by absorbing and dissipating light energy, they can protect the chlorophylls in the core light harvesting complex from inactivation by photodamage (Jagannathan and Golbeck, 2009). Photoprotection in green algae is mostly achieved by induction of the xanthophyll cycle depoxidation state (DPS), i.e., conversion of the light harvesting violaxanthin to the photoprotective antheraxanthin and zeaxanthin (Kulk et al., 2013). This reaction can be reversed by the conversion of violaxanthin to neoxanthin (Figure 4.1). The depoxidation state correlates positively with non-photochemical quenching (NPQ,) which reduces damage to the cells from high irradiances (Six et al., 2009, Demmig-Adams, 1990). Relative xanthophyll pigment contents can therefore be used to determine photoacclimation to irradiance level.

Physiological responses to light quality have not been previously investigated in *Ostreococcus*. The analyses described in this chapter aim to test whether *Ostreococcus* responds to changes in light quality by adjusting its pigment composition and the function of its photosystems. The responses of the RCC809 and OTH95 ecotypes

sourced from distinct light quality environments are compared to assess how this may represent adaptive divergence.

The objectives of these analyses were as follows:

- To investigate changes in pigment content, photochemistry and metabolism in cells adapted to different light qualities.
- To assess how these changes affect the ability of the cells to harvest light and achieve photoprotection
- To compare the physiological responses of two *Ostreococcus* ecotypes: the deep ocean sourced RCC809, and the lagoon sourced OTH95

4.2 Methods

All measurements described are a mean of three independent replicates. Significance was determined using an ANOVA and subsequent student's t-tests and the level of significance was assessed as $p=<0.05$ unless otherwise stated.

4.2.1 Pigment analysis

To gain more detail on the pigment changes indicated in RCC809 in response to light quality, and to assess how these changes may affect photosynthesis, measurements of pigment content were taken. In order to determine which pigment or pigments were synthesised, accumulated, or degraded in response to changes in light quality, cultures were grown in white light until they reached the middle of the logarithmic growth phase (approximately 20 to 30 million cells ml^{-1}). The cultures were then transferred to low intensity monochromatic light (4μmol photons m^{-2} s^{-1}) for 72 hours, at which point they were sampled for pigment analyses as described in section 2.12 of the Methods chapter. Two chlorophyll *b*-like pigments were detected in the RCC809 ecotype which were not detected in OTH95, as illustrated by the HPLC chromatogram in Figure 4.2a-b.

The relative carotenoid content was assessed by comparing the percentage contribution of each pigment to total carotenoid content. Included in this analysis were, in descending order of abundance: prasinoxanthin, neoxanthin, violaxanthin, uriolide, micromonal, dihydrolutein, the unknown carotenoid, β-carotene, α-carotene, zeaxanthin, antheraxanthin, and lutein.

To assess how the depoxidation state (DPS) was affected by light quality, it was quantified according to (Munné-Bosch and Cela, 2006). DPS (also known as DES) was calculated as (Z + 0.5A) / (V + A + Z), where Z, A, and V correspond to relative levels of zeaxanthin, antheraxanthin, and violaxanthin respectively.

4.2.2 Photosynthetic parameter analysis

To investigate how light quality responses affect photosynthetic activity, PAM (pulse-amplitude modulation) fluorometry analysis was used. This allowed insight into changes in the function of photosystem II after acclimation to the different light qualities. This method uses chlorophyll fluorescence to measure the efficiency of PSII and to infer the effects of non-photochemical quenching (NPQ).

Cultures were acclimated to the different light treatments for 72 hours as described in section 4.2.1. For each measurement, aliquots of culture were diluted to around 5 million cells ml^{-1} in Keller medium in a cuvette and subjected to light pulses of varied intensity to measure the resulting fluorescence. Different light qualities were used for excitation (blue at 470nm, green at 520nm, red at 645nm and dark red at 665nm). The measurements shown in the following analyses are based on excitation at 470nm as green algae show the greatest response to this wavelength (Heinz and Walz, 2003). Analyses based on excitation at other wavelengths were compared (data not shown,) and the resulting light quality responses were not different to those described here at 470nm, other than a change in the maximum quantum yield of PSII in OTH95 which will be discussed.

The maximum quantum yield of PSII photochemistry indicates the maximum proportion of photons absorbed by PSII which can potentially be used in photosynthesis (Maxwell and Johnson, 2000). Lower quantum yields indicate a lower photosynthetic efficiency which is likely the result of reduced PSII content. To detect the background fluorescence while all the electron accepting reaction centres downstream of PSII are open (Fo), the sample is acclimated to darkness for 5 minutes then subjected to a weak light which will not stimulate photochemistry. Next, a high intensity saturating light pulse is applied which closes the reaction centres to measure maximum fluorescence, Fm. Fv, the variable fluorescence, is the size of the increase in fluorescence between the background Fo and the maximum Fm. The maximum quantum yield of PSII is calculated as Fv/Fm.

The maximum relative electron transport rate through PSII (rETR) is calculated as (Yield x PAR x 0.5 x 0.84 μmol electrons $m^{-2}s^{-1}$), where PAR refers to the intensity of the photosynthetically active radiation (Heinz and Walz, 2003). This equation uses standard constants as estimates of the proportion of light reaching cells (0.84) and the proportion of light reaching PSII (0.5) and assumes a stable level of PSII content and an equal ratio of PSII to PSI (Murchie and Lawson, 2013). These constants were estimated for higher plants, so this calculation does not represent absolute ETR for *Ostreococcus*. However, it allows comparison between measurements taken using the same methods.

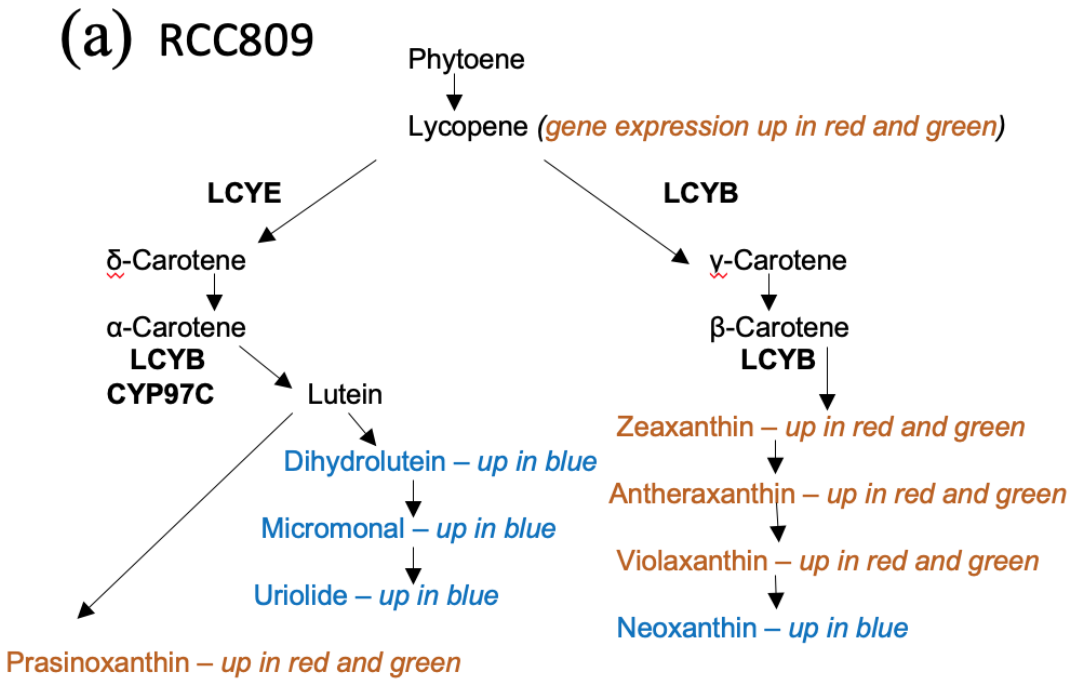

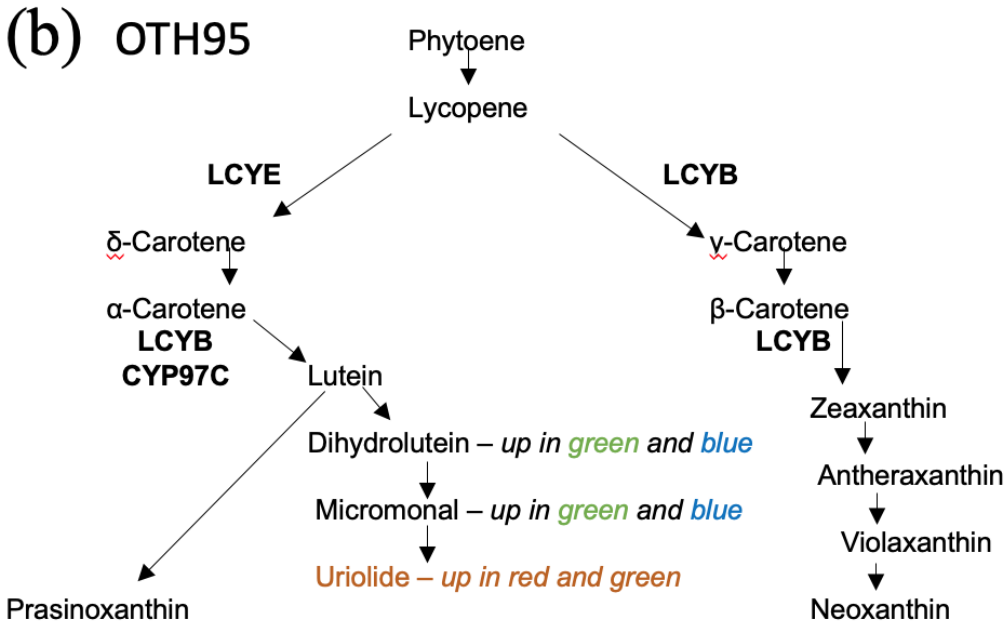

Figure 4.1 Simplified carotenoid biosynthetic pathway for Ostreococcus
(adapted from Blatt et al 2015). LCYB = lycopene β-cyclase; LCYE = lycopene ε-cyclase." The CP450 cryptochrome CYP97C is also shown. Light responses are annotated in terms of significant changes in relative pigment contents derived from HPLC measurements. (a) RCC809 (b) OTH95 https://onlinelibrary.wiley.com/doi/full/10.1111/tpj.12826

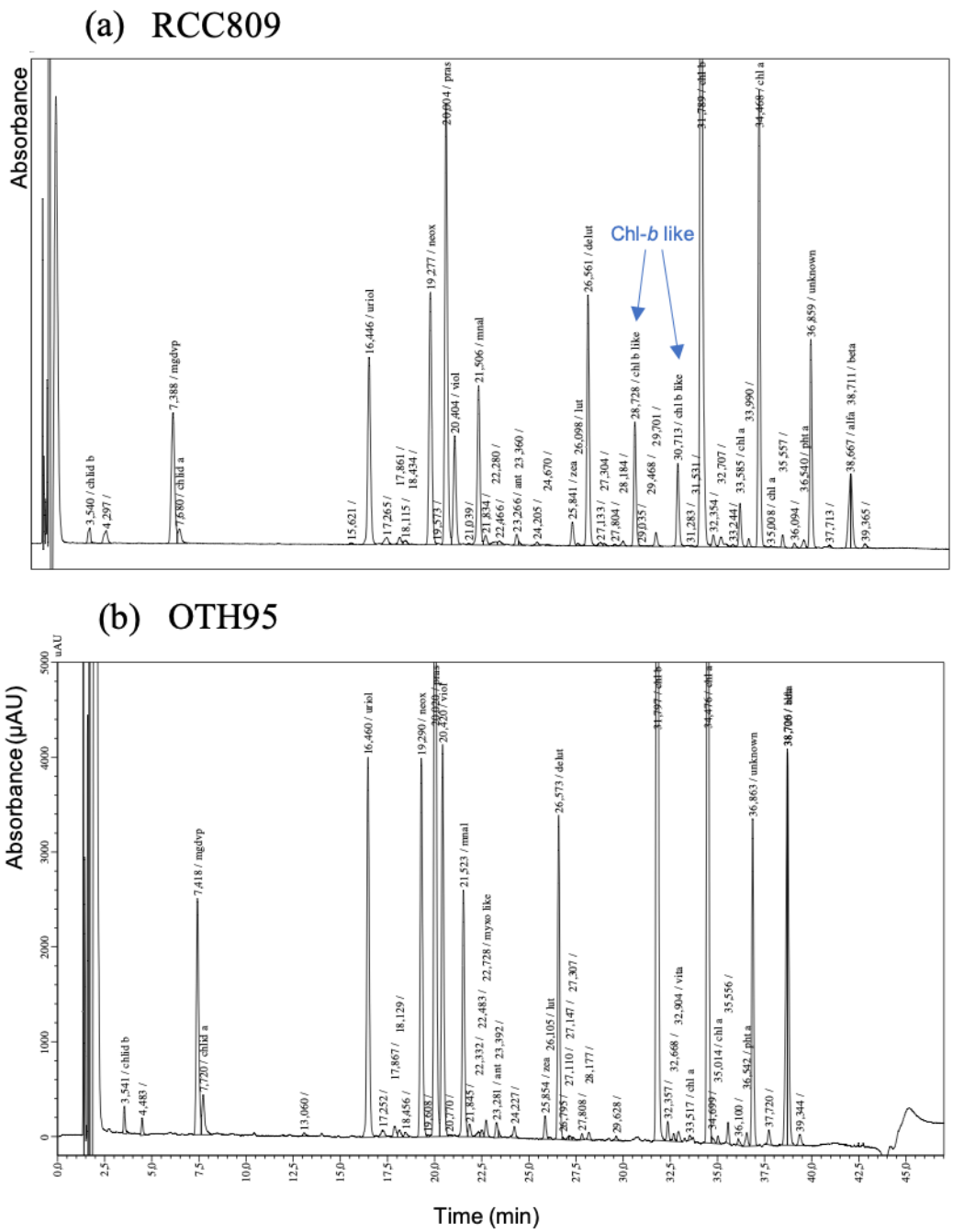

Figure 4.2 HPLC chromatograms of *Ostreococcus* sp. RCC809 and OTH95 pigments grown under different light qualities

(a) RCC809 exposed to 72 hours of low intensity blue light. The presence and separation time for the two chlorophyll *b*-like pigments can be seen just before chl-*b* and are marked with blue arrows. (b) OTH95 exposed to 72 hours of low intensity red light. The chlorophyll *b*-like pigments seen in RCC809 were not found in OTH95.

4.3 Results

4.3.1 Effect of light quality on pigment content

In the ocean ecotype RCC809, pigment composition differed in blue light versus red and green light (Figure 4.3a). The relative contributions of the following pigments increased by the given approximate percentages under blue light compared to red and green light: uriolide (12%), neoxanthin (29%), the unknown carotenoid (40%), micromonal (43%), and dihydrolutein (52%). The relative contents of the pigments prasinoxanthin and zeaxanthin increased in red and green light versus blue light by approximately 11% and 47% respectively. There were no significant changes in the relative contents of lutein, antheraxanthin, violaxanthin, α-carotene, and β-carotene. No significant differences between carotenoid percentages were seen between red and green light responses. While transcription of genes associated with lutein synthesis was reduced in RCC809 under blue light, no significant changes in lutein content were seen in the pigment data. Lutein levels were comparatively low in all light treatments. The pigment composition changes demonstrate a different response to blue light compared to red or green light in RCC809. As pigments affect both the levels of light harvesting and the wavelengths of light absorbed as well as photoprotection, the light quality responses identified here will affect the efficiency of light capture for photosynthesis.

In the lagoon ecotype OTH95, only two changes in carotenoid composition were observed in response to light quality: the relative contents of micromonal and dihydrolutein increased significantly in blue versus red light treatments (Figure 4.3b). These changes were low in amplitude compared to those seen in RCC809, the approximate increases in blue light were around 9% in micromonal (compared to the 43% in RCC809), and 14% in dihydrolutein (compared to the 52% in RCC809). This

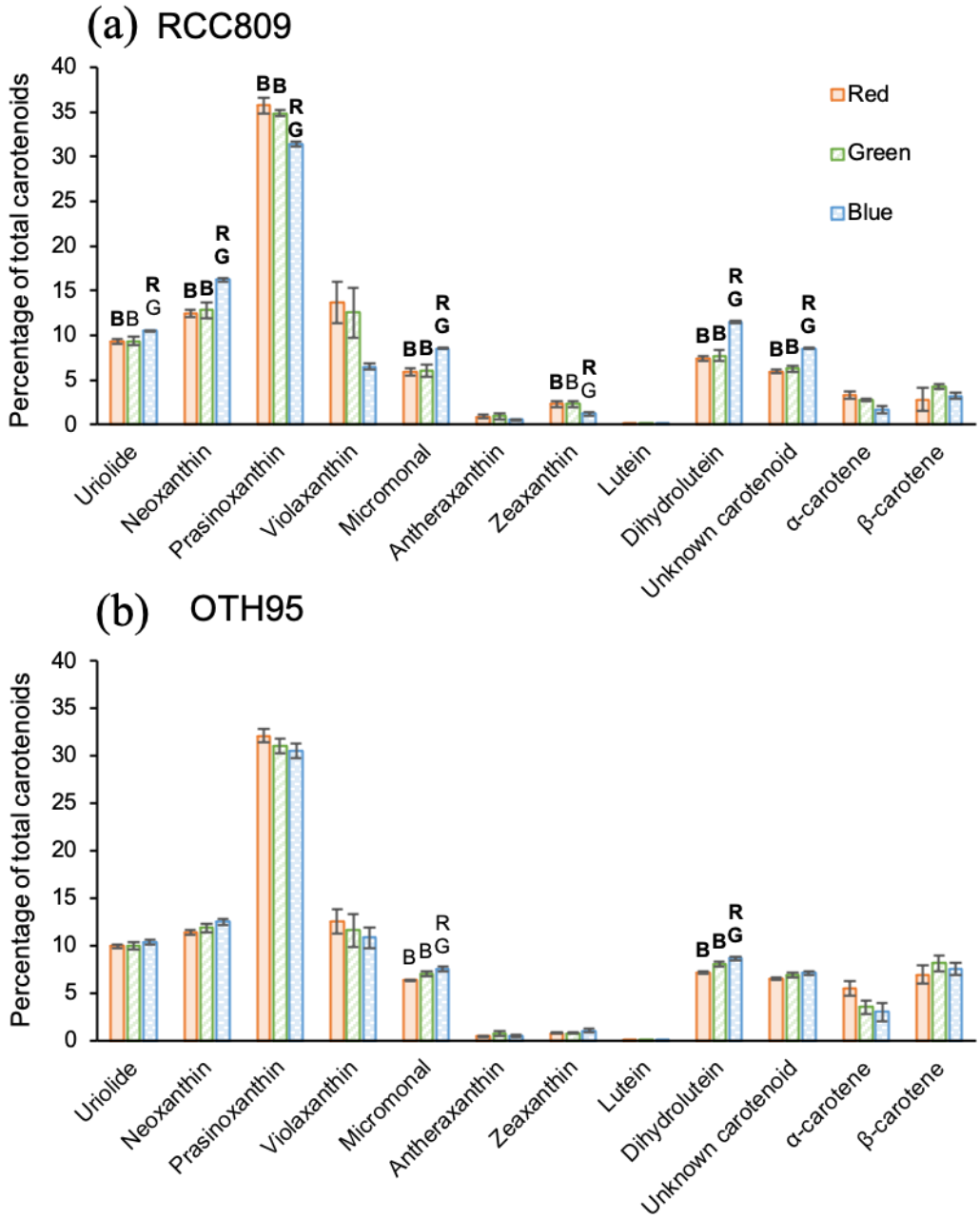

Figure 4.3 Comparative percentages of total carotenoid extracted after growth in red, green, and blue monochromatic light.
(a) RCC809 (b) OTH95. Letters indicate significant (p=<0.05) differences with either red (R), green (G), and blue (B) conditions. Significance was determined using ANOVA and subsequent student's t-tests. Letters are in bold if P<0.01.

demonstrates minor changes in pigment composition in OTH95 which will produce smaller effects on light capture.

When comparing the two ecotypes' pigment content, (Six et al., 2008) found higher levels of prasinoxanthin, neoxanthin, uriolide, MgDVP, micromonal, dihydrolutein, and α-carotene in RCC809 in low light (15μmol photons m^{-2} s^{-1}) than in OTH95 but lower β-carotene. These comparisons are also consistent with those seen in this work. This shows that the differences between the ecotypes are maintained in the experimental conditions applied here.

4.3.2 Chlorophylls and chlorophyll metabolites

In RCC809, the light harvesting accessory pigment and chlorophyll metabolite MgDVP (Mg-2,4-divinyl pheoporphyrin a5 monomethylester) increased significantly relative to chlorophyll *a*, almost doubling in blue light compared to both red and green light (Figure 4.4a).

Chl-*b* levels also significantly increased relative to chl-*a* in blue light, showing a positive ratio of chl-*b* to chl-*a* (1.1±0.04) compared to smaller ratios in red and green light 0.94±0.05 and 0.97±0.1 respectively) (Figure 4.4c). This high chl-*b* to chl-*a* ratio reflects the ratio found in RCC809 by Cardol et al. (2008): 1.01 after growth in 10μmol photons m^{-2} s^{-1} of blue light. The effect of this increase in chl-*b* in blue light is likely compounded by the large rise in content of the two chlorophyll *b*-like pigments only detected in RCC809. Levels of these pigments were around tenfold higher in blue light compared to red or green (Figure 4.4a). On the other hand, the chl-*b* precursor, chlorophyllide *b*, accumulated to half the levels in blue than under red and green light, consistent with it being converted to chl-*b*. These increases in MgDVP, chl-*b*, and chlorophyll *b*-like pigments in blue light RCC809 represent a specific light quality response which will affect the amount of light capture and the spectrum of light absorbance for photosynthesis.

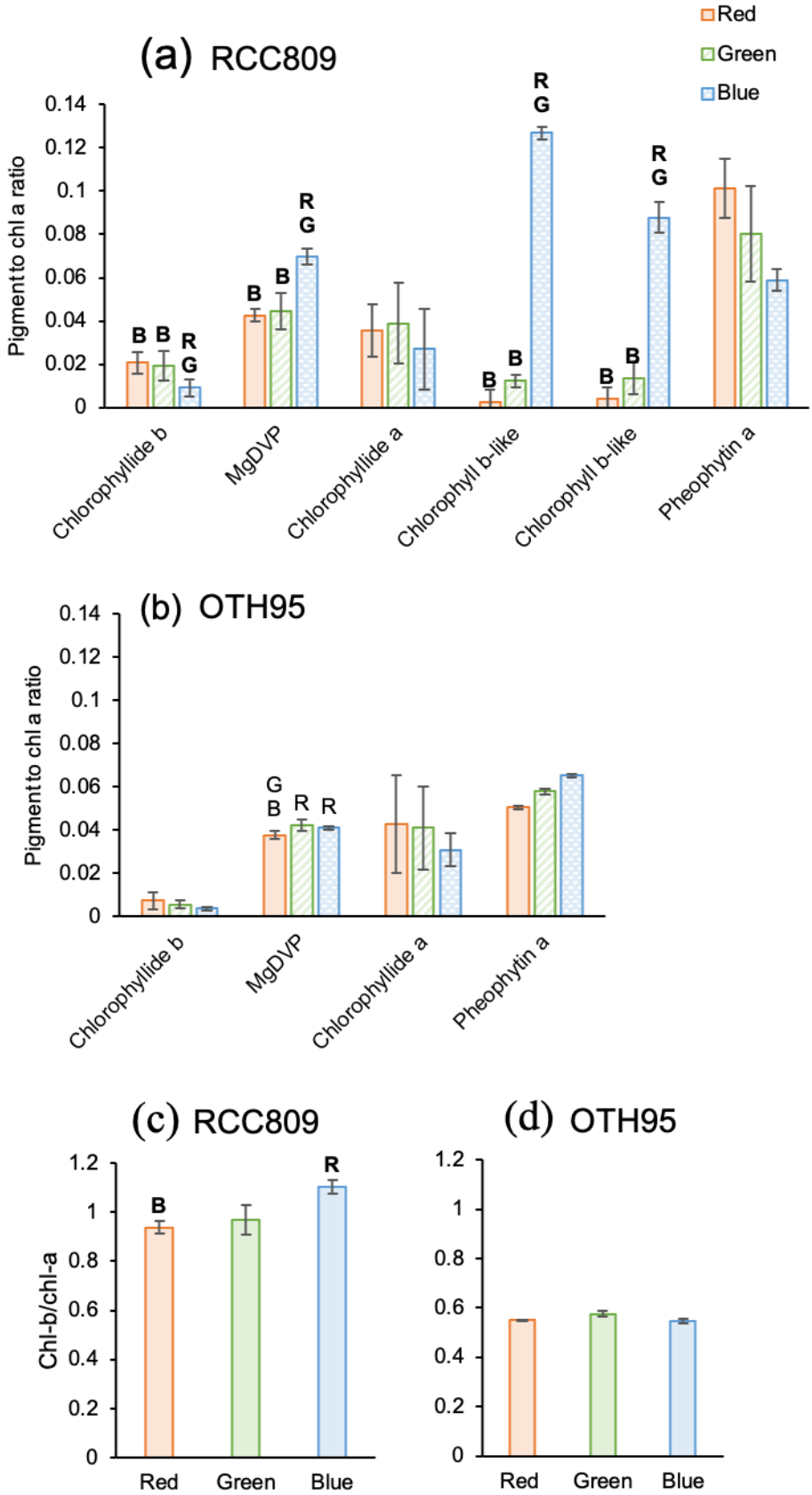

Figure 4.4 Pigment to chl-*a* ratios
(a) RCC809 (b) OTH95. Chl-*b* to chl-*a* ratio of (c) RCC809 and (d) OTH95. Letters indicate significant ($p < 0.05$) comparisons between light responses R red, G green, and B blue. Significance was determined using ANOVA and subsequent student's t-tests. Letters are in bold if $P < 0.01$.

Ratios of chlorophyllide *a* to chl-*a* were variable between experimental replicates in both RCC809 and OTH95, likely reflecting dynamic changes in chl-*a* synthesis in all conditions (Figure 4.4a-b). The relative levels of chl-*b* and chlorophyll metabolites to chl-*a* were lower in OTH95, likely reflecting its constitutively higher chl-*a* content than RCC809 regardless of light intensity (Six et al., 2008). OTH95 maintained a much smaller ratio of chl-*b* to chl-*a* than RCC809 (around 0.55) in all light qualities (Figure 4.4d). This value is lower than that previously reported for cultures of OTH95 grown in white light at 100μmol photons m^{-2} s^{-1} (0.65) but is consistent with the value (0.56) obtained under the lower light level of 10μmol photons m^{-2} s^{-1} (Cardol et al., 2008, Laviale and Jacques, 2011). The only chlorophyll metabolite content change relative to chl-*a* in OTH95 in response to light quality was a small decrease (around 10%) of MgDVP in red light compared to both blue and green light (Figure 4.4b). As with the accessory pigment data, this demonstrates fewer light quality responses in OTH95 which will produce fewer effects on light capture.

4.3.3 Effect of light quality on the xanthophyll cycle

To assess whether any light quality induces photoprotection through NPQ, the relative contents of xanthophyll cycle pigments were compared. No significant shifts in violaxanthin levels were seen in RCC809, but the relative content of zeaxanthin decreased in blue light while neoxanthin increased. In contrast, xanthophyll levels didn't respond to light quality in OTH95.

The depoxidation state was higher overall in RCC809 than in OTH95 and did not show a significant change between light treatments in either ecotype (Figure 4.5a-b). These results were consistent with previous observations, that levels of NPQ were higher in RCC809 than in OTH95 under all intensities of white light (Six et al., 2009). In addition, they suggested that levels of NPQ were not affected by light quality in either strain.

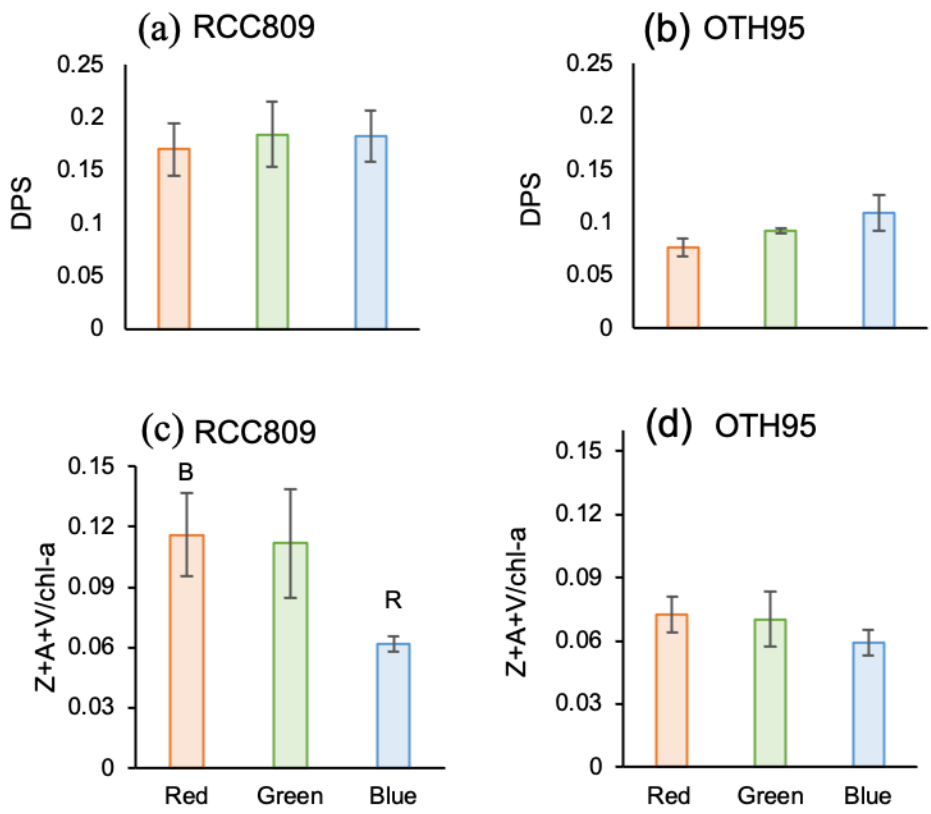

Figure 4.5 Pigment data showing the depoxidation state
(DPS/DES) (Z + 0.5A)/(V + A + Z) of (a) RCC809 and (b) OTH95 as well as the xanthophyll to chl-*a* ratio indicating the xanthophyll pool size of (c) RCC809 and (d) OTH95. Letters indicate significant ($p < 0.05$) comparisons between light responses R red, G green, and B blue. Significance was determined using ANOVA and subsequent student's t-tests. Letters are in bold if $P < 0.01$.

4.3.4 Size of the xanthophyll pool

Total xanthophyll content is higher in light adapted plants than in shade adapted; the larger the xanthophyll pool, the greater the potential for xanthophyll cycle induction for photoprotection (Demmig-Adams, 1990). To indicate the size of the xanthophyll pool, total xanthophyll to chlorophyll *a* (chl-*a*) ratio was calculated as Z+A+V/chl-*a*, where Z, A and V correspond to relative levels of zeaxanthin, antheraxanthin and violaxanthin, respectively. In RCC809, this ratio was smaller (0.06±0.003) under blue light than in red (0.12±0.02) or green light (0.11±0.03). This is likely due to conversion of violaxanthin to neoxanthin (Figure 4.5c). This smaller xanthophyll pool in blue light would be expected to reduce the potential level of xanthophyll cycle induction for photoprotection. The xanthophyll pool size observed here in RCC809 under low intensity blue light was consistent with previous observations across blue light intensities from 25 to 250µmol quanta m^{-2} s^{-1} (Six et al., 2009). This suggests that,

compared to red and green light, blue light signals a decrease in the xanthophyll pool size which is not dependant on light intensity.

No such light quality responsive changes were seen in OTH95 and its xanthophyll pool size was comparable in all conditions to that of RCC809 under blue light (Figure 4.5d).

4.3.5 Ratio of light harvesting pigments to photoprotective pigments

To ascertain whether changes in the accessory pigment contents in response to light quality were strategized for light harvesting or photoprotection, the ratio of light harvesting pigments to photoprotective pigments was compared between light conditions. Pigments were assigned as either light harvesting or photoprotective according to the hypothesised designations from the literature summarised in Table 4.1. Uriolide, micromonal, dihydrolutein, and prasinoxanthin are accessory pigments only found in prasinophyte algae and these are not as well described as the more commonly found pigments such as zeaxanthin (Blatt et al., 2015).

Table 4.1 Details of pigments derived from HPLC measurements

Pigment	Functional detail in literature on prasinophytes	Peaks of light absorbance (nm)	Light quality in which relative content increased	
			RCC809	OTH95
Chlorophyll a	Synthesis increases in low light (7)	~430 + ~660 violet + red (5)	Blue	-
Chlorophyll b	Synthesis increases in low light (7)	~450 +~645 blue + red (5)	Blue	-
Chlorophyllide a	Chlorophyll precursor	~435 + ~663 violet + red (6)	-	-
Chlorophyllide b	Chlorophyll precursor	~470 + ~654 blue + red (8)	Red + green	-
Chlorophyll b-like	Calculated from chlorophyll b response factor. Only found in RCC809 within this experiment	Unknown	Blue	-
Chlorophyll b-like	Calculated from chlorophyll b response factor. Only found in RCC809 within this experiment	Unknown	Blue	-
α-carotene	Also named b,ε-Carotene Increases with light intensity (7)	~422-477 violet-blue (5)	-	-
β-carotene	Increases with light intensity (4) Role in photoprotection (7)	~450-480 violet-blue (5)	-	-

MgDVP	Chl-c like pigment. Light harvesting role (3) Decreases with light intensity (2)	~438 + ~636 blue + red (5) +small ~580 yellow (8)	Blue	Blue + green
Uriolide	Only in prasinophytes. Decreases with light intensity (2,4)	~450-500 blue-green (8)	Blue	Blue
Micromonal	Only in prasinophytes. Decreases with light intensity (2,4)	~440-500 blue-green	Blue	Blue + green
Violaxanthin	Xanthophyll. Light harvesting role, decreases with light intensity (7)	~437-454 violet-blue (5)	-	-
Prasinoxanthin	Only in prasinophytes Light harvesting role (7)	~430-500 violet-green (8)	Red + green	Red
Antheraxanthin	Xanthophyll. Increases with light intensity (7) May be photoprotective (1)	~445-446 violet (5)	-	-
Zeaxanthin	Xanthophyll. Increases with light intensity (7) Photoprotective (1)	~450-483 violet-blue (5)	Red + green	-
Neoxanthin	Light harvesting role (1,7) Decreases with light intensity (7)	~437-455 violet-blue (5)	Blue	Green
Lutein	Increases with light intensity (1,7) Role in PSII photoprotection (1)	~444-474 violet-blue (5)	-	-
Dihydrolutein	Only in prasinophytes. Increases with light intensity (2,7)	~405-456 violet-blue (8)	Blue	Blue + green
Pheophytin a	Degradation product of chlorophyll. Associated with PSII	~418 + ~666 violet + red (5)	-	-
Unknown carotenoid	Decreases with light intensity (2)	Unknown	Blue	-
	(1) (Lopes Dos Santos et al., 2016) (2) (Six et al., 2008) (3) (Six et al., 2005) (4) (Egeland et al., 1995) (5) (Roy et al., 2011) (6) (Lorenzen and Newton Downs, 1986) (7) (Böhme et al., 2002) (8) (Egeland et al., 2011)			

Light harvesting pigments included in calculations were: MgDVP, uriolide, micromonal, violaxanthin, prasinoxanthin, neoxanthin, and the unknown carotenoid. Photoprotective pigments included were α-carotene, β-carotene, antheraxanthin, zeaxanthin, lutein, and dihydrolutein. Pheophytin a was not taken into account because its role is not understood in *Ostreococcus*. Neither ecotype showed significant differences in this ratio between light qualities, although RCC809 showed a higher proportion of light harvesting pigments to photoprotective pigments than OTH95 (p-value = 3.88E-05) (Figure 4.6). This fits the well documented low light adaptation of RCC809 compared to the OTH95 adaptation to higher light intensities (Six et al., 2008, Cardol et al., 2008, Six et al., 2009, Rodríguez et al., 2005).

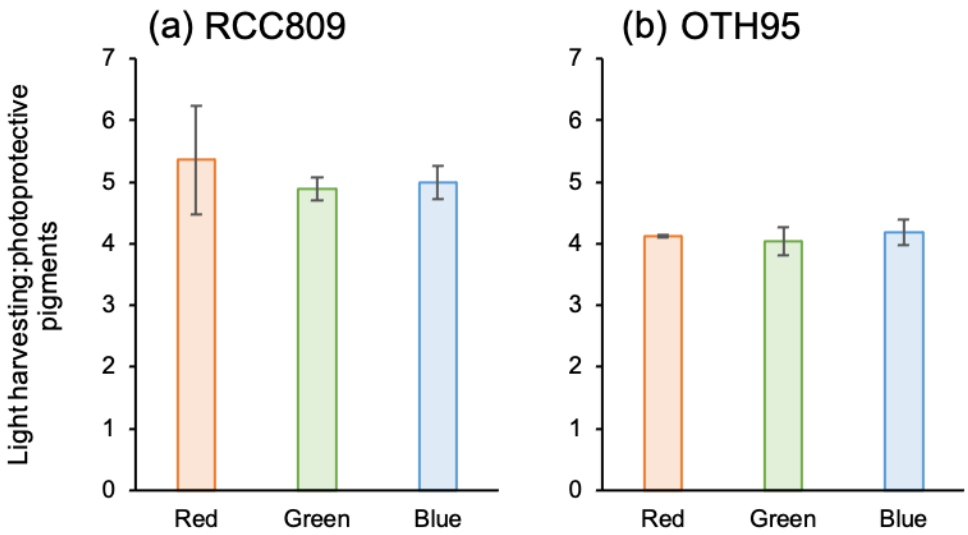

Figure 4.6 Ratio of light harvesting pigments to photoprotective pigments.
Pigments were assigned according to the designations in Table 4.1. Light harvesting pigments: MgDVP, uriolide, micromonal, violaxanthin, prasinoxanthin, neoxanthin, and the unknown carotenoid. Photoprotective pigments: α-carotene, β-carotene, antheraxanthin, zeaxanthin, lutein, and dihydrolutein. (a) RCC809 (b) OTH95.

4.3.6 Effect of light quality on photosynthetic parameters

4.3.7 Maximum quantum yield of PSII

In RCC809 the maximum quantum yield of PSII (Fv/Fm) was significantly different between light qualities, being highest in red (0.63±0.0045), then green (0.57±0.014), and lowest after blue (0.52±0.010) light acclimation (Figure 4.7a). These data are derived from excitation at 470nm. Similar results were observed when different light wavelengths were used for excitation. These quantum yield values were all lower than the Fv/Fm values of about 0.65 reported to be optimal in *Ostreococcus* strains under

standard culture conditions, but they were closer to the value (0.59) reported in RCC809 (in constant blue light at 25µmol quanta m^{-2} s^{-1}) (Botebol et al., 2017, Six et al., 2009).

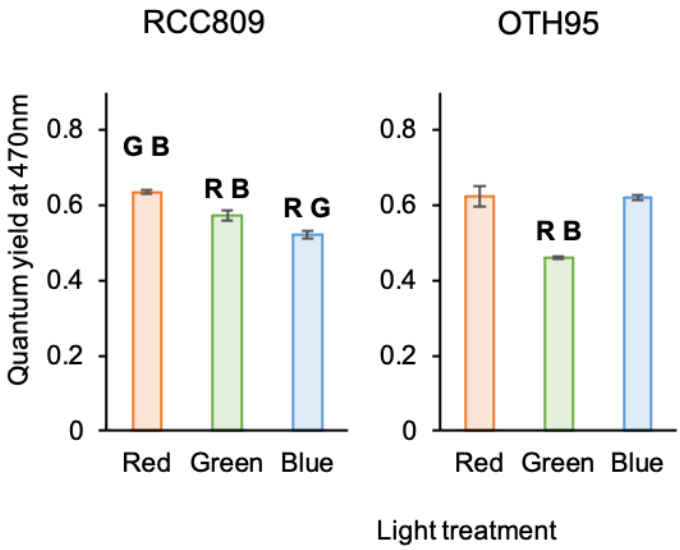

Figure 4.7 Maximum quantum yields of PSII (Fv/Fm)
(a) RCC809 and (b) OTH95. Letters indicate significant (p=<0.05) differences between light responses R red, G green, and B blue. Significance was determined using ANOVA and subsequent student's t-tests. Letters are in bold if P < 0.01.

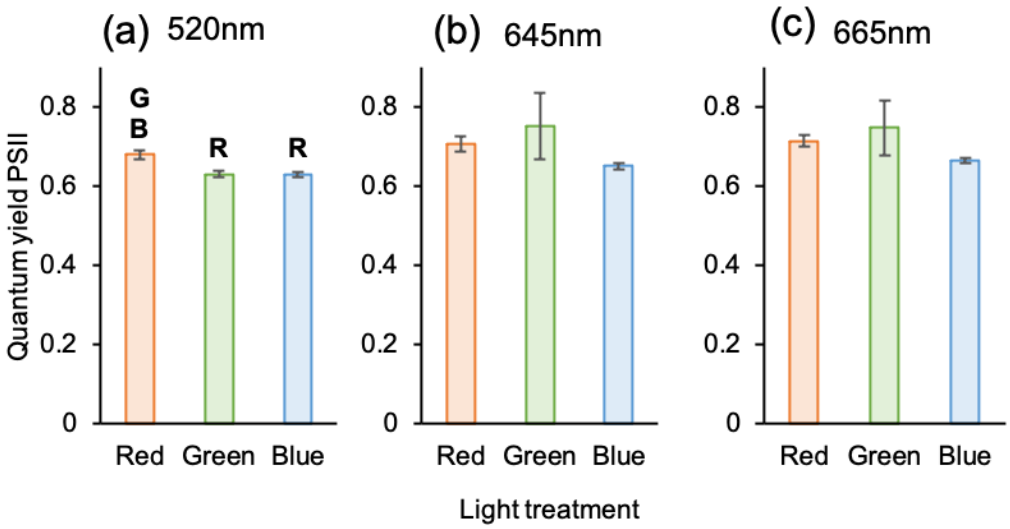

Figure 4.8 Maximum quantum yields of PSII (Fv/Fm) for *Ostreococcus* OTH95 using excitation beams of different wavelengths.
Letters indicate significant (p=<0.05) differences between light responses R red, G green, and B blue. (a to c) indicate 520nm, 645nm and 665nm respectively. Significance was determined using ANOVA and subsequent student's t-tests. Letters are in bold if P < 0.01.

Unlike RCC809, OTH95 showed a different quantum yield response when excited with beams of different wavelengths (Figure 4.8a-c). When excited using blue light at 470 nm, the maximum quantum yield of PSII was lower in cells acclimated to green light (0.46±0.10) compared to red and blue light (0.62±0.020 and 0.62±0.012 respectively) (Figure 4.7b). This was not seen when cells were excited at 520 nm, 635 nm or 665 nm, suggesting that this reduced yield is not due to a reduction in PSII efficiency, but to a reduced relative absorbance of the shorter wavelengths of blue light.

4.3.8 Maximum relative electron transport rate of PSII

rETRmax values give an indication of the maximum relative electron transport rate through PSII. A higher relative electron transport rate (rETR) can indicate stress in plants. Increased rETR may also be explained by an increase in RuBisCO activity as the ratio of RuBisCO content or active sites to PSII positively correlate with ETR values (Sukenik et al., 1987, Zorz et al., 2015, Vandenhecke et al., 2015).

In RCC809, rETRmax was highest in cells acclimated to red light (9.48±1.03), followed by green (6.31±0.56), and blue (3.67±0.70) (Figure 4.9a). This was consistent with the observed decrease in RuBisCO activase gene expression under blue light compared to red and green light (Figure 3.15a). RuBisCO small subunit gene expression was also reduced in blue light compared to green light and was most increased in red light (Figure 3.14).

rETRmax values were much higher in OTH95 (approximately 21) than in RCC809 but did not vary significantly between light conditions (Figure 4.9b). No changes in RuBisCO gene expression between light conditions were seen in OTH95 (Figure 3.15b).

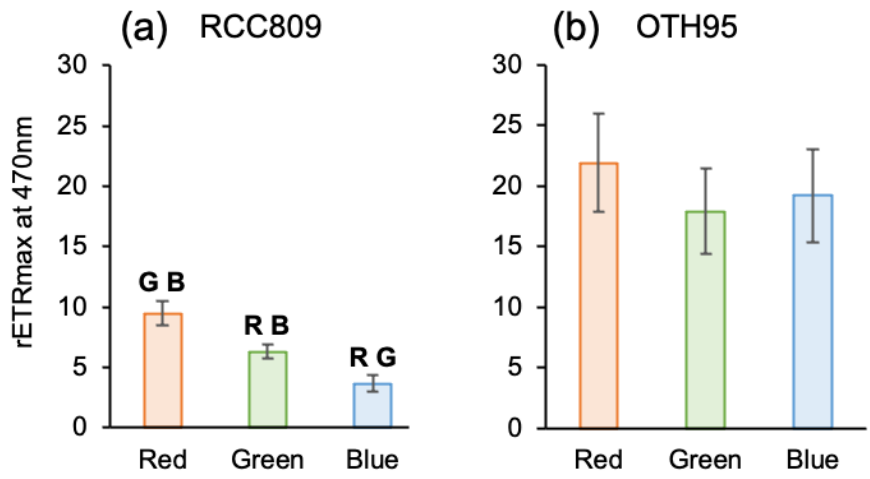

Figure 4.9 Relative ETRmax values recorded at 470nm
(a) RCC809 and (b) OTH95. Letters indicate significance (p=<0.05) compared between light responses R red, G green, and B blue. Significance was determined using ANOVA and subsequent student's t-tests. Letters are in bold if P < 0.01.

4.3.9 Rapid light curves of maximum relative electron transport rate and quantum yield

To determine the effects of light intensity challenge during a short term acclimation, the cells' photosynthetic capacities, and the point of PSII reaction centre saturation by light, rapid light curves were used (Ralph and Gademann, 2005). rETR and quantum yield were measured in rapid light curves of increasing intensities of PAR, section 2.11. The rETR rapid light curve results were in accordance with the rETRmax values recorded for each strain. At all light intensities above PAR 36µmol photons m^{-2} s^{-1}, RCC809 showed higher rETR in red light compared to green and the lowest rETR in blue light (Figure 4.10c). In contrast, OTH95 showed no significant differences in rETR at any light intensity (Figure 4.10d). These results are consistent with previous observations that OTH95 is able to tolerate higher light intensities than RCC809 (Cardol et al., 2008, Demir-Hilton et al., 2011, Six et al., 2008, Six et al., 2009). In addition, they suggest that RCC809 is more able to tolerate high light intensities after acclimation to red light and are saturated at the lowest light intensities after blue light acclimation. The green light acclimated cultures showed an intermediate response.

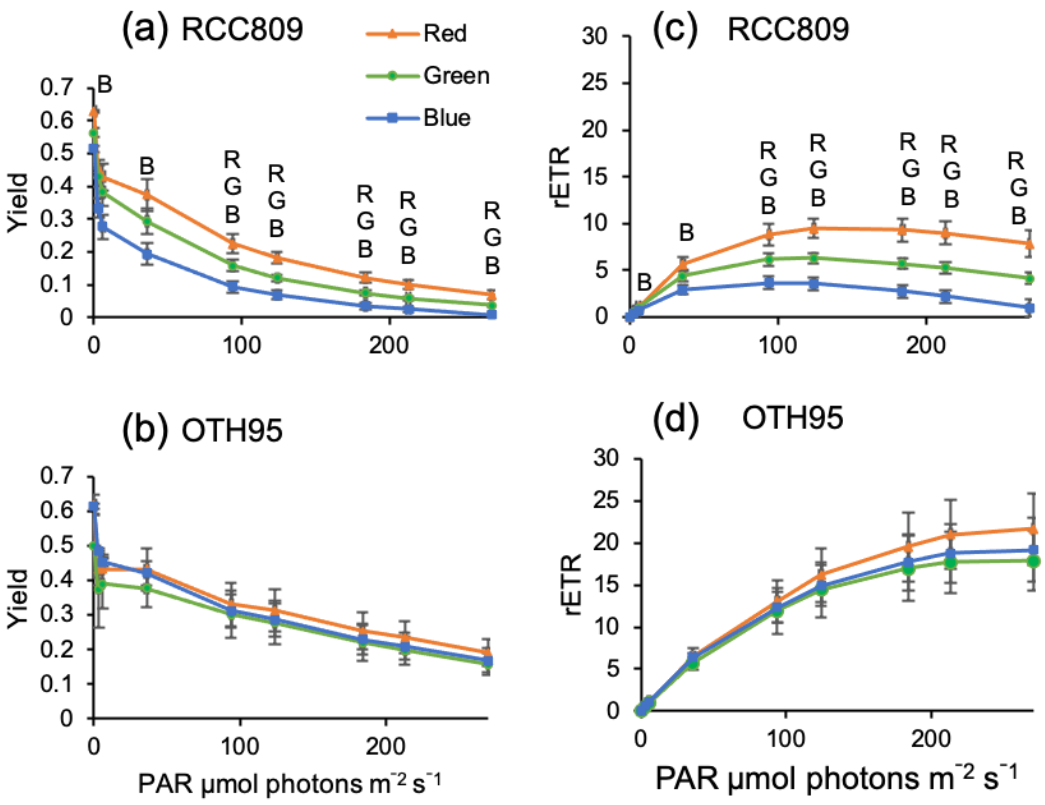

Figure 4.10 rETR and yield along light curves of increasing PAR (µmol photons m^{-2} s^{-1}) at 470nm. Letters for RCC809 rETR and yield curves indicate significance (p=<0.05) compared between light responses R red, G green, and B blue. Significance was determined using ANOVA and subsequent student's t-tests. OTH95 rETR and yield curves did not show any significant differences. (a to b) show yield vs PAR for RCC809 and OTH95 respectively. (c to d) show rETR vs PAR for RCC809 and OTH95 respectively.

PSII quantum yield curve measurements are calculated as ΦPSII= (F'm−Ft)/ F'm where F'm is the maximum fluorescence in the light exposed sample and Ft is the steady state of fluorescence in the light between saturating light pulses (Heinz and Walz, 2003). During a quantum yield curve, increased PAR intensities cause a reduced yield as the reaction centres of PSII close and NPQ increases. The fluorescence yield is also decreased due to photochemical quenching as electron transfer is increased, and this can be seen by the corresponding rise in rETR (Maxwell and Johnson, 2000). As with the rETR rapid light curves, RCC809 showed significantly different quantum yield curves between cells acclimated to red, green or blue light (Figure 4.10a). The RCC809 yield was highest in the red light and lowest in the blue light acclimated cultures. This is evidence of significantly different responses to each light quality in this ecotype and that red light acclimated cultures are saturated at higher light intensities than the blue light acclimated cultures. In contrast, OTH95 showed no

significant differences in quantum yield at any stage of the rapid light curve (Figure 4.10b).

4.3.10 Alpha and Ik values

The alpha value indicates the photosynthetic efficiency and changes in this value may be explained by a number of factors: the level of NPQ, the levels of light harvesting accessory pigments, the ratio of PSI to PSII, the efficiency of energy transfer from the antennae to the PSII reaction centres, and the activity of RuBisCO (Serôdio et al., 2006, Behrenfeld et al., 2004). A change in NPQ may be ruled out as the pigment content analysis showed no evidence for increased NPQ or photoprotective pigments as a response to light quality. The alpha value is measured as the maximal slope of the light response curve (rETR vs PAR) and indicates the efficiency of light absorption in terms of the maximal PSII quantum yield. This is calculated as the maximal yield multiplied by 0.42 (a PSII absorptivity constant for measurements derived from relative ETR). In RCC809 the alpha value was significantly lower in the blue light (0.12 ± 0.017) treated cultures than in the red (0.19 ± 0.030) suggesting that the efficiency of PSII has been reduced (Figure 4.11a-b).

The Ik values demonstrate the irradiance at which light saturation occurs, the covariance of the Ik values with the alpha values indicate that the differences in these values between the light conditions is due to photoacclimation. The Ik (alternatively known as Ek) value is measured as alpha/rETR max and corresponds to the irradiance in µmol photons m^{-2} s^{-1} at the onset of light saturation. In RCC809, the Ik values were significantly lower in blue light (31.4µmol photons m^{-2} s^{-1} ± 2.40) than in red (50.4µmol photons m^{-2} s^{-1} ± 8.30) or green (43.6µmol photons m^{-2} s^{-1} ± 3.08) light (Figure 4.11c-d). This shows that light saturation occurred at a lower PAR intensity in the RCC809 cultures which had been acclimated to blue light. In OTH95, Ik values were significantly higher (approximately 100µmol photons m^{-2} s^{-1}) than in RCC809, but no significant differences were seen between the light treatments indicating an absence of light quality response in OTH95. Higher Ik values, and therefore saturation at higher light intensities, are expected in OTH95 as this ecotype is well described as a high light adapted species compared to the low light RCC809 (Six et al., 2008, Six et al., 2009, Cardol et al., 2008, Rodríguez et al., 2005).

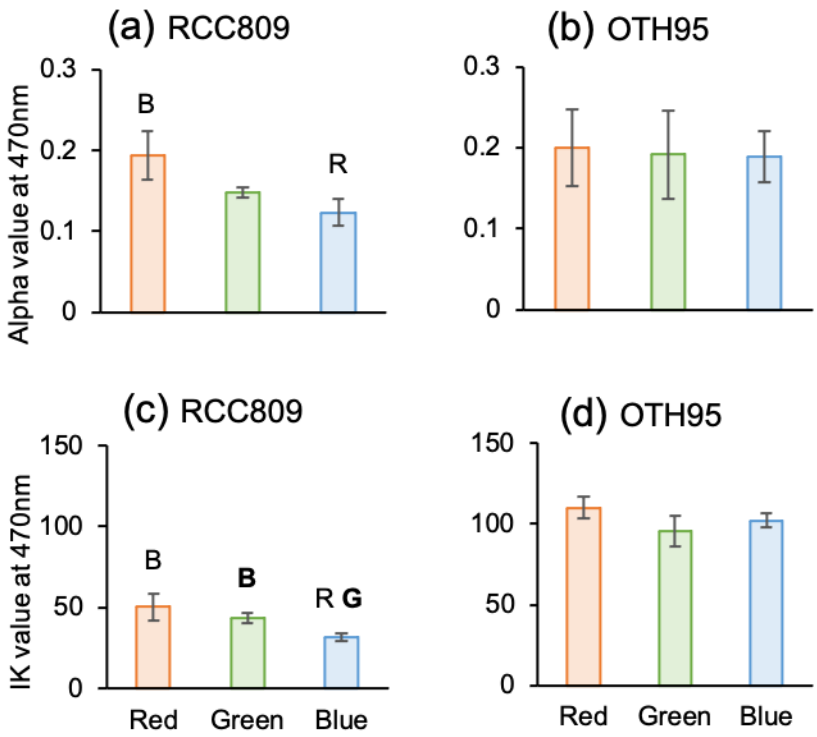

Figure 4.11 Alpha and IK values for *Ostreococcus* under different light qualities.
Letters indicate significance (p=<0.05) compared between light responses: R red, G green, and B blue. (a to b) show alpha values for RCC809 and OTH95 respectively. (c to d) IK values for RCC809 and OTH95 respectively. Significance was determined using ANOVA and subsequent student's t-tests. Letters in bold are if P=<0.01.

4.4 Discussion

The experiments in this chapter revealed physiological changes in RCC809 in response to light quality. These changes were seen in pigment content and photosynthetic parameters.

4.4.1 The ocean *Ostreococcus* ecotype RCC809 shows changes in pigment content in response to light quality

Consistent with the transcriptomic data in chapter 3, the physiological changes after blue light acclimation in RCC809 were most different from the red and green light responses. The transcriptional data showed that expression of chlorophyll synthesis genes was reduced after blue light acclimation, but gene annotations were not sufficient to specify changes in chl-*a* versus chl-*b*. Pigment analyses revealed that relative contents of chlorophylls and accessory pigments in RCC809 varied in response to light quality. The most pronounced of these responses was that of the

higher chl-*b* to chl-*a* ratios in blue light as well as greatly increased levels of two novel chlorophyll *b*-like pigments only seen in RCC809. The relative contents of several accessory pigments also showed significant changes after blue light acclimation when compared to red and green light. The gene expression data in Chapter 3 showed reduced expression of genes with roles in violaxanthin and lutein synthesis under blue light which suggested an increase in NPQ for photoprotection. Analysis of the relative levels of xanthophylls to determine the depoxidation state showed that NPQ was not induced under any light quality, but that the size of the total xanthophyll pool was smaller after blue light acclimation.

4.4.2 Chromatic adaptation

The pigment content experiments in this chapter show evidence of complementary chromatic adaptation in *Ostreococcus* RCC809. The ratio of chl-*b* to chl-*a* increased significantly from red light to a positive value in blue light. This increase in chl-*b* optimises capture of blue light wavelengths present in deep water environments as chl-*b* maximally absorbs blue light (Kume et al., 2018, Lichtenthaler, 1987, Bouman et al., 2000). Two chlorophyll *b*-like pigments only seen in RCC809 also increased under blue light and may also assist in the efficient absorption of blue light.

The accessory pigments in RCC809 do not show evidence of contribution to chromatic adaptation as changes in their abundance were not consistent with increased light absorption under any light quality (Table 4.1). Furthermore, changes in these pigments are small compared to the large changes in chl-*b* and the two chlorophyll *b*-like pigments.

4.4.3 RCC809 shows changes in photosynthetic parameters in response to light quality

As seen in the pigment data, the measured changes in photosynthetic parameters in response to light were most pronounced when comparing red and blue light, although here the green light acclimated cultures also showed some intermediate responses. This shows acclimation to the light treatments and that RCC809 responds specifically to each condition.

The maximum PSII quantum yield (Fv/Fm) and rETRmax values were lowest in blue light and highest in red light. The rapid light curves of quantum PSII yield and ETR also showed lower values after blue light acclimation (Figures 4.10 a and c). These changes in photosynthetic parameters indicate that in blue light the photosynthetic

efficiency of PSII is reduced and that this photosystem is saturated by light at lower intensities than after red and green light acclimation. The results suggest that PSII content or PSII activity is reduced in blue light in RCC809. The PhytoPAM measurements taken do not enable PSII content or PSI activity to be measured although the transcriptional data add context for these responses (Murchie and Lawson, 2013). The relative increase in chl-*b*, normally associated with PSII antennae (Melis, 1989), and the elevated expression of genes associated with PSII assembly and ferritin synthesis under blue light, together suggest that the reduced efficiency of PSII in blue light is most likely caused by a reduced PSII activity, rather than reduction in PSII content.

Photosystem II, antennae, and light harvesting complexes

Chl-*b* mostly is bound to the PSII antenna in light harvesting complexes (LHCs) whilst chl-*a* is also present in the reaction centres (Melis, 1989). Antennae are used for light harvesting and transfer of energy to the photosystems, their pigment contents may vary to efficiently capture light of different spectral qualities (Six et al., 2005, Wlodarczyk et al., 2015). Antennae can also protect the core photosystem complexes from damage by excess light (Saito et al., 2010, Alboresi et al., 2009). The ratio of chl-*b* to chl-*a* is almost twice as high in RCC809 than in OTH95; this was proposed to be linked to higher LHCP levels in RCC809 (Cardol et al., 2008). LHCPs are prasinophyte light-harvesting chlorophyll *a*/*b* binding proteins associated with the antenna; MgDVP is also bound to these complexes (Six et al., 2005). The rise in chl-*b* to chl-*a* ratio and the MgDVP content in blue light may both be related to an increased LHCP content in RCC809. Of the five genes in RCC809 with inferred annotations of 'prasinophyte specific chlorophyll *a*/*b*-binding protein', three did not show specific transcriptional light responses (Od01g01780, Od06g06020/30, and Od17g03160), but two were upregulated in blue light when compared to red light: Od07g02900 and Od14g00280. The expression profiles for these two genes are strikingly similar (Figure 4.12) which warrants further investigation. Increased expression of these LHCP proteins under blue light is again inconsistent with a decrease in PSII content under blue light.

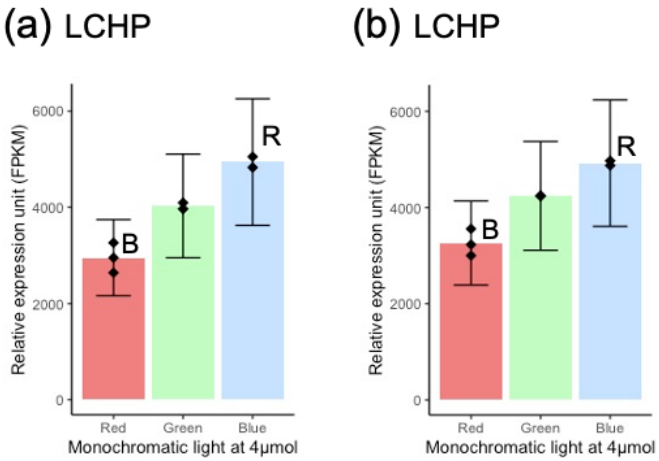

Figure 4.12 Expression levels of light responsive putative LHCP genes in RCC809
(a) Od14g00280 (b) Od07g02900. Letters indicate significant (p=<0.05) differences after false discovery rate correction with either red (R) red, green (G), and blue (B) conditions.

RuBisCO content and activity are limiting factors for ETR

Rather than changes in PSII activity, the lower rETRmax in blue light may alternatively be explained by a decrease in RuBisCO activity. The transcriptional expression of the RuBisCO small subunit and RuBisCO activase enzyme were reduced in blue light in RCC809 (Figures 3.14 and 3.15a-b). RuBisCO is a rate limiting factor in electron transport and its activity correlates with ETR (Zorz et al., 2015, Vandenhecke et al., 2015, Sukenik et al., 1987). It has been shown that silencing RuBisCO activase results in lower ETR values in *Oryza sativa* (Yamori et al., 2012).

4.4.4 Comparison with light intensity responses

Some RCC809 blue light quality responses resemble low light responses

In a higher light environment prasinophyte green algae produce more photoprotective pigments, and in a low light environment these pigments are converted to light harvesting pigments to maximise light capture (Six et al., 2008). In blue light, the increase in the low light associated and light harvesting MgDVP, uriolide, micromonal, and the unknown carotenoid, and the decrease in the photoprotective zeaxanthin, are consistent with this (Figures 4.3a and 4.4a). Neoxanthin has been shown to have a photoprotective role in higher plants by functioning as an antioxidant in PSII (Dall'Osto et al., 2007). In a mamiellophyte, however, neoxanthin accumulated in low light through conversion from violaxanthin and was degraded in high light (Böhme et al., 2002). From this, it was hypothesised that neoxanthin was involved in

light capture at low light intensities and was degraded for synthesis of photoprotective pigments at higher light intensities (Böhme et al., 2002). The increase in neoxanthin in blue light in RCC809 may therefore also be similar to a low light response. The increase of MgDVP in blue light relative to chl-*a* may also cause an accumulation of Chl *c* CS-170 which is found in RCC809 but not in OTH95. Chl c CS-170 was not quantified in this study due to lack of an appropriate standard but it is related to MgDVP and also accumulates at low light intensities (Álvarez et al., 2013, Rodríguez et al., 2005).

Higher relative levels of chl-*b* were observed in RCC809 in blue light; this also shows similarity to a low light response. The chl-*b* to chl-*a* ratio in OTH95 decreases with increasing light irradiance (Laviale and Jacques, 2011), and it was hypothesised that clade B *Ostreococcus* strains maintain higher chl-*b* to chl-*a* ratios to maximise light capture in low light environments (Rodríguez et al., 2005). This increase in chl-*b* in blue light suggests a shift towards maximising light capture by more efficient absorption of this wavelength by acclimating to the depth environment associated with the prevalence of blue light. Levels of chlorophyll as well as the ratio of chl-*b* to chl-*a* have been shown to increase with depth in the oceans and, although this reflects the shifts in dominant phytoplankton species at depth, it also illustrates the benefit of altering chlorophyll content strategy (Letelier et al., 2017, Bouman et al., 2000). This shows that light quality as well as light intensity can affect the ratio of chl-*b* to chl-*a* in *Ostreococcus*, and that in RCC809 this ratio increases in blue light.

Increased PSII content in blue light, suggested by the higher chl-*b* to chl-*a* ratio and the transcriptomic data, is also expected in low light intensities in RCC809 (Six et al., 2008). RCC809 and OTH95 respond differently to low light intensities (15-18μmol quanta m^{-2} s^{-1}); in low light OTH95 increases PSII content (as measured by the absorption cross-section of PSII), and RCC809 increases PSII antenna size (as determined by changes in antenna protein content) (Six et al., 2008). The hypothesis of that study was that RCC809 photoacclimates to low light by increasing antenna size as this strategy incurs a smaller nutrient cost than antenna synthesis, OTH95 in its lagoon source environment is not limited in this way (Six et al., 2008). PSI has a high iron content and the lower PSI:PSII ratio in RCC809 than in OTH95 is attributed to the ecological constraint of low iron levels available in the oligotrophic RCC809 source environment (Cardol et al., 2008).

After acclimation to red and green light, RCC809 also exhibited some specific responses which prepare the cells for higher light intensities; the Ik values showed saturation at higher light intensities than in blue light, and the xanthophyll pool sizes increased. The larger xanthophyll pool after acclimation to red and green light increases potential for NPQ (Demmig-Adams, 1990). The Ik values which describe the onset of light saturation varied with light quality in RCC809. The higher Ik values in red and green light than in blue light may be explained by the optical depth signalled by the light treatments. An analysis of Ik in phytoplankton communities at various depths found that the average Ik decreased rapidly with depth from around 75-150µmol photons m^{-2} s^{-1} in the top 20m to around 25µmol photons m^{-2} s^{-1} at a depth of 100m (Bouman et al., 2018, Bouman et al., 2000). These values are comparable to those determined in this chapter (Figure 4.11c-d)). Bouman et al. (2000) explained this reduction in Ik values with depth as being a result of photoacclimation and photoadaptation. From this, it may be expected that Ik would be lowest in a deep water ecotype like RCC809 which has acclimated to low intensity blue light. An increase in the alpha values (the initial slope of light curves) with depth was also observed in the same studies of phytoplankton communities but this was shown to be due to variation in nitrogen with depth (a nitracline) rather than due to irradiance or spectral qualities associated with depth (Bouman et al., 2000).

Higher relative levels of chl-*b* were observed in RCC809 in blue light, this also shows similarity to a low light response. The chl-*b* to chl-*a* ratio in OTH95 decreases with increasing light irradiance (Laviale and Jacques, 2011), and it was hypothesised that clade B *Ostreococcus* strains maintain higher chl-*b* to chl-*a* ratios to maximise light capture in low light environments (Rodríguez et al., 2005). This shows that light quality as well as light intensity can affect the ratio of chl-*b* to chl-*a* in *Ostreococcus*, and that in RCC809 this ratio increases in blue light.

In the aquatic environment, light quality responses may allow photosynthetic algae to anticipate other environmental parameters associated with different depths. A possible hypothesis is that RCC809 senses red light as an environmental indicator of proximity to surface waters, where red light wavelengths are found, and uses this signal to adjust its photosynthetic machinery in anticipation of higher light intensities. This idea has been posited as an explanation of red light responses in the diatom *Phaeodactylum tricornutum* (Fortunato et al., 2016). On the other hand, this ecotype may use blue light, or a low red to blue light ratio, as an indicator of depth, as it persists in deeper

water. It may then respond by adjusting its physiology to maximise light capture under low light intensities. The increase in relative chl-*b* content in blue light presents the strongest evidence that low intensity blue light signals depth in RCC809 as it stimulates physiological responses that maximise light capture which are not induced in low intensity red or green light qualities. This allows acclimation to the depth environment associated with the prevalence of blue light.

The blue light responses in RCC809 recorded in these experiments also show evidence for the anticipation of other environmental factors associated with depth. The reduced relative maximum electron transfer rate (quantified as rETRmax) in blue light, and its increase under red light (Figure 4.9a), was linked to corresponding changes in expression levels of the RuBisCO small subunit and RuBisCO activase (Figure 3.14 and 3.15a). The effect of reduced RuBisCO activase on rETR can be compensated for by sufficiently high CO_2 concentrations, as demonstrated in the green alga *Chlamydomonas reinhardtii* (Pollock et al., 2003). CO_2 increases with depth so less RuBisCO activase synthesis is required in the deep ocean environment to maintain RuBisCO activity. Pollock et al also showed that the growth rate in *Chlamydomonas reinhardtii* was reduced in the absence of RuBisCO activase. Here, the growth rate was found to be fastest in blue light in RCC809, although in this case RuBisCO activase is reduced rather than absent. This may explain the decrease in RuBisCO activase transcription in blue light in RCC809, as well as the reduction in rETRmax as the CO_2 levels would not have increased correspondingly to compensate for this. Blue light may therefore induce a reduction in RuBisCO activase activity in anticipation of a CO_2-rich environment. These changes in RuBisCO gene expression and in rETR show how blue light may induce responses in RCC809 which allow it to anticipate and adapt to environmental change.

Some of the pigment changes do not fit this hypothesis of blue light as a signal for depth: the decrease in blue light of the light harvesting prasinoxanthin, the lack of changes in the photoprotective α-carotene, β-carotene, antheraxanthin, and lutein contents, and the lack of change in the light harvesting violaxanthin (Table 4.1) (Böhme et al., 2002). The relative xanthophyll pigment contents also showed no evidence of induction for NPQ in any light quality which shows that, while blue light responses may resemble low light intensity responses, the red and green light responses do not resemble high light intensity responses. A study of RCC809 carotenoid content changes with light intensity showed that in high light dihydrolutein

increased while uriolide, the unknown carotenoid, MgDVP, micromonal, and Chl CS-170 all decreased (Six et al., 2008). Uriolide, the unknown carotenoid, MgDVP and micromonal did follow this pattern by decreasing in blue light compared to red and green, but dihydrolutein levels increased in blue (Figures 4.3a and 4.4a). Laviale and Jacques (2011) studied pigment contents in OTH95 and found that dihydrolutein did not vary with light intensity. These changes, particularly that of dihydrolutein show that, although there are similarities to light, the light quality responses are distinct from light intensity responses. Furthermore, these changes show that no light quality response in terms of pigment content changes can be solely explained by either an increase in photoprotective pigments, or light harvesting pigments.

4.4.5 Light qualities as a function of their energy and relative absorbance for photosynthesis

While equal light intensities were used for all monochromatic light treatments, it was possible that the energy levels of the different wavelengths of light may result in effectively different light intensity responses. Most of the light harvesting in *Ostreococcus* is by chlorophylls *a* and *b* which primarily absorb light in the red and blue areas of the visible light spectrum and of these the shorter wavelengths of blue light are higher energy (Bouman et al., 2018, Kume et al., 2018, Lichtenthaler, 1987, Lanoue et al., 2019). If the light quality responses seen in these experiments could be explained by reactions to differing effective light intensities produced by the light qualities, then it would be expected that responses to the higher energy blue light would match that of higher light intensity, and the responses to red and green light would resemble a low light response. These experiments do not show this pattern, instead showing that the blue light responses are more similar to low light intensity responses. This allows a rejection of this hypothesis by demonstrating that the responses observed are responses to specific light qualities rather than to different energy levels provided by the different wavelengths.

4.4.6 Comparison with the lagoon ecotype OTH95

Fewer light quality responses were detected in the lagoon ecotype OTH95 than in the ocean ecotype RCC809, both in terms of pigment content and in photosynthetic parameters. As in RCC809, OTH95 showed a small increase in relative contents of the accessory pigments micromonal and dihydrolutein in blue light compared to red or

green (Figure 4.3b). Other changes in pigment content seen in RCC809 in response to light quality were not demonstrated in OTH95.

The photosynthetic measurements of OTH95, as with the pigment data, revealed fewer light quality responses and those seen were only in green light (in terms of a lower quantum PSII yield) compared to red and blue light (Figure 4.7b). Uniquely among these measurements, the quantum yield of PSII in green light in OTH95 was dependant on the wavelength of the measuring beam. The green light acclimated yields were lowest when excited with a blue measuring beam (470nm), higher from the green beam (520nm) and higher again in the two higher wavelength red beams (645nm and 665nm) in which the yield was not different from the other light acclimated cultures (Figure 4.8a-c). This effect is not explained by the pigment data but suggests that the efficiency of PSII in green light acclimated OTH95 is dependent on the incident light quality. Kula et al found that in the green alga *Chlorella* the quantum yield of PSII (Fv/Fm) was not affected by light quality but reduced sharply once the cultures reached a high density (Kula et al., 2014). This effect would not explain the lower yield in green light in OTH95 as growth rates did not differ in this ecotype with light quality (Figures 3.1 and 4.7).

No light responsive changes in rETRmax were found in OTH95. Correspondingly, as shown in Chapter 3, no transcriptional changes were seen in OTH95 for RuBisCO small subunit genes or the RuBisCO activase gene (Figure 3.15b). Although direct comparisons of absolute expression values cannot be accurately compared between the ecotypes due to differences in their genomes (such as GC content and level of duplication), the data suggest a lower RuBisCO activase expression in OTH95.

As demonstrated by the rapid light curve derived Ik values (Figure 4.11 c and d), the differences between RCC809 and OTH95 are explained by their well described adaptations to light intensity. The Ik values derived from the rapid light curve of rETRmax showed that OTH95 was predicably saturated at higher PAR levels than RCC809. It was expected that the onset of light saturation in OTH95 would occur at a higher intensity as adaptation to higher light intensities is well established in this ecotype (Six et al., 2008, Six et al., 2009, Cardol et al., 2008, Rodríguez et al., 2005).

4.5 Conclusions

Changes in pigment content suggest that blue light acclimation in RCC809 induces a shift towards maximising capture of blue light wavelengths. The photosynthetic data from the PhytoPAM measurements suggest either a reduction of PSII activity, or an induction of NPQ after blue light acclimation causing lower quantum yields of PSII. The context provided by the pigment data concerning xanthophyll cycle comparisons show that the changes seen in blue light in RCC809 are not due to increased NPQ. The pigment data however, particularly the chl-*b* to chl-*a* ratios, suggest that PSII modification in blue light takes the form of increased PSII antenna size and reduced PSII activity. Both OTH95 and RCC809 show physiological responses to light quality, although compared to RCC809, OTH95 exhibited specific light quality responses in fewer of the parameters measured. Not all of the differences between the ecotypes are explained by their established differing adaptations to light intensity (Six et al., 2008, Six et al., 2009, Cardol et al., 2008, Rodríguez et al., 2005).

The differences in light responses described in this chapter reflect the predominant light qualities in the ecotypes' source environments and present further evidence of adaptation to their ecological niches. For RCC809, sourced at a depth of 105m in the Atlantic Ocean, the light quality in its environment is predominantly low intensity blue unless upwelling causes occasional exposure to red and green light as part of the broader spectrum in surface waters. The light quality environment for RCC809 is therefore variable and perception of red and blue light (or of the ratio between the two) may enable it to gain information about depth and so to adjust its physiology in anticipation of higher or lower light intensities. For OTH95, sourced from the shallow, nutrient rich Thau lagoon, the depth is not variable beyond 10 metres and so the light quality is predominantly higher intensity green light, although wavelengths of both red and blue are also present (Potes et al., 2013). The observation that different ecotypes have evolved light responses that are specific to their environment suggests that responses to light quality contribute to fitness of photosynthetic organisms in the aquatic environment.

Chapter 5: Mechanism of light responses

5.1 Introduction

Chapters 3 and 4 uncovered distinct responses to red, green, and blue light in the ocean *Ostreococcus* ecotype RCC809, in terms of gene expression, photosynthetic activity, growth rate, and pigment composition. Differences in photosynthetic activity and pigment composition were also noted in the lagoon *Ostreococcus* ecotype OTH95 in green light when compared to both red and blue treatments. This chapter presents an investigation of the regulatory mechanisms which may be involved in the coordination of these transcriptional light quality responses.

Regulation of gene expression by environmental inputs such as photoperiod is achieved in higher plants through signalling cascades coordinated by photoreceptors. This allows an organism to respond quickly and sensitively to its environment in order to coordinate processes such as metabolism, or to efficiently maximise light capture for energy (Pireyre and Burow, 2015). Responses to light in plants and phytoplankton are mainly initiated by photoreceptors which contain light sensing domains that undergo conformational changes in response to light. This initiates a cascade of complex downstream responses including autophosphorylation and binding to partner proteins resulting in changes in activity of transcription factors, or chromatin remodelling (Falciatore and Bowler, 2005). In plants, photoreceptors include blue light sensing cryptochromes and phototropins, UVR8 which senses UVB light, and red and far-red light sensing phytochromes (Möglich et al., 2010).

In higher plants, regulation of gene expression by light is mediated by specific transcription factors binding conserved DNA sequence motifs in the promoters of light-responsive genes, leading either to inhibition or to upregulation of transcription (Guilfoyle, 1997, Hiratsuka and Chua, 1997). Light-responsive transcription factors are either more highly expressed in response to light signals, or undergo posttranslational modifications or degradation in the light (Jiao et al., 2007). For example, in *Arabidopsis*, the bZIP transcription factor ELONGATED HYPOCOTYL 5 (HY5) negatively regulates hypocotyl elongation and promotes de-etiolation under red, blue and UV light. *HY5* transcription increases in response to light, and HY5 protein stability also increases due to decreased degradation by CONSTITUTIVE PHOTOMORPHOGENIC FACTOR 1 (COP1) (Jiao et al., 2007, Oyama et al., 1997, Gangappa and Botto, 2016). HY5 binds sequence motifs in the promoters of its target genes, containing the core sequence motif ACGT. This includes the G-box motif

CACGTG, the similar Z-box TACGTG, the CG hybrid GACGTG, and the CA hybrid GACGTA, (Lee et al., 2007). On the other hand, the bHLH phytochrome interacting factors (PIFs) promote expression of genes with roles in hypocotyl elongation and dark-specific phenotypes (Leivar et al., 2008, Franco-Zorrilla et al., 2014, Kim et al., 2003, Monte et al., 2004, Soy et al., 2016). These transcription factors are degraded in response to phytochrome activation by red light. Like HY5, the PIF proteins also bind promoter sequences including G-box motifs (Jiao et al., 2007, Ezer et al., 2017), as does the bHLH transcription factor MYC2, which mediates blue light responses in higher plants (Mallappa et al., 2006, Lee et al., 2007).

Five photoreceptors have been identified in *Ostreococcus:* two histidine kinases (LOV-HK and Rhod-HK), two cryptochromes (CPF1 and CPF2), and phototropin (Phot). However, the light sensing and resultant signalling functions of these photoreceptors have not yet been fully elucidated. In *Ostreococcus,* the LOV-HK photoreceptor has been shown to maximally sense blue light at 450nm, suggesting a role in blue light responses. However, it was also implicated in circadian entrainment by light-dark cycles composed of red light (Djouani-Tahri et al., 2011). On the other hand, Rhod-HK is implicated in circadian entrainment of *Ostreococcus* and shows a shift towards blue light absorbance in response to orange/green light, and a red shifted absorbance in response to blue light (Luck et al., 2019, Thommen et al., 2015). The OTH95 phototropin (OtPhot ostta16g02540) contains two LOV domains, which are distinct from the LOV-HK LOV domains and maximally absorb blue light at 449nm, and a serine threonine kinase domain (Djouani-Tahri et al., 2011). When OtPhot is expressed in transgenic *Arabidopsis*, its described functions include light responsive chloroplast accumulation and stomatal opening (Sullivan et al., 2016).

Transcription factors (TFs) have been identified in *Ostreococcus* based on domain homology to known transcription factors in plants, although little is known about their targets and downstream effects. Two databases: CIS-BP and PlantTFDB show similar information for *Ostreococcus* with some differences in transcription factor total numbers and family allocation. Discrepancies were assessed using BLAST on an individual basis when comparing families in this analysis so that ecotype comparisons could be made. This enabled the identification of 183 transcription factor loci in 26 families for OTH95 (Monnier et al., 2010, Weirauch et al., 2014). Only 123 factors within 29 families were inferred for RCC809 (Riano-Pachon et al., 2007, Weirauch et al., 2014), but this smaller number of transcription factors in RCC809 is by no means

exhaustive and more are likely to be described. Complex regulatory effects may also be produced by the formation of heterodimers between different transcription factors as has been found in bHLH, bZIP, and Myb factor families in higher plants (Jiao et al., 2007). Due to the small size of the *Ostreococcus* genome with little duplication, 97% of its genes are considered orthologous to either *Arabidopsis* or the green algae *Chlamydomonas reinhardtii*, and so these comparisons are informative (de Los Reyes et al., 2017). Of the 183 transcription factor genes in OTH95, 170 show rhythmic expression under light-dark cycles, suggesting regulation by light and/or a circadian clock (Monnier et al., 2010). DNA binding sites have been described for a subset of the *Ostreococcus* transcription factors (Weirauch et al., 2014). The genes which they specifically target have not yet been identified, but this knowledge of transcription factor binding sites is an important resource for identification of candidate regulators of transcriptional responses based on identification of regulatory motifs within promoters.

The aim of this chapter is to begin to elucidate aspects of signal transduction pathways for light regulation of gene expression in *Ostreococcus*. The primary light signalling mechanism was investigated by taking advantage of an existing OTH95 *ko-lovhk* mutant to determine the contribution of the LOV-HK photoreceptor to light quality responsive changes in photosynthetic parameters. Next, to identify transcription factors which may be involved in the light quality response signalling cascades, candidate regulatory motifs were then identified in the promoters of light quality responsive genes. These motifs may represent DNA binding sites for transcription factors which function downstream of photoreceptors and allow insight into the signalling cascades that may be enacted in response to different light qualities.

The objectives of these analyses were as follows:

- To test the role of the LOV-HK photoreceptor in light-quality responses by demonstrating the effect of knocking out the LOV-HK gene on photosynthetic parameters seen in response to light quality in OTH95 in Chapter 4
- To investigate potential mechanisms behind the transcriptional light quality responses by identifying candidate regulatory motifs which may present binding sites for transcription factors resulting in changes in transcriptional gene expression

5.2 Methods

5.2.1 Investigation of the OTH95 LOV-HK photoreceptor

To test whether LOV-HK plays a role in the physiological light quality responses seen in photosynthetic parameters in Chapter 4, the effects of loss of function of this photoreceptor were tested. A knock-out mutant in the OTH95 background was available and obtained from François-Yves Bouget.

Photosynthetic parameters were measured in the OTH95 *ko-lovhk* mutant using pulse-amplitude modulation (PhytoPAM) technology to detect chlorophyll fluorescence as for the two wild type strains in Chapter 4. Cells were acclimated to red, green, or blue light for 72 hours before measurement with light pulses of varying intensity and beams of different wavelengths. Measurements described are a mean of three independent replicates. Significance was determined using an ANOVA and subsequent student's t-tests and the level of significance was assessed as $p=<0.05$ unless otherwise stated.

5.2.1 Investigation of candidate regulatory motifs in the light quality response of RCC809

The deep ocean ecotype RCC809 exhibited extensive differences in gene expression between different light qualities (Chapter 3). To obtain initial clues to the transcription factors that may be involved in coordinating these responses, an investigation was made to find candidate regulatory motifs which may represent binding sites for these factors. Dreme and FIMO tools within the Meme suite were used to identify and locate short motifs of up to 8 bases that were overrepresented within the promoter regions of red, blue, or green light responsive genes, compared to promoter sequences genome wide, full details in section 2.10 (Bailey, 2011). For the purpose of this analysis, promoters were defined as the 250 base region upstream of each gene.

To identify candidates for the transcription factors that bind these motifs, the motifs were compared visually to *Ostreococcus* transcription factor binding site logos in the Catalog of Inferred Sequence Binding Preferences (CIS-BP) database compiled by Weirauch et al. (2014). The binding sites identified in *Ostreococcus* have been predicted for a selection of its transcription factor families. For this database, the closest *Arabidopsis* homologues were identified based on homology within DNA binding domains. DNA binding sites for *Ostreococcus* transcription factors were then

inferred on the basis of this similarity. In addition, a subset of transcription factor binding sites in OTH95 have been determined experimentally using the protein binding microarray (PBM) method. The RCC809 DNA binding sites of transcription factors were then inferred from binding sites of OTH95 homologues (Weirauch et al., 2014).

As the binding site identification for *Ostreococcus* to date in the CIS-BP database was limited in depth and coverage, the promoter motifs were also compared to known transcription factor binding sites in *Arabidopsis* databases which allowed the likely transcription factor family associated with a motif to be determined. These databases were the JASPAR (non-redundant) DNA database/JASPAR Core (2018) plants, and *Arabidopsis* DNA Plant (motifs in these databases are determined using two methods: DNA affinity purification (DAP-seq) or protein-binding microarray (PBM) (O'Malley et al., 2016, Fornes et al., 2020). This comparison was made by detecting the similarity of the promoter motif sequences to binding sites of *Arabidopsis* transcription factors using the TOMTOM alignment tool in the MEME suite as detailed in section 2.10 (Gupta et al., 2007).

5.3 Results and discussion

5.2.1 Investigation of the OTH95 LOV-HK photoreceptor effect on photosynthetic activity in response to light quality

As photoreceptors in plants and green algae are a primary mechanism for sensing light and coordinating responses, these receptors are key to understanding light quality response mechanisms. The LOV domain containing histidine kinase photoreceptor, LOV-HK has been shown to have a role in controlling blue light responses and the entrainment of the circadian clock to red and blue light signals in the OTH95 ecotype of *Ostreococcus* (Djouani-Tahri et al., 2011). However, its effect on photosynthetic parameters has not been tested.

As with OTH95, this *ko-lovhk* mutant showed few changes in photosynthetic parameters in response to light quality. As shown in Chapter 4.23, the wild type showed a lower maximum quantum yield of PSII when excited by blue light at 470nm after growth in green light, as compared to after growth in red or blue light. This response was abolished in the *ko-lovhk* mutant which demonstrated similar yields in

all light treatments (Figure 5.1a, b). The quantum yield of PSII in green light was significantly lower in the OTH95 wild type compared to the *ko-lovhk* mutant ($p = 0.017$). Ik values were also higher in the *ko-lovhk* mutant after acclimation to red light compared to green light (Figure 5.1c-d). On comparison of the mutant and wild type responses, it would appear that this is due to an increase in light intensity required for saturation in the red light acclimated mutant as the green light response is not altered.

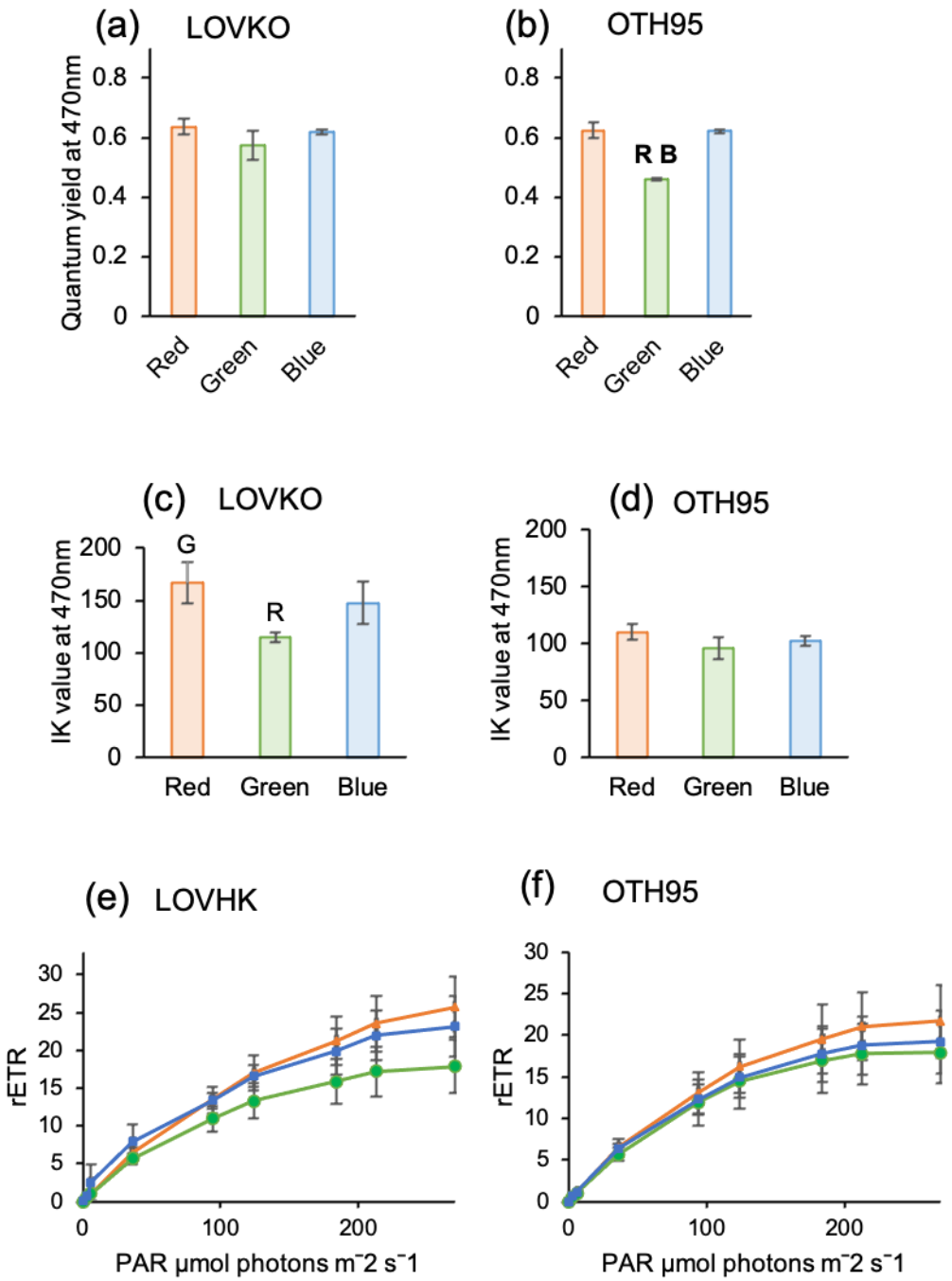

Figure 5.1 Light quality responses in the photosynthetic machinery.
Maximum quantum yields of PSII (Fv/Fm) in (a) LOV-HK mutant and (b) OTH95. IK values in (c) LOVHK mutant and (d) OTH95. rETR along light curves of increasing PAR (µmol photons m^{-2} s^{-1}) at 470nm in (e) LOVHK mutant and (f) OTH95. Letters indicate significant ($p < 0.05$) differences between light responses R red, G green, and B blue. Letters in bold if $P < 0.01$.

These results demonstrate that, in the OTH95 ecotype, the LOV-HK photoreceptor acts to modulate the quantum yield and the light harvesting capacity of PSII, resulting in decreased photosynthetic activity in red and green light. This suggests a role for LOV-HK in the perception of green light, or alternatively, the absence of red and blue light.

The PSII yield and electron transfer rate showing PSII photosynthetic activity did not increase significantly in red light alongside the Ik in the *ko-lovhk* mutant, and it is not possible from these data to determine whether this increased light intensity required for saturation results from changes in photosynthetic activity or non-photochemical quenching (Figure 5.1). It may be that the LOV-HK reduces the intensity of light absorbed by red light acclimated cells as a photoprotective mechanism due to the high light levels and presence of red light in the shallow environments to which OTH95 is adapted (Demir-Hilton et al., 2011). The lack of light quality responsive changes in transcriptional expression of the LOV-HK gene in OTH95 (Figure 5.2c) show that the differences in photosynthetic parameters between the wild type and *ko-lovhk* mutant are induced by the LOV-HK photoreceptor rather than by regulation by changes in its level of gene expression (Figure 5.1)

RCC809 photoreceptor activity

As RCC809 showed a greater physiological light quality response in photosynthetic parameter changes than OTH95, it can be predicted that further effects induced by the LOV-HK photoreceptor may be seen and an RCC809 *ko-lovhk* mutant would prove informative. The possibility of altered LOV-HK function in light quality responses in RCC809 is further supported by the elevated expression of both the LOV-HK genes in red light in this ecotype when compared to both blue and green light, (fold changes between red and blue: 1.1 Od09g04310 and 0.49 Od09g04300) which contrasts with the absence of response in OTH95 (Figure 5.2a-c).

Other *Ostreococcus* photoreceptors in RCC809 may also play roles in light quality sensing and regulatory responses that the photoreceptors in OTH95 do not. The RCC809 phototropin (Od15g00300) was also more highly expressed in red light compared to blue light (fold change 0.49) (Figure 5.2d). In contrast, the expression of the OTH95 gene was not affected by light quality.

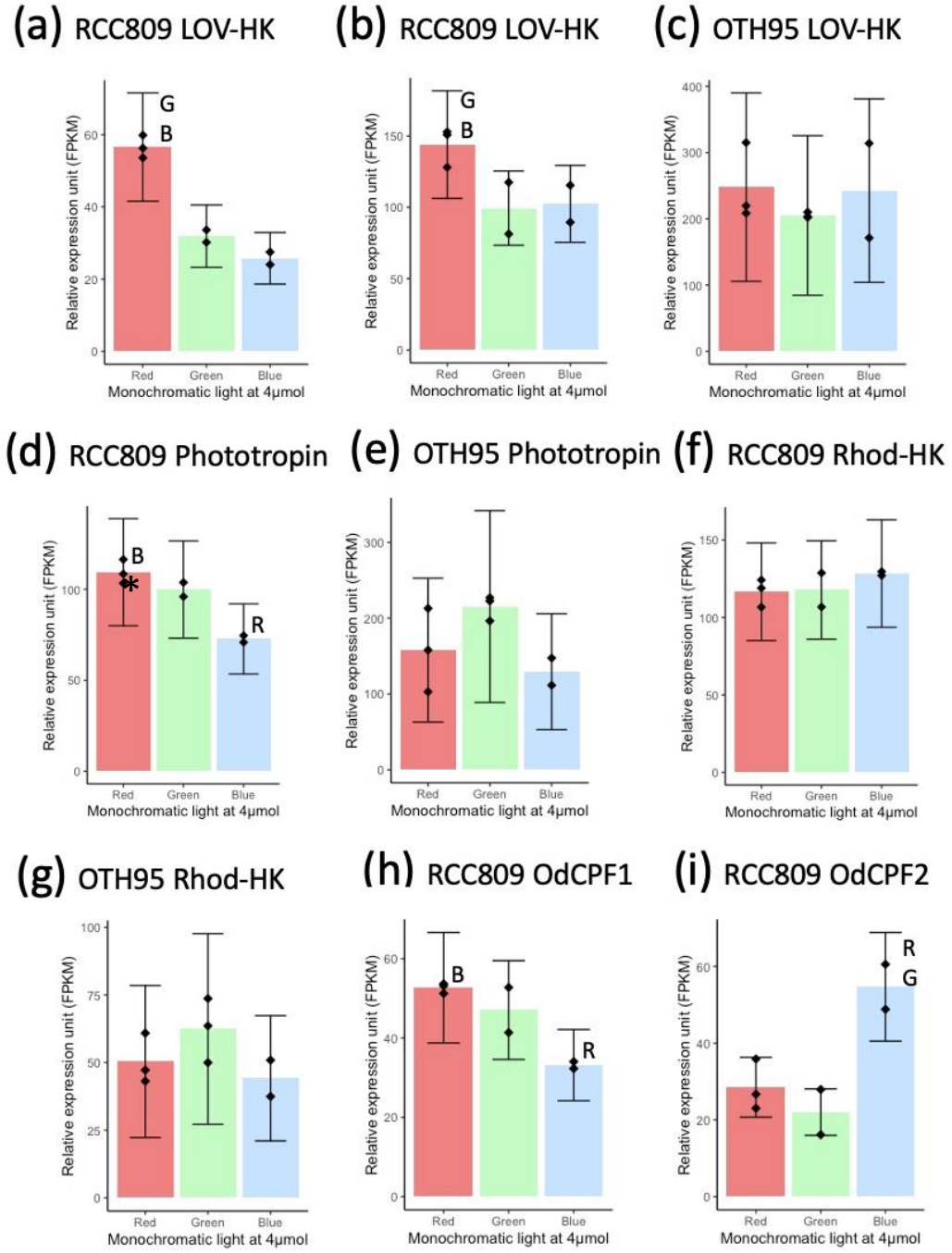

Figure 5.2 Photoreceptor expression
(a) RCC809 Od09g04310 and (b) RCC809 Od09g04300 both show significant rise in red light (c) OTH95 homologue ostta09g02190 showing no light quality response (d) Od15g00300 phototropin (e) OTH95 ostta16g02540 Phototropin (OtPhot) showing no response (f) Od16g01400 Rhod-HK (g) OTH95 Rhod-HK ostta17g01230 showing no response (h) OdCPF1 Od05g00310 (i) OdCPF2 Od01g00210. Letters indicate significant (p=<0.05) differences after false discovery rate correction with either red (R) red, green (G), and blue (B) conditions.

Rhod-HK is encoded by a single gene in OTH95 (ostta17g01230) and neither this gene nor its homologue in RCC809 (Od16g01400) showed any significant differences in expression level in response to the light quality treatments (Figure 5.2f-g).

Photoreceptor genes from two cryptochrome families have been analysed in OTH95: OtCPF1 (ostta05g00270) which is required for circadian entrainment in OTH95, and OtCPF2 (ostta01g06470) which is in the family of Cry-DASH cryptochromes (Kottke et al., 2017, Heijde et al., 2010). The two RCC809 homologues for the OTH95 cryptochrome genes, as identified here by reciprocal BLAST, showed opposing light quality transcriptional responses: OdCPF1 (Od05g00310) increased expression in red versus blue light (fold change 1.67) (Figure 5.2h), and OdCPF2 (Od01g00210) was more highly expressed in blue light (fold change 1.94) (Figure 5.2i). This suggests that the light quality responses of these two cryptochromes are divergent from one another in RCC809.

5.4 Regulatory element investigation – Identification of overrepresented promoter motifs in RCC809 light responsive genes

At least one motif was overrepresented in the promoters of genes in RCC809 which were responsive to each of the light quality treatments as described in Table 5.1. The numbers of light responsive genes containing each of these promoter motifs is shown in Figure 5.3.

Table 5.1 Overrepresented promoter motifs in light responsive genes in RCC809.

Light responsive numbers show how often this promoter motif occurred in sets of light responsive genes.

Genome wide numbers show the number of times this promoter motif is present genome wide.

Light response	Motif	Light responsive	Genome wide	Motif 2	Light responsive	Genome wide
Up Red		9 in 32 p = 1.4E-07	213 in 7923			
Up Green		37 in 60 p = 1.0E-06	2454 in 7923			
Up Blue		33 in 536 p = 1.7E-10	117 in 7923		163 in 536 p = 1.6E-07	1632 in 7923
Down Red		7 in 14 p = 2.1E-10	100 in 7923			
Down Blue		91 in 472 p = 2.1E-25	404 in 7923		24 in 472 p = 3.5E-12	55 in 7923

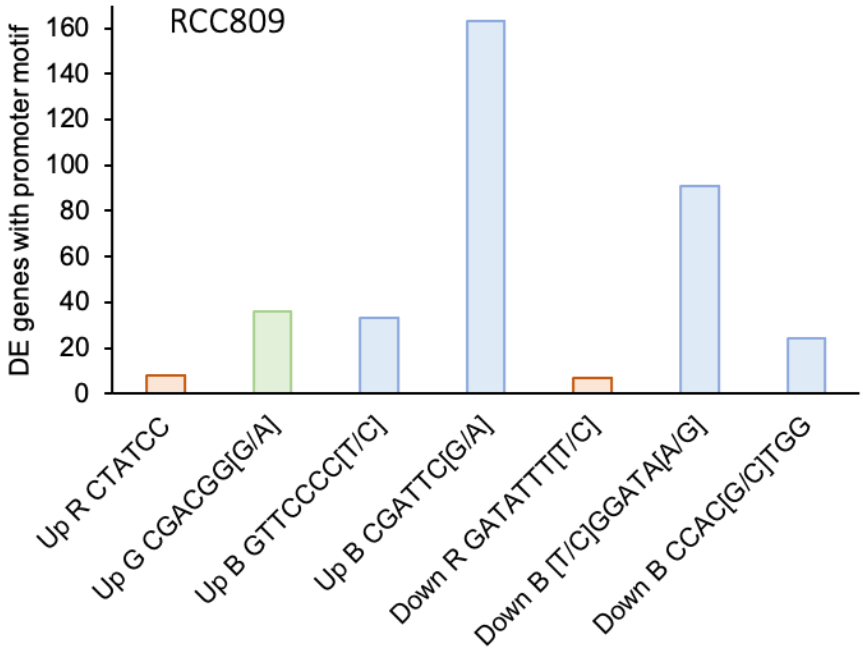

Figure 5.3 Overrepresented motifs in RCC809 light responsive differentially expressed (DE) genes.
Light qualities abbreviated as follows: Red (R), Green (G), Blue (B)

To identify candidates for the transcription factors that bind these motifs, the motifs were compared visually to *Ostreococcus* transcription factor binding site logos in the Catalog of Inferred Sequence Binding Preferences (CIS-BP) database compiled by Weirauch et al. (2014). Table 5.2 shows the best transcription factor DNA binding site matches from *Arabidopsis* and *Ostreococcus* to the promoter motifs. *Arabidopsis* matches were identified based on significant similarity to the motifs after correction for false discovery rate (FDR) $q < 0.05$, whereas *Ostreococcus* matches in the CIS-BP database were selected on the basis of visual similarity. This identified transcription factors, or families of transcription factors, which may control transcriptional responses to different light qualities.

Table 5.2 Transcription factor binding site matches for the candidate regulatory promoter motifs

RCC809 motif and light response	Transcription factor binding site matches	Transcription factor
Up Red 	No significant match to a transcription factor DNA binding site	N/A
Up Blue 		Myb *Ostreococcus* Od01g04240
Up Blue 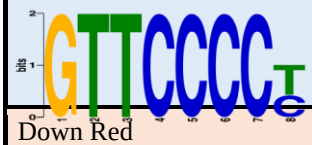		Myb *Ostreococcus* Od03g02230
Down Red 	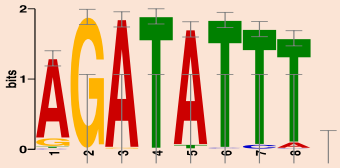	CCA1 Myb-like, *Arabidopsis* q < 0.05
Down blue 		Myb/SANT *Ostreococcus* Od06g01160
Down Blue 	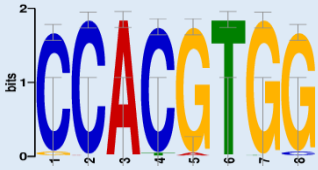	bHLH phytochrome interacting factor (PIF3) *Arabidopsis* q < 0.01
		bZIP, basic leucine zipper *Ostreococcus* Od14g01500 Motif also occurs twice in promoter

The CTATCC promoter motif associated with genes upregulated in red light

The CTATCC motif was overrepresented in the promoter sequences of 9 of the 32 genes upregulated in red compared to the genome-wide background (Table 5.1). The motif did not occur more than once in any of the promoter sequences. The annotations of the 9 genes containing this promoter motif show similarity in function, containing genes related to gluconeogenesis and the electron transport chain (Appendix 5). It is likely that this motif is involved in the regulation of a specific light responsive change identified as increasing in red and green light compared to blue in the gene expression analyses described in RCC809 in Chapter 3 involving macromolecular synthesis for energy storage as the annotated functions of the genes containing the promoter motif represent many of those functions.

The best matches for this motif to known transcription factor binding sites were those of a Cysteine2-Histidine2 (C2H2) zinc finger factor in *Arabidopsis,* as well as a poor match to a Myb domain transcription factor binding site in *Ostreococcus*. However, these were not statistically significant. A closer match to a DNA binding site may exist in an undescribed *Ostreococcus* Myb transcription factor. 26 Myb domain or Myb related transcription factors, and 4 C2H2 zinc finger factors have been described in RCC809 to date, Table 5.3, and of these only 10 Myb transcription factors had binding sites available for comparison of which 5 have been directly determined by PBM in OTH95 (Riano-Pachon et al., 2007, Weirauch et al., 2014).

Table 5.3 Myb transcription factors inferred in RCC809, candidates for binding to light quality responsive motifs

Gene	Binding site available	TF binding site match to a motif	Transcriptional light quality response	Function
Od01g04240	PBM in OTH95 homologue	Up blue CGATTC[G/A]	Up in red vs blue	Also contains receiver domain
Od03g02230	PBM in OTH95 homologue	Up blue GTTCCCC[T/C]	Down in blue	Probable repressor
Od06g01160	PBM in OTH95 homologue	Down blue [T/C]GGATA[A/G]	Up in green vs blue	
Od09g05870	Y		Up in blue	
Od07g02920	N	NA	Down in green	Also contains zinc finger
Od14g02540	N	NA	Down in blue	
Od06g04450	PBM in OTH95 homologue		Down in blue	
Od06g02270	Y		Down in blue	LHY homologue
Od13g03160	N	NA	Down in blue	Probable inducer
Od04g00700	Y		Down in blue	
Od14g01100	N	NA	Down in blue	
Od06g03360	N	NA	Up in blue vs red	Telomere binding
Od09g01640	N	NA	Up in blue vs red	Probable inducer
Od14g01870	N	NA	Up in green vs blue	Probable inducer
Od05g00570	Y		Up in green vs blue	
Od13g02520	PBM in OTH95 homologue		None	Probable telomere binding
Od02g03570	N	NA	None	Glycosyltransferase
Od11g04130	N	NA	None	Telomere binding
Od01g01750	N	NA	None	Probable TFIIIB inducer
Od17g02070	Y		None	
Od01g00660	N	NA	None	
Od12g02140	N	NA	None	
Od05g01860	N	NA	None	
Od06g01890	N	NA	None	
Od11g00550	N	NA	None	
Od05g01380	N	NA	None	

The [T/C]GGATA[A/G] motif associated with genes downregulated in blue light

The [T/C]GGATA[A/G] motif was overrepresented in the promoters of 91 of the 472 genes downregulated in blue light. It was mostly found singly in the promoter sequences of genes downregulated in blue light, only occurring more than once in 6 promoters of the 91 genes downregulated in blue light in which it was found. This motif is almost a reverse complement of the CTATCC motif found in promoters of genes upregulated in red light (Table 5.1), and two of the 9 genes containing the CTATCC motif (Od08g03040 and Od03g028500) also contained the [T/C]GGATA[A/G] motif. This suggests that these motifs are related and likely to be recognised by the same transcription factor. Analysis of Biological Processes GO terms associated with these genes revealed overrepresented functions related to amino acid metabolism, starch biosynthesis, chlorophyll biosynthesis, lipid biosynthesis, and gluconeogenesis (Appendix 5), implicating this promoter motif in the regulation of these blue light responsive changes in RCC809.

This motif contains the core GATA sequence commonly found in the promoters of light responsive genes and known as a light responsive element (LRE) in plants (Guilfoyle, 1997, Hiratsuka and Chua, 1997, Jiao et al., 2007, Manfield et al., 2007). The best matches to previously described transcription factor binding sites were, as for the CTATCC motif, a less than significant match to a Cysteine2-Histidine2 (C2H2) zinc finger factor in *Arabidopsis*, and a better visual match to a Myb domain transcription factor binding site determined in *Ostreococcus* (Table 5.2). This *Ostreococcus* Myb factor is the RCC809 homologue (Od06g01160) of a Myb-like transcription factor in OTH95 (ostta06g01220). Expression of this Myb transcription factor decreased in blue light compared to green light (Figure 5.4a), which indicates a positive regulatory role as the genes containing this motif were also downregulated.

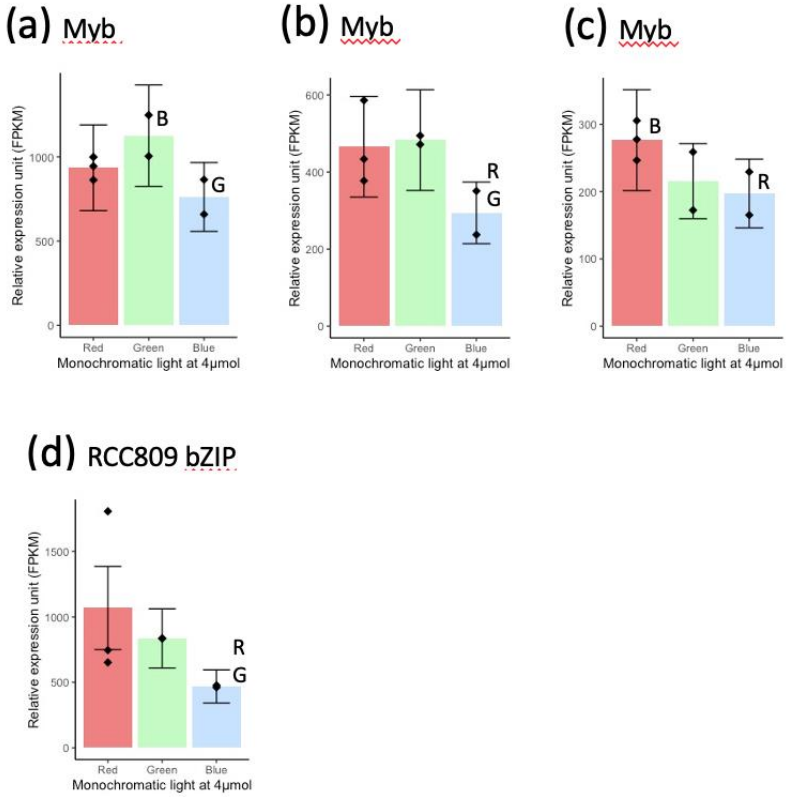

Figure 5.4 Expression of transcription factor matches to promoter motifs
(a) [T/C]GGATA[A/G] match Myb factor with similarity to CCA1 Od06g01160 (b) GTTCCCC[T/C] match Myb factor Od03g02230 (c) GTTCCCC[T/C] match Myb factor Od01g04240 (d) CCAC[G/C]TGG match bZIP factor Od14g01500. Letters indicate significant (p=<0.05) differences after false discovery rate correction with either red (R) red, green (G), and blue (B) conditions.

This Myb factor shows homology to the *Arabidopsis* Circadian clock associated 1 (CCA1) gene and the OTH95 homologue (ostta06g01220) was described as the *Ostreococcus* CCA1 homologue by de Los Reyes et al. (2017). A closer homologue of the *Arabidopsis* CCA1 gene, was however identified in OTH95 (ostta06g02340, RCC809 homologue Od06g02270) by Corellou et al. (2009). This Myb transcription factor gene (Od06g01160) may also be clock related, and investigation of the effect of light quality on RCC809 circadian clock entrainment over light dark cycles would prove informative. Blue light is prevalent in deeper waters where other wavelengths have been scattered or absorbed so that it is a more dependable signal for circadian entrainment of the ocean ecotype RCC809.

The CGACGG[G/A] promoter motif associated with genes upregulated in green light

The CGACGG[G/A] promoter motif was overrepresented in genes upregulated in green light, being present in 37 of the 60 gene set (Table 5.1). A low level of repetition within promoters was found for this motif; only 3 of the 38 genes had more than one copy in their promoter sequence. The functions of the genes containing this promoter motif were mainly related to protein modification and RNA binding, such as peptidases, protein folding, methyltransferases, and mRNA splicing (Appendix 5).

The CGACGG[G/A] motif showed some similarity to the binding site of a Myb-like domain-containing trihelix transcription factor from *Arabidopsis,* although this match was not significant after FDR correction (Willmann et al., 2011).

The GTTCCCC[T/C] promoter motif associated with genes upregulated in blue light

The GTTCCCC[T/C] motif was overrepresented in the promoters of genes upregulated in blue light, being present in 33 of the 536 of these genes (Table 5.1). The motif was only found once per promoter sequence. Functions related to cell cycle and mitosis were significantly overrepresented within the genes containing this motif. This group of genes also included functions related to transcription and photosystem II assembly (Appendix 5).

The GTTCCCC[T/C] motif was a good visual match to the binding site of the RCC809 homologue Od03g02230 of the OTH95 Myb transcription factor (ostta03g00840). (Weirauch et al., 2014). Expression of this Myb gene decreased under blue light compared to red and green light (Figure 5.4b), suggesting that increased gene expression in blue light may result from lifting of transcriptional repression by this transcription factor.

The CGATTC[G/A] promoter motif associated with genes upregulated in blue light

The promoter motif CGATTC[G/A] was also overrepresented in genes upregulated in blue light, being present in 163 in 536 of these genes (Table 5.1). Duplication of the CGATTC[G/A] motif within promoter sequences was more common than for the other motifs in this analysis, occurring two or more times in 17% of the promoters of genes upregulated in blue light in which it was found. 13 genes upregulated in blue light

contained both this motif and the GTTCCCC[T/C] motif discussed above, which suggests some overlap in function and regulation. The 163 light responsive genes containing this promoter motif were annotated with functions mainly related to cell cycle, transmembrane ion transport, protein binding and modification, and DNA repair (Appendix 5). These candidate regulatory promoter motifs (CGATTC[G/A] and GTTCCCC[T/C]) may therefore be both directly related to the regulation of the increased cell division identified as upregulated in blue light in the analyses described in Chapter 3, as well as to the regulation of further light quality responsive changes in gene expression through post transcriptional modifications within the light quality response cascade.

The CGATTC[G/A] motif showed good visual similarity to the binding site of an *Ostreococcus* Myb transcription factor (ostta16g01340) (Table 5.2). The RCC809 homologue of this transcription factor (Od01g04240) showed increased expression in blue light compared to red (Figure 5.4c). As genes containing the CGATTC[G/A] motif are upregulated under blue light, this transcription factor may promote the transcription of these putative target genes. Interestingly, this transcription factor contains a receiver (REC) domain which suggests that its activity may be regulated by one of the two photoreceptors containing histidine kinase domains, LOV-HK and Rhod-HK.

The GATATTT[T/C] promoter motif associated with genes downregulated in red light

The AT-rich GATATTT[T/C] promoter motif was overrepresented in promoters of genes downregulated in red light, being found in half of this 14 gene set. This motif was found in single copies only per promoter sequence. The 7 RCC809 genes containing this candidate regulatory promoter motif were not informatively annotated as little to no sequence homology to described genes in other species was identified. It is therefore difficult to determine the physiological consequences of the potential regulatory effects of the presence of this promoter motif.

The motif also contains the core GATA sequence and was a significant match to the binding site of the Circadian clock associated 1 (CCA1) Myb-like transcription factor in *Arabidopsis* (Table 5.2). The DNA binding site of the RCC809 homologue of the CCA1 transcription factor in OTH95 was however, a closer match for the

[T/C]GGATA[A/G] promoter motif found in genes downregulated in blue light. As illustrated by Table 5.3, few binding sites of Myb transcription factor genes in RCC809 were available for comparison and a better match may well exist among this undescribed set. Despite the lack of detail in the annotation of genes containing this promoter motif, its association with a transcription factor which is a light responsive *Arabidopsis* clock gene suggests that this motif is part of a red light responsive signalling cascade in RCC809.

The CCAC[G/C]TGG promoter motif associated with genes downregulated in blue light

A second promoter motif was overrepresented in genes downregulated in blue light, the palindromic CCAC[G/C]TGG. This motif has the highest incidence of repetition within promoters of any of the candidate regulatory motifs, appearing at least twice in the promoters of 18 of the total 24 genes. Repetition of the same motif within a promoter may intensify the regulatory effect on gene expression as well as increasing the specificity of transcription factor binding (Guilfoyle, 1997). Genes containing this promoter motif were mainly annotated as transmembrane protein, solute and ion transport, or related to protein modification such as proteases and protein binding (Appendix 5). 14 of the 24 genes were assigned GO terms related to 'Biological Processes' which allowed the identification of transport related overrepresented terms such as intracellular transport and proton transport.

The CCAC[G/C]TGG motif contains the regulatory sequence ACGT which is the core of the G-box CACGTG motif. G-box motifs are often present in light responsive genes and are a binding site for both basic helix-loop-helix (bHLH) and basic and leucine zipper (bZIP) transcription factors. In *Arabidopsis*, this includes multiple light responsive transcription factors such as the bZIP protein HY5, and the bHLH proteins MYC2 and phytochrome interacting factors (PIFs) (Guilfoyle, 1997, Jakoby et al., 2002, Hiratsuka and Chua, 1997, Gangappa and Botto, 2016, Lee et al., 2007).

The CCAC[G/C]TGG motif was a significant match to the binding site of *Arabidopsis* PIF3 (Table 5.2), suggesting that it might be recognised by a bHLH protein in *Ostreococcus*. 4 bHLH and 4 bZIP transcription factors have been described in RCC809 to date (Table 5.4), as compared to 7 bZIP and 1 bHLH in OTH95 (Riano-Pachon et al., 2007).

The HY5 homologue in RCC809 (Od01g02870) did not show a transcriptional response to light quality, and the binding site of its OTH95 homologue did not match any of the light-responsive promoter motifs identified here. However, the CCAC[G/C]TGG motif was a strong visual match to the binding site for another *Ostreococcus* bZIP transcription factor, ostta15g01060 (Table 5.2). Expression of the RCC809 homologue (Od14g01500) decreased in blue light (Figure 5.4d), and the motif appeared twice in its promoter sequence, suggesting autoregulation by this transcription factor. As expression of both this transcription factor and genes containing the CCAC[G/C]TGG motif decrease in blue light compared to red and green light, this transcription factor is likely to function as a transcriptional activator so that its reduced expression causes reduced expression of the target genes. The OTH95 homologue, ostta15g01060, also known as OtbZIP7, was found to be divergent from homologues of known function suggesting that the function of this bZIP may be unique to *Ostreococcus* (Corrêa et al., 2008).

Table 5.4 bZIP and bHLH transcription factors in RCC809

Gene	Binding site inferred	Binding site match to a motif	Transcriptional light quality response	Function
bZIP Od14g01500	PBM in OTH95 homologue	Down in blue CCAC[G/C]TGG	Down in blue	
bZIP Od07g00750	N	NA	Up in red vs blue	
bZIP Od01g02870	PBM in OTH95 homologue		None	HY5 homologue Cell division related
bZIP Od03g00300	PBM in OTH95 homologue		None	
bHLH Od19g00020	N	NA	None	Clock/ARNT/BMAL/ PAS domain (PTHR23042)
bHLH Od17g02270	N	NA	None	clock/ARNT/BMAL/ PAS domain (PTHR23042)
bHLH Od19g00170	N	NA	None	Clock/ARNT/BMAL/ PAS domain (PTHR23042)
bHLH Od20g02280	PBM in OTH95 homologue		None	Clock/ARNT/BMAL/ PAS domain (PTHR23042)

Transcriptional changes specific to a single light quality condition (red, green or blue,) were also detected in the expression of 26 transcription factor genes in RCC809 (Table 5.5). Transcription factors showing expression changes are likely to be controlled by other transcription factors in an upstream primary light response. These genes include transcription factor domains of several families, including zinc finger and Myb, and are therefore likely involved in secondary regulation in the signalling cascades of the light quality responses. Other transcriptional factors may also be affected by light quality signals and show post translational modifications or degradation undetected in this analysis (Jiao et al., 2007).

Table 5.5 Transcription factor genes which showed significant changes in expression in response to monochromatic light treatments

Light response	Gene	Transcription factor
Up in red	Od04g05270	DNA binding, regulation of transcription
Up in green	Od07g02150	Zinc finger CCHC domain 9, positive regulation
Up in blue	Od09g00610	Zinc finger C2H2
Up in blue	Od08g02120	DNA binding WRKY transcription factor domain
Up in blue	Od09g05870	Myb related transcription factor
Up in blue	Od17g00150	Zinc finger CCCH domain-containing protein 14-like
Up in blue	Od17g01360	Transcription factor complex, RNA pol II cofactor Med13
Up in blue	Od19g00350	Tesmin/TSO1-like CXC domain, transcription factor activity
Down in green	Od07g02920	Myb related factor with SANT/Myb and Zinc domains
Down in blue	Od06g02270	LHY homologue Chromatin binding, SANT/Myb domain
Down in blue	Od04g01800	CONSTANS, CO-like, and TOC1 (CCT) domain
Down in blue	Od09g05010	CONSTANS, CO-like, and TOC1 (CCT) domain with zinc finger domain
Down in blue	Od04g00700	Myb related factor, chromatin binding
Down in blue	Od14g01100	Myb factor
Down in blue	Od04g00460	DNA-binding and serine/threonine protein kinase domain containing transcription factor
Down in blue	Od04g02510	Zinc finger, Dof-type transcription factor
Down in blue	Od05g02290	DNA-binding transcription factor activity, zinc ion binding
Down in blue	Od05g03380	Maf1 negative regulation of transcription by RNA pol III binding

Down in blue	Od06g01000	RNA pol sigma factor, transcription initiation
Down in blue	Od06g04450	Myb related transcription factor
Down in blue	Od06g07010	Transcription factor, BAH and zinc PHD domains, chromatin associated
Down in blue	Od08g01810	Zinc finger CCCH domain, protein ubiquitination
Down in blue	Od13g03160	RNA pol II Myb transcription factor
Down in blue	Od14g01500	Transcription factor, basic-leucine zipper domain
Down in blue	Od14g02540	Myb transcription factor
Down in blue	Od19g01230	Heat shock transcription factor, winged helix domain

5.4.2 Are the candidate regulatory elements identified in RCC809 retained in OTH95?

As the transcriptional light quality responses identified in RCC809 were not seen in OTH95, the mechanisms behind these light quality responses would not be expected to be active in OTH95. Consequently, the regulatory motifs identified in promoters of light-quality responsive genes in RCC809 may be lost in OTH95 homologues. To test this hypothesis, homologues of RCC809 light quality responsive genes which contained putative regulatory motifs in their promoters were identified in OTH95, and the promoters of these genes were searched for the motifs found in RCC809. The percentages of OTH95 homologues which retained each promoter motif are shown in Figure 5.5. In all cases the motifs were present in OTH95, but at a much lower incidence level than in RCC809. For example, in RCC809 168 genes which showed increased expression in blue light contained the CGATTC[G/A] motif in their promoters, but, of the 145 homologues identified in OTH95, only 35 (24%) contained the motif. This may indicate either a loss of motifs in OTH95 or a novel adaptation in RCC809.

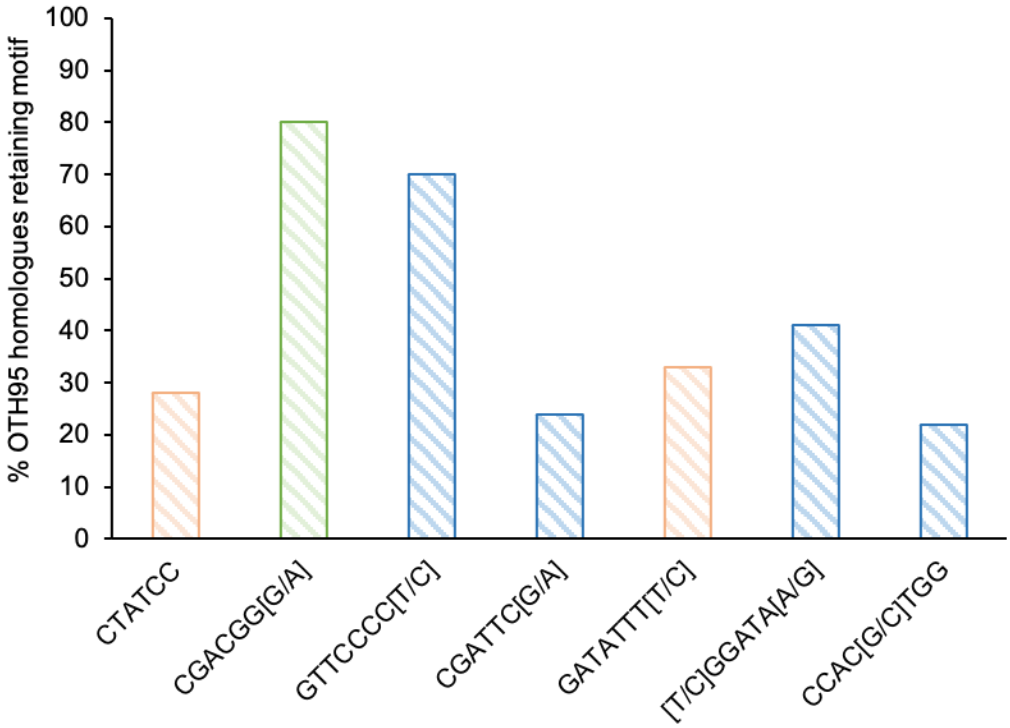

Figure 5.5 Percentage retention of promoter motifs in OTH95 homologues of light responsive genes in RCC809.

5.5 Conclusion

Analysis of the LOV-HK knockout mutant of OTH95 in terms of its photosynthetic parameters demonstrated that, although transcription of the LOV-HK gene was not affected by light quality in this ecotype (Figure 5.2c), this photoreceptor is involved in the regulation of light quality responses in terms of photosystem II activity and light saturation in OTH95 (Figure 5.1). A knockout mutant of these genes in RCC809 would prove informative as to the involvement of this photoreceptor in the broader range of physiological light quality responses seen in Chapter 4. Transcription of the RCC809 photoreceptor genes encoding LOV-HK, phototropin, and CPF1 cryptochrome photoreceptors all increased in red light compared to blue light, while CPF2 expression increased in blue light and the Rhod-HK showed no changes (Figure 5.2). The OTH95 homologues showed no light quality responsive changes which suggests that the transcriptional expression of RCC809 photoreceptors is under more sensitive control by feedback from light quality signalling networks.

The analysis of promoter motifs in RCC809 uncovered evidence for specific transcription factors controlling light quality responses in this deep ocean ecotype. Individual light-quality responsive motifs were associated with genes with related functions (Appendix 5). The function of these transcription factors in light quality responses seems likely to have been lost in the lagoon *Ostreococcus* ecotype OTH95 as the motifs identified in RCC809 are present in fewer of the promoters of homologues of these genes in OTH95 (Figure 5.5). All except two of the promoter motifs are greatly reduced in the OTH95 homologues, only being retained in 22-41% in each set. The two with greater retention in OTH95 are the green light associated motif CGACGG[G/A] found in regulatory genes (80% retained) and the up in blue cell cycle associated motif GTTCCCC[T/C] (70% retained). The motifs are likely to have been retained in RCC809 due to evolutionary constraints as the ability to respond to light quality presents an adaptive advantage for efficient light capture in the variable light spectra of the ocean environment compared to the broad spectrum of light wavelengths present in a shallow lagoon. Alternatively, it may have been important for OTH95 to lose these responses in its coastal environments where light across the full visible spectrum is present at all times so that light quality specific signals would induce inappropriate responses. A single transcription factor can be involved in more than one regulatory process and its regulatory function may change during an organism's lifecycle (Pireyre and Burow, 2015). The motifs retained in greater numbers in OTH95 may retain regulatory function in response to other signals. Crossovers between signals controlling regulation are often seen in higher plants, such as the integration of light and temperature signals allowing a coordinated response (Jiao et al., 2007).

Differences in the transcription factors identified in the RCC809 and OTH95 ecotypes show evidence of divergence upstream of the promoter motifs in the signalling cascades, allowing the loss of motifs in OTH95 by abolishing the downstream responses. For example, the 4 bZIP and 4 bHLH transcription factors listed for RCC809 contrast with the 7 bZIP and 1 bHLH factors listed for OTH95 on the Plant transcription factor database (PlantTFBD) (Riano-Pachon et al., 2007). The 4 bZIP factors in RCC809 have homologues in OTH95 while the bHLH factors show discrepancy between the ecotypes (Table 5.6). The one bHLH in OTH95 (ostta14g01990) shows homology to three of the RCC809 bHLH genes (Od17g02270, Od19g00170, and Od20g02280), which may be the result of duplication in RCC809,

and the fourth RCC809 bHLH (Od19g00020) has no strong homology to any OTH95 gene. This leaves 3 OTH95 bZIP factor genes, two of which (ostta03g03120 and ostta04g01490) showed poor homology (less than 40% identity) to the same RCC809 gene (Od04g03880), and the third gene (ostta15g01440) was a moderate homologue (48% identity) for an RCC809 gene (Od14g01880). These RCC809 genes also appear to be transcription factors which were not listed on the PlantTFDB database. Thus, it appears that the light quality response cascades differ between the ecotypes at every level.

Table 5.6 Comparison of bZIP and bHLH transcription factors in OTH95 and RCC809

RCC809 Gene	Transcription factor family	Homologue in OTH95
Od14g01500	bZIP	ostta15g01060 41% identity
Od07g00750	bZIP	ostta07g00490 58% identity
Od01g02870	bZIP	ostta01g03880 65% identity
Od03g00300	bZIP	ostta03g02740 62% identity
Od19g00020	bHLH	None
Od17g02270	bHLH	**ostta14g01990 54% identity**
Od19g00170	bHLH	**ostta14g01990 61% identity**
Od20g02280	bHLH	**ostta14g01990 54% identity**
Od04g03880	bZIP not on PlantTFDB	ostta03g03120 39% identity
Od04g03880	bZIP not on PlantTFDB	ostta04g01490 52% identity
Od14g01880	bZIP not on PlantTFDB	ostta15g01440 45% identity

Chapter 6: Conclusions and future directions

6.1 Findings

This work revealed that *Ostreococcus* is able to respond to different light qualities and that these responses differ between ecotypes sourced from different light quality environments.

The deep ocean ecotype RCC809 showed differentiated transcriptional responses to red, green, and blue light qualities, with gene expression under blue light being most distinct from red and green light. Consistent with its faster growth rate under blue light, blue light adaptation resulted in elevated expression of genes associated with the cell cycle and decreased expression of enzymes involved in macromolecular synthesis for energy storage. RCC809 also demonstrated changes in pigment content in response to light quality. Under blue light, the chl-*b* to chl-*a* ratio and levels of two novel chlorophyll *b*-like pigments only seen in RCC809 were greatly increased. These changes favour increased absorption of blue light wavelengths. In the open ocean, this may be important for continued photosynthesis at depths to which only low intensities of blue light penetrate. Photosynthetic parameters were also altered, including lower rETR and PSII quantum yields under blue light, which may result from reduced RuBisCO activity and also indicate reduced PSII efficiency. As blue light wavelengths are comparatively well absorbed by the chlorophylls and accessory pigments, it may be that these adjustments save energy and nutrients by reducing photosynthetic activity without detriment to the cell. The red and green light responses in RCC809 were less differentiated from one another but do show some distinction in terms of the level of change in photosynthetic parameters compared to blue light responses, so that the green light response was intermediate between the red and blue light responses.

In contrast, the coastal and lagoon ecotype, OTH95 did not exhibit significant changes in transcription in response to different monochromatic light treatments. Physiological differences were shown under green light, compared to red and blue light, but these were much less extensive than in RCC809. These changes included minor pigment changes and a reduced PSII quantum yield on exposure to blue light after green light acclimation which may represent an adaptive response to changes in green light levels in the environment. This ecotype originates from shallow environments where it is not greatly affected by the narrowing of spectral availability associated with depth. Instead, the spectral quality varies mostly according to the level of suspended sediment and other photosynthetic organisms. It may therefore be less important for this ecotype

to be able to perceive the blue-light enriched environment associated with depth, and to adjust its photosystems accordingly. This may explain why OTH95 only exhibits a limited range of light-quality responses.

Altogether these observations demonstrate that this important phytoplankton responds to light quality in its environment. Light intensity is considered to be the primary abiotic factor which determines the distribution of *Ostreococcus* ecotypes, and the high light intensity adapted OTH95 is known to differ from RCC809 which is adapted for efficient light harvesting at low light intensities (Six et al., 2005, Six et al., 2009, Demir-Hilton et al., 2011, Cardol et al., 2008). However, the difference in light quality responses of these two ecotypes suggest that light quality is also an important factor in adaptation to distinct ecological niches in the environment. This work also demonstrated evidence for chromatic adaptation in a eukaryotic phytoplankton, a response which had previously only been described in cyanobacteria (Grébert et al., 2018).

To obtain clues to the molecular mechanisms controlling light quality responsive changes in gene expression in RCC809, candidate regulatory elements were identified in the promoters of light-regulated genes. Interestingly, these promoter motifs were largely absent in the OTH95 homologues of these light quality-responsive genes, suggesting that they may have been lost since divergence of these two strains.

The identified promoter motifs were then compared to known DNA binding sites for *Ostreococcus* as well as higher plant transcription factors, and this identified candidate transcription factors, or transcription factor families that may control different aspects of the light quality response. Of these transcription factors, those which are absent in OTH95, or for which only matches of low homology are present, may explain the reduced light quality responsiveness compared to RCC809. For example, only one bHLH transcription factor is known in OTH95, as compared to four in RCC809. Those that are missing in OTH95 are candidate regulators for light quality responses in RCC809. These transcription factors may represent useful markers to study the prevalence of light-quality responsive strains in metagenomic studies of ocean communities.

6.2 Further questions

There may be further complexity in the light quality responses of *Ostreococcus* than is detected by experiments using monochromatic light. In higher plants for example, an increased ratio of far-red light to red light stimulates a shade response, and the application of varied red to blue light ratios promotes a suite of physiological changes (Hader et al., 1998, Silva et al., 2020, Pennisi et al., 2019). Applying varying ratios of the light qualities used in this study would allow these effects to be understood in *Ostreococcus*. The proportion of red versus blue light is likely to be an important signal for RCC809 based on its original light quality environment, whereas the proportion of green light versus other light qualities is likely to be more important for OTH95. The adaptive advantages conferred by light quality responses in *Ostreococcus* may be further interrogated by assessing competition effects between the ecotypes in monochromatic light conditions, or under different ratios of light wavelengths.

The contribution of specific transcription factor genes to the light quality responses in RCC809 may be tested by mutagenesis. If mutagenesis of a transcription factor abolishes a light quality response, this would demonstrate its regulatory function. Candidate light quality-responsive regulatory elements may be tested by fusing promoters containing these motifs to a luciferase reporter gene and testing their light-responsiveness in transgenic lines following the mutagenesis of a transcription factor, or of the transcription factor binding site within the promoter. Once their role in light quality response is confirmed, these transcription factors will represent useful markers for light quality responsiveness in populations of *Ostreococcus* ecotypes in diverse marine environments. An assessment of the prevalence of light responsiveness in communities of eukaryotic phytoplankton in different light quality environments, would then be enabled by a metagenomics investigation demonstrating the incidence level of these markers. This would give an overview of the light quality environments which promote light quality responses and allow the importance of these adaptations to be evaluated.

Similarly, greater understanding of how phytoplankton respond to light quality in situ, and how this contributes to ecological niche adaptation, would be enabled by a metatranscriptomic investigation demonstrating how the gene expression changes identified in this work map on to specific light quality environments. Targets for further investigation are key genes involved in the major processes which were found

to be regulated by light quality. For example, expression of RuBisCO small subunit (Od17g01990, Od17g02000, and Od17g02010) and RuBisCO activase (Od04g02820) genes decreased in blue light so it would be informative to compare their expression levels between sampling sites of different depths and between ocean sites and the more turbulent and greener coastal sites. The expression of certain prasinophyte light harvesting complex genes which increased expression in blue light (Od07g02900 and Od14g00280) would also be informative to analyse in this way, as the rise in chl-*b* to chl-*a* ratio may be due to increased prasinophyte light-harvesting chlorophyll *a*/*b* binding proteins (LHCP) content in RCC809 (Cardol et al., 2008). Other genes highlighted in the transcriptomic analyses of Chapter 3 may also prove informative, particularly those which enzymes for which reduced expression indicated reduced macromolecular synthesis in blue light, although preliminary tests would be necessary to determine the most relevant of these targets due to the limited detail provided by gene annotations. These analyses would provide ecological context for the transcriptional and physiological light quality responses demonstrated in Chapters 3 and 4 and would utilise metagenomic and metatranscriptomic data from Tara Oceans surveys (Villar et al., 2018).

In conclusion, this thesis provides novel experimental evidence for light quality responses in *Ostreococcus*, demonstrates that these responses are ecotype-specific and that they represent niche adaptation to the ecotypes' different light quality environments. This differentiation in light quality responses enhances understanding of adaptive ability in *Ostreococcus*. The presence of these adaptive light quality responses indicates the importance of light quality for this genus of green algae in the marine environment and implies that light quality adaptations may be seen in communities of other photosynthetic eukaryotes. Candidate regulatory elements were also identified, and the transcription factors that bind these motifs may represent useful markers for cells' ability to respond to light quality in the context of environmental studies.

References

ALBORESI, A., BALLOTTARI, M., HIENERWADEL, R., GIACOMETTI, G. M. & MOROSINOTTO, T. 2009. Antenna complexes protect Photosystem I from photoinhibition. *BioMed Central Plant Biology,* 9**,** 71.

ALTSCHUL, S. F., GISH, W., MILLER, W., MYERS, E. W. & LIPMAN, D. J. 1990. Basic local alignment search tool. *Journal of Molecular Biology,* 215**,** 403-10.

ALTSCHUL, S. F., MADDEN, T. L., SCHÄFFER, A. A., ZHANG, J., ZHANG, Z., MILLER, W. & LIPMAN, D. J. 1997. Gapped BLAST and PSI-BLAST: a new generation of protein database search programs. *Nucleic Acids Research,* 25**,** 3389-402.

ÁLVAREZ, S., RODRÍGUEZ, F., RIOBÓ, P., GARRIDO, J. & VAZ, B. 2013. Chlorophyll c(CS-170) isolated from *Ostreococcus* sp. is [7-methoxycarbonyl-8-vinyl]protochlorophyllide a. *Organic letters,* 15 17**,** 4430-3.

ANDREWS, S. 2015. FastQC: A Quality Control Tool for High Throughput Sequence Data [Online] Available Online at http://www.bioinformatics.babraham.ac.uk/projects/fastqc/.

ARP, T. B., KISTNER-MORRIS, J., AJI, V., COGDELL, R. J., VAN GRONDELLE, R. & GABOR, N. M. 2020. Quieting a noisy antenna reproduces photosynthetic light-harvesting spectra. *Science,* 368**,** 1490-1495.

ARRIGO, K. R. & VAN DIJKEN, G. L. 2015. Continued increases in Arctic Ocean primary production. *Progress in Oceanography,* 136**,** 60-70.

ASHBURNER, M., BALL, C. A., BLAKE, J. A., BOTSTEIN, D., BUTLER, H., CHERRY, J. M., DAVIS, A. P., DOLINSKI, K., DWIGHT, S. S., EPPIG, J. T., HARRIS, M. A., HILL, D. P., ISSEL-TARVER, L., KASARSKIS, A., LEWIS, S., MATESE, J. C., RICHARDSON, J. E., RINGWALD, M., RUBIN, G. M. & SHERLOCK, G. 2000. Gene ontology: tool for the unification of biology. The Gene Ontology Consortium. *Nature Genetics,* 25**,** 25-9.

BAILEY, T. L. 2011. DREME: motif discovery in transcription factor ChIP-seq data. *Bioinformatics,* 27**,** 1653-9.

BARTON, S., JENKINS, J., BUCKLING, A., SCHAUM, C. E., SMIRNOFF, N., RAVEN, J. A. & YVON-DUROCHER, G. 2020. Evolutionary temperature compensation of carbon fixation in marine phytoplankton. *Ecology Letters,* 23**,** 722-733.

BATES, N. R., ASTOR, Y. M., CHURCH, M. J., CURRIE, K. I. M., DORE, J. E., GONZÁLEZ-DÁVILA, M., LORENZONI, L., MULLER-KARGER, F., OLAFSSON, J. O. N. & SANTANA-CASIANO, J. M. 2014. A time-series view of changing surface ocean chemistry due to ocean uptake of anthropogenic co_2 and ocean acidification. *Oceanography,* 27**,** 126-141.

BATTLE, M. W., VEGLIANI, F. & JONES, M. A. 2020. Shades of green: untying the knots of green photoperception. *Journal of Experimental Botany,* 71**,** 5764-5770.

BEEL, B., MÜLLER, N., KOTTKE, T. & MITTAG, M. 2013. News about cryptochrome photoreceptors in algae. *Plant Signaling & Behavior,* 8**,** e22870.

BEEL, B., PRAGER, K., SPEXARD, M., SASSO, S., WEISS, D., MULLER, N., HEINNICKEL, M., DEWEZ, D., IKOMA, D., GROSSMAN, A., KOTTKE, T. & MITTAG, M. 2012. A flavin binding cryptochrome photoreceptor responds to both blue and red light in *Chlamydomonas reinhardtii*. *Plant Cell,* 24**,** 2992-3008.

BEHRENFELD, M. J., PRASIL, O., BABIN, M. & BRUYANT, F. 2004. in search of a physiological basis for covariations in light-limited and light-saturated photosynthesis. *Journal of Phycology,* 40**,** 4-25.

BENNER, I., IRWIN, A. J. & FINKEL, Z. V. 2020. Capacity of the common Arctic picoeukaryote *Micromonas* to adapt to a warming ocean. *Limnology and Oceanography Letters,* 5**,** 221-227.

BLANC-MATHIEU, R., KRASOVEC, M., HEBRARD, M., YAU, S., DESGRANGES, E., MARTIN, J., SCHACKWITZ, W., KUO, A., SALIN, G., DONNADIEU, C., DESDEVISES, Y., SANCHEZ-FERANDIN, S., MOREAU, H., RIVALS, E., GRIGORIEV, I. V., GRIMSLEY, N., EYRE-

WALKER, A. & PIGANEAU, G. 2017. Population genomics of picophytoplankton unveils novel chromosome hypervariability. *Science Advances,* 3**,** e1700239.

BLANC-MATHIEU, R., VERHELST, B., DERELLE, E., ROMBAUTS, S., BOUGET, F., CARRE, I., CHATEAU, A., EYRE-WALKER, A., GRIMSLEY, N., MOREAU, H., PIEGU, B., RIVALS, E., SCHACKWITZ, W., VAN DE PEER, Y. & PIGANEAU, G. 2014. An improved genome of the model marine alga *Ostreococcus tauri* unfolds by assessing Illumina de novo assemblies. *BioMed Central Genomics,* 15.

BLATT, A., BAUCH, M., PORSCHKE, Y. & LOHR, M. 2015. A lycopene β-cyclase/lycopene ε-cyclase/light-harvesting complex-fusion protein from the green alga *Ostreococcus lucimarinus* can be modified to produce α-carotene and β-carotene at different ratios. *Plant Journal,* 82**,** 582-595.

BLONDEAU-PATISSIER, D., GOWER, J. F. R., DEKKER, A. G., PHINN, S. R. & BRANDO, V. E. 2014. A review of ocean color remote sensing methods and statistical techniques for the detection, mapping and analysis of phytoplankton blooms in coastal and open oceans. *Progress in Oceanography,* 123**,** 123-144.

BÖHME, K., WILHELM, C. & GOSS, R. 2002. Light regulation of carotenoid biosynthesis in the prasinophycean alga *Mantoniella squamata*. *Photochemical and Photobiological Sciences,* 1**,** 619-28.

BOLAÑOS, L. M., CHOI, C. J., WORDEN, A. Z., BAETGE, N., CARLSON, C. A. & GIOVANNONI, S. 2021. Seasonality of the Microbial Community Composition in the North Atlantic. *Frontiers in Marine Science,* 8.

BOLGER, A. M., LOHSE, M. & USADEL, B. 2014. Trimmomatic: a flexible trimmer for Illumina sequence data. *Bioinformatics,* 30**,** 2114-20.

BORLONGAN, I. A., SUZUKI, S., NISHIHARA, G. N., KOZONO, J. & TERADA, R. 2020. Effects of light quality and temperature on the photosynthesis and pigment content of a subtidal edible red alga *Meristotheca papulosa (Solieriaceae, Gigartinales)* from Japan. *Journal of Applied Phycology,* 32**,** 1329-1340.

BOTEBOL, H., LELANDAIS, G., SIX, C., LESUISSE, E., MENG, A., BITTNER, L., LECROM, S., SUTAK, R., LOZANO, J. C., SCHATT, P., VERGÉ, V., BLAIN, S. & BOUGET, F. Y. 2017. Acclimation of a low iron adapted *Ostreococcus* strain to iron limitation through cell biomass lowering. *Scientific Reports,* 7**,** 327.

BOTEBOL, H., LESUISSE, E., SUTAK, R., SIX, C., LOZANO, J., SCHATT, P., VERGE, V., KIRILOVSKY, A., MORRISSEY, J., LEGER, T., CAMADRO, J., GUENEUGUES, A., BOWLER, C., BLAIN, S. & BOUGET, F. 2015. Central role for ferritin in the day/night regulation of iron homeostasis in marine phytoplankton. *Proceedings of the National Academy of Sciences of the United States of America,* 112**,** 14652-14657.

BOUMAN, H. A., PLATT, T., DOBLIN, M., FIGUEIRAS, F. G., GUDMUNDSSON, K., GUDFINNSSON, H. G., HUANG, B., HICKMAN, A., HISCOCK, M., JACKSON, T., LUTZ, V. A., MÉLIN, F., REY, F., PEPIN, P., SEGURA, V., TILSTONE, G. H., VAN DONGEN-VOGELS, V. & SATHYENDRANATH, S. 2018. Photosynthesis–irradiance parameters of marine phytoplankton: synthesis of a global data set. *Earth System Science Data,* 10**,** 251-266.

BOUMAN, H. A., PLATT, T., KRAAY, G. W., SATHYENDRANATH, S. & IRWIN, B. D. 2000. Bio-optical properties of the subtropical North Atlantic. I. Vertical variability. *Marine Ecology Progress Series,* 200**,** 3-18.

BRACHER, A. U. & TILZER, M. M. 2001. Underwater light field and phytoplankton absorbance in different surface water masses of the Atlantic sector of the Southern Ocean. *Polar Biology,* 24**,** 687-696.

BUITENHUIS, E. T., LI, W. K. W., VAULOT, D., LOMAS, M. W., LANDRY, M. R., PARTENSKY, F., KARL, D. M., ULLOA, O., CAMPBELL, L., JACQUET, S., LANTOINE, F., CHAVEZ, F., MACIAS, D., GOSSELIN, M. & MCMANUS, G. B. 2012. Picophytoplankton biomass distribution in the global ocean. *Earth System Science Data,* 4**,** 37-46.

CAMACHO, C., COULOURIS, G., AVAGYAN, V., MA, N., PAPADOPOULOS, J., BEALER, K. & MADDEN, T. L. 2009. BLAST+: architecture and applications. *BioMed Central Bioinformatics,* 10**,** 421.

CAMPBELL, D., HOUMARD, J. & DE MARSAC, N. T. 1993. Electron transport regulates cellular differentiation in the filamentous Cyanobacterium *Calothrix*. *Plant Cell,* 5**,** 451-463.

CARDOL, P., BAILLEUL, B., RAPPAPORT, F., DERELLE, E., BEAL, D., BREYTON, C., BAILEY, S., WOLLMAN, F., GROSSMAN, A., MOREAU, H. & FINAZZI, G. 2008. An original adaptation of photosynthesis in the marine green alga *Ostreococcus*. *Proceedings of the National Academy of Sciences of the United States of America,* 105**,** 7881-7886.

CASAL, J. J. 2013. Photoreceptor signaling networks in plant responses to shade. *Annual Review of Plant Biology,* 64**,** 403-27.

CHOI, D. H., AN, S. M., CHUN, S., YANG, E. C., SELPH, K. E., LEE, C. M. & NOH, J. H. 2016. Dynamic changes in the composition of photosynthetic picoeukaryotes in the northwestern Pacific Ocean revealed by high-throughput tag sequencing of plastid 16S rRNA genes. *FEMS Microbiology Ecology,* 92.

CHRETIENNOT-DINET, M., COURTIES, C., VAQUER, A., NEVEUX, J., CLAUSTRE, H., LAUTIER, J. & MACHADO, M. 1995. A new marine picoeucaryote - *Ostreococcus tauri* gen et sp-nov (Chlorophyta, Prasinophyceae). *Phycologia,* 34**,** 285-292.

CHURILOVA, T. Y., SUSLIN, V. V., MOISEEVA, N. A. & EFIMOVA, T. V. 2020. Phytoplankton bloom and photosynthetically active radiation in coastal waters. *Journal of Applied Spectroscopy,* 86**,** 1084-1091.

CLAYTON, S., LIN, Y. C., FOLLOWS, M. J. & WORDEN, A. Z. 2017. Co-existence of distinct *Ostreococcus* ecotypes at an oceanic front. *Limnology and Oceanography,* 62**,** 75-88.

CLOERN, J. E., FOSTER, S. Q. & KLECKNER, A. E. 2014. Phytoplankton primary production in the world's estuarine-coastal ecosystems. *Biogeosciences,* 11**,** 2477-2501.

CORELLOU, F., CAMASSES, A., LIGAT, L., PEAUCELLIER, G. & BOUGET, F. 2005. Atypical regulation of a green lineage-specific B-type cyclin-dependent kinase. *Plant Physiology,* 138**,** 1627-1636.

CORELLOU, F., SCHWARTZ, C., MOTTA, J., DJOUANI-TAHRI, E., SANCHEZ, F. & BOUGET, F. 2009. Clocks in the green lineage: comparative functional analysis of the circadian architecture of the Picoeukaryote *Ostreococcus*. *Plant Cell,* 21**,** 3436-3449.

CORRÊA, L. G., RIAÑO-PACHÓN, D. M., SCHRAGO, C. G., DOS SANTOS, R. V., MUELLER-ROEBER, B. & VINCENTZ, M. 2008. The role of bZIP transcription factors in green plant evolution: adaptive features emerging from four founder genes. *PLoS One,* 3**,** e2944.

COURTIES, C., VAQUER, A., TROUSSELIER, M., LAUTIER, J., CHRÉTIENNOT-DINET, M. J., NEVEUX, J., MACHADO, C. & CLAUSTRE, H. 1994. Smallest eukarotic organism. *Nature,* 370.

COUSO, I., VILA, M., VIGARA, J., CORDERO, B. F., VARGAS, M. Á., RODRÍGUEZ, H. & LEÓN, R. 2012. Synthesis of carotenoids and regulation of the carotenoid biosynthesis pathway in response to high light stress in the unicellular microalga *Chlamydomonas reinhardtii*. *European Journal of Phycology,* 47**,** 223-232.

CUI, H., YU, X., WANG, Y., CUI, Y., LI, X., LIU, Z. & QIN, S. 2013. Evolutionary origins, molecular cloning and expression of carotenoid hydroxylases in eukaryotic photosynthetic algae. *BioMed Central Genomics,* 14**,** 457.

DALL'OSTO, L., CAZZANIGA, S., NORTH, H., MARION-POLL, A. & BASSI, R. 2007. The *Arabidopsis* aba4-1 mutant reveals a specific function for neoxanthin in protection against photooxidative stress. *Plant Cell,* 19**,** 1048-64.

DARKO, E., HEYDARIZADEH, P., SCHOEFS, B. & SABZALIAN, M. R. 2014. Photosynthesis under artificial light: the shift in primary and secondary metabolism. *Philosophical Transactions of the Royal Society B: Biological Sciences* 369**,** 20130243.

DE LOS REYES, P., ROMERO-CAMPERO, F. J., RUIZ, M. T., ROMERO, J. M. & VALVERDE, F. 2017. Evolution of Daily Gene Co-expression Patterns from Algae to Plants. *Front Plant Sci,* 8**,** 1217.

DELLAPORTA, S. L., WOOD, J. & HICKS, J. B. 1983. A plant DNA minipreparation: Version II. *Plant Molecular Biology Reporter,* 1**,** 19-21.

DEMIR-HILTON, E., SUDEK, S., CUVELIER, M., GENTEMANN, C., ZEHR, J. & WORDEN, A. 2011. Global distribution patterns of distinct clades of the photosynthetic picoeukaryote *Ostreococcus*. *ISME Journal: Multidisciplinary Journal of Microbial Ecology* 5**,** 1095-1107.

DEMMIG-ADAMS, B. 1990. Carotenoids and photoprotection in plants: A role for the xanthophyll zeaxanthin. *Biochimica et Biophysica Acta (BBA) - Bioenergetics,* 1020**,** 1-24.

DERELLE, E., FERRAZ, C., LAGODA, P., EYCHENIE, S., COOKE, R., REGAD, F., SABAU, X., COURTIES, C., DELSENY, M., DEMAILLE, J., PICARD, A. & MOREAU, H. 2002. DNA libraries for sequencing the genome of *Ostreococcus tauri* (Chlorophyta, Prasinophyceae): The smallest free-living eukaryotic cell. *Journal of Phycology,* 38**,** 1150-1156.

DERELLE, E., FERRAZ, C., ROMBAUTS, S., ROUZE, P., WORDEN, A., ROBBENS, S., PARTENSKY, F., DEGROEVE, S., ECHEYNIE, S., COOKE, R., SAEYS, Y., WUYTS, J., JABBARI, K., BOWLER, C., PANAUD, O., PIEGU, B., BALL, S., RAL, J., BOUGET, F., PIGANEAU, G., DE BAETS, B., PICARD, A., DELSENY, M., DEMAILLE, J., VAN DE PEER, Y. & MOREAU, H. 2006. Genome analysis of the smallest free-living eukaryote *Ostreococcus tauri* unveils many unique features. *Proceedings of the National Academy of Sciences of the United States of America,* 103**,** 11647-11652.

DEVLIN, P. F. 2016. Plants wait for the lights to change to red. *Proceedings of the National Academy of Sciences of the United States of America,* 113**,** 7301-3.

DJOUANI-TAHRI, E., CHRISTIE, J., SANCHEZ-FERANDIN, S., SANCHEZ, F., BOUGET, F. & CORELLOU, F. 2011. A eukaryotic LOV-histidine kinase with circadian clock function in the picoalga *Ostreococcus*. *Plant Journal,* 65**,** 578-588.

DUANMU, D., BACHY, C., SUDEK, S., WONG, C.-H., JIMÉNEZ, V., ROCKWELL, N. C., MARTIN, S. S., NGAN, C. Y., REISTETTER, E. N., VAN BAREN, M. J., PRICE, D. C., WEI, C.-L., REYES-PRIETO, A., LAGARIAS, J. C. & WORDEN, A. Z. 2014. Marine algae and land plants share conserved phytochrome signaling systems. *Proceedings of the National Academy of Sciences,* 111**,** 15827-15832.

DUTKIEWICZ, S., HICKMAN, A., JAHN, O., HENSON, S., BEAULIEU, C. & MONIER, E. 2019. Ocean colour signature of climate change. *Nature Communications,* 10.

EGELAND, E. S., EIKREM, W., THRONDSEN, J. & WILHELM, C. 1995. Carotenoids from Further Prasinophytes. *Biochemical Systematics and Ecology,,* 23**,** 747-755.

EGELAND, E. S., GARRIDO, J., CLEMENTSON, L., ANDRESEN, K., THOMAS, C., ZAPATA, M., AIRS, R. L., LLEWELLYN, C., NEWMAN, G. L., RODRÍGUEZ, F. & ROY, S. 2011. Phytoplankton pigments: data sheets aiding identification of phytoplankton carotenoids and chlorophylls. *Phytoplankton Pigments Characterization, Chemotaxonomy and Applications in Oceanography.* Cambridge: Cambridge University Press.

ERGA, S., SSEBIYONGA, N., FRETTE, O., HAMRE, B., AURE, J., STRAND, O. & STROHMEIER, T. 2012. Dynamics of phytoplankton distribution and photosynthetic capacity in a western Norwegian fjord during coastal upwelling: Effects on optical properties. *Estuarine Coastal and Shelf Science,* 97**,** 91-103.

ESKINS, K., JIANG, C. Z. & SHIBLES, R. 1991. Light-quality and irradiance effects on pigments, light-harvesting proteins and Rubisco activity in a chlorophyll- and light- harvesting-deficient soybean mutant. *Physiologia Plantarum,* 83**,** 47-53.

EVRIN, C., CLARKE, P., ZECH, J., LURZ, R., SUN, J., UHLE, S., LI, H., STILLMAN, B. & SPECK, C. 2009. A double-hexameric MCM2-7 complex is loaded onto origin DNA during licensing of eukaryotic DNA replication. *Proceedings of the National Academy of Sciences,* 106**,** 20240-5.

EZER, D., SHEPHERD, S. J. K., BRESTOVITSKY, A., DICKINSON, P., CORTIJO, S., CHAROENSAWAN, V., BOX, M. S., BISWAS, S., JAEGER, K. E. & WIGGE, P. A. 2017. The G-Box Transcriptional Regulatory Code in Arabidopsis. *Plant Physiol,* 175**,** 628-640.

FALCIATORE, A. & BOWLER, C. 2005. The evolution and function of blue and red light photoreceptors. *Curr Top Dev Biol,* 68**,** 317-50.

FARINAS, B., MARY, C., DE O MANES, C. L., BHAUD, Y., PEAUCELLIER, G. & MOREAU, H. 2006. Natural synchronisation for the study of cell division in the green unicellular alga *Ostreococcus tauri*. *Plant Molecular Biology,* 60**,** 277-92.

FLOMBAUM, P., WANG, W.-L., PRIMEAU, F. W. & MARTINY, A. C. 2020. Global picophytoplankton niche partitioning predicts overall positive response to ocean warming. *Nature Geoscience,* 13**,** 116-120.

FORBES-STOVALL, J., HOWTON, J., YOUNG, M., DAVIS, G., CHANDLER, T., KESSLER, B., RINEHART, C. A. & JACOBSHAGEN, S. 2014. *Chlamydomonas reinhardtii* strain CC-124 is highly sensitive to blue light in addition to green and red light in resetting its circadian clock, with the blue-light photoreceptor plant cryptochrome likely acting as negative modulator. *Plant Physiology and Biochemistry,* 75**,** 14-23.

FORNES, O., CASTRO-MONDRAGON, J. A., KHAN, A., VAN DER LEE, R., ZHANG, X., RICHMOND, P. A., MODI, B. P., CORREARD, S., GHEORGHE, M., BARANAŠIĆ, D., SANTANA-GARCIA, W., TAN, G., CHÈNEBY, J., BALLESTER, B., PARCY, F., SANDELIN, A., LENHARD, B., WASSERMAN, W. W. & MATHELIER, A. 2020. JASPAR 2020: update of the open-access database of transcription factor binding profiles. *Nucleic Acids Research,* 48**,** D87-D92.

FORTUNATO, A. E., JAUBERT, M., ENOMOTO, G., BOULY, J.-P., RANIELLO, R., THALER, M., MALVIYA, S., BERNARDES, J. S., RAPPAPORT, F., GENTILI, B., HUYSMAN, M. J. J., CARBONE, A., BOWLER, C., D'ALCALÀ, M. R., IKEUCHI, M. & FALCIATORE, A. 2016. Diatom phytochromes reveal the existence of far-red-light-based sensing in the ocean. *The Plant Cell,* 28**,** 616-628.

FRANCO-ZORRILLA, J. M., LÓPEZ-VIDRIERO, I., CARRASCO, J. L., GODOY, M., VERA, P. & SOLANO, R. 2014. DNA-binding specificities of plant transcription factors and their potential to define target genes. *Proc Natl Acad Sci U S A,* 111**,** 2367-72.

FRANK, A., MATIOLLI, C. C., VIANA, A. J. C., HEARN, T. J., KUSAKINA, J., BELBIN, F. E., WELLS NEWMAN, D., YOCHIKAWA, A., CANO-RAMIREZ, D. L., CHEMBATH, A., CRAGG-BARBER, K., HAYDON, M. J., HOTTA, C. T., VINCENTZ, M., WEBB, A. A. R. & DODD, A. N. 2018. Circadian entrainment in *Arabidopsis* by the sugar-responsive transcription factor bzip63. *Current Biology,* 28**,** 2597-2606.e6.

FRECHILLA, S., ZHU, J., TALBOTT, L. D. & ZEIGER, E. 1999. Stomata from npq1, a zeaxanthin-less *Arabidopsis* mutant, lack a specific response to blue light. *Plant Cell Physiology,* 40**,** 949-54.

GANGAPPA, S. N. & BOTTO, J. F. 2016. The Multifaceted Roles of HY5 in Plant Growth and Development. *Mol Plant,* 9**,** 1353-1365.

GAO, K., ZHANG, Y. & HÄDER, D.-P. 2018. Individual and interactive effects of ocean acidification, global warming, and UV radiation on phytoplankton. *Journal of Applied Phycology,* 30**,** 743-759.

GOFF, L., TRAPNELL, C. & KELLEY, D. 2020. Analysis, exploration, manipulation, and visualization of Cufflinks high-throughput sequencing data. R package version 2.30.0 ed.

GÖTZ, S., GARCÍA-GÓMEZ, J. M., TEROL, J., WILLIAMS, T. D., NAGARAJ, S. H., NUEDA, M. J., ROBLES, M., TALÓN, M., DOPAZO, J. & CONESA, A. 2008. High-throughput functional

annotation and data mining with the Blast2GO suite. *Nucleic Acids Research,* 36**,** 3420-35.

GRANT, C. E., BAILEY, T. L. & NOBLE, W. S. 2011. FIMO: scanning for occurrences of a given motif. *Bioinformatics,* 27**,** 1017-1018.

GRÉBERT, T., DORÉ, H., PARTENSKY, F., FARRANT, G. K., BOSS, E. S., PICHERAL, M., GUIDI, L., PESANT, S., SCANLAN, D. J., WINCKER, P., ACINAS, S. G., KEHOE, D. M. & GARCZAREK, L. 2018. Light color acclimation is a key process in the global ocean distribution of. *Proceedings of the National Academy of Sciences,* 115**,** E2010-E2019.

GRIGORIEV, I. V., NORDBERG, H., SHABALOV, I., AERTS, A., CANTOR, M., GOODSTEIN, D., KUO, A., MINOVITSKY, S., NIKITIN, R., OHM, R. A., OTILLAR, R., POLIAKOV, A., RATNERE, I., RILEY, R., SMIRNOVA, T., ROKHSAR, D. & DUBCHAK, I. 2012. The genome portal of the Department of Energy Joint Genome Institute. *Nucleic Acids Research,* 40**,** D26-32.

GRIMSLEY, N., PEQUIN, B., BACHY, C., MOREAU, H. & PIGANEAU, G. 2010. Cryptic sex in the smallest eukaryotic marine green alga. *Molecular Biology and Evolution,* 27**,** 47-54.

GROOM, S., SATHYENDRANATH, S., BAN, Y., BERNARD, S., BREWIN, R., BROTAS, V., BROCKMANN, C., CHAUHAN, P., CHOI, J.-K., CHUPRIN, A., CIAVATTA, S., CIPOLLINI, P., DONLON, C., FRANZ, B., HE, X., HIRATA, T., JACKSON, T., KAMPEL, M., KRASEMANN, H., LAVENDER, S., PARDO-MARTINEZ, S., MÉLIN, F., PLATT, T., SANTOLERI, R., SKAKALA, J., SCHAEFFER, B., SMITH, M., STEINMETZ, F., VALENTE, A. & WANG, M. 2019. Satellite ocean colour: current status and future perspective. *Frontiers in Marine Science,* 6.

GROSS, J., CHO, W. K., LEZHNEVA, L., FALK, J., KRUPINSKA, K., SHINOZAKI, K., SEKI, M., HERRMANN, R. G. & MEURER, J. 2006. A plant locus essential for phylloquinone (vitamin K1) biosynthesis originated from a fusion of four eubacterial genes. *Journal of Biological Chemistry,* 281**,** 17189-96.

GRUENING, B. A. 2014. Galaxy Wrapper [ONLINE] https://github.com/bgruening/galaxytools.

GUILFOYLE, T. J. 1997. The Structure of Plant Gene Promoters. *In:* SETLOW, J. K. (ed.) *Genetic Engineering: Principles and Methods.* Boston, MA: Springer US.

GUILLOU, L., EIKREM, W., CHRETIENNOT-DINET, M., LE GALL, F., MASSANA, R., ROMARI, K., PEDROS-ALIO, C. & VAULOT, D. 2004. Diversity of picoplanktonic prasinophytes assessed by direct nuclear SSU rDNA sequencing of environmental samples and novel isolates retrieved from oceanic and coastal marine ecosystems. *Protist,* 155**,** 193-214.

GUPTA, S., STAMATOYANNOPOULOS, J. A., BAILEY, T. L. & NOBLE, W. S. 2007. Quantifying similarity between motifs. *Genome Biology,* 8**,** R24.

GUYON, J. B., VERGÉ, V., SCHATT, P., LOZANO, J. C., LIENNARD, M. & BOUGET, F. Y. 2018. Comparative analysis of culture conditions for the optimization of carotenoid production in several strains of the Picoeukaryote *Ostreococcus*. *Marine Drugs,* 16.

HADER, D., KUMAR, H., SMITH, R. & WORREST, R. 1998. Effects on aquatic ecosystems. *Journal of Photochemistry and Photobiology B-Biology,* 46**,** 53-68.

HEIJDE, M., ZABULON, G., CORELLOU, F., ISHIKAWA, T., BRAZARD, J., USMAN, A., SANCHEZ, F., PLAZA, P., MARTIN, M., FALCIATORE, A., TODO, T., BOUGET, F. & BOWLER, C. 2010. Characterization of two members of the cryptochrome/photolyase family from Ostreococcus tauri provides insights into the origin and evolution of cryptochromes. *Plant Cell and Environment,* 33**,** 1614-1626.

HEINZ & WALZ 2003. Phytoplankton Analyzer PHYTO-PAM and Phyto-Win Software V 1.45 System Components and Principles of Operation. *In:* WALZ (ed.) 2 ed. Germany.

HENRÍQUEZ-CASTILLO, C., BOTEBOL, H., MOUTON, A., RAMÍREZ-FLANDES, S., LOZANO, J.-C., LELANDAIS, G., ANDRADE, S., TREFAULT, N., DE LA IGLESIA, R. & BOUGET, F.-Y. 2018. *Ostreococcus tauri* luminescent reporter lines as biosensors for detecting pollution

from copper-mine tailing effluents in coastal environments. *Frontiers in Environmental Science,* 6.

HERNÁNDEZ-RUIZ, M., BARBER-LLUCH, E., PRIETO, A., ÁLVAREZ-SALGADO, X. A., LOGARES, R. & TEIRA, E. 2018. Seasonal succession of small planktonic eukaryotes inhabiting surface waters of a coastal upwelling system. *Environmental Microbiology,* 20**,** 2955-2973.

HIRATSUKA, K. & CHUA, N. H. 1997. Light regulated transcription in higher plants. *J Plant Res,* 110**,** 131-9.

HOOKER, S. B. & CENTER, G. S. F. 2005. *Second SeaWiFS HPLC Analysis Round-robin Experiment (SeaHARRE-2)*, National Aeronautics and Space Administration, Goddard Space Flight Center.

HOPPE, C. J. M., FLINTROP, C. M. & ROST, B. 2018. The Arctic picoeukaryote *Micromonas pusilla* benefits synergistically from warming and ocean acidification. *Biogeosciences,* 15**,** 4353-4365.

HUMPHREYS, M. P. 2016. Climate sensitivity and the rate of ocean acidification: future impacts, and implications for experimental design. *ICES Journal of Marine Science,* 74**,** 934-940.

HYUN, B., KIM, J.-M., JANG, P.-G., JANG, M.-C., CHOI, K.-H., LEE, K., YANG, E. J., NOH, J. H. & SHIN, K. 2020. The effects of ocean acidification and warming on growth of a natural community of coastal phytoplankton. *Journal of Marine Science and Engineering,* 8**,** 821.

JAGANNATHAN, B. & GOLBECK, J. H. 2009. Photosynthesis: Microbial. *In:* SCHAECHTER, M. (ed.) *Encyclopedia of Microbiology (Third Edition).* Oxford: Academic Press.

JAKOBY, M., WEISSHAAR, B., DRÖGE-LASER, W., VICENTE-CARBAJOSA, J., TIEDEMANN, J., KROJ, T., PARCY, F. & GROUP, B. R. 2002. bZIP transcription factors in Arabidopsis. *Trends Plant Sci,* 7**,** 106-11.

JARDILLIER, L., ZUBKOV, M., PEARMAN, J. & SCANLAN, D. 2010. Significant CO_2 fixation by small prymnesiophytes in the subtropical and tropical northeast Atlantic Ocean. *The ISME Journal: Multidisciplinary Journal of Microbial Ecology,* 4**,** 1180-1192.

JIAO, Y., LAU, O. S. & DENG, X. W. 2007. Light-regulated transcriptional networks in higher plants. *Nat Rev Genet,* 8**,** 217-30.

KANEHISA, M. & GOTO, S. 2000. KEGG: kyoto encyclopedia of genes and genomes. *Nucleic Acids Research,* 28**,** 27-30.

KEHOE, D. M. & GROSSMAN, A. R. 1994. Complementary chromatic adaptation: photoperception to gene regulation. *Seminars in Cell and Developmental Biology,* 5**,** 303-13.

KELLER, M. D., SELVIN, R. C., CLAUS, W. & GUILLARD, R. R. L. 1987. Media for the culture of oceanic ultraphytoplankton. *Journal of Phycology,* 23**,** 633-638.

KIM, D., PERTEA, G., TRAPNELL, C., PIMENTEL, H., KELLEY, R. & SALZBERG, S. L. 2013. TopHat2: accurate alignment of transcriptomes in the presence of insertions, deletions and gene fusions. *Genome Biology,* 14**,** R36.

KIM, J., YI, H., CHOI, G., SHIN, B. & SONG, P. S. 2003. Functional characterization of phytochrome interacting factor 3 in phytochrome-mediated light signal transduction. *Plant Cell,* 15**,** 2399-407.

KIRKHAM, A. R., LEPÈRE, C., JARDILLIER, L. E., NOT, F., BOUMAN, H., MEAD, A. & SCANLAN, D. J. 2013. A global perspective on marine photosynthetic picoeukaryote community structure. *The ISME Journal: Multidisciplinary Journal of Microbial Ecology,* 7**,** 922-36.

KOBAYASHI, M., KAKIZONO, T., NISHIO, N. & NAGAI, S. 1992. Effects of light intensity, light quality, and illumination cycle on astaxanthin formation in a green alga, *Haematococcus pluvialis*. *Journal of Fermentation and Bioengineering,* 74**,** 61-63.

KOLDE, R. 2019. pheatmap: Pretty Heatmaps. R package version 1.0.12 ed.

KOTTKE, T., OLDEMEYER, S., WENZEL, S., ZOU, Y. & MITTAG, M. 2017. Cryptochrome photoreceptors in green algae: Unexpected versatility of mechanisms and functions. *J Plant Physiol,* 217**,** 4-14.

KULA, M., RYS, M., MOŻDŻEŃ, K. & SKOCZOWSKI, A. 2014. Metabolic activity, the chemical composition of biomass and photosynthetic activity of *Chlorella vulgaris* under different light spectra in photobioreactors. *Engineering in Life Sciences,* 14**,** 57-67.

KULK, G., VRIES, P., VAN DE POLL, W., VISSER, R. & BUMA, A. 2013. Temperature-dependent photoregulation in oceanic picophytoplankton during excessive irradiance exposure. *Marine Ecology Progress Series***,** 209-228.

KUME, A., AKITSU, T. & NASAHARA, K. N. 2018. Why is chlorophyll b only used in light-harvesting systems? *Journal of Plant Research,* 131**,** 961-972.

LAIN, L. R. & BERNARD, S. 2018. The fundamental contribution of phytoplankton spectral scattering to ocean colour: implications for satellite detection of phytoplankton community structure. *Applied Sciences,* 8**,** 2681.

LANDSCHÜTZER, P., GRUBER, N., BAKKER, D. C. E., STEMMLER, I. & SIX, K. D. 2018. Strengthening seasonal marine CO2 variations due to increasing atmospheric CO2. *Nature Climate Change,* 8**,** 146-150.

LANGMEAD, B. & SALZBERG, S. L. 2012. Fast gapped-read alignment with Bowtie 2. *Nature Methods,* 9**,** 357-9.

LANOUE, J., LEONARDOS, E. D. & GRODZINSKI, B. 2019. 4.68 - Artificial lighting technologies for agricultural production. *In:* MOO-YOUNG, M. (ed.) *Comprehensive Biotechnology (Third Edition).* Oxford: Pergamon.

LAVIALE, M. & JACQUES, N. 2011. Relationships between pigment ratios and growth irradiance. *Marine Ecology Progress Series,* 425**,** 63-77.

LECONTE, J., BENITES, L. F., VANNIER, T., WINCKER, P., PIGANEAU, G. & JAILLON, O. 2020. Genome resolved biogeography of mamiellales. *Genes (Basel),* 11.

LEE, J., HE, K., STOLC, V., LEE, H., FIGUEROA, P., GAO, Y., TONGPRASIT, W., ZHAO, H., LEE, I. & DENG, X. W. 2007. Analysis of transcription factor HY5 genomic binding sites revealed its hierarchical role in light regulation of development. *Plant Cell,* 19**,** 731-49.

LEIVAR, P., MONTE, E., AL-SADY, B., CARLE, C., STORER, A., ALONSO, J. M., ECKER, J. R. & QUAIL, P. H. 2008. The Arabidopsis phytochrome-interacting factor PIF7, together with PIF3 and PIF4, regulates responses to prolonged red light by modulating phyB levels. *Plant Cell,* 20**,** 337-52.

LELANDAIS, G., SCHEIBER, I., PAZ-YEPES, J., LOZANO, J., BOTEBOL, H., PILATOVA, J., ZARSKY, V., LEGER, T., BLAISEAU, P., BOWLER, C., BOUGET, F., CAMADRO, J., SUTAK, R. & LESUISSE, E. 2016. *Ostreococcus tauri* is a new model green alga for studying iron metabolism in eukaryotic phytoplankton. *BioMed Central Genomics,* 17.

LETELIER, R. M., WHITE, A. E., BIDIGARE, R. R., BARONE, B., CHURCH, M. J. & KARL, D. M. 2017. Light absorption by phytoplankton in the North Pacific Subtropical Gyre. *Limnology and Oceanography,* 62**,** 1526-1540.

LEWANDOWSKA, A. M., STRIEBEL, M., FEUDEL, U., HILLEBRAND, H. & SOMMER, U. 2015. The importance of phytoplankton trait variability in spring bloom formation. *ICES Journal of Marine Science,* 72**,** 1908-1915.

LI, G., CHENG, L., ZHU, J., TRENBERTH, K. E., MANN, M. E. & ABRAHAM, J. P. 2020. Increasing ocean stratification over the past half-century. *Nature Climate Change,* 10**,** 1116-1123.

LICHTENTHALER, H. K. 1987. [34] Chlorophylls and carotenoids: Pigments of photosynthetic biomembranes. *Methods in Enzymology.* Academic Press.

LIM, G., CHANG, Y. & HUH, W.-K. 2020. Phosphoregulation of Rad51/Rad52 by CDK1 functions as a molecular switch for cell cycle–specific activation of homologous recombination. *Science Advances,* 6**,** eaay2669.

LIMARDO, A. J., SUDEK, S., CHOI, C. J., POIRIER, C., RII, Y. M., BLUM, M., ROTH, R., GOODENOUGH, U., CHURCH, M. J. & WORDEN, A. Z. 2017. Quantitative biogeography of picoprasinophytes establishes ecotype distributions and significant contributions to marine phytoplankton. *Environmental Microbiology,* 19**,** 3219-3234.

LIS, M. & WALTHER, D. 2016. The orientation of transcription factor binding site motifs in gene promoter regions: does it matter? *BioMed Central Genomics,* 17**,** 185.

LOPES DOS SANTOS, A., GOURVIL, P., RODRÍGUEZ, F., GARRIDO, J. L. & VAULOT, D. 2016. Photosynthetic pigments of oceanic Chlorophyta belonging to prasinophytes clade VII. *Journal of Phycology,* 52**,** 148-55.

LOPES DOS SANTOS, A., GOURVIL, P., TRAGIN, M., NOEL, M.-H., DECELLE, J., ROMAC, S. & VAULOT, D. 2017. Diversity and oceanic distribution of prasinophytes clade VII, the dominant group of green algae in oceanic waters. *ISME Journal,* 11**,** 512-528.

LÓPEZ-FIGUEROA, F. 1992. Diurnal variation in pigment content in *Porphyra laciniata* and *Chondrus crispus* and its relation to the diurnal changes of underwater light quality and quantity. *Marine Ecology,* 13**,** 285-305.

LORENZEN, C. J. & NEWTON DOWNS, J. 1986. The specific absorption coefficients of chlorophyllide a and pheophorbide a in 90% acetone, and comments on the fluorometric determination of chlorophyll and pheopigments. *Limnology and Oceanography,* 31**,** 449-452.

LOZANO, J., SCHATT, P., BOTEBOL, H., VERGE, V., LESUISSE, E., BLAIN, S., CARRE, I. & BOUGET, F. 2014. Efficient gene targeting and removal of foreign DNA by homologous recombination in the picoeukaryote *Ostreococcus*. *Plant Journal,* 78**,** 1073-1083.

LUCK, M., ESCOBAR, F. V., GLASS, K., SABOTKE, M.-I., HAGEDORN, R., CORELLOU, F., SIEBERT, F., HILDEBRANDT, P. & HEGEMANN, P. 2019. Photoreactions of the histidine kinase rhodopsin Ot-HKR from the marine picoalga *Ostreococcus tauri*. *Biochemistry,* 58**,** 1878-1891.

LUIMSTRA, V. M., SCHUURMANS, J. M., HELLINGWERF, K. J., MATTHIJS, H. C. P. & HUISMAN, J. 2020a. Blue light induces major changes in the gene expression profile of the cyanobacterium *Synechocystis sp. PCC 6803*. *Physiologia Plantarum,* 170**,** 10-26.

LUIMSTRA, V. M., VERSPAGEN, J. M. H., XU, T., SCHUURMANS, J. M. & HUISMAN, J. 2020b. Changes in water color shift competition between phytoplankton species with contrasting light-harvesting strategies. *Ecology,* 101**,** e02951-e02951.

MAERE, S., HEYMANS, K. & KUIPER, M. 2005. BiNGO: a Cytoscape plugin to assess overrepresentation of gene ontology categories in biological networks. *Bioinformatics,* 21**,** 3448-9.

MALLAPPA, C., YADAV, V., NEGI, P. & CHATTOPADHYAY, S. 2006. A basic leucine zipper transcription factor, G-box-binding factor 1, regulates blue light-mediated photomorphogenic growth in Arabidopsis. *J Biol Chem,* 281**,** 22190-22199.

MANFIELD, I. W., DEVLIN, P. F., JEN, C. H., WESTHEAD, D. R. & GILMARTIN, P. M. 2007. Conservation, convergence, and divergence of light-responsive, circadian-regulated, and tissue-specific expression patterns during evolution of the Arabidopsis GATA gene family. *Plant Physiol,* 143**,** 941-58.

MARKAGER, S. & VINCENT, W. F. 2001. Light absorption by phytoplankton: development of a matching parameter for algal photosynthesis under different spectral regimes. *Journal of Plankton Research,* 23**,** 1373-1384.

MAWPHLANG, O. I. L. & KHARSHIING, E. V. 2017. Photoreceptor mediated plant growth responses: implications for photoreceptor engineering toward improved performance in crops. *Frontiers in Plant Science,* 8**,** 1181.

MAXWELL, D. P., LAUDENBACH, D. E. & HUNER, N. 1995. Redox regulation of Light-Harvesting Complex II and cab mRNA abundance in *Dunaliella salina*. *Plant Physiology,* 109**,** 787-795.

MAXWELL, K. & JOHNSON, G. N. 2000. Chlorophyll fluorescence--a practical guide. *Journal of Experimental Botany,* 51**,** 659-68.

MELIS, A. 1989. Spectroscopic Methods in Photosynthesis: Photosystem Stoichiometry and Chlorophyll Antenna Size. *Philosophical Transactions of the Royal Society of London. Series B, Biological Sciences,* 323**,** 397-409.

MENG, R., ZHOU, C., ZHU, X., HUANG, H., XU, J., LUO, Q. & YAN, X. 2019. Critical light-related gene expression varies in two different strains of the dinoflagellate *Karlodinium veneficum* in response to the light spectrum and light intensity. *Journal of Photochemistry and Photobiology B-Biology,* 194**,** 76-83.

MODEL, M. A. 2018. Methods for cell volume measurement. *Cytometry A,* 93**,** 281-296.

MÖGLICH, A., YANG, X., AYERS, R. A. & MOFFAT, K. 2010. Structure and function of plant photoreceptors. *Annual Review of Plant Biology,* 61**,** 21-47.

MONNIER, A., LIVERANI, S., BOUVET, R., JESSON, B., SMITH, J., MOSSER, J., CORELLOU, F. & BOUGET, F. 2010. Orchestrated transcription of biological processes in the marine picoeukaryote *Ostreococcus* exposed to light/dark cycles. *BioMed Central Genomics,* 11.

MONTE, E., TEPPERMAN, J. M., AL-SADY, B., KACZOROWSKI, K. A., ALONSO, J. M., ECKER, J. R., LI, X., ZHANG, Y. & QUAIL, P. H. 2004. The phytochrome-interacting transcription factor, PIF3, acts early, selectively, and positively in light-induced chloroplast development. *Proc Natl Acad Sci U S A,* 101**,** 16091-8.

MOON-VAN DER STAAY, S. Y., DE WACHTER, R. & VAULOT, D. 2001. Oceanic 18S rDNA sequences from picoplankton reveal unsuspected eukaryotic diversity. *Nature,* 409**,** 607-10.

MORÁN, X. A. G., LÓPEZ-URRUITA, Á., CALVO-DÍAZ, A. & LI, W. K. W. 2010. Increasing importance of small phytoplankton in a warmer ocean. *Global Change Biology,* 16**,** 1137-1144.

MOULAGER, M., MONNIER, A., JESSON, B., BOUVET, R., MOSSER, J., SCHWARTZ, C., GARNIER, L., CORELLOU, F. & BOUGET, F. 2007. Light-dependent regulation of cell division in *Ostreococcus*: Evidence for a major transcriptional input. *Plant Physiology,* 144**,** 1360-1369.

MOYER, S. E., LEWIS, P. W. & BOTCHAN, M. R. 2006. Isolation of the Cdc45/Mcm2-7/GINS (CMG) complex, a candidate for the eukaryotic DNA replication fork helicase. *Proceedings of the National Academy of Sciences of the United States of America,* 103**,** 10236-10241.

MULLANEY, P. F., VAN DILLA, M. A., COULTER, J. R. & DEAN, P. N. 1969. Cell sizing: a light scattering photometer for rapid volume determination. *Review of Scientific Instruments,* 40**,** 1029-32.

MULLIN, M. M. 2001. Plankton. *In:* COCHRAN, J. K., BOKUNIEWICZ, H. J. & YAGER, P. L. (eds.) *Encyclopedia of Ocean Sciences (Third Edition).* Oxford: Academic Press.

MUNNÉ-BOSCH, S. & CELA, J. 2006. Effects of water deficit on photosystem II photochemistry and photoprotection during acclimation of lyreleaf sage (*Salvia lyrata L*.) plants to high light. *Journal of Photochemistry and Photobiology B-Biology,* 85**,** 191-7.

MURCHIE, E. H. & HORTON, P. 1997. Acclimation of photosynthesis to irradiance and spectral quality in British plant species: chlorophyll content, photosynthetic capacity and habitat preference. *Plant, Cell & Environment,* 20**,** 438-448.

MURCHIE, E. H. & LAWSON, T. 2013. Chlorophyll fluorescence analysis: a guide to good practice and understanding some new applications. *Journal of Experimental Botany,* 64**,** 3983-3998.

O'KELLY, C., SIERACKI, M., THIER, E. & HOBSON, I. 2003. A transient bloom of *Ostreococcus* (Chlorophyta, Prasinophyceae) in West Neck Bay, Long Island, New York. *Journal of Phycology,* 39**,** 850-854.

O'MALLEY, R. C., HUANG, S. C., SONG, L., LEWSEY, M. G., BARTLETT, A., NERY, J. R., GALLI, M., GALLAVOTTI, A. & ECKER, J. R. 2016. Cistrome and Epicistrome Features Shape the Regulatory DNA Landscape. *Cell,* 166**,** 1598.

OUZOUNIS, T., ROSENQVIST, E. & OTTOSEN, C.-O. 2015. Spectral Effects of Artificial Light on Plant Physiology and Secondary Metabolism: A Review. *HortScience horts,* 50**,** 1128.

OYAMA, T., SHIMURA, Y. & OKADA, K. 1997. The Arabidopsis HY5 gene encodes a bZIP protein that regulates stimulus-induced development of root and hypocotyl. *Genes & development,* 11**,** 2983-2995.

OZIEL, L., BAUDENA, A., ARDYNA, M., MASSICOTTE, P., RANDELHOFF, A., SALLÉE, J. B., INGVALDSEN, R. B., DEVRED, E. & BABIN, M. 2020. Faster Atlantic currents drive poleward expansion of temperate phytoplankton in the Arctic Ocean. *Nature Communications,* 11**,** 1705.

PALENIK, B. 2001. Chromatic adaptation in marine *Synechococcus* strains. *Applied and Environmental Microbiology,* 67**,** 991-4.

PALENIK, B., GRIMWOOD, J., AERTS, A., ROUZE, P., SALAMOV, A., PUTNAM, N., DUPONT, C., JORGENSEN, R., DERELLE, E., ROMBAUTS, S., ZHOU, K., OTILLAR, R., MERCHANT, S., PODELL, S., GAASTERLAND, T., NAPOLI, C., GENDLER, K., MANUELL, A., TAI, V., VALLON, O., PIGANEAU, G., JANCEK, S., HEIJDE, M., JABBARI, K., BOWLER, C., LOHR, M., ROBBENS, S., WERNER, G., DUBCHAK, I., PAZOUR, G., REN, Q., PAULSEN, I., DELWICHE, C., SCHMUTZ, J., ROKHSAR, D., VAN DE PEER, Y., MOREAU, H. & GRIGORIEV, I. 2007. The tiny eukaryote *Ostreococcus* provides genomic insights into the paradox of plankton speciation. *Proceedings of the National Academy of Sciences of the United States of America,* 104**,** 7705-7710.

PENNISI, G., BLASIOLI, S., CELLINI, A., MAIA, L., CREPALDI, A., BRASCHI, I., SPINELLI, F., NICOLA, S., FERNANDEZ, J. A., STANGHELLINI, C., MARCELIS, L. F. M., ORSINI, F. & GIANQUINTO, G. 2019. Unraveling the Role of Red:Blue LED Lights on Resource Use Efficiency and Nutritional Properties of Indoor Grown Sweet Basil. *Frontiers in Plant Science,* 10.

PFANNSCHMIDT, T., ALLEN, J. F. & OELMÜLLER, R. 2001. Principles of redox control in photosynthesis gene expression. *Physiologia Plantarum,* 112**,** 1-9.

PIREYRE, M. & BUROW, M. 2015. Regulation of MYB and bHLH transcription factors: a glance at the protein level. *Mol Plant,* 8**,** 378-88.

PLATT, T., GALLEGOS, C. L. & HARRISON, W. G. 1980. PHOTOINHIBITION OF PHOTOSYNTHESIS IN NATURAL ASSEMBLAGES OF MARINE PHYTOPLANKTON. *Journal of Marine Research,* 38**,** 687-701.

POLLOCK, S. V., COLOMBO, S. L., PROUT, D. L., GODFREY, A. C. & MORONEY, J. V. 2003. Rubisco activase is required for optimal photosynthesis in the green alga *Chlamydomonas reinhardtii* in a low-CO(2) atmosphere. *Plant Physiology,* 133**,** 1854-61.

POLOVINA, J. J., HOWELL, E. A. & ABECASSIS, M. 2008. Ocean's least productive waters are expanding. *Geophysical Research Letters,* 35.

PORTIS, A. R., JR. 2003. Rubisco activase - Rubisco's catalytic chaperone. *Photosynthesis Research,* 75**,** 11-27.

POTES, M., COSTA, M. J., SALGADO, R., BORTOLI, D., SERAFIM, A. & MOIGNE, P. L. 2013. Spectral measurements of underwater downwelling radiance of inland water bodies. *Tellus A: Dynamic Meteorology and Oceanography,* 65**,** 20774.

QUINLAN, A. R. & HALL, I. M. 2010. BEDTools: a flexible suite of utilities for comparing genomic features. *Bioinformatics,* 26**,** 841-2.

R CORE TEAM 2020. R: A language and environment for statistical computing. Vienna, Austria: R Foundation for Statistical Computing.

RABARA, R. C., BEHRMAN, G., TIMBOL, T. & RUSHTON, P. J. 2017. Effect of Spectral Quality of Monochromatic LED Lights on the Growth of Artichoke Seedlings. *Front Plant Sci,* 8**,** 190.

RALPH, P. J. & GADEMANN, R. 2005. Rapid light curves: A powerful tool to assess photosynthetic activity. *Aquatic Botany,* 82**,** 222-237.

RASTOGI, R. P., SONANI, R. R. & MADAMWAR, D. 2015. Cyanobacterial sunscreen scytonemin: role in photoprotection and biomedical research. *Applied Biochemistry and Biotechnology,* 176**,** 1551-1563.

REMUS, D., BEURON, F., TOLUN, G., GRIFFITH, J. D., MORRIS, E. P. & DIFFLEY, J. F. 2009. Concerted loading of Mcm2-7 double hexamers around DNA during DNA replication origin licensing. *Cell,* 139**,** 719-30.

RIANO-PACHON, D., RUZICIC, S., DREYER, I. & MUELLER-ROEBER, B. 2007. PlnTFDB: an integrative plant transcription factor database. *Bmc Bioinformatics,* 8.

RII, Y. M., DUHAMEL, S., BIDIGARE, R. R., KARL, D. M., REPETA, D. J. & CHURCH, M. J. 2016. Diversity and productivity of photosynthetic picoeukaryotes in biogeochemically distinct regions of the South East Pacific Ocean. *Limnology and Oceanography,* 61**,** 806-824.

RIVKIN, R. B. 1989. Influence of irradiance and spectral quality on the carbon metabolism of phytoplankton. I. Photosynthesis, chemical composition and growth. *Marine Ecology Progress Series,* 55**,** 291-304.

RODRÍGUEZ, F., DERELLE, E., GUILLOU, L., LE GALL, F., VAULOT, D. & MOREAU, H. 2005. Ecotype diversity in the marine picoeukaryote *Ostreococcus* (Chlorophyta, Prasinophyceae). *Environmental Microbiology,* 7**,** 853-9.

ROY, S., LLEWELLYN, C., EGELAND, E. & JOHNSEN, G. 2011. Specific absorption coefficients for major algal chlorophylls, bacteriochlorophylls and carotenoids. *Phytoplankton pigments: characterization, chemotaxonomy and applications in oceanography.* Cambridge: Cambridge University Press.

SAITO, A., IINO, T., SONOIKE, K., MIWA, E. & HIGUCHI, K. 2010. Remodeling of the major light-harvesting antenna protein of PSII protects the young leaves of barley (*Hordeum vulgare L.*) from photoinhibition under prolonged iron deficiency. *Plant Cell Physiology,* 51**,** 2013-30.

SANCHEZ, F., GEFFROY, S., NOREST, M., YAU, S., MOREAU, H. & GRIMSLEY, N. 2019. Simplified Transformation of. *Genes (Basel),* 10.

SAWBRIDGE, T. I., LÓPEZ-JUEZ, E., KNIGHT, M. R. & JENKINS, G. I. 1993. A blue-light photoreceptor mediates the fluence-rate-dependent expression of genes encoding the small subunit of ribulose 1,5-bisphosphate carboxylase/oxygenase in light-grown Phaseolus vulgaris primary leaves. *Planta,* 192**,** 1-8.

SCHAUM, C. E. & COLLINS, S. 2014. Plasticity predicts evolution in a marine alga. *Proceedings of the Royal Society B-Biological Sciences,* 281.

SCHAUM, E., ROST, B., MILLAR, A. & COLLINS, S. 2013. Variation in plastic responses of a globally distributed picoplankton species to ocean acidification. *Nature Climate Change,* 3**,** 298-302.

SCHMIDTKO, S., STRAMMA, L. & VISBECK, M. 2017. Decline in global oceanic oxygen content during the past five decades. *Nature,* 542**,** 335-339.

SCHUBERT, H., SAGERT, S. & FORSTER, R. 2001. Evaluation of the different levels of variability in the underwater light field of a shallow estuary. *Helgoland Marine Research,* 55**,** 12-22.

SCHULZ, K. G., BACH, L. T., BELLERBY, R. G. J., BERMÚDEZ, R., BÜDENBENDER, J., BOXHAMMER, T., CZERNY, J., ENGEL, A., LUDWIG, A., MEYERHÖFER, M., LARSEN, A., PAUL, A. J., SSWAT, M. & RIEBESELL, U. 2017. Phytoplankton blooms at increasing levels of atmospheric carbon dioxide: experimental evidence for negative effects on

Prymnesiophytes and positive on small picoeukaryotes. *Frontiers in Marine Science,* 4.

SEIFERT, M., ROST, B., TRIMBORN, S. & HAUCK, J. 2020. Meta-analysis of multiple driver effects on marine phytoplankton highlights modulating role of pCO2. *Global Change Biology,* 26**,** 6787-6804.

SERÔDIO, J., VIEIRA, S., CRUZ, S. & COELHO, H. 2006. Rapid light-response curves of chlorophyll fluorescence in microalgae: relationship to steady-state light curves and non-photochemical quenching in benthic diatom-dominated assemblages. *Photosynthesis Research,* 90**,** 29-43.

SILVA, T. D., BATISTA, D. S., FORTINI, E. A., CASTRO, K. M. D., FELIPE, S. H. S., FERNANDES, A. M., SOUSA, R. M. D. J., CHAGAS, K., SILVA, J. V. S. D., CORREIA, L. N. D. F., FARIAS, L. M., LEITE, J. P. V., ROCHA, D. I. & OTONI, W. C. 2020. Blue and red light affects morphogenesis and 20-hydroxyecdisone content of in vitro Pfaffia glomerata accessions. *Journal of Photochemistry and Photobiology B: Biology,* 203**,** 111761.

SIMMONS, M., SUDEK, S., MONIER, A., LIMARDO, A., JIMENEZ, V., PERLE, C., ELROD, V., PENNINGTON, J. & WORDEN, A. 2016. Abundance and biogeography of Picoprasinophyte ecotypes and other phytoplankton in the Eastern North Pacific Ocean. *Applied and Environmental Microbiology,* 82**,** 1693-1705.

SIX, C., FINKEL, Z., RODRIGUEZ, F., MARIE, D., PARTENSKY, F. & CAMPBELL, D. 2008. Contrasting photoacclimation costs in ecotypes of the marine eukaryotic picoplankter *Ostreococcus*. *Limnology and Oceanography,* 53**,** 255-265.

SIX, C., SHERRARD, R., LIONARD, M., ROY, S. & CAMPBELL, D. 2009. Photosystem II and pigment dynamics among ecotypes of the green alga *Ostreococcus*. *Plant Physiology,* 151**,** 379-390.

SIX, C., THOMAS, J.-C., GARCZAREK, L., OSTROWSKI, M., DUFRESNE, A., BLOT, N., SCANLAN, D. J. & PARTENSKY, F. 2007. Diversity and evolution of phycobilisomes in marine *Synechococcus spp*.: a comparative genomics study. *Genome Biology,* 8**,** R259.

SIX, C., WORDEN, A., RODRIGUEZ, F., MOREAU, H. & PARTENSKY, F. 2005. New insights into the nature and phylogeny of prasinophyte antenna proteins: *Ostreococcus tauri*, a case study. *Molecular Biology and Evolution,* 22**,** 2217-2230.

SOJA-WOŹNIAK, M., DARECKI, M., WOJTASIEWICZ, B. & BRADTKE, K. 2018. Laboratory measurements of remote sensing reflectance of selected phytoplankton species from the Baltic Sea. *Oceanologia,* 60**,** 86-96.

SOY, J., LEIVAR, P., GONZÁLEZ-SCHAIN, N., MARTÍN, G., DIAZ, C., SENTANDREU, M., AL-SADY, B., QUAIL, P. H. & MONTE, E. 2016. Molecular convergence of clock and photosensory pathways through PIF3-TOC1 interaction and co-occupancy of target promoters. *Proc Natl Acad Sci U S A,* 113**,** 4870-5.

SPRINGER, P. S., HOLDING, D. R., GROOVER, A., YORDAN, C. & MARTIENSSEN, R. A. 2000. The essential Mcm7 protein PROLIFERA is localized to the nucleus of dividing cells during the G(1) phase and is required maternally for early *Arabidopsis* development. *Development,* 127**,** 1815-22.

STOMP, M., HUISMAN, J., DE JONGH, F., VERAART, A. J., GERLA, D., RIJKEBOER, M., IBELINGS, B. W., WOLLENZIEN, U. I. & STAL, L. J. 2004. Adaptive divergence in pigment composition promotes phytoplankton biodiversity. *Nature,* 432**,** 104-7.

STOWE, W. C., BRODIE-KOMMIT, J. & STOWE-EVANS, E. 2011. Characterization of complementary chromatic adaptation in *Gloeotrichia UTEX 583* and identification of a transposon-like insertion in the cpeBA operon. *Plant Cell Physiology,* 52**,** 553-62.

SUBIRANA, L., PEQUIN, B., MICHELY, S., ESCANDE, M., MEILLAND, J., DERELLE, E., MARIN, B., PIGANEAU, G., DESDEVISES, Y., MOREAU, H. & GRIMSLEY, N. 2013. Morphology, genome plasticity, and phylogeny in the genus *Ostreococcus* reveal a cryptic species, *O. mediterraneus sp nov* (Mamiellales, Mamiellophyceae). *Protist,* 164**,** 643-659.

SUKENIK, A., BENNETT, J. & FALKOWSKI, P. 1987. Light-saturated photosynthesis—limitation by electron transport or carbon fixation? *Biochimica et Biophysica Acta (BBA) - Bioenergetics,* 891**,** 205-215.

SULLIVAN, S., PETERSEN, J., BLACKWOOD, L., PAPANATSIOU, M. & CHRISTIE, J. 2016. Functional characterization of *Ostreococcus tauri* phototropin. *New Phytologist,* 209**,** 612-623.

SUN, D., LI, Y., WANG, Q., LV, H., LE, C., HUANG, C. & GONG, S. 2010. Partitioning particulate scattering and absorption into contributions of phytoplankton and non-algal particles in winter in Lake Taihu (China). *Hydrobiologia,* 644**,** 337-349.

TARDU, M., DIKBAS, U. M., BARIS, I. & KAVAKLI, I. H. 2016. RNA-seq analysis of the transcriptional response to blue and red light in the extremophilic red alga, *Cyanidioschyzon merolae*. *Functional & Integrative Genomics,* 16**,** 657-669.

TARENTO, T. D. C., MCCLURE, D. D., TALBOT, A. M., REGTOP, H. L., BIFFIN, J. R., VALTCHEV, P., DEHGHANI, F. & KAVANAGH, J. M. 2019. A potential biotechnological process for the sustainable production of vitamin K. *Critical Reviews in Biotechnology,* 39**,** 1-19.

THE GENE ONTOLOGY CONSORTIUM 2019. The Gene Ontology Resource: 20 years and still GOing strong. *Nucleic Acids Res,* 47**,** D330-D338.

THE UNIPROT CONSORTIUM 2020. UniProt: the universal protein knowledgebase in 2021. *Nucleic Acids Research*.

THOMMEN, Q., PFEUTY, B., SCHATT, P., BIJOUX, A., BOUGET, F. & LEFRANC, M. 2015. Probing entrainment of *Ostreococcus* tauri circadian clock by green and blue light through a mathematical modeling approach. *Frontiers in Genetics,* 6.

THOMY, J., SANCHEZ, F., GUT, M., CRUZ, F., ALIOTO, T., PIGANEAU, G., GRIMSLEY, N. & YAU, S. 2021. Combining nanopore and illumina sequencing permits detailed analysis of insertion mutations and structural variations produced by PEG-mediated transformation in *Ostreococcus tauri*. *Cells,* 10**,** 664.

TILZER, M., STAMBLER, N. & LOVENGREEN, C. 1995. The role of phytoplankton in determining the underwater light climate in Lake Constance. *Hydrobiologia,* 316**,** 161-172.

TRAGIN, M. & VAULOT, D. 2019. Novel diversity within marine Mamiellophyceae (Chlorophyta) unveiled by metabarcoding. *Scientific Reports,* 9**,** 5190.

TRAPNELL, C., HENDRICKSON, D. G., SAUVAGEAU, M., GOFF, L., RINN, J. L. & PACHTER, L. 2013. Differential analysis of gene regulation at transcript resolution with RNA-seq. *Nature Biotechnology,* 31**,** 46-53.

TUTEJA, N., TRAN, N. Q., DANG, H. Q. & TUTEJA, R. 2011. Plant MCM proteins: role in DNA replication and beyond. *Plant Molecular Biology,* 77**,** 537-45.

V-BALOGH, K., NEMETH, B. & VOROS, L. 2009. Specific attenuation coefficients of optically active substances and their contribution to the underwater ultraviolet and visible light climate in shallow lakes and ponds. *Hydrobiologia,* 632**,** 91-105.

VALLE, K. C., NYMARK, M., AAMOT, I., HANCKE, K., WINGE, P., ANDRESEN, K., JOHNSEN, G., BREMBU, T. & BONES, A. M. 2014. System responses to equal doses of photosynthetically usable radiation of blue, green, and red light in the marine diatom *Phaeodactylum tricornutum*. *PLoS One,* 9**,** e114211.

VAN BAREN, M. J., BACHY, C., REISTETTER, E. N., PURVINE, S. O., GRIMWOOD, J., SUDEK, S., YU, H., POIRIER, C., DEERINCK, T. J., KUO, A., GRIGORIEV, I. V., WONG, C.-H., SMITH, R. D., CALLISTER, S. J., WEI, C.-L., SCHMUTZ, J. & WORDEN, A. Z. 2016. Evidence-based green algal genomics reveals marine diversity and ancestral characteristics of land plants. *BioMed Central Genomics,* 17**,** 267.

VAN HEUKELEM, L. & THOMAS, C. S. 2001. Computer-assisted high-performance liquid chromatography method development with applications to the isolation and analysis of phytoplankton pigments. *The Journal of Chromatography A,* 910**,** 31-49.

VAN OOIJEN, G., KNOX, K., KIS, K., BOUGET, F. & MILLAR, A. 2012. Genomic transformation of the Picoeukaryote *Ostreococcus tauri*. *Jove-Journal of Visualized Experiments*.

VANDENHECKE, J. M., BASTEDO, J., COCKSHUTT, A. M., CAMPBELL, D. A. & HUOT, Y. 2015. Changes in the Rubisco to photosystem ratio dominates photoacclimation across phytoplankton taxa. *Photosynthesis Research,* 124**,** 275-91.

VILLAR, E., VANNIER, T., VERNETTE, C., LESCOT, M., CUENCA, M., ALEXANDRE, A., BACHELERIE, P., ROSNET, T., PELLETIER, E., SUNAGAWA, S. & HINGAMP, P. 2018. The Ocean Gene Atlas: exploring the biogeography of plankton genes online. *Nucleic Acids Res,* 46**,** W289-W295.

WANG, H., GU, M., CUI, J., SHI, K., ZHOU, Y. & YU, J. 2009. Effects of light quality on CO2 assimilation, chlorophyll-fluorescence quenching, expression of Calvin cycle genes and carbohydrate accumulation in *Cucumis sativus*. *Journal of Photochemistry and Photobiology B: Biology,* 96**,** 30-37.

WEIRAUCH, M. T., YANG, A., ALBU, M., COTE, A. G., MONTENEGRO-MONTERO, A., DREWE, P., NAJAFABADI, H. S., LAMBERT, S. A., MANN, I., COOK, K., ZHENG, H., GOITY, A., VAN BAKEL, H., LOZANO, J. C., GALLI, M., LEWSEY, M. G., HUANG, E., MUKHERJEE, T., CHEN, X., REECE-HOYES, J. S., GOVINDARAJAN, S., SHAULSKY, G., WALHOUT, A. J. M., BOUGET, F. Y., RATSCH, G., LARRONDO, L. F., ECKER, J. R. & HUGHES, T. R. 2014. Determination and inference of eukaryotic transcription factor sequence specificity. *Cell,* 158**,** 1431-1443.

WILLMANN, M. R., MEHALICK, A. J., PACKER, R. L. & JENIK, P. D. 2011. MicroRNAs regulate the timing of embryo maturation in Arabidopsis. *Plant Physiol,* 155**,** 1871-84.

WLODARCZYK, L. M., SNELLENBURG, J. J., IHALAINEN, J. A., VAN GRONDELLE, R., VAN STOKKUM, I. H. & DEKKER, J. P. 2015. Functional rearrangement of the light-harvesting antenna upon state transitions in a green alga. *Biophysical Journal,* 108**,** 261-71.

WORDEN, A., NOLAN, J. & PALENIK, B. 2004. Assessing the dynamics and ecology of marine picophytoplankton: The importance of the eukaryotic component. *Limnology and Oceanography,* 49**,** 168-179.

WU, H. 2016. Effect of different light qualities on growth, pigment content, chlorophyll fluorescence, and antioxidant enzyme activity in the red alga *Pyropia haitanensis* (Bangiales, Rhodophyta). *BioMed Research International,* 2016**,** 7383918.

YAMORI, W., MASUMOTO, C., FUKAYAMA, H. & MAKINO, A. 2012. Rubisco activase is a key regulator of non-steady-state photosynthesis at any leaf temperature and, to a lesser extent, of steady-state photosynthesis at high temperature. *Plant Journal,* 71**,** 871-80.

YANG, D., SEATON, D. D., KRAHMER, J. & HALLIDAY, K. J. 2016a. Photoreceptor effects on plant biomass, resource allocation, and metabolic state. *Proceedings of the National Academy of Sciences,* 113**,** 7667-72.

YANG, J., PAN, Y., BOWLER, C., ZHANG, L. & HU, H. 2016b. Knockdown of phosphoenolpyruvate carboxykinase increases carbon flux to lipid synthesis in *Phaeodactylum tricornutum*. *Algal Research-Biomass Biofuels and Bioproducts,* 15**,** 50-58.

ZEIGER, E. & ZHU, J. 1998. Role of zeaxanthin in blue light photoreception and the modulation of light-CO2 interactions in guard cells. *Journal of Experimental Botany,* 49**,** 433-442.

ZORZ, J. K., ALLANACH, J. R., MURPHY, C. D., ROODVOETS, M. S., CAMPBELL, D. A. & COCKSHUTT, A. M. 2015. The RUBISCO to Photosystem II Ratio limits the maximum photosynthetic rate in Picocyanobacteria. *Life (Basel),* 5**,** 403-17.

Appendix 1 All significantly differentially expressed genes from RNASeq

OTH95 genes

Gene ID	Light condition 1	Light condition 2	FPKM 1	FPKM 2	log2 fold change	FDR corrected q value
ostta03g05340	Blue	Green	4.53	15.03	1.730	0.0072
ostta08g04240	Blue	Green	144.96	432.66	1.578	0.0072
ostta01g02840	Blue	Green	7.24	18.90	1.384	0.0072
ostta15g01710	Blue	Green	32.91	79.21	1.267	0.0194
ostta05g01150	Blue	Green	18.75	44.27	1.239	0.0173
ostta06g02350	Blue	Green	30.31	70.78	1.224	0.0114
ostta07g02530	Blue	Green	2337.71	5405.02	1.209	0.0390
ostta05g04970	Blue	Green	8.14	18.31	1.169	0.0317
ostta06g02940	Blue	Green	35.41	75.09	1.084	0.0438
ostta01g04715	Blue	Green	22.76	0.00	22.760	0.0242
ostta06g00450	Blue	Green	4.08	0.00	4.085	0.0194
ostta14g01070	Blue	Green	388.42	194.13	-1.001	0.0390
ostta09g03820	Blue	Green	77.77	38.54	-1.013	0.0438
ostta08g02870	Blue	Green	103.50	48.94	-1.080	0.0467
ostta13g02780	Blue	Green	12.99	6.13	-1.084	0.0438
ostta06g03500	Blue	Green	460.96	214.36	-1.105	0.0406
ostta17g01070	Blue	Green	42.50	19.57	-1.119	0.0406
ostta07g02070	Blue	Green	57.51	26.44	-1.121	0.0390
ostta12g00280	Blue	Green	23.15	10.44	-1.149	0.0302
ostta15g00410	Blue	Green	52.78	23.68	-1.156	0.0390
ostta15g02360	Blue	Green	795.89	356.61	-1.158	0.0390
ostta02g03260	Blue	Green	461.56	206.64	-1.159	0.0317
ostta13g02890	Blue	Green	41.33	18.44	-1.164	0.0302
ostta02g04760	Blue	Green	40.10	17.85	-1.168	0.0194
ostta18g01120	Blue	Green	194.73	86.61	-1.169	0.0453
ostta02g03540	Blue	Green	122.78	54.59	-1.169	0.0425
ostta13g00380	Blue	Green	161.06	71.36	-1.174	0.0146
ostta03g01070	Blue	Green	326.74	144.03	-1.182	0.0302
ostta12g00080	Blue	Green	126.43	55.63	-1.184	0.0339
ostta07g03520	Blue	Green	68.86	30.28	-1.185	0.0406
ostta07g03010	Blue	Green	38.03	16.72	-1.185	0.0146
ostta03g04970	Blue	Green	84.46	37.11	-1.186	0.0357
ostta07g01530	Blue	Green	65.58	28.79	-1.188	0.0317
ostta01g01810	Blue	Green	35.47	15.55	-1.190	0.0317
ostta10g00565	Blue	Green	93.36	40.85	-1.192	0.0406
ostta03g02370	Blue	Green	138.12	60.38	-1.194	0.0453
ostta06g04480	Blue	Green	51.22	22.36	-1.196	0.0242
ostta15g02325	Blue	Green	138.24	60.25	-1.198	0.0377
ostta11g01680	Blue	Green	53.74	23.38	-1.201	0.0072
ostta02g03920	Blue	Green	59.73	25.71	-1.216	0.0453
ostta07g02870	Blue	Green	118.68	51.04	-1.217	0.0390
ostta04g04370	Blue	Green	96.92	41.64	-1.219	0.0377
ostta05g02690	Blue	Green	104.02	44.38	-1.229	0.0467
ostta15g00640	Blue	Green	986.83	420.64	-1.230	0.0453
ostta02g05480	Blue	Green	515.28	219.32	-1.232	0.0453

ostta10g00280	Blue	Green	91.99	38.88	-1.242	0.0221
ostta14g00750	Blue	Green	45.86	19.35	-1.245	0.0317
ostta14g01555	Blue	Green	72.65	30.60	-1.247	0.0194
ostta06g03332	Blue	Green	530.30	222.91	-1.250	0.0194
ostta06g00660	Blue	Green	120.91	50.75	-1.252	0.0173
ostta05g04990	Blue	Green	51.54	21.42	-1.266	0.0285
ostta12g02660	Blue	Green	11.50	4.74	-1.279	0.0221
ostta07g01160	Blue	Green	78.79	32.43	-1.280	0.0173
ostta04g00810	Blue	Green	78.30	32.12	-1.285	0.0221
ostta13g01920	Blue	Green	36.70	15.04	-1.287	0.0173
ostta01g01490	Blue	Green	37.78	15.41	-1.294	0.0114
ostta01g00180	Blue	Green	258.54	105.32	-1.296	0.0285
ostta12g01760	Blue	Green	1009.57	410.30	-1.299	0.0453
ostta17g01520	Blue	Green	72.55	29.43	-1.302	0.0194
ostta01g00150	Blue	Green	55.07	22.33	-1.303	0.0285
ostta18g00160	Blue	Green	132.77	53.70	-1.306	0.0242
ostta07g02310	Blue	Green	104.86	42.41	-1.306	0.0194
ostta04g04310	Blue	Green	91.55	37.01	-1.307	0.0173
ostta16g01770	Blue	Green	1077.35	435.35	-1.307	0.0242
ostta01g04760	Blue	Green	102.75	41.26	-1.316	0.0194
ostta14g02080	Blue	Green	226.29	90.81	-1.317	0.0114
ostta18g01660	Blue	Green	134.94	54.09	-1.319	0.0302
ostta01g01220	Blue	Green	392.51	157.11	-1.321	0.0467
ostta18g00590	Blue	Green	585.55	232.72	-1.331	0.0390
ostta15g01750	Blue	Green	31.55	12.51	-1.334	0.0242
ostta18g01690	Blue	Green	82.00	32.50	-1.335	0.0242
ostta05g03040	Blue	Green	549.64	217.66	-1.336	0.0377
ostta02g04030	Blue	Green	295.46	116.78	-1.339	0.0438
ostta10g02130	Blue	Green	135.03	53.35	-1.340	0.0242
ostta03g01320	Blue	Green	255.52	100.82	-1.342	0.0390
ostta17g00250	Blue	Green	54.45	21.44	-1.344	0.0438
ostta03g03690	Blue	Green	79.60	31.28	-1.348	0.0221
ostta06g04260	Blue	Green	87.38	34.27	-1.350	0.0285
ostta08g01890	Blue	Green	753.60	293.41	-1.361	0.0221
ostta09g00760	Blue	Green	675.44	262.76	-1.362	0.0357
ostta11g00780	Blue	Green	629.55	244.68	-1.363	0.0242
ostta01g00530	Blue	Green	84.80	32.88	-1.367	0.0114
ostta04g05280	Blue	Green	347.93	134.81	-1.368	0.0357
ostta01g05110	Blue	Green	55.17	21.33	-1.371	0.0265
ostta06g03010	Blue	Green	25.98	10.03	-1.372	0.0146
ostta15g00930	Blue	Green	329.75	127.33	-1.373	0.0194
ostta05g02300	Blue	Green	125.62	48.49	-1.373	0.0302
ostta03g02960	Blue	Green	526.35	202.64	-1.377	0.0072
ostta05g03750	Blue	Green	80.53	30.98	-1.378	0.0194
ostta06g01550	Blue	Green	9.59	3.69	-1.379	0.0317
ostta15g01830	Blue	Green	139.51	53.59	-1.380	0.0390
ostta03g02210	Blue	Green	118.74	45.43	-1.386	0.0221
ostta07g00210	Blue	Green	102.38	39.13	-1.388	0.0357
ostta16g00770	Blue	Green	605.41	231.38	-1.388	0.0114
ostta15g02200	Blue	Green	313.10	119.52	-1.389	0.0173
ostta10g02530	Blue	Green	92.24	35.21	-1.390	0.0357

ostta02g04650	Blue	Green	238.48	89.93	-1.407	0.0173
ostta03g00620	Blue	Green	16.41	6.18	-1.409	0.0146
ostta12g01500	Blue	Green	252.19	94.82	-1.411	0.0390
ostta14g00690	Blue	Green	87.65	32.94	-1.412	0.0114
ostta03g05760	Blue	Green	348.73	130.91	-1.414	0.0194
ostta16g02025	Blue	Green	115.90	43.47	-1.415	0.0146
ostta07g00710	Blue	Green	57.40	21.52	-1.415	0.0114
ostta12g02010	Blue	Green	251.42	94.03	-1.419	0.0194
ostta11g01100	Blue	Green	188.13	69.58	-1.435	0.0377
ostta13g01120	Blue	Green	384.67	142.16	-1.436	0.0357
ostta09g00270	Blue	Green	982.70	363.14	-1.436	0.0453
ostta09g02360	Blue	Green	24.92	9.20	-1.437	0.0302
ostta16g00530	Blue	Green	1465.64	540.72	-1.439	0.0265
ostta16g00550	Blue	Green	19.96	7.36	-1.440	0.0146
ostta03g03960	Blue	Green	79.75	29.35	-1.442	0.0425
ostta07g04040	Blue	Green	43.01	15.82	-1.443	0.0285
ostta09g02180	Blue	Green	29.78	10.95	-1.443	0.0146
ostta04g04080	Blue	Green	157.41	57.86	-1.444	0.0317
ostta07g03190	Blue	Green	258.61	95.03	-1.444	0.0072
ostta07g01150	Blue	Green	31.97	11.73	-1.447	0.0072
ostta16g00330	Blue	Green	414.20	151.92	-1.447	0.0146
ostta07g01760	Blue	Green	182.63	66.96	-1.447	0.0072
ostta16g00500	Blue	Green	15.56	5.68	-1.454	0.0194
ostta11g03070	Blue	Green	217.20	79.23	-1.455	0.0317
ostta07g03635	Blue	Green	96.25	35.06	-1.457	0.0072
ostta13g00130	Blue	Green	175.90	63.61	-1.467	0.0438
ostta04g00090	Blue	Green	256.62	92.79	-1.468	0.0146
ostta12g02520	Blue	Green	206.10	74.39	-1.470	0.0242
ostta07g03260	Blue	Green	81.50	29.34	-1.474	0.0146
ostta13g00720	Blue	Green	580.76	208.88	-1.475	0.0317
ostta05g03590	Blue	Green	66.50	23.89	-1.477	0.0317
ostta20g00570	Blue	Green	314.62	112.37	-1.485	0.0114
ostta08g01630	Blue	Green	182.88	65.22	-1.488	0.0173
ostta06g01960	Blue	Green	264.26	93.75	-1.495	0.0357
ostta14g00490	Blue	Green	115.50	40.96	-1.496	0.0114
ostta09g03580	Blue	Green	146.50	51.84	-1.499	0.0317
ostta08g03070	Blue	Green	228.85	80.69	-1.504	0.0194
ostta02g05290	Blue	Green	189.70	66.86	-1.504	0.0194
ostta12g00590	Blue	Green	153.29	53.93	-1.507	0.0146
ostta10g01900	Blue	Green	24.72	8.69	-1.508	0.0072
ostta01g06200	Blue	Green	93.27	32.77	-1.509	0.0146
ostta02g02790	Blue	Green	337.36	118.44	-1.510	0.0173
ostta09g00890	Blue	Green	85.30	29.92	-1.511	0.0114
ostta07g02900	Blue	Green	325.54	114.16	-1.512	0.0317
ostta10g00010	Blue	Green	25.51	8.95	-1.512	0.0242
ostta08g01340	Blue	Green	43.79	15.32	-1.515	0.0265
ostta08g00480	Blue	Green	437.78	152.84	-1.518	0.0285
ostta03g02650	Blue	Green	402.07	140.36	-1.518	0.0265
ostta06g01470	Blue	Green	246.25	85.69	-1.523	0.0114
ostta07g02060	Blue	Green	238.79	83.06	-1.523	0.0265
ostta01g00190	Blue	Green	246.56	85.73	-1.524	0.0242

ostta07g03380	Blue	Green	906.63	314.98	-1.525	0.0072
ostta07g01200	Blue	Green	639.66	222.21	-1.525	0.0265
ostta14g00940	Blue	Green	57.92	20.07	-1.529	0.0242
ostta01g06390	Blue	Green	179.08	62.00	-1.530	0.0114
ostta03g02350	Blue	Green	272.59	94.25	-1.532	0.0265
ostta13g00885	Blue	Green	420.96	144.93	-1.538	0.0072
ostta15g00580	Blue	Green	252.67	86.89	-1.540	0.0072
ostta05g04770	Blue	Green	666.10	228.80	-1.542	0.0265
ostta01g00450	Blue	Green	47.49	16.30	-1.543	0.0072
ostta07g04020	Blue	Green	105.66	36.17	-1.546	0.0173
ostta07g04660	Blue	Green	230.54	78.79	-1.549	0.0265
ostta02g04930	Blue	Green	222.54	75.77	-1.554	0.0072
ostta06g02970	Blue	Green	96.86	32.85	-1.560	0.0072
ostta16g00700	Blue	Green	42.98	14.56	-1.561	0.0173
ostta20g00560	Blue	Green	34.79	11.78	-1.562	0.0114
ostta14g00290	Blue	Green	28.41	9.61	-1.564	0.0114
ostta07g00750	Blue	Green	150.30	50.80	-1.565	0.0072
ostta03g01170	Blue	Green	457.93	154.43	-1.568	0.0072
ostta06g00580	Blue	Green	252.99	85.27	-1.569	0.0357
ostta19g00170	Blue	Green	139.25	46.85	-1.572	0.0221
ostta01g05620	Blue	Green	33.58	11.29	-1.573	0.0173
ostta08g03090	Blue	Green	103.16	34.58	-1.577	0.0072
ostta05g02870	Blue	Green	373.44	125.07	-1.578	0.0072
ostta08g03170	Blue	Green	73.37	24.51	-1.582	0.0072
ostta04g04870	Blue	Green	744.95	248.78	-1.582	0.0072
ostta11g03210	Blue	Green	202.84	67.66	-1.584	0.0285
ostta05g03820	Blue	Green	505.42	168.51	-1.585	0.0072
ostta06g02410	Blue	Green	1233.69	410.56	-1.587	0.0221
ostta18g00630	Blue	Green	662.90	219.73	-1.593	0.0072
ostta08g01400	Blue	Green	87.75	28.98	-1.598	0.0285
ostta01g04980	Blue	Green	120.75	39.73	-1.604	0.0114
ostta06g00860	Blue	Green	618.52	202.20	-1.613	0.0072
ostta09g03130	Blue	Green	90.93	29.67	-1.616	0.0146
ostta06g04610	Blue	Green	105.19	34.28	-1.618	0.0146
ostta06g01030	Blue	Green	356.95	116.12	-1.620	0.0072
ostta02g05070	Blue	Green	70.86	22.90	-1.629	0.0114
ostta03g00690	Blue	Green	539.23	173.93	-1.632	0.0194
ostta06g01830	Blue	Green	280.73	90.35	-1.635	0.0221
ostta04g00570	Blue	Green	204.11	65.65	-1.637	0.0146
ostta03g00770	Blue	Green	200.96	64.62	-1.637	0.0072
ostta12g03000	Blue	Green	122.55	39.39	-1.637	0.0114
ostta01g05230	Blue	Green	135.41	43.51	-1.638	0.0114
ostta05g02120	Blue	Green	256.17	82.25	-1.639	0.0242
ostta16g01720	Blue	Green	478.68	153.39	-1.642	0.0072
ostta07g04330	Blue	Green	91.58	29.19	-1.650	0.0194
ostta06g04000	Blue	Green	77.55	24.69	-1.651	0.0072
ostta01g04840	Blue	Green	232.86	74.08	-1.652	0.0173
ostta03g05370	Blue	Green	58.12	18.43	-1.657	0.0072
ostta16g01170	Blue	Green	40.76	12.80	-1.671	0.0072
ostta05g03560	Blue	Green	106.01	33.20	-1.675	0.0242
ostta05g00440	Blue	Green	12.91	4.02	-1.683	0.0438

ostta18g01680	Blue	Green	243.26	75.73	-1.684	0.0114
ostta06g01640	Blue	Green	619.90	192.74	-1.685	0.0072
ostta08g04210	Blue	Green	161.64	50.20	-1.687	0.0173
ostta07g03200	Blue	Green	179.50	55.18	-1.702	0.0194
ostta10g00320	Blue	Green	133.64	41.07	-1.702	0.0114
ostta01g06120	Blue	Green	32.99	10.11	-1.706	0.0072
ostta01g05470	Blue	Green	146.49	44.51	-1.719	0.0173
ostta06g00670	Blue	Green	156.09	47.28	-1.723	0.0072
ostta14g01060	Blue	Green	231.46	70.02	-1.725	0.0072
ostta14g02520	Blue	Green	51.19	15.39	-1.734	0.0072
ostta15g00740	Blue	Green	63.97	19.19	-1.737	0.0146
ostta05g04360	Blue	Green	127.10	37.93	-1.745	0.0146
ostta06g01120	Blue	Green	181.58	53.96	-1.751	0.0146
ostta15g01300	Blue	Green	167.69	49.47	-1.761	0.0173
ostta16g00990	Blue	Green	73.99	21.79	-1.764	0.0072
ostta05g00690	Blue	Green	238.39	70.16	-1.765	0.0072
ostta01g03480	Blue	Green	54.81	16.08	-1.769	0.0072
ostta03g05040	Blue	Green	347.44	101.90	-1.770	0.0072
ostta04g00970	Blue	Green	107.19	31.31	-1.776	0.0072
ostta09g00785	Blue	Green	91.99	26.83	-1.778	0.0072
ostta02g03840	Blue	Green	38.84	11.25	-1.788	0.0072
ostta18g01070	Blue	Green	466.57	133.21	-1.808	0.0072
ostta06g01610	Blue	Green	126.74	36.08	-1.813	0.0072
ostta08g02420	Blue	Green	31.57	8.98	-1.813	0.0072
ostta13g02140	Blue	Green	135.81	38.57	-1.816	0.0072
ostta17g01600	Blue	Green	93.46	26.53	-1.817	0.0072
ostta04g02880	Blue	Green	49.21	13.96	-1.818	0.0072
ostta07g04450	Blue	Green	131.17	37.18	-1.819	0.0072
ostta11g02020	Blue	Green	180.21	50.98	-1.822	0.0242
ostta15g02660	Blue	Green	141.06	39.48	-1.837	0.0072
ostta12g02110	Blue	Green	98.05	27.33	-1.843	0.0072
ostta01g00570	Blue	Green	157.53	43.85	-1.845	0.0072
ostta10g01740	Blue	Green	120.52	33.52	-1.846	0.0072
ostta03g02220	Blue	Green	90.64	25.11	-1.852	0.0072
ostta05g01450	Blue	Green	206.11	57.05	-1.853	0.0072
ostta05g00360	Blue	Green	163.35	44.79	-1.867	0.0072
ostta15g02560	Blue	Green	86.56	23.57	-1.877	0.0072
ostta17g01310	Blue	Green	76.11	20.38	-1.901	0.0072
ostta10g00150	Blue	Green	150.51	40.28	-1.902	0.0072
ostta06g03980	Blue	Green	865.44	230.85	-1.906	0.0072
ostta16g02347	Blue	Green	81.07	21.50	-1.915	0.0072
ostta15g01840	Blue	Green	199.81	52.94	-1.916	0.0072
ostta03g04380	Blue	Green	285.03	75.37	-1.919	0.0072
ostta15g01560	Blue	Green	55.90	14.55	-1.942	0.0072
ostta12g00070	Blue	Green	111.43	28.92	-1.946	0.0072
ostta04g01120	Blue	Green	298.60	76.81	-1.959	0.0072
ostta17g02160	Blue	Green	211.28	54.33	-1.959	0.0072
ostta07g04430	Blue	Green	30.88	7.93	-1.962	0.0072
ostta04g04050	Blue	Green	70.55	18.03	-1.968	0.0072
ostta08g01690	Blue	Green	107.15	27.26	-1.975	0.0072
ostta08g02930	Blue	Green	423.35	107.46	-1.978	0.0072

ostta07g01810	Blue	Green	155.23	39.01	-1.993	0.0072
ostta17g02220	Blue	Green	576.14	144.63	-1.994	0.0072
ostta07g00780	Blue	Green	642.12	160.42	-2.001	0.0072
ostta05g00190	Blue	Green	211.62	52.77	-2.004	0.0072
ostta18g01220	Blue	Green	59.18	14.73	-2.007	0.0072
ostta01g00720	Blue	Green	354.44	87.96	-2.011	0.0072
ostta01g06010	Blue	Green	310.21	75.54	-2.038	0.0072
ostta13g01240	Blue	Green	84.61	20.55	-2.042	0.0072
ostta08g01000	Blue	Green	72.37	17.32	-2.063	0.0072
ostta10g02520	Blue	Green	35.18	8.41	-2.064	0.0072
ostta01g04380	Blue	Green	251.95	59.96	-2.071	0.0072
ostta11g03220	Blue	Green	58.09	13.79	-2.075	0.0072
ostta05g04180	Blue	Green	311.80	73.93	-2.076	0.0072
ostta05g03410	Blue	Green	50.79	12.00	-2.082	0.0072
ostta09g01210	Blue	Green	79.82	18.73	-2.091	0.0072
ostta02g04010	Blue	Green	99.31	23.15	-2.101	0.0072
ostta05g01080	Blue	Green	113.74	26.42	-2.106	0.0072
ostta16g01760	Blue	Green	164.78	38.13	-2.111	0.0072
ostta15g01610	Blue	Green	270.23	62.04	-2.123	0.0072
ostta18g00680	Blue	Green	47.06	10.76	-2.129	0.0072
ostta04g00340	Blue	Green	58.76	13.34	-2.139	0.0072
ostta14g01110	Blue	Green	114.30	25.87	-2.143	0.0072
ostta04g04930	Blue	Green	18.50	4.17	-2.151	0.0072
ostta16g00610	Blue	Green	105.60	23.75	-2.153	0.0072
ostta11g02120	Blue	Green	138.08	31.00	-2.155	0.0072
ostta16g01790	Blue	Green	69.35	15.46	-2.166	0.0072
ostta14g00780	Blue	Green	124.14	27.05	-2.198	0.0072
ostta04g00770	Blue	Green	77.56	16.83	-2.204	0.0072
ostta04g02770	Blue	Green	155.97	33.72	-2.210	0.0072
ostta03g00060	Blue	Green	170.91	36.82	-2.215	0.0072
ostta09g01960	Blue	Green	243.90	51.82	-2.235	0.0072
ostta05g04940	Blue	Green	198.70	41.83	-2.248	0.0072
ostta17g00640	Blue	Green	214.26	43.91	-2.287	0.0072
ostta09g01190	Blue	Green	234.46	47.75	-2.296	0.0072
ostta05g00450	Blue	Green	235.72	47.94	-2.298	0.0072
ostta13g01100	Blue	Green	302.29	59.74	-2.339	0.0072
ostta09g00290	Blue	Green	271.39	53.31	-2.348	0.0072
ostta11g00160	Blue	Green	117.08	22.92	-2.353	0.0072
ostta05g03090	Blue	Green	71.31	13.63	-2.387	0.0072
ostta03g04840	Blue	Green	116.02	21.28	-2.447	0.0072
ostta05g02880	Blue	Green	236.79	42.81	-2.468	0.0072
ostta01g02040	Red	Blue	3.91	15.09	1.948	0.0221
ostta03g00910	Red	Blue	8.30	23.93	1.527	0.0146
ostta01g02040	Red	Green	3.91	29.75	2.928	0.0072
ostta10g00950	Red	Green	229.14	685.22	1.580	0.0173
ostta10g00930	Red	Green	97.03	289.13	1.575	0.0265
ostta18g01920	Red	Green	59.87	174.76	1.545	0.0072
ostta12g00660	Red	Green	17.97	52.22	1.539	0.0072
ostta10g02040	Red	Green	9.14	26.49	1.535	0.0114
ostta08g04020	Red	Green	88.92	251.72	1.501	0.0072
ostta01g03880	Red	Green	208.29	574.00	1.462	0.0072

ostta10g00920	Red	Green	181.92	500.02	1.459	0.0194
ostta07g00920	Red	Green	36.92	98.10	1.410	0.0072
ostta10g00940	Red	Green	1193.79	3110.45	1.382	0.0146
ostta03g00910	Red	Green	8.30	21.43	1.368	0.0114
ostta01g05380	Red	Green	21.84	55.53	1.346	0.0072
ostta03g02380	Red	Green	308.78	726.80	1.235	0.0242
ostta15g01710	Red	Green	33.85	79.21	1.226	0.0194
ostta08g04300	Red	Green	9.21	21.39	1.216	0.0302
ostta07g04470	Red	Green	125.60	290.96	1.212	0.0072
ostta05g04790	Red	Green	38.32	86.80	1.179	0.0072
ostta10g00970	Red	Green	9.91	22.33	1.172	0.0285
ostta13g02380	Red	Green	20.34	44.99	1.145	0.0339
ostta16g01960	Red	Green	24.60	53.89	1.131	0.0194
ostta03g05620	Red	Green	23.46	50.86	1.116	0.0072
ostta08g04240	Red	Green	200.71	432.66	1.108	0.0425
ostta05g04350	Red	Green	34.31	71.81	1.066	0.0173
ostta10g00960	Red	Green	11.25	23.27	1.049	0.0406
ostta05g04970	Red	Green	9.02	18.31	1.021	0.0302
ostta12g01970	Red	Green	96.62	194.62	1.010	0.0406
ostta09g00780	Red	Green	90.78	176.39	0.958	0.0285
ostta02g03930	Red	Green	227.78	439.34	0.948	0.0425
ostta16g00650	Red	Green	154.25	296.12	0.941	0.0285
ostta08g00690	Red	Green	26.01	48.69	0.905	0.0339
ostta16g01110	Red	Green	28.38	52.93	0.899	0.0406
ostta04g01510	Red	Green	140.83	261.19	0.891	0.0406
ostta01g02080	Red	Green	54.84	100.69	0.877	0.0302
ostta17g01050	Red	Green	78.37	39.15	-1.001	0.0438
ostta05g04990	Red	Green	43.10	21.42	-1.009	0.0438
ostta13g00690	Red	Green	11.79	5.82	-1.019	0.0377
ostta17g01520	Red	Green	59.77	29.43	-1.022	0.0377
ostta04g04310	Red	Green	76.00	37.01	-1.038	0.0467
ostta05g03820	Red	Green	346.47	168.51	-1.040	0.0377
ostta13g00070	Red	Green	292.55	141.86	-1.044	0.0302
ostta11g00660	Red	Green	15.95	7.68	-1.054	0.0242
ostta10g00565	Red	Green	84.86	40.85	-1.055	0.0317
ostta05g02870	Red	Green	261.77	125.07	-1.066	0.0285
ostta01g00150	Red	Green	46.75	22.33	-1.066	0.0317
ostta14g00690	Red	Green	69.09	32.94	-1.069	0.0467
ostta14g02080	Red	Green	191.31	90.81	-1.075	0.0285
ostta16g00700	Red	Green	30.86	14.56	-1.083	0.0467
ostta03g01070	Red	Green	310.20	144.03	-1.107	0.0265
ostta18g00160	Red	Green	115.67	53.70	-1.107	0.0453
ostta07g02070	Red	Green	57.19	26.44	-1.113	0.0357
ostta01g00530	Red	Green	71.14	32.88	-1.113	0.0406
ostta16g00550	Red	Green	16.05	7.36	-1.126	0.0489
ostta07g02060	Red	Green	181.50	83.06	-1.128	0.0302
ostta03g01170	Red	Green	340.01	154.43	-1.139	0.0242
ostta14g00290	Red	Green	21.30	9.61	-1.149	0.0242
ostta18g01120	Red	Green	192.52	86.61	-1.152	0.0339
ostta16g00530	Red	Green	1209.74	540.72	-1.162	0.0390
ostta20g00560	Red	Green	26.50	11.78	-1.169	0.0453

ostta03g04970	Red	Green	83.89	37.11	-1.177	0.0114
ostta14g00490	Red	Green	92.93	40.96	-1.182	0.0221
ostta16g00330	Red	Green	344.76	151.92	-1.182	0.0339
ostta02g05260	Red	Green	20.16	8.87	-1.184	0.0146
ostta07g01760	Red	Green	153.10	66.96	-1.193	0.0114
ostta06g01030	Red	Green	265.70	116.12	-1.194	0.0285
ostta11g01100	Red	Green	159.23	69.58	-1.194	0.0467
ostta06g01550	Red	Green	8.44	3.69	-1.196	0.0317
ostta03g05760	Red	Green	299.92	130.91	-1.196	0.0339
ostta07g03380	Red	Green	723.52	314.98	-1.200	0.0377
ostta16g01720	Red	Green	353.22	153.39	-1.203	0.0194
ostta09g03580	Red	Green	119.40	51.84	-1.204	0.0302
ostta07g00710	Red	Green	49.74	21.52	-1.209	0.0173
ostta10g01900	Red	Green	20.11	8.69	-1.210	0.0317
ostta06g01960	Red	Green	217.31	93.75	-1.213	0.0425
ostta02g04930	Red	Green	175.94	75.77	-1.215	0.0357
ostta13g00720	Red	Green	486.12	208.88	-1.219	0.0406
ostta12g03000	Red	Green	91.68	39.39	-1.219	0.0302
ostta07g04450	Red	Green	86.58	37.18	-1.219	0.0146
ostta05g00690	Red	Green	163.60	70.16	-1.221	0.0302
ostta13g00130	Red	Green	148.72	63.61	-1.225	0.0390
ostta06g02410	Red	Green	961.24	410.56	-1.227	0.0467
ostta07g03260	Red	Green	69.01	29.34	-1.234	0.0285
ostta05g03750	Red	Green	73.49	30.98	-1.246	0.0221
ostta02g04500	Red	Green	18.34	7.73	-1.246	0.0146
ostta03g02650	Red	Green	333.06	140.36	-1.247	0.0438
ostta14g01060	Red	Green	166.60	70.02	-1.251	0.0173
ostta02g05290	Red	Green	159.17	66.86	-1.251	0.0453
ostta06g02970	Red	Green	78.26	32.85	-1.252	0.0072
ostta03g03300	Red	Green	2068.08	867.39	-1.254	0.0072
ostta05g02690	Red	Green	106.00	44.38	-1.256	0.0406
ostta06g01640	Red	Green	460.82	192.74	-1.258	0.0302
ostta12g00590	Red	Green	129.45	53.93	-1.263	0.0467
ostta06g04610	Red	Green	82.95	34.28	-1.275	0.0265
ostta18g00630	Red	Green	535.70	219.73	-1.286	0.0146
ostta15g00740	Red	Green	47.04	19.19	-1.294	0.0357
ostta07g04020	Red	Green	89.23	36.17	-1.303	0.0390
ostta08g03170	Red	Green	60.98	24.51	-1.315	0.0317
ostta09g00890	Red	Green	74.93	29.92	-1.324	0.0173
ostta07g00750	Red	Green	127.84	50.80	-1.332	0.0114
ostta06g00860	Red	Green	510.29	202.20	-1.336	0.0146
ostta07g04660	Red	Green	199.43	78.79	-1.340	0.0194
ostta01g05470	Red	Green	113.73	44.51	-1.354	0.0438
ostta10g00320	Red	Green	105.35	41.07	-1.359	0.0390
ostta02g02790	Red	Green	306.28	118.44	-1.371	0.0317
ostta08g04210	Red	Green	129.99	50.20	-1.373	0.0339
ostta01g06120	Red	Green	26.31	10.11	-1.380	0.0265
ostta06g00670	Red	Green	123.02	47.28	-1.380	0.0390
ostta01g03480	Red	Green	42.19	16.08	-1.392	0.0194
ostta03g05040	Red	Green	267.83	101.90	-1.394	0.0194
ostta06g01610	Red	Green	95.62	36.08	-1.406	0.0146

ostta16g01170	Red	Green	34.09	12.80	-1.414	0.0072
ostta04g00970	Red	Green	83.94	31.31	-1.423	0.0425
ostta06g04000	Red	Green	66.49	24.69	-1.429	0.0173
ostta03g05370	Red	Green	49.72	18.43	-1.431	0.0173
ostta05g03560	Red	Green	89.96	33.20	-1.438	0.0194
ostta09g03130	Red	Green	80.53	29.67	-1.440	0.0302
ostta01g04840	Red	Green	202.20	74.08	-1.449	0.0221
ostta10g01740	Red	Green	91.58	33.52	-1.450	0.0221
ostta03g02220	Red	Green	68.83	25.11	-1.455	0.0072
ostta09g00785	Red	Green	74.07	26.83	-1.465	0.0146
ostta18g01070	Red	Green	369.07	133.21	-1.470	0.0072
ostta17g01600	Red	Green	73.93	26.53	-1.479	0.0072
ostta18g01680	Red	Green	211.97	75.73	-1.485	0.0114
ostta15g02560	Red	Green	66.21	23.57	-1.490	0.0072
ostta16g00990	Red	Green	61.41	21.79	-1.495	0.0438
ostta06g01120	Red	Green	152.30	53.96	-1.497	0.0221
ostta16g02347	Red	Green	60.84	21.50	-1.501	0.0146
ostta11g02020	Red	Green	144.45	50.98	-1.502	0.0173
ostta03g04380	Red	Green	213.97	75.37	-1.505	0.0146
ostta15g01840	Red	Green	150.40	52.94	-1.506	0.0339
ostta15g02660	Red	Green	112.75	39.48	-1.514	0.0467
ostta14g02520	Red	Green	43.98	15.39	-1.515	0.0114
ostta13g02140	Red	Green	110.64	38.57	-1.520	0.0072
ostta05g01450	Red	Green	165.68	57.05	-1.538	0.0194
ostta10g00150	Red	Green	117.35	40.28	-1.543	0.0173
ostta17g02160	Red	Green	158.72	54.33	-1.547	0.0114
ostta07g03200	Red	Green	161.56	55.18	-1.550	0.0114
ostta07g01810	Red	Green	114.35	39.01	-1.552	0.0072
ostta17g01310	Red	Green	60.09	20.38	-1.560	0.0072
ostta17g02220	Red	Green	429.09	144.63	-1.569	0.0194
ostta15g01560	Red	Green	43.26	14.55	-1.572	0.0285
ostta04g01120	Red	Green	229.59	76.81	-1.580	0.0146
ostta04g02880	Red	Green	41.83	13.96	-1.583	0.0072
ostta06g03980	Red	Green	695.56	230.85	-1.591	0.0114
ostta05g00360	Red	Green	135.68	44.79	-1.599	0.0072
ostta04g04050	Red	Green	54.63	18.03	-1.599	0.0194
ostta01g00570	Red	Green	133.39	43.85	-1.605	0.0146
ostta01g00720	Red	Green	271.10	87.96	-1.624	0.0114
ostta05g00190	Red	Green	163.23	52.77	-1.629	0.0114
ostta11g03220	Red	Green	43.17	13.79	-1.647	0.0173
ostta07g00780	Red	Green	502.42	160.42	-1.647	0.0114
ostta04g00340	Red	Green	41.81	13.34	-1.648	0.0072
ostta08g02930	Red	Green	337.45	107.46	-1.651	0.0114
ostta12g00070	Red	Green	90.81	28.92	-1.651	0.0114
ostta05g01080	Red	Green	84.31	26.42	-1.674	0.0173
ostta08g02420	Red	Green	28.74	8.98	-1.678	0.0072
ostta10g02520	Red	Green	27.16	8.41	-1.691	0.0072
ostta08g01000	Red	Green	55.98	17.32	-1.693	0.0114
ostta18g01220	Red	Green	47.69	14.73	-1.695	0.0072
ostta05g03410	Red	Green	38.96	12.00	-1.700	0.0242
ostta18g00680	Red	Green	35.24	10.76	-1.712	0.0072

ostta01g04380	Red	Green	196.69	59.96	-1.714	0.0302
ostta13g01240	Red	Green	67.44	20.55	-1.714	0.0221
ostta05g04180	Red	Green	244.44	73.93	-1.725	0.0265
ostta16g01760	Red	Green	126.63	38.13	-1.731	0.0114
ostta09g01210	Red	Green	62.36	18.73	-1.735	0.0114
ostta02g04010	Red	Green	77.27	23.15	-1.739	0.0146
ostta07g04430	Red	Green	26.78	7.93	-1.756	0.0072
ostta01g06010	Red	Green	255.42	75.54	-1.758	0.0146
ostta05g04940	Red	Green	141.61	41.83	-1.759	0.0072
ostta04g02770	Red	Green	114.57	33.72	-1.764	0.0173
ostta15g01610	Red	Green	215.11	62.04	-1.794	0.0072
ostta14g01110	Red	Green	91.37	25.87	-1.820	0.0146
ostta03g04840	Red	Green	75.31	21.28	-1.823	0.0072
ostta14g00780	Red	Green	96.39	27.05	-1.833	0.0072
ostta11g02120	Red	Green	110.50	31.00	-1.834	0.0194
ostta16g00610	Red	Green	84.81	23.75	-1.836	0.0114
ostta04g00770	Red	Green	60.13	16.83	-1.837	0.0072
ostta03g00060	Red	Green	132.79	36.82	-1.851	0.0072
ostta17g00640	Red	Green	159.43	43.91	-1.860	0.0072
ostta09g00290	Red	Green	194.00	53.31	-1.864	0.0072
ostta04g04930	Red	Green	15.28	4.17	-1.875	0.0114
ostta16g01790	Red	Green	56.90	15.46	-1.880	0.0072
ostta09g01960	Red	Green	193.42	51.82	-1.900	0.0072
ostta09g01190	Red	Green	180.41	47.75	-1.918	0.0072
ostta05g00450	Red	Green	186.10	47.94	-1.957	0.0072
ostta05g02880	Red	Green	168.89	42.81	-1.980	0.0072
ostta13g01100	Red	Green	237.64	59.74	-1.992	0.0072
ostta11g00160	Red	Green	92.30	22.92	-2.010	0.0072
ostta05g03090	Red	Green	59.04	13.63	-2.115	0.0072

RCC809 genes

Gene ID	Light condition 1	Light condition 2	FPKM 1	FPKM 2	log2 fold change	FDR corrected q value
Od15g01270	Red	Blue	43.60	281.66	2.692	0.0009
Od03g03140	Red	Blue	2.18	14.04	2.689	0.0009
Od01g06420	Red	Blue	12.60	78.19	2.634	0.0009
Od08g02000	Red	Blue	8.83	46.84	2.408	0.0009
Od10g02190	Red	Blue	1.63	8.51	2.385	0.0009
Od07g00170	Red	Blue	1.30	6.78	2.383	0.0009
Od06g00550	Red	Blue	1.71	8.58	2.331	0.0357
Od02g00200	Red	Blue	8.88	44.41	2.322	0.0009
Od04g04760	Red	Blue	2.77	13.81	2.318	0.0009

Od07g03400	Red	Blue	1.04	4.90	2.237	0.0363
Od04g03190	Red	Blue	10.72	50.03	2.223	0.0009
Od09g01360	Red	Blue	4.93	22.42	2.185	0.0009
Od09g02300	Red	Blue	44.82	200.61	2.162	0.0009
Od19g00300	Red	Blue	4.75	20.90	2.138	0.0009
Od07g02550	Red	Blue	4.06	17.75	2.128	0.0009
Od20g03310	Red	Blue	5.23	22.61	2.112	0.0009
Od15g01190	Red	Blue	0.79	3.38	2.101	0.0392
Od06g07360	Red	Blue	10.05	42.75	2.088	0.0009
Od08g00870	Red	Blue	36.19	151.85	2.069	0.0009
Od16g00070	Red	Blue	14.09	58.64	2.058	0.0041
Od01g06650	Red	Blue	15.91	66.16	2.056	0.0009
Od07g03280	Red	Blue	4.97	20.40	2.037	0.0009
Od11g03720	Red	Blue	2.99	12.13	2.021	0.0029
Od13g01200	Red	Blue	8.56	33.81	1.981	0.0009
Od16g00040	Red	Blue	1.38	5.43	1.979	0.0009
Od04g00010	Red	Blue	4.86	19.02	1.968	0.0009
Od14g00130	Red	Blue	41.62	162.67	1.967	0.0009
Od09g05770	Red	Blue	3.16	12.18	1.948	0.0009
Od04g05000	Red	Blue	1.26	4.87	1.945	0.0009
Od08g03260	Red	Blue	3.91	14.96	1.934	0.0009
Od15g00940	Red	Blue	1.59	6.05	1.927	0.0029
Od11g00070	Red	Blue	66.62	252.45	1.922	0.0009
Od01g00560	Red	Blue	20.56	77.56	1.915	0.0009
Od07g00820	Red	Blue	2.09	7.89	1.915	0.0046
Od07g03850	Red	Blue	11.17	41.90	1.908	0.0009
Od07g00400	Red	Blue	17.63	64.09	1.862	0.0009
Od11g01330	Red	Blue	8.48	30.29	1.837	0.0009
Od12g01040	Red	Blue	20.65	72.47	1.811	0.0009
Od02g03820	Red	Blue	4.23	14.66	1.793	0.0352
Od20g00270	Red	Blue	23.94	82.85	1.791	0.0009
Od02g00320	Red	Blue	13.48	46.61	1.790	0.0009
Od16g00230	Red	Blue	1.01	3.46	1.779	0.0331
Od12g01020	Red	Blue	4.98	17.07	1.777	0.0009
Od07g02560	Red	Blue	9.83	32.56	1.727	0.0009
Od06g04270	Red	Blue	2.44	8.04	1.718	0.0100
Od14g00930	Red	Blue	10.16	33.04	1.702	0.0009
Od01g04620	Red	Blue	0.93	3.02	1.698	0.0104
Od05g00920	Red	Blue	2.93	9.51	1.697	0.0009
Od07g04620	Red	Blue	31.45	101.21	1.686	0.0009
Od17g01800	Red	Blue	26.36	84.66	1.684	0.0009
Od05g01470	Red	Blue	7.57	24.18	1.675	0.0009
Od06g04090	Red	Blue	24.79	79.02	1.673	0.0009

Od16g02610	Red	Blue	1.31	4.15	1.658	0.0492
Od02g03170	Red	Blue	7.55	23.71	1.652	0.0009
Od07g00180	Red	Blue	72.06	225.13	1.643	0.0009
Od17g00150	Red	Blue	2.84	8.83	1.634	0.0108
Od20g00700	Red	Blue	1.36	4.23	1.634	0.0405
Od11g04460	Red	Blue	67.02	207.26	1.629	0.0009
Od02g00300	Red	Blue	182.62	564.13	1.627	0.0138
Od01g04760	Red	Blue	24.58	75.50	1.619	0.0009
Od16g02330	Red	Blue	9.23	28.09	1.605	0.0122
Od20g01170	Red	Blue	11.84	35.95	1.603	0.0009
Od04g00640	Red	Blue	1.00	3.04	1.600	0.0224
Od20g00470	Red	Blue	6.59	19.92	1.597	0.0057
Od11g02280	Red	Blue	0.71	2.13	1.595	0.0275
Od14g03320	Red	Blue	24.38	73.39	1.590	0.0009
Od02g03540	Red	Blue	15.19	45.17	1.572	0.0009
Od01g06640	Red	Blue	7.47	22.21	1.572	0.0009
Od15g00900	Red	Blue	6.27	18.63	1.571	0.0009
Od11g00400	Red	Blue	5.56	16.48	1.568	0.0009
Od14g00740	Red	Blue	15.37	45.32	1.560	0.0009
Od04g05390	Red	Blue	1.09	3.20	1.547	0.0252
Od10g01870	Red	Blue	74.83	218.38	1.545	0.0009
Od05g03110	Red	Blue	11.89	34.31	1.529	0.0009
Od15g00600	Red	Blue	8.63	24.87	1.527	0.0009
Od12g00140	Red	Blue	174.21	495.77	1.509	0.0009
Od13g00190	Red	Blue	37.79	107.42	1.507	0.0009
Od12g00180	Red	Blue	7.59	21.56	1.507	0.0009
Od08g02560	Red	Blue	3.29	9.33	1.505	0.0009
Od12g02770	Red	Blue	5.26	14.92	1.504	0.0095
Od08g01720	Red	Blue	4.06	11.44	1.494	0.0016
Od13g00760	Red	Blue	5.57	15.40	1.466	0.0009
Od07g03640	Red	Blue	10.02	27.62	1.463	0.0081
Od01g06980	Red	Blue	12.06	33.08	1.456	0.0009
Od04g00100	Red	Blue	1.39	3.77	1.443	0.0046
Od01g06080	Red	Blue	2.97	8.02	1.433	0.0482
Od09g02770	Red	Blue	0.76	2.04	1.432	0.0213
Od16g00130	Red	Blue	2.18	5.88	1.432	0.0023
Od02g04240	Red	Blue	3.11	8.32	1.417	0.0130
Od13g02310	Red	Blue	4.50	11.93	1.408	0.0009
Od05g00890	Red	Blue	40.52	106.18	1.390	0.0009
Od02g04350	Red	Blue	205.62	536.13	1.383	0.0009
Od04g03210	Red	Blue	7.40	19.21	1.377	0.0009
Od20g03270	Red	Blue	12.08	31.32	1.374	0.0046
Od11g03080	Red	Blue	77.64	201.23	1.374	0.0009

Od11g02550	Red	Blue	1.14	2.94	1.371	0.0122
Od05g01450	Red	Blue	11.39	29.36	1.366	0.0009
Od15g00350	Red	Blue	10.97	28.28	1.366	0.0009
Od05g00220	Red	Blue	23.40	60.18	1.363	0.0009
Od08g01730	Red	Blue	24.43	62.70	1.360	0.0009
Od06g02450	Red	Blue	9.45	24.26	1.360	0.0041
Od10g01650	Red	Blue	10.59	27.04	1.352	0.0009
Od08g01230	Red	Blue	6.68	17.00	1.347	0.0009
Od16g01060	Red	Blue	9.08	23.08	1.346	0.0009
Od13g03060	Red	Blue	6.33	16.08	1.345	0.0035
Od14g00290	Red	Blue	1.21	3.06	1.340	0.0076
Od04g01690	Red	Blue	23.61	59.58	1.336	0.0009
Od03g01650	Red	Blue	19.69	49.66	1.334	0.0009
Od05g03390	Red	Blue	3.18	7.99	1.328	0.0009
Od14g00870	Red	Blue	0.96	2.41	1.324	0.0009
Od14g02910	Red	Blue	4.55	11.36	1.318	0.0041
Od13g01790	Red	Blue	9.97	24.75	1.312	0.0009
Od19g01210	Red	Blue	2.43	6.03	1.312	0.0041
Od13g01990	Red	Blue	17.05	42.22	1.308	0.0009
Od07g00310	Red	Blue	21.82	53.86	1.304	0.0009
Od08g00250	Red	Blue	10.92	26.94	1.303	0.0041
Od02g02690	Red	Blue	727.30	1779.39	1.291	0.0009
Od01g05320	Red	Blue	19.20	46.92	1.289	0.0009
Od01g02570	Red	Blue	10.69	26.11	1.288	0.0009
Od12g00030	Red	Blue	24.01	58.32	1.280	0.0009
Od04g00260	Red	Blue	12.84	31.04	1.273	0.0009
Od14g03310	Red	Blue	51.99	125.26	1.269	0.0009
Od06g01470	Red	Blue	8.55	20.51	1.263	0.0009
Od04g04730	Red	Blue	7.75	18.53	1.258	0.0009
Od10g02340	Red	Blue	19.16	45.78	1.256	0.0009
Od19g00350	Red	Blue	5.57	13.26	1.251	0.0035
Od04g00830	Red	Blue	11.33	26.95	1.249	0.0009
Od11g02410	Red	Blue	4.19	9.96	1.249	0.0234
Od16g02500	Red	Blue	30.39	71.93	1.243	0.0009
Od15g00850	Red	Blue	6.41	15.17	1.242	0.0009
Od07g00480	Red	Blue	17.48	41.29	1.240	0.0009
Od04g04740	Red	Blue	9.01	21.26	1.238	0.0046
Od01g05030	Red	Blue	77.97	183.89	1.238	0.0009
Od05g01170	Red	Blue	390.73	918.57	1.233	0.0009
Od15g00840	Red	Blue	4.07	9.53	1.229	0.0023
Od14g01080	Red	Blue	45.84	106.93	1.222	0.0009
Od05g03930	Red	Blue	19.06	44.35	1.218	0.0009
Od14g02780	Red	Blue	10.25	23.81	1.216	0.0009

Od11g00700	Red	Blue	19.66	45.29	1.204	0.0009
Od10g02150	Red	Blue	109.90	253.01	1.203	0.0009
Od09g02830	Red	Blue	6.46	14.83	1.200	0.0035
Od01g01650	Red	Blue	17.56	40.32	1.199	0.0009
Od09g03810	Red	Blue	3.16	7.25	1.198	0.0086
Od12g00290	Red	Blue	17.75	40.58	1.193	0.0009
Od11g00170	Red	Blue	49.90	113.95	1.191	0.0009
Od09g05100	Red	Blue	28.56	65.13	1.189	0.0009
Od08g00520	Red	Blue	69.17	157.67	1.189	0.0009
Od01g01230	Red	Blue	57.22	130.38	1.188	0.0009
Od02g00310	Red	Blue	762.35	1735.42	1.187	0.0009
Od09g03260	Red	Blue	6.53	14.85	1.184	0.0029
Od04g00790	Red	Blue	13.01	29.40	1.177	0.0009
Od06g02440	Red	Blue	3.65	8.25	1.175	0.0281
Od02g03580	Red	Blue	36.03	81.15	1.171	0.0009
Od06g04290	Red	Blue	95.22	214.31	1.170	0.0009
Od01g03410	Red	Blue	18.24	41.05	1.170	0.0009
Od12g00470	Red	Blue	10.02	22.55	1.170	0.0009
Od20g00460	Red	Blue	14.94	33.60	1.170	0.0035
Od04g05300	Red	Blue	36.94	82.96	1.167	0.0009
Od01g05390	Red	Blue	3.58	8.03	1.167	0.0381
Od09g05490	Red	Blue	8.62	19.30	1.163	0.0062
Od12g00160	Red	Blue	49.48	110.67	1.161	0.0009
Od14g01370	Red	Blue	1.21	2.69	1.157	0.0431
Od17g00270	Red	Blue	13.12	29.18	1.153	0.0009
Od14g01000	Red	Blue	19.99	44.44	1.152	0.0009
Od06g07370	Red	Blue	42.38	94.20	1.152	0.0009
Od09g01150	Red	Blue	16.21	35.96	1.149	0.0009
Od05g01230	Red	Blue	26.95	59.71	1.148	0.0016
Od20g00040	Red	Blue	19.66	43.46	1.144	0.0009
Od06g01410	Red	Blue	6.90	15.20	1.140	0.0009
Od06g06460	Red	Blue	5.92	13.01	1.135	0.0095
Od16g01220	Red	Blue	14.60	31.89	1.127	0.0009
Od15g00790	Red	Blue	20.16	43.78	1.119	0.0009
Od19g00370	Red	Blue	35.40	76.82	1.118	0.0009
Od17g02170	Red	Blue	23.13	49.89	1.109	0.0009
Od09g00990	Red	Blue	517.66	1112.81	1.104	0.0009
Od07g04150	Red	Blue	20.30	43.63	1.104	0.0016
Od09g01340	Red	Blue	11.65	25.01	1.103	0.0009
Od06g02030	Red	Blue	5.76	12.34	1.100	0.0150
Od09g01330	Red	Blue	13.28	28.44	1.098	0.0113
Od17g03260	Red	Blue	7.98	17.05	1.096	0.0016
Od11g04240	Red	Blue	155.12	328.77	1.084	0.0009

Od19g00740	Red	Blue	238.55	505.52	1.083	0.0009
Od17g03230	Red	Blue	1.38	2.93	1.080	0.0009
Od06g04890	Red	Blue	96.52	203.82	1.078	0.0009
Od13g01980	Red	Blue	5.84	12.31	1.077	0.0052
Od10g02380	Red	Blue	131.33	277.01	1.077	0.0009
Od09g04520	Red	Blue	7.14	15.05	1.075	0.0170
Od12g03660	Red	Blue	10.62	22.34	1.073	0.0071
Od10g01930	Red	Blue	1.62	3.40	1.073	0.0009
Od09g05920	Red	Blue	18.58	39.02	1.071	0.0009
Od08g02180	Red	Blue	16.33	34.29	1.070	0.0009
Od17g00980	Red	Blue	7.85	16.45	1.067	0.0016
Od01g03680	Red	Blue	11.67	24.40	1.063	0.0016
Od06g00540	Red	Blue	8.87	18.50	1.061	0.0009
Od17g00110	Red	Blue	74.57	155.25	1.058	0.0009
Od01g02880	Red	Blue	9.91	20.62	1.056	0.0009
Od11g01790	Red	Blue	1.21	2.52	1.056	0.0281
Od09g00610	Red	Blue	10.12	21.00	1.054	0.0009
Od12g01050	Red	Blue	13.94	28.92	1.053	0.0016
Od01g03480	Red	Blue	14.71	30.52	1.053	0.0009
Od07g00010	Red	Blue	5.30	10.98	1.052	0.0009
Od09g04040	Red	Blue	15.30	31.69	1.051	0.0029
Od01g02710	Red	Blue	8.85	18.33	1.051	0.0016
Od05g03690	Red	Blue	3.85	7.94	1.044	0.0177
Od04g05100	Red	Blue	25.25	51.97	1.042	0.0126
Od09g00150	Red	Blue	51.37	105.66	1.041	0.0009
Od01g02300	Red	Blue	27.83	57.19	1.039	0.0009
Od06g01240	Red	Blue	24.53	50.35	1.038	0.0009
Od12g00150	Red	Blue	59.02	121.01	1.036	0.0009
Od03g03210	Red	Blue	130.85	268.20	1.035	0.0009
Od04g04460	Red	Blue	23.99	49.01	1.031	0.0009
Od09g05840	Red	Blue	6.48	13.22	1.030	0.0009
Od14g00990	Red	Blue	4.59	9.37	1.029	0.0023
Od04g05220	Red	Blue	69.58	141.83	1.028	0.0009
Od11g03350	Red	Blue	3.37	6.87	1.027	0.0417
Od12g02100	Red	Blue	23.58	48.04	1.026	0.0009
Od09g02310	Red	Blue	15.82	32.18	1.025	0.0046
Od20g00710	Red	Blue	2.28	4.64	1.024	0.0372
Od20g02460	Red	Blue	32.07	65.20	1.024	0.0009
Od06g00230	Red	Blue	8.79	17.86	1.022	0.0057
Od06g03940	Red	Blue	16.91	34.33	1.022	0.0009
Od06g06240	Red	Blue	43.17	87.36	1.017	0.0009
Od19g00750	Red	Blue	13.19	26.66	1.015	0.0009
Od16g00380	Red	Blue	34.21	68.95	1.011	0.0009

Od10g00970	Red	Blue	15.89	31.98	1.009	0.0009
Od01g00800	Red	Blue	21.93	44.03	1.005	0.0009
Od02g04830	Red	Blue	14.09	28.18	1.000	0.0009
Od01g05640	Red	Blue	3.12	6.24	0.999	0.0016
Od13g02870	Red	Blue	16.91	33.62	0.991	0.0009
Od04g05020	Red	Blue	21.86	43.42	0.990	0.0009
Od20g02320	Red	Blue	11.80	23.42	0.989	0.0009
Od13g00360	Red	Blue	12.29	24.39	0.988	0.0067
Od12g00240	Red	Blue	300.54	595.29	0.986	0.0009
Od14g01240	Red	Blue	21.52	42.61	0.986	0.0009
Od16g00290	Red	Blue	76.66	151.62	0.984	0.0234
Od09g06220	Red	Blue	9.54	18.87	0.984	0.0192
Od09g00660	Red	Blue	11.34	22.38	0.981	0.0009
Od11g00680	Red	Blue	13.15	25.96	0.981	0.0016
Od04g02770	Red	Blue	28.13	55.45	0.979	0.0009
Od07g00100	Red	Blue	106.93	210.40	0.976	0.0009
Od02g03200	Red	Blue	33.24	65.39	0.976	0.0009
Od09g04910	Red	Blue	71.09	139.84	0.976	0.0009
Od12g00120	Red	Blue	11.35	22.32	0.976	0.0009
Od09g05630	Red	Blue	19.06	37.47	0.975	0.0009
Od10g00880	Red	Blue	54.06	106.05	0.972	0.0009
Od06g02850	Red	Blue	176.55	345.45	0.968	0.0009
Od05g01080	Red	Blue	19.55	38.23	0.967	0.0009
Od15g00120	Red	Blue	11.20	21.90	0.967	0.0086
Od11g03030	Red	Blue	37.98	74.08	0.964	0.0009
Od11g04450	Red	Blue	43.78	85.21	0.961	0.0009
Od02g00440	Red	Blue	18.88	36.70	0.959	0.0130
Od11g03280	Red	Blue	13.72	26.65	0.958	0.0046
Od01g00580	Red	Blue	14.66	28.44	0.956	0.0009
Od12g00690	Red	Blue	168.69	326.95	0.955	0.0009
Od16g01180	Red	Blue	12.49	24.20	0.954	0.0009
Od07g02910	Red	Blue	19.58	37.85	0.951	0.0009
Od03g03030	Red	Blue	9.23	17.81	0.949	0.0009
Od20g02780	Red	Blue	7.27	13.96	0.942	0.0104
Od17g00780	Red	Blue	31.74	60.97	0.942	0.0009
Od01g00210	Red	Blue	28.53	54.69	0.939	0.0009
Od16g01870	Red	Blue	54.98	105.37	0.938	0.0009
Od07g02340	Red	Blue	24.06	46.04	0.936	0.0009
Od11g00410	Red	Blue	60.68	115.91	0.934	0.0009
Od06g01250	Red	Blue	36.04	68.68	0.931	0.0009
Od14g00920	Red	Blue	28.93	55.06	0.928	0.0009
Od16g01050	Red	Blue	18.96	36.07	0.928	0.0009
Od06g01270	Red	Blue	8.43	16.03	0.927	0.0016

Od08g01990	Red	Blue	5.65	10.72	0.925	0.0041
Od01g05260	Red	Blue	98.50	186.20	0.919	0.0009
Od04g03550	Red	Blue	53.88	101.73	0.917	0.0009
Od06g02130	Red	Blue	8.81	16.63	0.917	0.0100
Od03g01340	Red	Blue	36.63	68.92	0.912	0.0009
Od06g04320	Red	Blue	16.11	30.30	0.912	0.0009
Od01g01160	Red	Blue	8.06	15.15	0.911	0.0126
Od07g03450	Red	Blue	7.76	14.59	0.910	0.0220
Od19g01100	Red	Blue	73.23	137.62	0.910	0.0009
Od09g05470	Red	Blue	163.15	306.40	0.909	0.0016
Od04g04880	Red	Blue	25.45	47.65	0.905	0.0009
Od05g03260	Red	Blue	7.10	13.28	0.904	0.0255
Od02g00280	Red	Blue	35.63	66.54	0.901	0.0009
Od13g01020	Red	Blue	586.96	1094.84	0.899	0.0009
Od13g01540	Red	Blue	25.56	47.66	0.899	0.0126
Od08g03280	Red	Blue	18.15	33.76	0.895	0.0009
Od01g04830	Red	Blue	11.43	21.22	0.893	0.0104
Od01g04670	Red	Blue	10.96	20.34	0.892	0.0062
Od06g06820	Red	Blue	24.89	46.15	0.891	0.0009
Od06g04940	Red	Blue	65.96	122.21	0.890	0.0009
Od19g01270	Red	Blue	16.95	31.39	0.889	0.0009
Od09g01680	Red	Blue	17.22	31.89	0.889	0.0213
Od07g03210	Red	Blue	12.10	22.29	0.881	0.0029
Od12g02690	Red	Blue	17.40	31.95	0.877	0.0035
Od05g01480	Red	Blue	10.12	18.56	0.875	0.0009
Od19g01000	Red	Blue	13.38	24.50	0.873	0.0009
Od11g01910	Red	Blue	13.18	24.10	0.871	0.0009
Od06g04390	Red	Blue	8.75	15.97	0.867	0.0009
Od09g02120	Red	Blue	10.81	19.65	0.863	0.0009
Od01g03470	Red	Blue	55.63	101.11	0.862	0.0009
Od01g01620	Red	Blue	18.72	34.01	0.862	0.0029
Od17g00090	Red	Blue	45.97	83.30	0.858	0.0009
Od15g01260	Red	Blue	5.11	9.25	0.856	0.0130
Od20g01520	Red	Blue	13.25	23.97	0.855	0.0134
Od20g00500	Red	Blue	18.47	33.38	0.854	0.0290
Od07g03870	Red	Blue	6.13	11.07	0.853	0.0067
Od04g03740	Red	Blue	19.71	35.58	0.852	0.0023
Od06g01640	Red	Blue	30.50	55.02	0.851	0.0009
Od02g03670	Red	Blue	67.53	121.80	0.851	0.0009
Od20g02870	Red	Blue	44.28	79.82	0.850	0.0009
Od07g03320	Red	Blue	21.35	38.47	0.850	0.0009
Od15g00200	Red	Blue	14.02	25.26	0.850	0.0442
Od05g01850	Red	Blue	41.91	75.32	0.846	0.0009

Od05g00020	Red	Blue	9.03	16.22	0.844	0.0484
Od01g03690	Red	Blue	13.75	24.68	0.844	0.0009
Od12g02080	Red	Blue	21.58	38.73	0.844	0.0023
Od16g00280	Red	Blue	68.14	122.12	0.842	0.0016
Od06g03360	Red	Blue	32.07	57.26	0.836	0.0023
Od14g03140	Red	Blue	4.47	7.97	0.834	0.0067
Od11g01890	Red	Blue	39.53	70.42	0.833	0.0009
Od02g04740	Red	Blue	89.74	159.51	0.830	0.0009
Od06g05210	Red	Blue	11.91	21.15	0.829	0.0122
Od12g02680	Red	Blue	18.44	32.70	0.827	0.0009
Od09g05220	Red	Blue	43.06	76.32	0.826	0.0009
Od11g00490	Red	Blue	16.95	30.00	0.824	0.0009
Od10g01020	Red	Blue	41.66	73.72	0.823	0.0016
Od01g05270	Red	Blue	16.38	28.98	0.823	0.0041
Od01g05590	Red	Blue	13.35	23.61	0.823	0.0029
Od06g04770	Red	Blue	12.54	22.12	0.819	0.0134
Od20g01140	Red	Blue	43.44	76.62	0.819	0.0009
Od06g05070	Red	Blue	8.76	15.44	0.817	0.0009
Od14g02480	Red	Blue	57.42	101.10	0.816	0.0009
Od11g02800	Red	Blue	2.57	4.52	0.814	0.0104
Od16g01980	Red	Blue	6.94	12.19	0.814	0.0378
Od09g06210	Red	Blue	16.25	28.53	0.812	0.0016
Od15g00150	Red	Blue	12.31	21.59	0.811	0.0041
Od06g04880	Red	Blue	24.09	42.22	0.809	0.0086
Od12g02860	Red	Blue	90.86	159.18	0.809	0.0009
Od20g00380	Red	Blue	44.65	78.22	0.809	0.0016
Od08g01280	Red	Blue	162.24	284.20	0.809	0.0009
Od06g06390	Red	Blue	10.22	17.86	0.806	0.0041
Od06g02460	Red	Blue	5.97	10.43	0.806	0.0234
Od03g00950	Red	Blue	16.19	28.28	0.804	0.0302
Od07g04510	Red	Blue	63.29	110.52	0.804	0.0009
Od06g00340	Red	Blue	16.70	29.15	0.804	0.0076
Od05g03240	Red	Blue	9.51	16.59	0.802	0.0470
Od16g01550	Red	Blue	212.18	369.74	0.801	0.0009
Od11g00060	Red	Blue	44.20	76.97	0.800	0.0009
Od01g00310	Red	Blue	36.91	64.21	0.799	0.0009
Od12g00850	Red	Blue	25.80	44.87	0.798	0.0076
Od04g04470	Red	Blue	57.58	100.13	0.798	0.0046
Od20g01580	Red	Blue	152.42	264.37	0.795	0.0009
Od03g02870	Red	Blue	9.17	15.90	0.794	0.0071
Od19g00570	Red	Blue	137.16	237.77	0.794	0.0009
Od05g04810	Red	Blue	22.00	38.11	0.793	0.0009
Od11g01100	Red	Blue	3.14	5.45	0.793	0.0035

Od20g01510	Red	Blue	5.02	8.68	0.789	0.0023
Od16g02460	Red	Blue	100.05	172.46	0.786	0.0009
Od12g03830	Red	Blue	5.61	9.65	0.783	0.0009
Od09g00670	Red	Blue	33.27	57.12	0.780	0.0035
Od11g03980	Red	Blue	11.11	19.07	0.779	0.0090
Od20g02070	Red	Blue	36.24	62.06	0.776	0.0023
Od14g03010	Red	Blue	30.99	53.04	0.775	0.0009
Od04g01720	Red	Blue	11.85	20.25	0.773	0.0108
Od08g03230	Red	Blue	23.43	40.00	0.772	0.0057
Od14g02600	Red	Blue	15.97	27.25	0.771	0.0041
Od03g00630	Red	Blue	13.76	23.47	0.771	0.0108
Od17g01360	Red	Blue	17.78	30.33	0.770	0.0041
Od01g04930	Red	Blue	6.86	11.69	0.768	0.0234
Od03g02830	Red	Blue	957.47	1629.82	0.767	0.0009
Od12g00040	Red	Blue	22.17	37.71	0.766	0.0009
Od03g00260	Red	Blue	36.87	62.71	0.766	0.0057
Od11g00130	Red	Blue	84.14	143.09	0.766	0.0009
Od15g00210	Red	Blue	54.29	92.28	0.765	0.0016
Od09g06080	Red	Blue	35.97	61.14	0.765	0.0009
Od09g00550	Red	Blue	18.68	31.75	0.765	0.0076
Od01g02820	Red	Blue	19.08	32.42	0.765	0.0009
Od06g04750	Red	Blue	100.31	170.43	0.765	0.0009
Od07g04590	Red	Blue	17.25	29.28	0.763	0.0255
Od17g02180	Red	Blue	11.22	19.04	0.763	0.0195
Od16g02450	Red	Blue	20.36	34.53	0.762	0.0076
Od12g00110	Red	Blue	10.69	18.11	0.760	0.0009
Od06g00070	Red	Blue	2311.16	3914.08	0.760	0.0009
Od17g00230	Red	Blue	18.33	31.01	0.758	0.0062
Od03g03160	Red	Blue	108.76	183.75	0.757	0.0009
Od20g01820	Red	Blue	33.02	55.73	0.755	0.0009
Od08g02850	Red	Blue	30.44	51.35	0.754	0.0009
Od08g00470	Red	Blue	22.68	38.26	0.754	0.0206
Od05g00160	Red	Blue	6.52	10.99	0.752	0.0009
Od10g02330	Red	Blue	7.35	12.38	0.751	0.0067
Od04g00500	Red	Blue	25.34	42.63	0.750	0.0029
Od20g02360	Red	Blue	7.85	13.20	0.750	0.0104
Od13g02590	Red	Blue	41.66	70.06	0.750	0.0113
Od12g03340	Red	Blue	15.34	25.79	0.750	0.0071
Od09g01440	Red	Blue	76.37	128.42	0.750	0.0009
Od08g01740	Red	Blue	46.11	77.49	0.749	0.0009
Od01g00810	Red	Blue	25.66	43.10	0.748	0.0035
Od07g02950	Red	Blue	12.60	21.16	0.748	0.0113
Od03g02700	Red	Blue	15.38	25.83	0.748	0.0174

Od20g01370	Red	Blue	27.14	45.49	0.745	0.0174
Od12g02220	Red	Blue	100.00	167.57	0.745	0.0009
Od16g02050	Red	Blue	23.94	40.10	0.744	0.0130
Od19g00930	Red	Blue	54.35	91.00	0.744	0.0041
Od14g00280	Red	Blue	2952.30	4940.05	0.743	0.0009
Od07g03710	Red	Blue	10.69	17.87	0.741	0.0086
Od19g00990	Red	Blue	2.48	4.15	0.741	0.0029
Od17g01730	Red	Blue	29.49	49.22	0.739	0.0062
Od08g02120	Red	Blue	7.48	12.49	0.739	0.0439
Od01g00970	Red	Blue	24.91	41.56	0.738	0.0035
Od06g02210	Red	Blue	18.08	30.11	0.736	0.0041
Od07g04860	Red	Blue	40.72	67.79	0.735	0.0095
Od07g04070	Red	Blue	19.05	31.70	0.734	0.0046
Od04g05040	Red	Blue	25.41	42.25	0.734	0.0052
Od08g03860	Red	Blue	52.22	86.82	0.733	0.0009
Od04g03830	Red	Blue	11.61	19.29	0.733	0.0146
Od20g02900	Red	Blue	101.91	169.29	0.732	0.0009
Od05g04960	Red	Blue	83.31	138.22	0.730	0.0009
Od01g05600	Red	Blue	33.80	55.93	0.727	0.0009
Od11g00080	Red	Blue	15.05	24.89	0.726	0.0071
Od12g01750	Red	Blue	58.42	96.64	0.726	0.0009
Od05g01670	Red	Blue	13.80	22.82	0.726	0.0104
Od12g02550	Red	Blue	19.70	32.56	0.725	0.0071
Od01g07020	Red	Blue	102.59	169.55	0.725	0.0009
Od06g00130	Red	Blue	100.17	165.51	0.725	0.0009
Od10g01390	Red	Blue	21.25	35.09	0.724	0.0023
Od11g01940	Red	Blue	28.68	47.33	0.722	0.0166
Od02g00150	Red	Blue	11.95	19.64	0.717	0.0016
Od12g03460	Red	Blue	31.62	51.93	0.716	0.0041
Od11g01460	Red	Blue	10.79	17.71	0.715	0.0231
Od06g02230	Red	Blue	88.14	144.64	0.715	0.0009
Od09g01640	Red	Blue	17.71	29.05	0.714	0.0029
Od12g03040	Red	Blue	47.20	77.29	0.712	0.0067
Od12g03250	Red	Blue	16.66	27.25	0.710	0.0029
Od05g04730	Red	Blue	77.87	127.31	0.709	0.0035
Od17g01120	Red	Blue	28.00	45.77	0.709	0.0057
Od09g00260	Red	Blue	102.06	166.75	0.708	0.0016
Od08g01470	Red	Blue	37.10	60.52	0.706	0.0029
Od10g00780	Red	Blue	9.68	15.78	0.705	0.0302
Od05g03410	Red	Blue	12.98	21.15	0.704	0.0126
Od14g00810	Red	Blue	12.27	19.94	0.701	0.0062
Od01g01190	Red	Blue	34.98	56.83	0.700	0.0009
Od11g01470	Red	Blue	22.18	36.03	0.700	0.0016

Od05g00700	Red	Blue	30.71	49.77	0.696	0.0076
Od12g03740	Red	Blue	16.61	26.89	0.694	0.0052
Od10g00760	Red	Blue	150.50	243.53	0.694	0.0067
Od09g06130	Red	Blue	521.54	843.75	0.694	0.0023
Od11g00340	Red	Blue	13.14	21.25	0.694	0.0241
Od06g07420	Red	Blue	79.53	128.35	0.691	0.0009
Od06g02880	Red	Blue	66.22	106.88	0.690	0.0029
Od09g01260	Red	Blue	66.80	107.80	0.690	0.0016
Od06g00830	Red	Blue	36.14	58.29	0.690	0.0023
Od11g01680	Red	Blue	22.63	36.49	0.689	0.0108
Od16g02570	Red	Blue	67.05	107.93	0.687	0.0071
Od01g06790	Red	Blue	53.58	86.16	0.685	0.0071
Od02g03890	Red	Blue	32.13	51.60	0.683	0.0023
Od06g00900	Red	Blue	27.21	43.70	0.683	0.0122
Od15g01180	Red	Blue	23.29	37.39	0.683	0.0081
Od16g00870	Red	Blue	20.94	33.62	0.683	0.0062
Od01g03970	Red	Blue	36.76	59.00	0.683	0.0329
Od06g00290	Red	Blue	12.77	20.49	0.682	0.0071
Od04g00120	Red	Blue	23.67	37.94	0.681	0.0210
Od02g03320	Red	Blue	18.64	29.83	0.679	0.0117
Od12g02460	Red	Blue	27.65	44.25	0.678	0.0258
Od07g03500	Red	Blue	75.43	120.55	0.676	0.0016
Od04g00270	Red	Blue	15.38	24.57	0.676	0.0134
Od05g04750	Red	Blue	10.70	17.07	0.674	0.0113
Od09g00970	Red	Blue	85.04	135.68	0.674	0.0016
Od17g01290	Red	Blue	6.16	9.82	0.674	0.0278
Od05g04350	Red	Blue	14.40	22.97	0.673	0.0346
Od07g03740	Red	Blue	33.58	53.51	0.672	0.0057
Od06g05680	Red	Blue	24.00	38.18	0.670	0.0166
Od20g00290	Red	Blue	52.44	83.42	0.670	0.0041
Od14g00700	Red	Blue	64.54	102.54	0.668	0.0016
Od12g02090	Red	Blue	40.94	65.02	0.667	0.0046
Od13g01210	Red	Blue	19.41	30.79	0.666	0.0052
Od08g01430	Red	Blue	5.48	8.69	0.666	0.0062
Od11g01050	Red	Blue	64.00	101.50	0.665	0.0023
Od20g01930	Red	Blue	4.43	7.02	0.665	0.0057
Od12g03840	Red	Blue	119.12	188.81	0.665	0.0023
Od07g02670	Red	Blue	30.78	48.78	0.664	0.0041
Od01g06230	Red	Blue	23.99	38.01	0.664	0.0057
Od11g01670	Red	Blue	111.00	175.83	0.664	0.0029
Od04g05090	Red	Blue	37.23	58.93	0.663	0.0150
Od09g02820	Red	Blue	11.21	17.75	0.662	0.0468
Od07g04760	Red	Blue	15.78	24.97	0.662	0.0231

Od09g06120	Red	Blue	31.73	50.12	0.660	0.0067
Od06g03180	Red	Blue	26.89	42.46	0.659	0.0104
Od08g00070	Red	Blue	50.88	80.31	0.658	0.0046
Od02g04480	Red	Blue	45.22	71.34	0.658	0.0170
Od12g02990	Red	Blue	27.76	43.77	0.657	0.0142
Od16g01170	Red	Blue	46.48	73.27	0.657	0.0090
Od06g02660	Red	Blue	16.25	25.61	0.656	0.0041
Od13g00120	Red	Blue	17.60	27.73	0.656	0.0041
Od06g00520	Red	Blue	19.35	30.48	0.655	0.0199
Od05g04200	Red	Blue	11.61	18.28	0.655	0.0046
Od12g00100	Red	Blue	22.39	35.24	0.655	0.0071
Od18g00090	Red	Blue	36.66	57.66	0.653	0.0029
Od11g01290	Red	Blue	13.17	20.71	0.653	0.0052
Od12g00840	Red	Blue	11.18	17.58	0.653	0.0220
Od02g03690	Red	Blue	8.54	13.43	0.652	0.0331
Od17g01040	Red	Blue	69.06	108.45	0.651	0.0029
Od10g00450	Red	Blue	179.52	281.85	0.651	0.0104
Od07g00530	Red	Blue	69.46	109.02	0.650	0.0023
Od09g03390	Red	Blue	64.21	100.75	0.650	0.0035
Od06g07570	Red	Blue	12.15	19.05	0.649	0.0237
Od03g02520	Red	Blue	9.94	15.57	0.648	0.0352
Od14g01220	Red	Blue	70.31	110.17	0.648	0.0057
Od17g01560	Red	Blue	118.64	185.83	0.647	0.0023
Od01g04880	Red	Blue	73.54	115.13	0.647	0.0041
Od13g01180	Red	Blue	50.46	78.99	0.647	0.0029
Od02g00970	Red	Blue	31.37	49.09	0.646	0.0126
Od08g00650	Red	Blue	32.35	50.61	0.646	0.0041
Od14g02680	Red	Blue	68.28	106.81	0.645	0.0057
Od06g01970	Red	Blue	28.97	45.29	0.645	0.0312
Od05g01880	Red	Blue	17.78	27.79	0.644	0.0041
Od06g01710	Red	Blue	52.59	82.18	0.644	0.0130
Od13g02610	Red	Blue	27.88	43.54	0.643	0.0023
Od13g01110	Red	Blue	11.91	18.60	0.643	0.0095
Od05g04770	Red	Blue	42.23	65.92	0.642	0.0188
Od14g00410	Red	Blue	61.85	96.49	0.642	0.0052
Od06g02430	Red	Blue	74.84	116.76	0.642	0.0071
Od13g02570	Red	Blue	41.72	65.08	0.642	0.0052
Od06g03670	Red	Blue	19.92	31.07	0.641	0.0023
Od01g05400	Red	Blue	18.35	28.62	0.641	0.0271
Od04g03140	Red	Blue	76.10	118.52	0.639	0.0081
Od09g00850	Red	Blue	12.25	19.08	0.639	0.0076
Od02g00160	Red	Blue	48.92	76.17	0.639	0.0076
Od06g07000	Red	Blue	17.89	27.84	0.638	0.0258

Od07g03470	Red	Blue	14.79	23.02	0.638	0.0067
Od12g02800	Red	Blue	51.81	80.62	0.638	0.0041
Od19g00380	Red	Blue	23.80	37.02	0.638	0.0177
Od02g03870	Red	Blue	78.52	122.04	0.636	0.0081
Od20g01040	Red	Blue	44.33	68.64	0.631	0.0071
Od10g00720	Red	Blue	58.05	89.75	0.629	0.0046
Od16g00170	Red	Blue	74.52	115.15	0.628	0.0095
Od07g04040	Red	Blue	24.44	37.72	0.626	0.0357
Od11g02930	Red	Blue	29.38	45.32	0.625	0.0217
Od13g02790	Red	Blue	22.31	34.40	0.625	0.0071
Od08g00490	Red	Blue	13.33	20.54	0.624	0.0166
Od06g05270	Red	Blue	22.98	35.40	0.623	0.0463
Od09g03510	Red	Blue	395.92	609.60	0.623	0.0041
Od09g03330	Red	Blue	51.24	78.87	0.622	0.0057
Od02g00370	Red	Blue	15.97	24.54	0.620	0.0452
Od16g00730	Red	Blue	90.44	138.93	0.619	0.0041
Od07g01860	Red	Blue	63.13	96.95	0.619	0.0142
Od06g03060	Red	Blue	37.10	56.96	0.619	0.0170
Od08g03400	Red	Blue	34.13	52.40	0.619	0.0057
Od17g01170	Red	Blue	18.81	28.86	0.617	0.0154
Od05g02520	Red	Blue	12.77	19.56	0.615	0.0100
Od06g03680	Red	Blue	25.25	38.65	0.614	0.0113
Od04g02090	Red	Blue	56.88	86.89	0.611	0.0076
Od20g00250	Red	Blue	27.51	42.02	0.611	0.0067
Od04g00670	Red	Blue	85.46	130.46	0.610	0.0057
Od16g01850	Red	Blue	35.47	54.11	0.609	0.0170
Od07g00510	Red	Blue	21.21	32.35	0.609	0.0086
Od09g00390	Red	Blue	27.05	41.22	0.608	0.0192
Od11g02720	Red	Blue	97.12	147.99	0.608	0.0071
Od13g01870	Red	Blue	14.69	22.39	0.608	0.0463
Od05g04620	Red	Blue	21.29	32.41	0.606	0.0355
Od09g01760	Red	Blue	22.74	34.59	0.605	0.0346
Od14g00640	Red	Blue	9.71	14.76	0.605	0.0327
Od04g02100	Red	Blue	53.45	81.20	0.603	0.0302
Od01g06620	Red	Blue	5.86	8.89	0.602	0.0192
Od04g03500	Red	Blue	20.78	31.54	0.602	0.0071
Od04g05310	Red	Blue	126.89	192.52	0.601	0.0104
Od02g04560	Red	Blue	72.38	109.67	0.599	0.0138
Od11g02480	Red	Blue	42.86	64.90	0.599	0.0108
Od01g02860	Red	Blue	184.39	279.13	0.598	0.0126
Od02g04950	Red	Blue	61.59	93.22	0.598	0.0188
Od06g07450	Red	Blue	42.47	64.25	0.597	0.0271
Od17g01280	Red	Blue	15.85	23.97	0.597	0.0271

Od07g02900	Red	Blue	3261.89	4921.91	0.594	0.0057
Od10g02210	Red	Blue	4.69	7.07	0.593	0.0086
Od03g00140	Red	Blue	34.17	51.44	0.590	0.0220
Od06g06590	Red	Blue	31.54	47.44	0.589	0.0180
Od10g00890	Red	Blue	57.92	87.08	0.588	0.0262
Od12g01340	Red	Blue	66.36	99.69	0.587	0.0126
Od20g02970	Red	Blue	20.54	30.85	0.587	0.0443
Od06g01950	Red	Blue	29.26	43.91	0.586	0.0142
Od07g02890	Red	Blue	17.62	26.43	0.586	0.0134
Od12g03130	Red	Blue	5.58	8.37	0.585	0.0357
Od14g01660	Red	Blue	57.89	86.60	0.581	0.0154
Od03g02080	Red	Blue	27.61	41.30	0.581	0.0162
Od11g03970	Red	Blue	40.47	60.50	0.580	0.0142
Od10g02090	Red	Blue	636.27	950.99	0.580	0.0117
Od02g00880	Red	Blue	36.08	53.91	0.579	0.0315
Od09g05870	Red	Blue	84.07	125.57	0.579	0.0117
Od12g00130	Red	Blue	79.82	119.20	0.578	0.0104
Od09g03150	Red	Blue	27.72	41.31	0.576	0.0162
Od12g03470	Red	Blue	27.08	40.34	0.575	0.0357
Od20g00920	Red	Blue	33.63	50.04	0.574	0.0117
Od07g04550	Red	Blue	8.98	13.35	0.572	0.0278
Od10g00810	Red	Blue	15.81	23.50	0.572	0.0420
Od07g00980	Red	Blue	24.45	36.32	0.571	0.0113
Od16g00630	Red	Blue	12.08	17.93	0.571	0.0262
Od06g04960	Red	Blue	26.31	39.03	0.569	0.0162
Od06g06940	Red	Blue	21.01	31.15	0.568	0.0262
Od06g00450	Red	Blue	80.30	118.90	0.566	0.0234
Od13g00400	Red	Blue	86.03	127.38	0.566	0.0188
Od11g03270	Red	Blue	45.36	67.03	0.563	0.0319
Od15g01330	Red	Blue	77.12	113.94	0.563	0.0210
Od06g07410	Red	Blue	63.19	93.26	0.562	0.0154
Od09g01350	Red	Blue	26.12	38.52	0.561	0.0479
Od01g00790	Red	Blue	77.48	114.28	0.561	0.0130
Od12g01220	Red	Blue	32.66	48.16	0.560	0.0202
Od05g00600	Red	Blue	33.73	49.68	0.559	0.0122
Od02g00430	Red	Blue	15.34	22.59	0.558	0.0312
Od09g00310	Red	Blue	188.78	277.92	0.558	0.0117
Od06g01870	Red	Blue	23.16	34.08	0.557	0.0210
Od05g01600	Red	Blue	1300.71	1911.91	0.556	0.0158
Od06g04160	Red	Blue	9.18	13.50	0.555	0.0492
Od03g02120	Red	Blue	6.91	10.16	0.555	0.0375
Od20g01910	Red	Blue	28.88	42.44	0.555	0.0349
Od07g01100	Red	Blue	43.10	63.28	0.554	0.0278

Od14g00910	Red	Blue	100.13	146.98	0.554	0.0138
Od14g00390	Red	Blue	24.50	35.96	0.554	0.0210
Od04g01970	Red	Blue	63.47	93.10	0.553	0.0258
Od14g02010	Red	Blue	22.22	32.59	0.552	0.0428
Od06g03190	Red	Blue	23.26	34.10	0.552	0.0217
Od04g01850	Red	Blue	20.87	30.59	0.551	0.0180
Od06g06580	Red	Blue	24.63	36.08	0.551	0.0210
Od14g01210	Red	Blue	236.46	346.30	0.550	0.0224
Od04g02200	Red	Blue	15.22	22.28	0.550	0.0392
Od05g00350	Red	Blue	127.28	186.29	0.550	0.0170
Od10g01130	Red	Blue	20.75	30.36	0.549	0.0278
Od12g01680	Red	Blue	22.75	33.20	0.546	0.0134
Od20g00280	Red	Blue	75.15	109.69	0.546	0.0213
Od04g01520	Red	Blue	48.97	71.47	0.545	0.0465
Od16g00890	Red	Blue	40.71	59.38	0.545	0.0150
Od01g01950	Red	Blue	51.48	75.08	0.544	0.0195
Od06g02940	Red	Blue	52.31	76.17	0.542	0.0484
Od06g00150	Red	Blue	102.77	149.52	0.541	0.0220
Od14g02670	Red	Blue	46.97	68.32	0.541	0.0202
Od04g04360	Red	Blue	23.54	34.22	0.540	0.0180
Od20g00930	Red	Blue	168.17	244.51	0.540	0.0227
Od06g06950	Red	Blue	30.14	43.81	0.540	0.0343
Od20g01710	Red	Blue	111.84	162.46	0.539	0.0213
Od10g02550	Red	Blue	6.40	9.29	0.539	0.0192
Od02g00750	Red	Blue	37.32	54.20	0.538	0.0449
Od13g00080	Red	Blue	22.76	33.03	0.538	0.0210
Od17g00240	Red	Blue	34.45	49.98	0.537	0.0227
Od03g01070	Red	Blue	22.02	31.92	0.536	0.0321
Od01g06450	Red	Blue	49.00	71.02	0.535	0.0294
Od11g03920	Red	Blue	107.13	155.23	0.535	0.0217
Od06g00250	Red	Blue	74.98	108.63	0.535	0.0166
Od02g03790	Red	Blue	20.31	29.38	0.533	0.0458
Od09g03320	Red	Blue	42.27	61.14	0.533	0.0439
Od17g00920	Red	Blue	43.13	62.32	0.531	0.0343
Od04g04750	Red	Blue	48.06	69.43	0.531	0.0237
Od15g00100	Red	Blue	64.16	92.69	0.531	0.0195
Od06g03900	Red	Blue	163.87	236.69	0.530	0.0227
Od09g04660	Red	Blue	54.74	79.03	0.530	0.0241
Od02g04230	Red	Blue	231.33	333.97	0.530	0.0436
Od19g00730	Red	Blue	77.49	111.84	0.529	0.0278
Od01g06580	Red	Blue	998.32	1439.11	0.528	0.0331
Od14g02920	Red	Blue	33.98	48.94	0.527	0.0378
Od03g01590	Red	Blue	54.76	78.88	0.527	0.0281

Od08g02940	Red	Blue	694.97	1000.16	0.525	0.0220
Od06g01820	Red	Blue	81.87	117.70	0.524	0.0192
Od02g00390	Red	Blue	170.20	244.46	0.522	0.0306
Od05g04090	Red	Blue	71.13	102.13	0.522	0.0258
Od17g03010	Red	Blue	124.45	178.61	0.521	0.0321
Od07g02850	Red	Blue	34.97	50.16	0.521	0.0309
Od07g00050	Red	Blue	26.11	37.46	0.521	0.0443
Od01g05760	Red	Blue	11.07	15.88	0.520	0.0290
Od09g04670	Red	Blue	18.57	26.61	0.519	0.0346
Od11g00030	Red	Blue	41.57	59.47	0.516	0.0284
Od10g00050	Red	Blue	424.67	607.04	0.515	0.0327
Od07g04240	Red	Blue	23.64	33.79	0.515	0.0327
Od13g01360	Red	Blue	17.71	25.29	0.514	0.0436
Od17g00420	Red	Blue	34.92	49.72	0.510	0.0324
Od09g06110	Red	Blue	37.12	52.86	0.510	0.0417
Od12g02320	Red	Blue	12.36	17.59	0.509	0.0443
Od03g01380	Red	Blue	15.61	22.19	0.507	0.0302
Od03g02690	Red	Blue	16.96	24.11	0.507	0.0375
Od06g06640	Red	Blue	117.15	166.44	0.507	0.0341
Od02g04980	Red	Blue	1017.95	1445.23	0.506	0.0329
Od11g01550	Red	Blue	34.99	49.59	0.503	0.0355
Od04g01430	Red	Blue	14.43	20.44	0.502	0.0402
Od11g03870	Red	Blue	87.13	123.29	0.501	0.0341
Od19g00260	Red	Blue	174.29	246.56	0.500	0.0357
Od08g03580	Red	Blue	168.39	237.79	0.498	0.0357
Od01g01640	Red	Blue	200.70	282.82	0.495	0.0297
Od09g06280	Red	Blue	89.71	126.41	0.495	0.0335
Od04g01190	Red	Blue	39.48	55.62	0.495	0.0473
Od19g00920	Red	Blue	14.07	19.82	0.494	0.0417
Od14g03150	Red	Blue	183.70	258.59	0.493	0.0349
Od11g03070	Red	Blue	27.84	39.10	0.490	0.0426
Od14g02450	Red	Blue	25.78	36.17	0.488	0.0458
Od10g01260	Red	Blue	27.56	38.66	0.488	0.0360
Od01g01310	Red	Blue	65.14	91.36	0.488	0.0411
Od20g01260	Red	Blue	100.34	140.68	0.487	0.0442
Od19g00720	Red	Blue	47.11	66.03	0.487	0.0487
Od19g00090	Red	Blue	148.37	207.89	0.487	0.0434
Od06g03090	Red	Blue	53.03	74.12	0.483	0.0414
Od17g01350	Red	Blue	123.90	173.12	0.483	0.0352
Od20g02080	Red	Blue	64.84	90.53	0.482	0.0443
Od07g02470	Red	Blue	219.67	306.12	0.479	0.0414
Od19g00280	Red	Blue	31.91	44.45	0.478	0.0500
Od12g01640	Red	Blue	429.94	598.71	0.478	0.0392

Od12g03510	Red	Blue	134.88	187.81	0.478	0.0414
Od12g03370	Red	Blue	81.98	114.11	0.477	0.0468
Od03g00090	Red	Blue	109.97	152.92	0.476	0.0484
Od07g01740	Red	Blue	112.91	156.97	0.475	0.0497
Od09g00960	Red	Blue	77.91	108.30	0.475	0.0473
Od13g02330	Red	Blue	24.19	33.62	0.475	0.0447
Od01g00330	Red	Blue	40.35	55.86	0.469	0.0500
Od20g03400	Red	Blue	66.03	91.23	0.467	0.0490
Od09g02620	Red	Blue	135.42	187.06	0.466	0.0468
Od08g02360	Red	Blue	415.86	301.80	-0.462	0.0497
Od02g02860	Red	Blue	570.41	412.13	-0.469	0.0473
Od06g00790	Red	Blue	165.58	119.28	-0.473	0.0473
Od09g02140	Red	Blue	77.86	56.09	-0.473	0.0473
Od01g04440	Red	Blue	43.38	31.24	-0.474	0.0479
Od03g02430	Red	Blue	120.09	86.47	-0.474	0.0443
Od06g02790	Red	Blue	566.58	407.79	-0.474	0.0449
Od01g05070	Red	Blue	324.89	233.81	-0.475	0.0468
Od11g03180	Red	Blue	70.18	50.47	-0.476	0.0428
Od01g06550	Red	Blue	574.62	413.23	-0.476	0.0417
Od15g00340	Red	Blue	177.81	127.84	-0.476	0.0497
Od04g00520	Red	Blue	211.46	151.87	-0.478	0.0465
Od06g04080	Red	Blue	138.13	99.10	-0.479	0.0495
Od06g00980	Red	Blue	1049.23	752.78	-0.479	0.0476
Od02g02000	Red	Blue	683.22	490.05	-0.479	0.0449
Od16g00010	Red	Blue	286.38	205.39	-0.480	0.0434
Od18g00360	Red	Blue	188.86	135.31	-0.481	0.0428
Od05g00090	Red	Blue	241.86	173.22	-0.482	0.0463
Od03g03020	Red	Blue	242.90	173.93	-0.482	0.0436
Od18g00570	Red	Blue	220.20	157.55	-0.483	0.0449
Od01g04350	Red	Blue	79.38	56.75	-0.484	0.0463
Od12g01950	Red	Blue	385.76	275.77	-0.484	0.0439
Od13g01560	Red	Blue	145.58	104.04	-0.485	0.0487
Od05g04140	Red	Blue	176.04	125.76	-0.485	0.0428
Od07g01360	Red	Blue	1141.23	815.02	-0.486	0.0482
Od08g00140	Red	Blue	589.31	420.82	-0.486	0.0458
Od01g06170	Red	Blue	187.81	133.98	-0.487	0.0372
Od01g04240	Red	Blue	276.61	197.28	-0.488	0.0408
Od13g02400	Red	Blue	758.46	540.82	-0.488	0.0443
Od06g01900	Red	Blue	98.51	70.18	-0.489	0.0390
Od06g03810	Red	Blue	789.70	562.43	-0.490	0.0357
Od09g04300	Red	Blue	143.92	102.48	-0.490	0.0369
Od10g02070	Red	Blue	31.27	22.27	-0.490	0.0408
Od07g00870	Red	Blue	1325.62	943.89	-0.490	0.0473

Od08g02350	Red	Blue	272.74	194.19	-0.490	0.0455
Od04g03710	Red	Blue	94.47	67.26	-0.490	0.0431
Od02g00480	Red	Blue	278.62	198.26	-0.491	0.0402
Od02g02850	Red	Blue	448.05	318.46	-0.493	0.0369
Od13g00270	Red	Blue	280.21	199.15	-0.493	0.0402
Od01g02310	Red	Blue	76.57	54.41	-0.493	0.0461
Od05g04570	Red	Blue	175.90	124.99	-0.493	0.0381
Od08g00180	Red	Blue	4778.48	3394.38	-0.493	0.0426
Od15g00670	Red	Blue	81.12	57.55	-0.495	0.0321
Od16g01600	Red	Blue	147.81	104.82	-0.496	0.0331
Od05g02220	Red	Blue	110.39	78.28	-0.496	0.0402
Od09g03360	Red	Blue	160.78	114.00	-0.496	0.0384
Od06g04820	Red	Blue	37.19	26.37	-0.496	0.0337
Od17g00120	Red	Blue	321.84	228.15	-0.496	0.0352
Od05g04450	Red	Blue	749.25	531.01	-0.497	0.0428
Od10g00380	Red	Blue	244.73	173.43	-0.497	0.0387
Od05g04600	Red	Blue	246.49	174.63	-0.497	0.0423
Od02g02380	Red	Blue	261.83	185.47	-0.497	0.0363
Od07g04750	Red	Blue	207.02	146.63	-0.498	0.0390
Od02g00190	Red	Blue	361.36	255.88	-0.498	0.0357
Od11g03770	Red	Blue	142.10	100.26	-0.503	0.0329
Od12g00990	Red	Blue	185.80	131.08	-0.503	0.0281
Od08g02500	Red	Blue	107.84	76.08	-0.503	0.0281
Od11g02320	Red	Blue	74.74	52.71	-0.504	0.0372
Od20g00950	Red	Blue	135.28	95.34	-0.505	0.0329
Od04g01900	Red	Blue	155.60	109.63	-0.505	0.0369
Od08g02100	Red	Blue	201.70	142.08	-0.505	0.0271
Od19g00510	Red	Blue	84.49	59.49	-0.506	0.0434
Od18g00390	Red	Blue	92.56	65.11	-0.508	0.0300
Od08g02170	Red	Blue	165.46	116.37	-0.508	0.0327
Od17g00670	Red	Blue	342.25	240.60	-0.508	0.0349
Od20g01780	Red	Blue	44.24	31.09	-0.509	0.0319
Od16g00460	Red	Blue	159.43	111.99	-0.510	0.0255
Od15g00860	Red	Blue	458.56	322.05	-0.510	0.0360
Od16g01660	Red	Blue	207.20	145.47	-0.510	0.0309
Od04g02650	Red	Blue	84.68	59.45	-0.510	0.0327
Od16g01580	Red	Blue	128.56	90.25	-0.510	0.0278
Od01g00470	Red	Blue	343.03	240.80	-0.511	0.0258
Od05g03960	Red	Blue	282.26	197.86	-0.513	0.0443
Od19g01010	Red	Blue	347.31	243.42	-0.513	0.0252
Od05g03750	Red	Blue	96.68	67.76	-0.513	0.0331
Od10g00290	Red	Blue	1135.54	795.84	-0.513	0.0309
Od10g02060	Red	Blue	13.74	9.63	-0.513	0.0329

Od04g02210	Red	Blue	128.14	89.77	-0.513	0.0360
Od09g03900	Red	Blue	109.96	77.03	-0.514	0.0309
Od04g04160	Red	Blue	89.45	62.61	-0.515	0.0265
Od04g03380	Red	Blue	31.89	22.32	-0.515	0.0281
Od06g01030	Red	Blue	158.50	110.90	-0.515	0.0284
Od06g01380	Red	Blue	66.03	46.18	-0.516	0.0262
Od12g00410	Red	Blue	60.76	42.47	-0.516	0.0287
Od04g02400	Red	Blue	860.26	600.91	-0.518	0.0252
Od20g02440	Red	Blue	188.47	131.61	-0.518	0.0337
Od11g00650	Red	Blue	554.74	387.32	-0.518	0.0312
Od07g01350	Red	Blue	908.97	634.47	-0.519	0.0309
Od02g03300	Red	Blue	259.43	181.01	-0.519	0.0287
Od07g01420	Red	Blue	623.07	434.36	-0.521	0.0300
Od09g04370	Red	Blue	130.79	91.16	-0.521	0.0241
Od14g00250	Red	Blue	306.61	213.66	-0.521	0.0434
Od17g03140	Red	Blue	411.25	286.32	-0.522	0.0331
Od06g06090	Red	Blue	654.60	455.59	-0.523	0.0281
Od20g01230	Red	Blue	3533.59	2456.74	-0.524	0.0241
Od06g02800	Red	Blue	110.92	77.11	-0.524	0.0170
Od09g05950	Red	Blue	484.10	336.50	-0.525	0.0331
Od02g02810	Red	Blue	160.15	111.30	-0.525	0.0297
Od02g04300	Red	Blue	124.10	86.21	-0.526	0.0210
Od19g01230	Red	Blue	355.47	246.70	-0.527	0.0245
Od09g04750	Red	Blue	56.12	38.92	-0.528	0.0324
Od14g03220	Red	Blue	308.37	213.81	-0.528	0.0188
Od01g01520	Red	Blue	1130.59	783.74	-0.529	0.0265
Od03g00760	Red	Blue	1306.42	905.41	-0.529	0.0248
Od05g05070	Red	Blue	255.44	176.94	-0.530	0.0284
Od04g02010	Red	Blue	750.62	519.71	-0.530	0.0309
Od12g00390	Red	Blue	210.41	145.68	-0.530	0.0248
Od05g01130	Red	Blue	88.92	61.53	-0.531	0.0180
Od02g01650	Red	Blue	61.49	42.51	-0.533	0.0297
Od01g01400	Red	Blue	306.20	211.59	-0.533	0.0234
Od20g02020	Red	Blue	102.95	71.11	-0.534	0.0329
Od13g02060	Red	Blue	101.30	69.95	-0.534	0.0258
Od04g04480	Red	Blue	60.32	41.63	-0.535	0.0411
Od16g01340	Red	Blue	1387.71	957.33	-0.536	0.0290
Od03g02530	Red	Blue	48.62	33.53	-0.536	0.0227
Od06g03460	Red	Blue	222.84	153.66	-0.536	0.0213
Od08g02690	Red	Blue	113.81	78.46	-0.537	0.0166
Od14g00370	Red	Blue	151.60	104.49	-0.537	0.0231
Od13g02710	Red	Blue	654.79	451.10	-0.538	0.0252
Od03g02190	Red	Blue	163.63	112.66	-0.538	0.0220

Od20g02670	Red	Blue	448.60	308.71	-0.539	0.0210
Od04g01890	Red	Blue	1076.78	740.99	-0.539	0.0248
Od20g01130	Red	Blue	1142.33	785.16	-0.541	0.0202
Od10g01300	Red	Blue	165.33	113.51	-0.542	0.0174
Od12g01870	Red	Blue	565.66	388.23	-0.543	0.0192
Od11g04440	Red	Blue	49.44	33.92	-0.543	0.0287
Od04g02960	Red	Blue	177.41	121.58	-0.545	0.0146
Od03g00700	Red	Blue	88.19	60.41	-0.546	0.0162
Od11g04350	Red	Blue	186.25	127.51	-0.547	0.0217
Od03g01280	Red	Blue	387.02	264.45	-0.549	0.0166
Od02g02040	Red	Blue	257.26	175.44	-0.552	0.0126
Od14g02160	Red	Blue	622.52	424.31	-0.553	0.0166
Od05g04640	Red	Blue	239.21	162.99	-0.554	0.0180
Od04g00690	Red	Blue	601.16	409.08	-0.555	0.0154
Od16g01890	Red	Blue	615.90	418.73	-0.557	0.0231
Od09g02220	Red	Blue	703.00	477.88	-0.557	0.0309
Od18g00230	Red	Blue	41.24	28.02	-0.557	0.0262
Od15g01150	Red	Blue	72.36	49.17	-0.557	0.0138
Od09g04740	Red	Blue	78.71	53.46	-0.558	0.0180
Od12g00420	Red	Blue	74.58	50.64	-0.558	0.0134
Od01g03880	Red	Blue	125.56	85.25	-0.559	0.0158
Od12g03850	Red	Blue	964.75	654.93	-0.559	0.0329
Od01g06030	Red	Blue	1015.47	688.48	-0.561	0.0158
Od12g01230	Red	Blue	294.48	199.65	-0.561	0.0150
Od01g00740	Red	Blue	33.64	22.77	-0.563	0.0180
Od04g00680	Red	Blue	41.49	28.07	-0.564	0.0146
Od02g00470	Red	Blue	464.12	313.72	-0.565	0.0174
Od04g02450	Red	Blue	3636.73	2457.39	-0.566	0.0150
Od03g01930	Red	Blue	55.76	37.68	-0.566	0.0130
Od12g03770	Red	Blue	200.09	135.11	-0.567	0.0142
Od09g01170	Red	Blue	159.31	107.53	-0.567	0.0122
Od11g01150	Red	Blue	58.07	39.19	-0.567	0.0138
Od02g04310	Red	Blue	82.83	55.88	-0.568	0.0331
Od16g00470	Red	Blue	2863.05	1930.41	-0.569	0.0113
Od06g07010	Red	Blue	79.40	53.53	-0.569	0.0378
Od03g02930	Red	Blue	124.25	83.76	-0.569	0.0146
Od10g02080	Red	Blue	23.51	15.85	-0.569	0.0134
Od02g02920	Red	Blue	1034.49	696.90	-0.570	0.0146
Od20g02230	Red	Blue	1673.53	1127.32	-0.570	0.0138
Od19g00470	Red	Blue	2242.44	1510.43	-0.570	0.0104
Od03g03040	Red	Blue	32.42	21.83	-0.571	0.0192
Od02g04200	Red	Blue	299.17	201.36	-0.571	0.0100
Od01g01970	Red	Blue	458.06	308.21	-0.572	0.0150

Od11g03110	Red	Blue	117.06	78.76	-0.572	0.0104
Od03g01090	Red	Blue	463.13	311.42	-0.573	0.0177
Od02g01550	Red	Blue	508.19	341.66	-0.573	0.0126
Od14g01060	Red	Blue	395.83	266.09	-0.573	0.0138
Od09g00010	Red	Blue	179.81	120.81	-0.574	0.0142
Od02g04030	Red	Blue	178.94	120.18	-0.574	0.0188
Od02g02610	Red	Blue	372.25	249.92	-0.575	0.0142
Od02g03140	Red	Blue	1414.59	949.54	-0.575	0.0113
Od09g01140	Red	Blue	128.68	86.36	-0.575	0.0126
Od01g03810	Red	Blue	106.13	71.18	-0.576	0.0104
Od04g02180	Red	Blue	236.47	158.51	-0.577	0.0134
Od19g00340	Red	Blue	48.19	32.30	-0.577	0.0138
Od17g00900	Red	Blue	72.67	48.70	-0.577	0.0130
Od09g06000	Red	Blue	129.20	86.58	-0.577	0.0231
Od08g02290	Red	Blue	524.11	351.18	-0.578	0.0117
Od02g02140	Red	Blue	452.99	303.51	-0.578	0.0113
Od12g01860	Red	Blue	400.71	268.36	-0.578	0.0095
Od04g02890	Red	Blue	157.46	105.37	-0.580	0.0095
Od05g00710	Red	Blue	209.19	139.85	-0.581	0.0126
Od13g02090	Red	Blue	166.04	110.94	-0.582	0.0130
Od04g01340	Red	Blue	250.35	167.05	-0.584	0.0126
Od13g00240	Red	Blue	89.04	59.36	-0.585	0.0090
Od17g00300	Red	Blue	95.71	63.79	-0.585	0.0108
Od11g00950	Red	Blue	572.49	381.49	-0.586	0.0090
Od06g01660	Red	Blue	168.79	112.33	-0.588	0.0138
Od07g01730	Red	Blue	85.29	56.75	-0.588	0.0081
Od02g01760	Red	Blue	157.08	104.48	-0.588	0.0117
Od04g00210	Red	Blue	315.23	209.66	-0.588	0.0108
Od15g00300	Red	Blue	109.39	72.73	-0.589	0.0100
Od02g02180	Red	Blue	652.94	434.04	-0.589	0.0090
Od01g04550	Red	Blue	384.23	255.36	-0.589	0.0142
Od01g07060	Red	Blue	104.89	69.70	-0.590	0.0081
Od09g03910	Red	Blue	106.11	70.49	-0.590	0.0113
Od14g03300	Red	Blue	76.09	50.54	-0.590	0.0278
Od07g00750	Red	Blue	484.97	322.07	-0.591	0.0117
Od20g01100	Red	Blue	242.76	161.10	-0.592	0.0057
Od09g02200	Red	Blue	26.70	17.71	-0.592	0.0302
Od07g00730	Red	Blue	537.90	356.74	-0.592	0.0146
Od06g03270	Red	Blue	131.21	86.94	-0.594	0.0113
Od17g00170	Red	Blue	406.29	269.13	-0.594	0.0100
Od03g01170	Red	Blue	408.04	270.23	-0.595	0.0062
Od16g00600	Red	Blue	85.85	56.86	-0.595	0.0052
Od02g02590	Red	Blue	1057.35	699.77	-0.595	0.0126

Od02g02790	Red	Blue	810.04	536.09	-0.596	0.0100
Od05g01030	Red	Blue	38.82	25.69	-0.596	0.0297
Od03g02030	Red	Blue	166.35	110.06	-0.596	0.0086
Od02g03280	Red	Blue	754.83	499.19	-0.597	0.0081
Od11g00770	Red	Blue	64.72	42.79	-0.597	0.0108
Od13g01680	Red	Blue	457.74	302.61	-0.597	0.0076
Od01g06560	Red	Blue	331.27	218.98	-0.597	0.0081
Od02g02070	Red	Blue	679.78	449.30	-0.597	0.0126
Od04g03220	Red	Blue	384.34	253.96	-0.598	0.0076
Od01g05180	Red	Blue	86.02	56.82	-0.598	0.0122
Od19g00060	Red	Blue	108.01	71.26	-0.600	0.0076
Od09g05080	Red	Blue	371.98	245.30	-0.601	0.0067
Od10g02450	Red	Blue	1516.49	1000.01	-0.601	0.0057
Od01g06380	Red	Blue	165.01	108.72	-0.602	0.0076
Od13g01850	Red	Blue	342.22	225.46	-0.602	0.0062
Od14g01250	Red	Blue	1649.75	1086.66	-0.602	0.0071
Od01g04840	Red	Blue	59.23	38.99	-0.603	0.0150
Od02g02080	Red	Blue	975.01	641.57	-0.604	0.0434
Od18g00550	Red	Blue	419.17	275.79	-0.604	0.0086
Od06g01910	Red	Blue	108.88	71.59	-0.605	0.0095
Od07g04680	Red	Blue	111.04	72.97	-0.606	0.0062
Od18g00320	Red	Blue	74.10	48.68	-0.606	0.0046
Od09g01000	Red	Blue	111.88	73.49	-0.606	0.0052
Od12g03690	Red	Blue	25.17	16.53	-0.607	0.0192
Od02g01600	Red	Blue	279.69	183.46	-0.608	0.0122
Od02g01410	Red	Blue	1783.14	1168.66	-0.610	0.0062
Od09g05350	Red	Blue	116.01	75.85	-0.613	0.0086
Od16g01920	Red	Blue	158.79	103.80	-0.613	0.0352
Od06g01630	Red	Blue	267.84	175.08	-0.613	0.0071
Od11g00830	Red	Blue	126.46	82.57	-0.615	0.0052
Od18g00560	Red	Blue	396.66	258.93	-0.615	0.0046
Od02g02780	Red	Blue	639.61	417.10	-0.617	0.0071
Od02g02260	Red	Blue	489.92	319.33	-0.618	0.0062
Od04g02360	Red	Blue	68.63	44.73	-0.618	0.0100
Od02g02580	Red	Blue	1402.40	913.27	-0.619	0.0057
Od05g02290	Red	Blue	2987.00	1945.05	-0.619	0.0081
Od14g01100	Red	Blue	1824.04	1187.45	-0.619	0.0035
Od09g02650	Red	Blue	578.38	376.49	-0.619	0.0095
Od12g00820	Red	Blue	292.77	190.47	-0.620	0.0138
Od13g00610	Red	Blue	116.22	75.50	-0.622	0.0046
Od07g02050	Red	Blue	2440.97	1582.54	-0.625	0.0035
Od17g00190	Red	Blue	199.89	129.57	-0.625	0.0321
Od06g04520	Red	Blue	369.02	239.16	-0.626	0.0052

Od04g03290	Red	Blue	97.69	63.30	-0.626	0.0071
Od09g00460	Red	Blue	775.64	501.62	-0.629	0.0062
Od06g00910	Red	Blue	40.86	26.42	-0.629	0.0046
Od02g02570	Red	Blue	76.26	49.27	-0.630	0.0052
Od09g02190	Red	Blue	91.99	59.43	-0.630	0.0041
Od13g02920	Red	Blue	322.94	208.54	-0.631	0.0067
Od16g00350	Red	Blue	108.67	70.13	-0.632	0.0071
Od16g02100	Red	Blue	461.42	297.77	-0.632	0.0041
Od11g04210	Red	Blue	71.40	46.00	-0.634	0.0057
Od06g01110	Red	Blue	242.63	156.23	-0.635	0.0057
Od17g00080	Red	Blue	400.63	257.92	-0.635	0.0023
Od10g01620	Red	Blue	41.09	26.45	-0.636	0.0095
Od17g03070	Red	Blue	149.95	96.48	-0.636	0.0052
Od06g03580	Red	Blue	366.69	235.91	-0.636	0.0052
Od04g01940	Red	Blue	261.25	167.91	-0.638	0.0029
Od12g01370	Red	Blue	186.44	119.70	-0.639	0.0046
Od11g00860	Red	Blue	1311.56	841.76	-0.640	0.0009
Od12g01380	Red	Blue	119.06	76.36	-0.641	0.0046
Od09g05010	Red	Blue	599.99	384.40	-0.642	0.0086
Od20g02850	Red	Blue	245.39	157.17	-0.643	0.0071
Od16g00450	Red	Blue	392.15	251.08	-0.643	0.0052
Od20g00770	Red	Blue	1706.87	1092.55	-0.644	0.0046
Od18g00480	Red	Blue	97.98	62.71	-0.644	0.0071
Od02g02150	Red	Blue	762.22	487.68	-0.644	0.0052
Od11g04260	Red	Blue	70.95	45.38	-0.645	0.0016
Od12g01810	Red	Blue	269.54	172.26	-0.646	0.0035
Od03g02200	Red	Blue	227.33	145.13	-0.647	0.0041
Od02g00710	Red	Blue	144.66	92.33	-0.648	0.0262
Od01g02120	Red	Blue	682.25	434.87	-0.650	0.0016
Od07g01440	Red	Blue	92.86	59.11	-0.652	0.0035
Od01g03340	Red	Blue	182.80	116.26	-0.653	0.0029
Od14g00500	Red	Blue	224.76	142.95	-0.653	0.0009
Od02g02210	Red	Blue	997.36	634.25	-0.653	0.0041
Od05g01980	Red	Blue	1495.66	948.91	-0.656	0.0046
Od06g06190	Red	Blue	387.93	245.71	-0.659	0.0035
Od06g05840	Red	Blue	96.53	61.11	-0.660	0.0035
Od07g03350	Red	Blue	146.56	92.71	-0.661	0.0248
Od08g02040	Red	Blue	87.28	55.21	-0.661	0.0029
Od16g00770	Red	Blue	168.38	106.36	-0.663	0.0029
Od03g02230	Red	Blue	465.62	293.98	-0.663	0.0023
Od07g02800	Red	Blue	3597.08	2270.76	-0.664	0.0023
Od08g01560	Red	Blue	220.39	139.11	-0.664	0.0035
Od16g01280	Red	Blue	93.18	58.80	-0.664	0.0009

Od13g00880	Red	Blue	124.83	78.71	-0.665	0.0029
Od01g03660	Red	Blue	70.70	44.57	-0.666	0.0158
Od05g03380	Red	Blue	963.77	607.36	-0.666	0.0029
Od04g02530	Red	Blue	88.17	55.52	-0.667	0.0016
Od05g00310	Red	Blue	52.69	33.17	-0.668	0.0016
Od01g00610	Red	Blue	163.49	102.90	-0.668	0.0035
Od11g01930	Red	Blue	110.28	69.39	-0.668	0.0009
Od04g05010	Red	Blue	635.60	399.90	-0.668	0.0035
Od02g04020	Red	Blue	585.87	368.44	-0.669	0.0016
Od17g02960	Red	Blue	128.29	80.64	-0.670	0.0035
Od16g02240	Red	Blue	470.08	295.40	-0.670	0.0035
Od01g00950	Red	Blue	162.60	102.14	-0.671	0.0399
Od01g06190	Red	Blue	1539.26	966.45	-0.671	0.0016
Od11g00940	Red	Blue	138.66	87.00	-0.672	0.0041
Od06g01610	Red	Blue	509.81	319.80	-0.673	0.0023
Od12g00670	Red	Blue	210.32	131.60	-0.676	0.0009
Od18g00500	Red	Blue	278.45	174.00	-0.678	0.0035
Od17g00580	Red	Blue	484.03	302.45	-0.678	0.0009
Od01g05190	Red	Blue	106.84	66.73	-0.679	0.0041
Od17g00860	Red	Blue	57.97	36.19	-0.680	0.0312
Od07g02790	Red	Blue	2257.59	1409.09	-0.680	0.0016
Od04g02270	Red	Blue	102.12	63.70	-0.681	0.0041
Od02g02020	Red	Blue	760.30	473.94	-0.682	0.0023
Od02g02880	Red	Blue	1174.33	731.87	-0.682	0.0016
Od20g03120	Red	Blue	83.61	52.06	-0.684	0.0016
Od01g04990	Red	Blue	197.07	122.64	-0.684	0.0035
Od10g00860	Red	Blue	656.49	408.41	-0.685	0.0016
Od04g00730	Red	Blue	81.98	50.98	-0.685	0.0009
Od06g01000	Red	Blue	936.31	582.13	-0.686	0.0029
Od14g02540	Red	Blue	378.08	234.89	-0.687	0.0016
Od18g00540	Red	Blue	452.03	280.78	-0.687	0.0016
Od18g00410	Red	Blue	132.14	81.92	-0.690	0.0016
Od01g01210	Red	Blue	141.61	87.66	-0.692	0.0016
Od16g01250	Red	Blue	58.31	36.03	-0.695	0.0023
Od02g01840	Red	Blue	690.04	426.12	-0.695	0.0023
Od01g07070	Red	Blue	10.06	6.21	-0.696	0.0095
Od07g04250	Red	Blue	269.14	165.89	-0.698	0.0009
Od13g01420	Red	Blue	22.48	13.85	-0.698	0.0341
Od12g01710	Red	Blue	893.13	550.21	-0.699	0.0009
Od06g04800	Red	Blue	593.88	365.84	-0.699	0.0035
Od11g02470	Red	Blue	29351.30	18077.70	-0.699	0.0052
Od17g03100	Red	Blue	113.22	69.72	-0.699	0.0009
Od13g02810	Red	Blue	118.49	72.94	-0.700	0.0016

Od09g02790	Red	Blue	1036.15	636.72	-0.702	0.0009
Od18g00370	Red	Blue	179.55	110.31	-0.703	0.0009
Od01g07080	Red	Blue	10.10	6.19	-0.705	0.0035
Od12g03120	Red	Blue	303.08	185.86	-0.705	0.0016
Od01g00820	Red	Blue	260.92	159.85	-0.707	0.0016
Od03g03050	Red	Blue	262.15	160.51	-0.708	0.0154
Od02g00530	Red	Blue	95.43	58.42	-0.708	0.0090
Od20g02410	Red	Blue	211.66	129.53	-0.708	0.0029
Od07g02830	Red	Blue	181.31	110.96	-0.708	0.0009
Od14g02610	Red	Blue	144.84	88.35	-0.713	0.0009
Od06g03120	Red	Blue	646.41	394.31	-0.713	0.0009
Od04g00700	Red	Blue	1571.67	958.32	-0.714	0.0029
Od16g00500	Red	Blue	144.29	87.91	-0.715	0.0009
Od18g00290	Red	Blue	232.26	141.46	-0.715	0.0016
Od17g02080	Red	Blue	249.93	151.98	-0.718	0.0009
Od14g01920	Red	Blue	86.21	52.37	-0.719	0.0009
Od04g05170	Red	Blue	26.85	16.29	-0.721	0.0174
Od06g04460	Red	Blue	198.20	120.02	-0.724	0.0009
Od10g01610	Red	Blue	16.88	10.22	-0.724	0.0449
Od06g04660	Red	Blue	896.54	541.93	-0.726	0.0009
Od02g01730	Red	Blue	664.13	401.25	-0.727	0.0009
Od07g02700	Red	Blue	83.74	50.56	-0.728	0.0009
Od04g00720	Red	Blue	279.64	168.45	-0.731	0.0009
Od08g03020	Red	Blue	170.12	102.41	-0.732	0.0009
Od19g00660	Red	Blue	172.54	103.69	-0.735	0.0081
Od09g00180	Red	Blue	793.20	475.47	-0.738	0.0023
Od18g00520	Red	Blue	492.57	295.24	-0.738	0.0009
Od02g03380	Red	Blue	303.07	181.51	-0.740	0.0009
Od13g01670	Red	Blue	258.88	154.94	-0.741	0.0009
Od09g04020	Red	Blue	26.26	15.71	-0.741	0.0016
Od07g00770	Red	Blue	199.33	119.21	-0.742	0.0016
Od13g02380	Red	Blue	842.60	503.45	-0.743	0.0009
Od09g05360	Red	Blue	319.15	190.64	-0.743	0.0009
Od16g01860	Red	Blue	153.06	91.32	-0.745	0.0016
Od17g00890	Red	Blue	133.93	79.87	-0.746	0.0349
Od17g00910	Red	Blue	336.20	200.42	-0.746	0.0009
Od16g02230	Red	Blue	107.76	64.23	-0.746	0.0016
Od18g00340	Red	Blue	399.21	237.93	-0.747	0.0016
Od17g00180	Red	Blue	476.90	283.74	-0.749	0.0016
Od17g00310	Red	Blue	3341.79	1981.37	-0.754	0.0009
Od06g00990	Red	Blue	206.14	122.22	-0.754	0.0009
Od06g04680	Red	Blue	663.95	393.27	-0.756	0.0009
Od20g00760	Red	Blue	112.52	66.60	-0.757	0.0009

Od12g03300	Red	Blue	273.41	161.83	-0.757	0.0009
Od10g00870	Red	Blue	418.74	247.73	-0.757	0.0009
Od04g02910	Red	Blue	213.58	126.22	-0.759	0.0009
Od05g01900	Red	Blue	80.51	47.50	-0.761	0.0009
Od04g01170	Red	Blue	1696.85	1000.93	-0.762	0.0009
Od09g05690	Red	Blue	655.53	386.64	-0.762	0.0009
Od18g00380	Red	Blue	94.93	55.95	-0.763	0.0009
Od18g00250	Red	Blue	96.95	57.10	-0.764	0.0067
Od05g01720	Red	Blue	579.63	340.67	-0.767	0.0009
Od02g03500	Red	Blue	41.89	24.62	-0.767	0.0041
Od05g00680	Red	Blue	91.01	53.44	-0.768	0.0009
Od09g03890	Red	Blue	4693.28	2752.29	-0.770	0.0009
Od18g00460	Red	Blue	530.21	310.82	-0.771	0.0009
Od16g01820	Red	Blue	94.45	55.30	-0.772	0.0009
Od16g02630	Red	Blue	455.85	266.88	-0.772	0.0009
Od08g00380	Red	Blue	56.37	33.00	-0.773	0.0009
Od04g02610	Red	Blue	177.26	103.71	-0.773	0.0009
Od07g02870	Red	Blue	4693.93	2743.96	-0.775	0.0009
Od17g01460	Red	Blue	464.88	271.71	-0.775	0.0009
Od02g02800	Red	Blue	318.54	185.95	-0.777	0.0009
Od04g05330	Red	Blue	107.06	62.46	-0.778	0.0009
Od04g01950	Red	Blue	146.03	85.18	-0.778	0.0009
Od02g02090	Red	Blue	1546.40	901.00	-0.779	0.0009
Od13g02780	Red	Blue	300.80	175.17	-0.780	0.0009
Od04g02820	Red	Blue	5868.24	3417.15	-0.780	0.0009
Od05g04700	Red	Blue	497.24	289.44	-0.781	0.0009
Od07g00800	Red	Blue	1842.03	1071.54	-0.782	0.0009
Od10g02140	Red	Blue	44.00	25.58	-0.782	0.0355
Od02g02890	Red	Blue	342.91	199.21	-0.784	0.0009
Od07g04640	Red	Blue	262.39	152.12	-0.786	0.0009
Od08g01520	Red	Blue	128.61	74.29	-0.792	0.0009
Od01g04720	Red	Blue	83.54	48.15	-0.795	0.0162
Od04g05270	Red	Blue	22.66	13.06	-0.795	0.0009
Od01g03440	Red	Blue	381.88	219.64	-0.798	0.0009
Od19g00640	Red	Blue	332.83	191.30	-0.799	0.0009
Od14g02210	Red	Blue	274.97	157.85	-0.801	0.0009
Od04g01470	Red	Blue	221.58	127.10	-0.802	0.0009
Od02g01720	Red	Blue	792.60	454.19	-0.803	0.0009
Od14g01880	Red	Blue	1057.79	605.77	-0.804	0.0009
Od06g03250	Red	Blue	667.97	382.02	-0.806	0.0009
Od09g03050	Red	Blue	173.30	99.09	-0.806	0.0009
Od07g01750	Red	Blue	1115.00	637.46	-0.807	0.0009
Od18g00310	Red	Blue	92.78	52.95	-0.809	0.0009

Od07g02380	Red	Blue	1352.88	770.66	-0.812	0.0009
Od01g01080	Red	Blue	119.06	67.79	-0.813	0.0009
Od17g03090	Red	Blue	215.58	122.68	-0.813	0.0009
Od07g02100	Red	Blue	299.54	170.26	-0.815	0.0009
Od02g04110	Red	Blue	93.84	53.33	-0.815	0.0009
Od17g00960	Red	Blue	15.92	9.04	-0.816	0.0062
Od06g07510	Red	Blue	67.10	38.13	-0.816	0.0009
Od01g04970	Red	Blue	232.61	132.10	-0.816	0.0009
Od02g02250	Red	Blue	1040.67	590.97	-0.816	0.0009
Od18g00300	Red	Blue	291.32	165.28	-0.818	0.0009
Od10g01780	Red	Blue	286.30	161.97	-0.822	0.0009
Od07g03510	Red	Blue	185.59	104.99	-0.822	0.0009
Od07g03830	Red	Blue	1440.65	813.82	-0.824	0.0009
Od01g03450	Red	Blue	911.41	513.31	-0.828	0.0009
Od01g00700	Red	Blue	405.37	228.05	-0.830	0.0009
Od07g00900	Red	Blue	245.54	138.12	-0.830	0.0009
Od09g00820	Red	Blue	334.01	187.87	-0.830	0.0009
Od13g00890	Red	Blue	145.27	81.66	-0.831	0.0009
Od06g06110	Red	Blue	169.88	95.43	-0.832	0.0009
Od06g04670	Red	Blue	525.66	294.38	-0.836	0.0071
Od19g00250	Red	Blue	54.87	30.71	-0.838	0.0009
Od06g04530	Red	Blue	721.77	403.47	-0.839	0.0009
Od06g01290	Red	Blue	352.25	196.86	-0.839	0.0009
Od17g01920	Red	Blue	192.54	107.55	-0.840	0.0009
Od13g03190	Red	Blue	386.08	215.56	-0.841	0.0009
Od05g00580	Red	Blue	400.60	223.42	-0.842	0.0009
Od02g01610	Red	Blue	1157.59	644.78	-0.844	0.0009
Od09g03710	Red	Blue	170.03	94.69	-0.845	0.0009
Od04g00660	Red	Blue	279.37	155.40	-0.846	0.0009
Od07g03190	Red	Blue	796.20	442.59	-0.847	0.0009
Od09g05650	Red	Blue	5783.72	3213.13	-0.848	0.0009
Od01g00710	Red	Blue	307.39	170.65	-0.849	0.0009
Od05g01350	Red	Blue	1039.70	576.78	-0.850	0.0009
Od14g03280	Red	Blue	662.40	367.29	-0.851	0.0009
Od16g02550	Red	Blue	702.75	389.02	-0.853	0.0009
Od02g03960	Red	Blue	12605.00	6969.13	-0.855	0.0009
Od03g01290	Red	Blue	112.31	61.93	-0.859	0.0009
Od06g04580	Red	Blue	448.20	247.16	-0.859	0.0009
Od09g03380	Red	Blue	213.95	117.83	-0.861	0.0009
Od12g02660	Red	Blue	346.07	190.38	-0.862	0.0126
Od07g01970	Red	Blue	440.71	242.39	-0.863	0.0009
Od11g00900	Red	Blue	62.95	34.61	-0.863	0.0009
Od01g03700	Red	Blue	1964.80	1079.64	-0.864	0.0009

Od07g04200	Red	Blue	751.08	412.52	-0.865	0.0009
Od05g03740	Red	Blue	223.40	122.67	-0.865	0.0009
Od05g01280	Red	Blue	164.45	90.21	-0.866	0.0009
Od01g06140	Red	Blue	62.60	34.25	-0.870	0.0009
Od13g01760	Red	Blue	181.59	99.14	-0.873	0.0009
Od19g01200	Red	Blue	634.74	346.33	-0.874	0.0009
Od03g01260	Red	Blue	763.28	415.88	-0.876	0.0009
Od03g02370	Red	Blue	40.58	22.10	-0.877	0.0009
Od14g02280	Red	Blue	208.57	113.49	-0.878	0.0009
Od07g03790	Red	Blue	68.94	37.40	-0.882	0.0009
Od10g02230	Red	Blue	1544.53	837.40	-0.883	0.0009
Od03g01080	Red	Blue	1247.98	676.18	-0.884	0.0009
Od12g00970	Red	Blue	257.56	139.52	-0.884	0.0067
Od10g02420	Red	Blue	2.92	1.58	-0.885	0.0428
Od04g05340	Red	Blue	320.30	173.17	-0.887	0.0009
Od16g00750	Red	Blue	301.09	162.40	-0.891	0.0009
Od20g00610	Red	Blue	634.23	341.73	-0.892	0.0009
Od17g02560	Red	Blue	12286.00	6619.11	-0.892	0.0009
Od17g00340	Red	Blue	45.06	24.26	-0.893	0.0009
Od10g01180	Red	Blue	318.02	171.13	-0.894	0.0009
Od01g03200	Red	Blue	1640.86	882.72	-0.894	0.0009
Od06g03260	Red	Blue	115.68	62.22	-0.895	0.0009
Od01g05480	Red	Blue	772.91	415.22	-0.896	0.0009
Od17g01930	Red	Blue	149.34	80.22	-0.897	0.0009
Od06g06100	Red	Blue	218.66	117.38	-0.898	0.0009
Od13g00740	Red	Blue	124.50	66.76	-0.899	0.0009
Od01g00600	Red	Blue	152.75	81.79	-0.901	0.0009
Od11g04000	Red	Blue	106.65	57.09	-0.901	0.0009
Od05g03760	Red	Blue	7.34	3.93	-0.904	0.0436
Od18g00470	Red	Blue	358.09	191.11	-0.906	0.0009
Od08g01380	Red	Blue	311.92	166.25	-0.908	0.0023
Od11g02010	Red	Blue	49.92	26.57	-0.910	0.0009
Od16g01370	Red	Blue	1271.39	675.69	-0.912	0.0009
Od11g00560	Red	Blue	19.32	10.27	-0.912	0.0009
Od09g03480	Red	Blue	65.51	34.81	-0.912	0.0009
Od02g03840	Red	Blue	14.17	7.53	-0.913	0.0180
Od01g02970	Red	Blue	1318.84	696.97	-0.920	0.0009
Od07g00560	Red	Blue	185.95	98.15	-0.922	0.0009
Od06g06880	Red	Blue	433.53	228.43	-0.924	0.0009
Od16g02700	Red	Blue	315.94	166.36	-0.925	0.0009
Od17g02000	Red	Blue	66.16	34.77	-0.928	0.0009
Od20g00600	Red	Blue	119.74	62.93	-0.928	0.0009
Od06g03820	Red	Blue	152.76	80.24	-0.929	0.0009

Od17g02010	Red	Blue	42.29	22.20	-0.930	0.0035
Od16g02690	Red	Blue	153.46	80.48	-0.931	0.0009
Od08g01130	Red	Blue	780.27	408.02	-0.935	0.0009
Od12g01760	Red	Blue	207.63	108.27	-0.939	0.0009
Od03g02360	Red	Blue	84.75	44.18	-0.940	0.0009
Od14g02240	Red	Blue	166.87	86.92	-0.941	0.0009
Od09g04780	Red	Blue	169.44	88.07	-0.944	0.0009
Od06g04640	Red	Blue	294.76	152.86	-0.947	0.0009
Od02g01640	Red	Blue	469.08	243.04	-0.949	0.0009
Od02g01370	Red	Blue	807.98	418.09	-0.951	0.0009
Od09g04760	Red	Blue	92.46	47.84	-0.951	0.0009
Od10g00160	Red	Blue	3017.20	1557.70	-0.954	0.0009
Od07g03480	Red	Blue	105.38	54.15	-0.961	0.0009
Od13g00750	Red	Blue	275.51	141.50	-0.961	0.0009
Od05g04230	Red	Blue	367.63	188.66	-0.962	0.0009
Od04g00340	Red	Blue	96.55	49.44	-0.966	0.0009
Od04g00140	Red	Blue	174.10	89.15	-0.966	0.0009
Od10g01790	Red	Blue	182.59	93.25	-0.969	0.0009
Od07g04840	Red	Blue	128.25	65.47	-0.970	0.0009
Od13g03030	Red	Blue	28601.40	14566.70	-0.973	0.0009
Od01g00910	Red	Blue	160.87	81.87	-0.974	0.0009
Od14g02230	Red	Blue	250.71	127.47	-0.976	0.0009
Od05g03200	Red	Blue	107.71	54.76	-0.976	0.0009
Od10g00670	Red	Blue	23.55	11.96	-0.978	0.0090
Od13g00950	Red	Blue	224.81	113.62	-0.985	0.0009
Od01g05230	Red	Blue	515.47	259.80	-0.989	0.0009
Od09g01770	Red	Blue	477.43	240.56	-0.989	0.0009
Od05g04710	Red	Blue	245.20	123.37	-0.991	0.0071
Od07g00470	Red	Blue	139.71	70.12	-0.994	0.0009
Od01g03260	Red	Blue	993.06	496.78	-0.999	0.0009
Od01g05730	Red	Blue	371.33	185.70	-1.000	0.0009
Od05g01370	Red	Blue	188.61	94.28	-1.000	0.0009
Od20g02980	Red	Blue	515.34	257.14	-1.003	0.0009
Od12g02640	Red	Blue	509.17	253.56	-1.006	0.0009
Od17g01480	Red	Blue	551.68	274.71	-1.006	0.0009
Od15g00140	Red	Blue	37.43	18.63	-1.007	0.0009
Od05g02490	Red	Blue	115.07	57.16	-1.009	0.0009
Od06g03340	Red	Blue	66.92	33.16	-1.013	0.0009
Od05g00590	Red	Blue	445.42	219.98	-1.018	0.0009
Od03g00560	Red	Blue	66.60	32.88	-1.018	0.0009
Od09g06250	Red	Blue	198.91	97.91	-1.023	0.0009
Od02g03030	Red	Blue	1390.45	680.41	-1.031	0.0009
Od07g00130	Red	Blue	236.82	115.57	-1.035	0.0009

Od01g03210	Red	Blue	942.51	459.69	-1.036	0.0009
Od05g01890	Red	Blue	89.50	43.48	-1.042	0.0009
Od04g00980	Red	Blue	41.68	20.21	-1.044	0.0009
Od07g04230	Red	Blue	972.57	471.40	-1.045	0.0009
Od07g03230	Red	Blue	743.17	359.62	-1.047	0.0009
Od04g02510	Red	Blue	887.45	429.39	-1.047	0.0009
Od11g02450	Red	Blue	339.53	163.65	-1.053	0.0009
Od05g01780	Red	Blue	149.57	71.94	-1.056	0.0009
Od03g02310	Red	Blue	2076.81	996.25	-1.060	0.0009
Od05g04650	Red	Blue	141.50	67.81	-1.061	0.0009
Od20g02470	Red	Blue	206.88	99.13	-1.061	0.0009
Od07g04720	Red	Blue	1294.55	619.31	-1.064	0.0009
Od05g05120	Red	Blue	451.72	215.64	-1.067	0.0009
Od09g03950	Red	Blue	33.12	15.80	-1.068	0.0009
Od02g00080	Red	Blue	348.64	166.22	-1.069	0.0009
Od19g00040	Red	Blue	479.73	228.70	-1.069	0.0009
Od15g01050	Red	Blue	67.18	32.00	-1.070	0.0009
Od02g00070	Red	Blue	518.45	246.80	-1.071	0.0009
Od02g02950	Red	Blue	1869.11	889.58	-1.071	0.0009
Od08g00340	Red	Blue	272.88	129.82	-1.072	0.0009
Od16g02600	Red	Blue	151.98	71.97	-1.078	0.0009
Od06g02270	Red	Blue	209.75	99.28	-1.079	0.0009
Od04g00330	Red	Blue	1305.68	617.73	-1.080	0.0009
Od11g04110	Red	Blue	1048.64	495.11	-1.083	0.0009
Od11g00960	Red	Blue	126.99	59.60	-1.091	0.0009
Od10g02270	Red	Blue	554.60	259.68	-1.095	0.0009
Od20g01770	Red	Blue	192.20	89.98	-1.095	0.0009
Od04g00460	Red	Blue	1426.23	667.53	-1.095	0.0009
Od07g03780	Red	Blue	52.39	24.46	-1.099	0.0009
Od03g02850	Red	Blue	649.95	303.32	-1.099	0.0009
Od07g00140	Red	Blue	1396.39	650.80	-1.101	0.0009
Od03g01710	Red	Blue	2106.96	980.68	-1.103	0.0009
Od10g01350	Red	Blue	1098.33	509.40	-1.108	0.0009
Od09g04790	Red	Blue	1800.89	833.19	-1.112	0.0009
Od06g03790	Red	Blue	30.80	14.22	-1.115	0.0009
Od06g04450	Red	Blue	2207.09	1015.90	-1.119	0.0009
Od12g01770	Red	Blue	1271.58	584.90	-1.120	0.0009
Od06g00660	Red	Blue	596.88	273.18	-1.128	0.0009
Od09g02460	Red	Blue	179.17	82.00	-1.128	0.0009
Od10g01360	Red	Blue	642.83	293.82	-1.130	0.0009
Od17g01990	Red	Blue	1059.45	484.18	-1.130	0.0009
Od17g03170	Red	Blue	3.39	1.55	-1.132	0.0104
Od05g02660	Red	Blue	295.62	134.77	-1.133	0.0009

Od09g04310	Red	Blue	56.58	25.75	-1.136	0.0009
Od18g00260	Red	Blue	65.15	29.60	-1.138	0.0009
Od12g02670	Red	Blue	208.01	94.42	-1.139	0.0009
Od15g00560	Red	Blue	2030.10	920.92	-1.140	0.0009
Od06g03440	Red	Blue	103.43	46.87	-1.142	0.0009
Od12g01140	Red	Blue	329.09	146.90	-1.164	0.0009
Od14g00760	Red	Blue	157.96	70.45	-1.165	0.0009
Od02g00490	Red	Blue	5.39	2.39	-1.173	0.0146
Od04g01630	Red	Blue	4541.32	2009.66	-1.176	0.0009
Od04g02810	Red	Blue	826.50	365.63	-1.177	0.0009
Od14g01500	Red	Blue	1068.06	468.97	-1.187	0.0009
Od06g03170	Red	Blue	145.62	63.90	-1.188	0.0009
Od06g00580	Red	Blue	687.09	301.47	-1.189	0.0009
Od05g03520	Red	Blue	728.45	317.64	-1.197	0.0009
Od07g03760	Red	Blue	224.77	97.94	-1.198	0.0009
Od07g03240	Red	Blue	350.83	152.51	-1.202	0.0009
Od19g00430	Red	Blue	246.43	106.84	-1.206	0.0009
Od01g04650	Red	Blue	504.83	218.52	-1.208	0.0009
Od02g03130	Red	Blue	170.05	73.30	-1.214	0.0009
Od07g01230	Red	Blue	797.46	340.32	-1.229	0.0009
Od18g00270	Red	Blue	50.75	21.58	-1.234	0.0009
Od13g03160	Red	Blue	1908.71	804.84	-1.246	0.0009
Od09g06240	Red	Blue	2862.66	1198.81	-1.256	0.0009
Od08g02950	Red	Blue	225.63	94.20	-1.260	0.0009
Od07g00720	Red	Blue	834.34	348.20	-1.261	0.0009
Od07g04740	Red	Blue	90.80	37.73	-1.267	0.0009
Od14g02940	Red	Blue	78.19	32.45	-1.269	0.0009
Od03g01850	Red	Blue	6764.68	2793.03	-1.276	0.0009
Od14g01690	Red	Blue	125.70	51.69	-1.282	0.0009
Od05g02670	Red	Blue	208.94	85.81	-1.284	0.0009
Od14g00300	Red	Blue	28.39	11.58	-1.294	0.0009
Od08g02490	Red	Blue	11513.90	4671.92	-1.301	0.0009
Od10g01170	Red	Blue	350.23	140.36	-1.319	0.0009
Od06g04490	Red	Blue	25.39	10.15	-1.323	0.0009
Od01g03140	Red	Blue	267.94	106.93	-1.325	0.0009
Od06g06980	Red	Blue	947.23	377.59	-1.327	0.0009
Od08g01040	Red	Blue	374.97	149.23	-1.329	0.0009
Od17g01680	Red	Blue	262.59	104.36	-1.331	0.0009
Od16g02340	Red	Blue	245.19	97.15	-1.336	0.0009
Od07g01310	Red	Blue	4947.18	1917.42	-1.367	0.0009
Od09g02470	Red	Blue	162.83	62.07	-1.391	0.0009
Od04g01620	Red	Blue	554.36	210.19	-1.399	0.0009
Od04g01800	Red	Blue	266.86	101.02	-1.401	0.0009

Od07g03920	Red	Blue	61.26	23.12	-1.406	0.0009
Od20g02710	Red	Blue	7.17	2.70	-1.408	0.0192
Od02g02960	Red	Blue	4170.56	1565.03	-1.414	0.0434
Od05g04740	Red	Blue	130.68	48.81	-1.421	0.0009
Od07g03670	Red	Blue	104.20	38.77	-1.426	0.0009
Od07g03910	Red	Blue	32.09	11.70	-1.455	0.0009
Od11g00840	Red	Blue	101.03	36.66	-1.463	0.0009
Od04g01770	Red	Blue	1265.62	456.98	-1.470	0.0009
Od01g02410	Red	Blue	6268.90	2250.20	-1.478	0.0009
Od08g01810	Red	Blue	369.95	132.20	-1.485	0.0009
Od06g07490	Red	Blue	270.21	96.40	-1.487	0.0009
Od17g01690	Red	Blue	271.45	96.63	-1.490	0.0009
Od01g01020	Red	Blue	464.96	164.12	-1.502	0.0009
Od13g00450	Red	Blue	2.90	1.01	-1.516	0.0487
Od02g02530	Red	Blue	1246.44	433.22	-1.525	0.0009
Od08g03150	Red	Blue	108.09	37.41	-1.531	0.0009
Od08g03040	Red	Blue	885.41	295.69	-1.582	0.0009
Od04g03820	Red	Blue	75.42	25.09	-1.588	0.0009
Od16g01420	Red	Blue	879.75	288.06	-1.611	0.0009
Od06g01010	Red	Blue	192.86	61.52	-1.648	0.0009
Od10g01560	Red	Blue	82.06	26.16	-1.649	0.0009
Od04g03730	Red	Blue	5310.22	1653.93	-1.683	0.0009
Od06g03610	Red	Blue	916.63	262.24	-1.805	0.0009
Od12g00050	Red	Blue	216.28	44.37	-2.285	0.0009
Od11g01480	Red	Blue	73.00	14.31	-2.350	0.0009
Od10g01940	Blue	Green	3.46	0.00	3.461	0.0265
Od06g07490	Blue	Green	96.40	431.08	2.161	0.0009
Od06g03610	Blue	Green	262.24	1162.35	2.148	0.0009
Od20g01770	Blue	Green	89.98	347.84	1.951	0.0009
Od11g01480	Blue	Green	14.31	52.12	1.865	0.0009
Od07g03670	Blue	Green	38.77	136.71	1.818	0.0009
Od17g00960	Blue	Green	9.04	30.72	1.764	0.0009
Od06g01010	Blue	Green	61.52	208.58	1.761	0.0009
Od06g07500	Blue	Green	9.88	32.86	1.733	0.0016
Od12g01140	Blue	Green	146.90	467.43	1.670	0.0009
Od10g01560	Blue	Green	26.16	82.81	1.662	0.0009
Od16g01420	Blue	Green	288.06	858.17	1.575	0.0009
Od09g06240	Blue	Green	1198.81	3522.72	1.555	0.0009
Od02g02960	Blue	Green	1565.03	4551.56	1.540	0.0076
Od01g01020	Blue	Green	164.12	473.59	1.529	0.0009
Od17g03170	Blue	Green	1.55	4.39	1.505	0.0009
Od04g03820	Blue	Green	25.09	70.53	1.491	0.0009
Od18g00260	Blue	Green	29.60	81.67	1.464	0.0009

Od13g00740	Blue	Green	66.76	183.69	1.460	0.0009
Od04g01770	Blue	Green	456.98	1251.31	1.453	0.0009
Od10g01360	Blue	Green	293.82	800.27	1.446	0.0009
Od06g03250	Blue	Green	382.02	1010.57	1.403	0.0009
Od03g02370	Blue	Green	22.10	58.11	1.395	0.0009
Od09g06250	Blue	Green	97.91	256.25	1.388	0.0009
Od17g01690	Blue	Green	96.63	252.34	1.385	0.0029
Od04g03730	Blue	Green	1653.93	4255.26	1.363	0.0009
Od05g03520	Blue	Green	317.64	817.03	1.363	0.0009
Od12g02660	Blue	Green	190.38	486.08	1.352	0.0009
Od07g01310	Blue	Green	1917.42	4869.77	1.345	0.0009
Od17g01680	Blue	Green	104.36	264.54	1.342	0.0009
Od10g01170	Blue	Green	140.36	354.40	1.336	0.0009
Od02g02530	Blue	Green	433.22	1089.88	1.331	0.0009
Od02g00080	Blue	Green	166.22	418.04	1.331	0.0009
Od04g00140	Blue	Green	89.15	223.99	1.329	0.0009
Od11g02450	Blue	Green	163.65	409.93	1.325	0.0009
Od01g06140	Blue	Green	34.25	84.72	1.307	0.0009
Od16g02550	Blue	Green	389.02	961.87	1.306	0.0009
Od01g02410	Blue	Green	2250.20	5548.05	1.302	0.0009
Od04g01800	Blue	Green	101.02	248.92	1.301	0.0009
Od10g00370	Blue	Green	22.34	55.05	1.301	0.0009
Od04g01630	Blue	Green	2009.66	4905.33	1.287	0.0009
Od16g02690	Blue	Green	80.48	196.25	1.286	0.0009
Od16g01370	Blue	Green	675.69	1646.60	1.285	0.0009
Od07g04840	Blue	Green	65.47	159.38	1.284	0.0009
Od09g02220	Blue	Green	477.88	1160.78	1.280	0.0009
Od13g03160	Blue	Green	804.84	1941.03	1.270	0.0009
Od03g01850	Blue	Green	2793.03	6716.65	1.266	0.0009
Od07g03910	Blue	Green	11.70	28.11	1.264	0.0009
Od14g01420	Blue	Green	63.45	152.29	1.263	0.0009
Od06g04670	Blue	Green	294.38	705.01	1.260	0.0009
Od06g05880	Blue	Green	63.19	150.23	1.249	0.0375
Od14g01690	Blue	Green	51.69	122.51	1.245	0.0009
Od15g00560	Blue	Green	920.92	2178.44	1.242	0.0009
Od08g01040	Blue	Green	149.23	352.42	1.240	0.0009
Od20g02470	Blue	Green	99.13	233.45	1.236	0.0009
Od18g00270	Blue	Green	21.58	50.80	1.235	0.0009
Od10g02270	Blue	Green	259.68	605.92	1.222	0.0009
Od09g02460	Blue	Green	82.00	189.97	1.212	0.0009
Od04g01620	Blue	Green	210.19	485.65	1.208	0.0009
Od05g04740	Blue	Green	48.81	112.38	1.203	0.0009
Od08g03150	Blue	Green	37.41	86.09	1.202	0.0009

Od08g01380	Blue	Green	166.25	378.95	1.189	0.0009
Od14g02210	Blue	Green	157.85	359.18	1.186	0.0009
Od08g02490	Blue	Green	4671.92	10595.20	1.181	0.0009
Od10g02140	Blue	Green	25.58	57.89	1.178	0.0009
Od10g01350	Blue	Green	509.40	1149.63	1.174	0.0009
Od05g01370	Blue	Green	94.28	212.56	1.173	0.0009
Od08g02950	Blue	Green	94.20	211.80	1.169	0.0009
Od12g00810	Blue	Green	340.21	763.53	1.166	0.0287
Od19g00430	Blue	Green	106.84	239.70	1.166	0.0009
Od11g00840	Blue	Green	36.66	82.19	1.165	0.0009
Od06g04460	Blue	Green	120.02	268.50	1.162	0.0009
Od19g00640	Blue	Green	191.30	426.98	1.158	0.0009
Od06g04580	Blue	Green	247.16	549.40	1.152	0.0009
Od01g02970	Blue	Green	696.97	1547.64	1.151	0.0009
Od01g04650	Blue	Green	218.52	484.00	1.147	0.0009
Od07g03510	Blue	Green	104.99	232.53	1.147	0.0009
Od04g04150	Blue	Green	53.78	119.03	1.146	0.0417
Od03g02310	Blue	Green	996.25	2202.38	1.144	0.0009
Od09g04790	Blue	Green	833.19	1840.87	1.144	0.0009
Od09g02470	Blue	Green	62.07	136.98	1.142	0.0009
Od05g02670	Blue	Green	85.81	188.97	1.139	0.0009
Od05g00590	Blue	Green	219.98	483.98	1.138	0.0009
Od13g00750	Blue	Green	141.50	311.32	1.138	0.0009
Od01g00600	Blue	Green	81.79	179.91	1.137	0.0009
Od09g04020	Blue	Green	15.71	34.53	1.136	0.0009
Od03g03050	Blue	Green	160.51	350.83	1.128	0.0009
Od07g03790	Blue	Green	37.40	81.12	1.117	0.0009
Od13g00950	Blue	Green	113.62	246.28	1.116	0.0009
Od07g03920	Blue	Green	23.12	49.87	1.109	0.0009
Od01g05730	Blue	Green	185.70	400.40	1.108	0.0009
Od18g00250	Blue	Green	57.10	122.67	1.103	0.0009
Od01g00710	Blue	Green	170.65	366.52	1.103	0.0009
Od07g03480	Blue	Green	54.15	116.28	1.103	0.0009
Od15g00340	Blue	Green	127.84	273.90	1.099	0.0009
Od06g06980	Blue	Green	377.59	806.65	1.095	0.0009
Od06g03790	Blue	Green	14.22	30.30	1.091	0.0009
Od02g01180	Blue	Green	39.74	84.62	1.090	0.0423
Od06g04800	Blue	Green	365.84	776.61	1.086	0.0009
Od07g01230	Blue	Green	340.32	721.22	1.084	0.0009
Od17g00340	Blue	Green	24.26	51.39	1.083	0.0009
Od04g00340	Blue	Green	49.44	104.64	1.082	0.0009
Od06g04450	Blue	Green	1015.90	2149.42	1.081	0.0009
Od05g01890	Blue	Green	43.48	91.81	1.078	0.0009

Od07g00470	Blue	Green	70.12	148.06	1.078	0.0009
Od01g03210	Blue	Green	459.69	964.52	1.069	0.0009
Od04g02910	Blue	Green	126.22	264.64	1.068	0.0009
Od07g04230	Blue	Green	471.40	987.48	1.067	0.0009
Od10g01790	Blue	Green	93.25	195.00	1.064	0.0009
Od12g00050	Blue	Green	44.37	92.66	1.062	0.0009
Od01g03260	Blue	Green	496.78	1034.77	1.059	0.0009
Od14g00760	Blue	Green	70.45	146.54	1.057	0.0009
Od04g02510	Blue	Green	429.39	893.21	1.057	0.0009
Od07g02830	Blue	Green	110.96	230.62	1.056	0.0009
Od13g01760	Blue	Green	99.14	205.87	1.054	0.0009
Od01g05230	Blue	Green	259.80	539.31	1.054	0.0009
Od07g03230	Blue	Green	359.62	745.60	1.052	0.0009
Od05g05120	Blue	Green	215.64	446.92	1.051	0.0009
Od11g04110	Blue	Green	495.11	1024.75	1.049	0.0009
Od06g07510	Blue	Green	38.13	78.73	1.046	0.0009
Od01g03130	Blue	Green	626.36	1286.28	1.038	0.0009
Od17g01990	Blue	Green	484.18	994.17	1.038	0.0009
Od06g00920	Blue	Green	94.33	193.61	1.037	0.0009
Od09g04760	Blue	Green	47.84	98.17	1.037	0.0009
Od07g03760	Blue	Green	97.94	200.07	1.031	0.0009
Od04g00460	Blue	Green	667.53	1359.73	1.026	0.0009
Od07g04740	Blue	Green	37.73	76.51	1.020	0.0009
Od02g02820	Blue	Green	98.01	198.73	1.020	0.0234
Od05g04710	Blue	Green	123.37	250.13	1.020	0.0057
Od06g02270	Blue	Green	99.28	201.24	1.019	0.0009
Od10g02230	Blue	Green	837.40	1694.91	1.017	0.0009
Od07g02870	Blue	Green	2743.96	5550.33	1.016	0.0009
Od02g03960	Blue	Green	6969.13	14074.80	1.014	0.0009
Od05g03200	Blue	Green	54.76	110.45	1.012	0.0009
Od17g00910	Blue	Green	200.42	403.57	1.010	0.0009
Od17g01480	Blue	Green	274.71	552.56	1.008	0.0009
Od16g01340	Blue	Green	957.33	1923.79	1.007	0.0009
Od12g02640	Blue	Green	253.56	509.06	1.005	0.0009
Od07g04200	Blue	Green	412.52	827.23	1.004	0.0009
Od16g02340	Blue	Green	97.15	194.70	1.003	0.0009
Od17g01920	Blue	Green	107.55	215.16	1.000	0.0009
Od04g00330	Blue	Green	617.73	1234.08	0.998	0.0009
Od02g00070	Blue	Green	246.80	492.89	0.998	0.0009
Od03g02360	Blue	Green	44.18	87.78	0.991	0.0009
Od13g00880	Blue	Green	78.71	156.29	0.990	0.0009
Od03g01080	Blue	Green	676.18	1340.97	0.988	0.0009
Od02g04650	Blue	Green	130.87	258.73	0.983	0.0009

Od09g03710	Blue	Green	94.69	187.15	0.983	0.0009
Od08g01130	Blue	Green	408.02	806.26	0.983	0.0009
Od04g01170	Blue	Green	1000.93	1972.02	0.978	0.0009
Od16g01540	Blue	Green	883.60	1740.69	0.978	0.0009
Od12g02670	Blue	Green	94.42	185.99	0.978	0.0009
Od11g02910	Blue	Green	18.51	36.44	0.978	0.0268
Od02g01260	Blue	Green	40.22	79.05	0.975	0.0009
Od02g03030	Blue	Green	680.41	1336.83	0.974	0.0009
Od17g00580	Blue	Green	302.45	592.08	0.969	0.0009
Od06g03440	Blue	Green	46.87	91.69	0.968	0.0009
Od02g02890	Blue	Green	199.21	389.51	0.967	0.0009
Od05g00580	Blue	Green	223.42	436.44	0.966	0.0009
Od09g05690	Blue	Green	386.64	755.06	0.966	0.0009
Od02g02950	Blue	Green	889.58	1736.14	0.965	0.0016
Od02g04200	Blue	Green	201.36	392.16	0.962	0.0009
Od12g01760	Blue	Green	108.27	210.86	0.962	0.0009
Od06g06190	Blue	Green	245.71	478.05	0.960	0.0009
Od01g03440	Blue	Green	219.64	426.98	0.959	0.0009
Od14g02610	Blue	Green	88.35	171.75	0.959	0.0009
Od11g00560	Blue	Green	10.27	19.94	0.958	0.0009
Od07g00730	Blue	Green	356.74	692.96	0.958	0.0009
Od02g03130	Blue	Green	73.30	142.38	0.958	0.0009
Od07g03780	Blue	Green	24.46	47.48	0.957	0.0076
Od05g02290	Blue	Green	1945.05	3767.49	0.954	0.0009
Od06g00580	Blue	Green	301.47	583.56	0.953	0.0009
Od06g03260	Blue	Green	62.22	119.89	0.946	0.0009
Od10g02420	Blue	Green	1.58	3.05	0.945	0.0458
Od16g00450	Blue	Green	251.08	483.40	0.945	0.0009
Od04g02810	Blue	Green	365.63	703.78	0.945	0.0009
Od06g02650	Blue	Green	46.17	88.70	0.942	0.0009
Od20g02020	Blue	Green	71.11	136.61	0.942	0.0009
Od09g00560	Blue	Green	21.79	41.75	0.938	0.0023
Od01g03060	Blue	Green	9.85	18.86	0.937	0.0331
Od19g00040	Blue	Green	228.70	437.43	0.936	0.0009
Od01g03200	Blue	Green	882.72	1687.83	0.935	0.0009
Od07g00770	Blue	Green	119.21	227.86	0.935	0.0009
Od02g01720	Blue	Green	454.19	867.69	0.934	0.0009
Od16g00400	Blue	Green	284.80	544.08	0.934	0.0009
Od07g00720	Blue	Green	348.20	663.87	0.931	0.0009
Od20g00610	Blue	Green	341.73	651.17	0.930	0.0009
Od20g02980	Blue	Green	257.14	489.48	0.929	0.0009
Od04g02530	Blue	Green	55.52	105.68	0.929	0.0009
Od11g04000	Blue	Green	57.09	108.58	0.927	0.0009

Od13g02090	Blue	Green	110.94	210.90	0.927	0.0009
Od05g01840	Blue	Green	900.26	1710.00	0.926	0.0009
Od13g00890	Blue	Green	81.66	155.04	0.925	0.0009
Od07g02100	Blue	Green	170.26	323.22	0.925	0.0009
Od11g02310	Blue	Green	80.10	152.05	0.925	0.0009
Od09g04740	Blue	Green	53.46	101.43	0.924	0.0009
Od01g03140	Blue	Green	106.93	202.84	0.924	0.0009
Od05g01350	Blue	Green	576.78	1093.62	0.923	0.0009
Od20g00760	Blue	Green	66.60	125.83	0.918	0.0009
Od09g06200	Blue	Green	114.04	215.37	0.917	0.0009
Od04g01900	Blue	Green	109.63	207.04	0.917	0.0009
Od07g01350	Blue	Green	634.47	1196.22	0.915	0.0009
Od12g00820	Blue	Green	190.47	358.80	0.914	0.0016
Od06g01290	Blue	Green	196.86	370.85	0.914	0.0009
Od07g03240	Blue	Green	152.51	287.29	0.914	0.0009
Od09g01770	Blue	Green	240.56	452.07	0.910	0.0016
Od20g02680	Blue	Green	1097.73	2056.75	0.906	0.0009
Od07g00140	Blue	Green	650.80	1216.38	0.902	0.0009
Od05g01280	Blue	Green	90.21	168.54	0.902	0.0009
Od02g00530	Blue	Green	58.42	109.01	0.900	0.0016
Od09g05650	Blue	Green	3213.13	5981.81	0.897	0.0009
Od05g02660	Blue	Green	134.77	250.66	0.895	0.0009
Od12g03860	Blue	Green	999.55	1854.85	0.892	0.0009
Od14g00300	Blue	Green	11.58	21.47	0.891	0.0023
Od02g01640	Blue	Green	243.04	450.57	0.891	0.0009
Od07g00560	Blue	Green	98.15	181.91	0.890	0.0009
Od05g04230	Blue	Green	188.66	349.64	0.890	0.0009
Od01g05480	Blue	Green	415.22	769.48	0.890	0.0009
Od19g00250	Blue	Green	30.71	56.90	0.890	0.0009
Od06g06880	Blue	Green	228.43	423.08	0.889	0.0009
Od01g00910	Blue	Green	81.87	151.39	0.887	0.0009
Od09g01870	Blue	Green	68.21	125.88	0.884	0.0009
Od05g01780	Blue	Green	71.94	132.63	0.883	0.0009
Od13g01850	Blue	Green	225.46	414.57	0.879	0.0009
Od09g01600	Blue	Green	178.41	327.42	0.876	0.0009
Od04g01050	Blue	Green	2143.09	3931.59	0.875	0.0009
Od07g01730	Blue	Green	56.75	104.02	0.874	0.0009
Od15g01150	Blue	Green	49.17	90.06	0.873	0.0009
Od04g02270	Blue	Green	63.70	116.66	0.873	0.0009
Od17g03100	Blue	Green	69.72	127.56	0.872	0.0009
Od04g00720	Blue	Green	168.45	307.43	0.868	0.0009
Od02g00710	Blue	Green	92.33	168.49	0.868	0.0041
Od02g01370	Blue	Green	418.09	762.28	0.867	0.0009

Od06g05350	Blue	Green	78.42	142.98	0.866	0.0009
Od02g03500	Blue	Green	24.62	44.88	0.866	0.0041
Od11g00650	Blue	Green	387.32	706.10	0.866	0.0009
Od08g02040	Blue	Green	55.21	100.60	0.866	0.0009
Od09g00060	Blue	Green	130.14	237.09	0.865	0.0009
Od16g02100	Blue	Green	297.77	542.46	0.865	0.0009
Od17g00860	Blue	Green	36.19	65.89	0.865	0.0108
Od16g00350	Blue	Green	70.13	127.63	0.864	0.0009
Od11g02010	Blue	Green	26.57	48.34	0.863	0.0023
Od08g00380	Blue	Green	33.00	60.03	0.863	0.0009
Od08g01560	Blue	Green	139.11	253.02	0.863	0.0009
Od12g01710	Blue	Green	550.21	1000.61	0.863	0.0009
Od02g03840	Blue	Green	7.53	13.67	0.861	0.0495
Od13g02780	Blue	Green	175.17	318.05	0.861	0.0009
Od04g01340	Blue	Green	167.05	303.15	0.860	0.0009
Od06g04660	Blue	Green	541.93	983.07	0.859	0.0009
Od05g02490	Blue	Green	57.16	103.58	0.858	0.0009
Od14g03280	Blue	Green	367.29	665.00	0.856	0.0009
Od20g00770	Blue	Green	1092.55	1975.14	0.854	0.0009
Od09g00630	Blue	Green	48.76	88.01	0.852	0.0029
Od14g02280	Blue	Green	113.49	204.77	0.851	0.0009
Od10g01780	Blue	Green	161.97	292.10	0.851	0.0009
Od01g02490	Blue	Green	131.48	236.94	0.850	0.0009
Od10g01990	Blue	Green	18.29	32.95	0.849	0.0009
Od05g00680	Blue	Green	53.44	96.27	0.849	0.0009
Od11g02960	Blue	Green	305.00	549.11	0.848	0.0009
Od08g00510	Blue	Green	64.51	115.90	0.845	0.0009
Od05g03380	Blue	Green	607.36	1090.95	0.845	0.0009
Od07g03350	Blue	Green	92.71	166.41	0.844	0.0062
Od06g06180	Blue	Green	31.14	55.83	0.842	0.0052
Od17g00180	Blue	Green	283.74	508.40	0.841	0.0016
Od10g01610	Blue	Green	10.22	18.30	0.841	0.0281
Od06g04310	Blue	Green	1310.70	2345.35	0.839	0.0154
Od10g00160	Blue	Green	1557.70	2787.18	0.839	0.0009
Od10g02060	Blue	Green	9.63	17.20	0.837	0.0009
Od08g00340	Blue	Green	129.82	231.79	0.836	0.0009
Od07g00130	Blue	Green	115.57	206.17	0.835	0.0009
Od04g05010	Blue	Green	399.90	713.05	0.834	0.0009
Od14g01500	Blue	Green	468.97	835.47	0.833	0.0009
Od16g01360	Blue	Green	35.65	63.51	0.833	0.0009
Od01g00820	Blue	Green	159.85	284.62	0.832	0.0016
Od02g02880	Blue	Green	731.87	1302.29	0.831	0.0009
Od12g03300	Blue	Green	161.83	287.93	0.831	0.0009

Od18g00230	Blue	Green	28.02	49.86	0.831	0.0009
Od06g00980	Blue	Green	752.78	1338.69	0.831	0.0009
Od09g03610	Blue	Green	35.39	62.82	0.828	0.0224
Od01g04970	Blue	Green	132.10	234.22	0.826	0.0009
Od16g00500	Blue	Green	87.91	155.79	0.826	0.0009
Od13g03190	Blue	Green	215.56	380.82	0.821	0.0009
Od16g00910	Blue	Green	872.44	1540.94	0.821	0.0009
Od06g03820	Blue	Green	80.24	141.54	0.819	0.0009
Od05g00410	Blue	Green	789.26	1391.27	0.818	0.0009
Od20g00600	Blue	Green	62.93	110.91	0.818	0.0009
Od07g04640	Blue	Green	152.12	268.08	0.817	0.0009
Od09g01170	Blue	Green	107.53	189.39	0.817	0.0009
Od06g06110	Blue	Green	95.43	167.53	0.812	0.0016
Od16g02700	Blue	Green	166.36	291.95	0.811	0.0009
Od09g02160	Blue	Green	38.00	66.60	0.810	0.0158
Od09g03380	Blue	Green	117.83	206.28	0.808	0.0009
Od04g01470	Blue	Green	127.10	222.21	0.806	0.0009
Od12g01380	Blue	Green	76.36	133.49	0.806	0.0009
Od17g00310	Blue	Green	1981.37	3463.30	0.806	0.0009
Od07g01340	Blue	Green	36.05	62.99	0.805	0.0046
Od09g00050	Blue	Green	89.25	155.91	0.805	0.0009
Od02g02280	Blue	Green	1440.77	2511.67	0.802	0.0009
Od03g01710	Blue	Green	980.68	1709.16	0.801	0.0009
Od01g06440	Blue	Green	226.69	394.13	0.798	0.0009
Od11g03590	Blue	Green	265.36	461.03	0.797	0.0009
Od14g03100	Blue	Green	236.26	410.43	0.797	0.0009
Od15g00730	Blue	Green	125.03	216.92	0.795	0.0009
Od10g00310	Blue	Green	49.20	85.25	0.793	0.0035
Od14g01880	Blue	Green	605.77	1049.21	0.792	0.0023
Od01g03230	Blue	Green	12.66	21.91	0.792	0.0420
Od05g04600	Blue	Green	174.63	302.26	0.792	0.0009
Od20g02620	Blue	Green	220.10	380.96	0.792	0.0023
Od01g00700	Blue	Green	228.05	394.68	0.791	0.0029
Od08g00630	Blue	Green	83.99	145.31	0.791	0.0009
Od05g04700	Blue	Green	289.44	499.30	0.787	0.0009
Od13g00600	Blue	Green	14.35	24.73	0.785	0.0009
Od10g00380	Blue	Green	173.43	298.72	0.784	0.0009
Od09g04780	Blue	Green	88.07	151.57	0.783	0.0009
Od01g07060	Blue	Green	69.70	119.92	0.783	0.0009
Od01g01080	Blue	Green	67.79	116.58	0.782	0.0009
Od06g04640	Blue	Green	152.86	262.68	0.781	0.0009
Od14g01100	Blue	Green	1187.45	2039.46	0.780	0.0016
Od14g01250	Blue	Green	1086.66	1863.72	0.778	0.0009

Od17g00130	Blue	Green	330.09	566.08	0.778	0.0029
Od09g03870	Blue	Green	174.47	298.34	0.774	0.0009
Od05g03740	Blue	Green	122.67	209.61	0.773	0.0009
Od10g01760	Blue	Green	225.43	385.05	0.772	0.0009
Od08g02800	Blue	Green	25.61	43.74	0.772	0.0016
Od09g03050	Blue	Green	99.09	168.98	0.770	0.0052
Od07g00800	Blue	Green	1071.54	1824.69	0.768	0.0023
Od05g01040	Blue	Green	50.23	85.41	0.766	0.0029
Od16g01250	Blue	Green	36.03	61.21	0.765	0.0023
Od09g02090	Blue	Green	36.74	62.37	0.763	0.0009
Od12g03120	Blue	Green	185.86	315.12	0.762	0.0009
Od06g06520	Blue	Green	31.79	53.88	0.761	0.0439
Od16g00770	Blue	Green	106.36	180.21	0.761	0.0009
Od15g01360	Blue	Green	57.87	97.93	0.759	0.0016
Od03g02200	Blue	Green	145.13	245.48	0.758	0.0016
Od20g01100	Blue	Green	161.10	272.38	0.758	0.0009
Od01g05530	Blue	Green	1084.24	1832.85	0.757	0.0009
Od06g03340	Blue	Green	33.16	55.91	0.754	0.0016
Od02g03280	Blue	Green	499.19	841.59	0.754	0.0016
Od12g03760	Blue	Green	74.78	125.50	0.747	0.0023
Od01g06180	Blue	Green	139.57	234.16	0.746	0.0029
Od06g05830	Blue	Green	204.16	341.87	0.744	0.0023
Od07g04290	Blue	Green	108.02	180.85	0.744	0.0023
Od15g01140	Blue	Green	45.06	75.41	0.743	0.0290
Od03g01260	Blue	Green	415.88	695.71	0.742	0.0035
Od13g01120	Blue	Green	541.33	905.44	0.742	0.0023
Od03g03060	Blue	Green	173.15	289.30	0.741	0.0035
Od01g01210	Blue	Green	87.66	146.44	0.740	0.0035
Od17g01930	Blue	Green	80.22	133.99	0.740	0.0052
Od06g01100	Blue	Green	75.66	126.36	0.740	0.0052
Od07g02380	Blue	Green	770.66	1286.80	0.740	0.0023
Od04g04320	Blue	Green	32.61	54.44	0.740	0.0210
Od02g04020	Blue	Green	368.44	614.87	0.739	0.0029
Od07g03190	Blue	Green	442.59	738.39	0.738	0.0029
Od06g00990	Blue	Green	122.22	203.86	0.738	0.0016
Od09g00820	Blue	Green	187.87	313.24	0.738	0.0041
Od11g02200	Blue	Green	53.37	88.95	0.737	0.0071
Od01g05070	Blue	Green	233.81	389.42	0.736	0.0016
Od08g00180	Blue	Green	3394.38	5653.55	0.736	0.0023
Od07g03830	Blue	Green	813.82	1355.39	0.736	0.0029
Od16g02600	Blue	Green	71.97	119.85	0.736	0.0035
Od17g00330	Blue	Green	1157.53	1925.44	0.734	0.0016
Od17g02560	Blue	Green	6619.11	11009.70	0.734	0.0016

Od06g04530	Blue	Green	403.47	671.07	0.734	0.0009
Od08g03040	Blue	Green	295.69	491.44	0.733	0.0052
Od04g05170	Blue	Green	16.29	27.06	0.732	0.0271
Od07g01440	Blue	Green	59.11	98.20	0.732	0.0009
Od04g02330	Blue	Green	182.62	303.27	0.732	0.0206
Od17g00080	Blue	Green	257.92	428.23	0.731	0.0009
Od03g00600	Blue	Green	436.38	724.38	0.731	0.0009
Od14g01120	Blue	Green	117.09	194.34	0.731	0.0023
Od04g00700	Blue	Green	958.32	1590.30	0.731	0.0023
Od02g04320	Blue	Green	120.89	200.60	0.731	0.0041
Od05g04640	Blue	Green	162.99	269.42	0.725	0.0041
Od06g03120	Blue	Green	394.31	651.79	0.725	0.0029
Od12g01850	Blue	Green	350.14	578.75	0.725	0.0035
Od07g01360	Blue	Green	815.02	1346.58	0.724	0.0046
Od20g02230	Blue	Green	1127.32	1861.80	0.724	0.0035
Od02g01610	Blue	Green	644.78	1064.48	0.723	0.0029
Od20g02440	Blue	Green	131.61	217.26	0.723	0.0071
Od11g04210	Blue	Green	46.00	75.91	0.723	0.0023
Od07g03890	Blue	Green	80.83	133.29	0.722	0.0076
Od01g01970	Blue	Green	308.21	507.73	0.720	0.0029
Od04g02180	Blue	Green	158.51	260.97	0.719	0.0029
Od03g00700	Blue	Green	60.41	99.33	0.717	0.0023
Od18g00470	Blue	Green	191.11	313.99	0.716	0.0035
Od03g02230	Blue	Green	293.98	482.92	0.716	0.0041
Od05g04140	Blue	Green	125.76	206.35	0.714	0.0016
Od04g03290	Blue	Green	63.30	103.81	0.714	0.0062
Od20g02940	Blue	Green	99.21	162.64	0.713	0.0035
Od14g02230	Blue	Green	127.47	208.92	0.713	0.0023
Od16g00750	Blue	Green	162.40	266.10	0.712	0.0041
Od16g00480	Blue	Green	56.10	91.87	0.712	0.0062
Od04g02520	Blue	Green	10.53	17.25	0.712	0.0067
Od07g02800	Blue	Green	2270.76	3716.93	0.711	0.0016
Od03g01290	Blue	Green	61.93	101.36	0.711	0.0029
Od14g02240	Blue	Green	86.92	142.25	0.711	0.0023
Od04g05340	Blue	Green	173.17	283.38	0.711	0.0023
Od16g02240	Blue	Green	295.40	483.11	0.710	0.0035
Od08g00110	Blue	Green	42.20	69.00	0.709	0.0041
Od01g02070	Blue	Green	278.02	454.49	0.709	0.0023
Od05g01720	Blue	Green	340.67	556.82	0.709	0.0035
Od04g00660	Blue	Green	155.40	253.95	0.709	0.0016
Od17g01810	Blue	Green	62.08	101.36	0.707	0.0023
Od04g02760	Blue	Green	290.67	474.42	0.707	0.0046
Od17g02000	Blue	Green	34.77	56.72	0.706	0.0086

Od06g01660	Blue	Green	112.33	183.15	0.705	0.0035
Od08g00410	Blue	Green	128.57	209.28	0.703	0.0052
Od19g00400	Blue	Green	63.36	103.08	0.702	0.0035
Od04g02650	Blue	Green	59.45	96.62	0.701	0.0029
Od03g00740	Blue	Green	655.80	1064.92	0.699	0.0035
Od09g02190	Blue	Green	59.43	96.50	0.699	0.0052
Od07g02280	Blue	Green	861.19	1398.17	0.699	0.0023
Od14g01440	Blue	Green	127.80	207.49	0.699	0.0023
Od06g00510	Blue	Green	111.26	180.49	0.698	0.0035
Od06g00660	Blue	Green	273.18	443.12	0.698	0.0009
Od05g01980	Blue	Green	948.91	1539.20	0.698	0.0046
Od01g06190	Blue	Green	966.45	1566.80	0.697	0.0029
Od17g02960	Blue	Green	80.64	130.70	0.697	0.0035
Od16g02630	Blue	Green	266.88	432.34	0.696	0.0067
Od07g04560	Blue	Green	134.10	217.19	0.696	0.0046
Od01g00470	Blue	Green	240.80	389.64	0.694	0.0029
Od12g00420	Blue	Green	50.64	81.93	0.694	0.0067
Od07g01840	Blue	Green	21.82	35.29	0.694	0.0306
Od04g00730	Blue	Green	50.98	82.45	0.694	0.0067
Od01g02120	Blue	Green	434.87	703.14	0.693	0.0057
Od17g01590	Blue	Green	24.79	40.06	0.692	0.0041
Od19g01010	Blue	Green	243.42	393.06	0.691	0.0046
Od09g03480	Blue	Green	34.81	56.21	0.691	0.0067
Od07g00790	Blue	Green	53.00	85.54	0.691	0.0052
Od02g04110	Blue	Green	53.33	86.04	0.690	0.0138
Od10g01180	Blue	Green	171.13	276.02	0.690	0.0108
Od09g02060	Blue	Green	449.27	724.58	0.690	0.0035
Od05g01340	Blue	Green	11.21	18.07	0.689	0.0029
Od16g01860	Blue	Green	91.32	147.19	0.689	0.0041
Od06g03460	Blue	Green	153.66	247.49	0.688	0.0062
Od06g02790	Blue	Green	407.79	656.74	0.687	0.0062
Od15g01370	Blue	Green	777.45	1251.49	0.687	0.0046
Od05g00710	Blue	Green	139.85	224.96	0.686	0.0086
Od05g01900	Blue	Green	47.50	76.40	0.686	0.0046
Od15g00140	Blue	Green	18.63	29.96	0.685	0.0158
Od08g01660	Blue	Green	301.11	484.11	0.685	0.0023
Od02g00380	Blue	Green	170.52	274.11	0.685	0.0046
Od02g02590	Blue	Green	699.77	1124.19	0.684	0.0062
Od20g01670	Blue	Green	27.60	44.29	0.682	0.0349
Od06g02280	Blue	Green	39.74	63.74	0.682	0.0192
Od04g02360	Blue	Green	44.73	71.73	0.681	0.0090
Od04g01890	Blue	Green	740.99	1187.09	0.680	0.0057
Od01g03660	Blue	Green	44.57	71.39	0.680	0.0357

Od05g03220	Blue	Green	66.31	106.08	0.678	0.0052
Od14g00560	Blue	Green	168.91	270.18	0.678	0.0081
Od01g01960	Blue	Green	230.25	368.18	0.677	0.0081
Od01g02360	Blue	Green	16.92	27.03	0.676	0.0343
Od03g02190	Blue	Green	112.66	179.99	0.676	0.0041
Od12g01770	Blue	Green	584.90	934.34	0.676	0.0067
Od14g00220	Blue	Green	97.13	155.10	0.675	0.0300
Od10g01620	Blue	Green	26.45	42.23	0.675	0.0100
Od04g02010	Blue	Green	519.71	829.74	0.675	0.0076
Od09g02650	Blue	Green	376.49	601.04	0.675	0.0062
Od16g01280	Blue	Green	58.80	93.83	0.674	0.0086
Od15g00670	Blue	Green	57.55	91.83	0.674	0.0041
Od12g03170	Blue	Green	82.14	130.92	0.673	0.0046
Od02g01400	Blue	Green	742.11	1182.67	0.672	0.0227
Od07g02000	Blue	Green	128.50	204.74	0.672	0.0076
Od02g00480	Blue	Green	198.26	315.70	0.671	0.0057
Od01g00900	Blue	Green	36.78	58.54	0.671	0.0154
Od11g04260	Blue	Green	45.38	72.21	0.670	0.0071
Od06g06080	Blue	Green	88.83	141.25	0.669	0.0108
Od14g02540	Blue	Green	234.89	373.23	0.668	0.0071
Od06g04820	Blue	Green	26.37	41.88	0.667	0.0052
Od03g02220	Blue	Green	168.70	267.89	0.667	0.0134
Od08g02690	Blue	Green	78.46	124.56	0.667	0.0046
Od06g06750	Blue	Green	258.37	409.87	0.666	0.0081
Od14g02970	Blue	Green	14.24	22.58	0.665	0.0081
Od04g01950	Blue	Green	85.18	135.07	0.665	0.0052
Od06g07010	Blue	Green	53.53	84.87	0.665	0.0275
Od11g00860	Blue	Green	841.76	1334.38	0.665	0.0057
Od20g01870	Blue	Green	26.35	41.77	0.665	0.0487
Od06g04990	Blue	Green	120.11	190.29	0.664	0.0071
Od12g02280	Blue	Green	144.31	228.61	0.664	0.0142
Od01g03830	Blue	Green	649.08	1026.54	0.661	0.0081
Od09g05080	Blue	Green	245.30	387.66	0.660	0.0062
Od01g02350	Blue	Green	13.18	20.82	0.660	0.0309
Od20g00950	Blue	Green	95.34	150.48	0.658	0.0071
Od09g04370	Blue	Green	91.16	143.86	0.658	0.0067
Od07g04160	Blue	Green	427.74	675.00	0.658	0.0076
Od19g01230	Blue	Green	246.70	389.23	0.658	0.0067
Od12g01240	Blue	Green	202.81	319.86	0.657	0.0076
Od08g01940	Blue	Green	22.79	35.91	0.656	0.0158
Od07g04210	Blue	Green	93.83	147.83	0.656	0.0057
Od02g00190	Blue	Green	255.88	403.07	0.656	0.0100
Od09g03950	Blue	Green	15.80	24.88	0.655	0.0170

Od01g06560	Blue	Green	218.98	344.66	0.654	0.0108
Od13g02930	Blue	Green	89.24	140.41	0.654	0.0062
Od17g02080	Blue	Green	151.98	239.05	0.653	0.0062
Od07g04940	Blue	Green	64.32	101.12	0.653	0.0076
Od15g01050	Blue	Green	32.00	50.29	0.652	0.0184
Od20g00660	Blue	Green	67.39	105.85	0.651	0.0076
Od02g01840	Blue	Green	426.12	668.71	0.650	0.0076
Od19g00660	Blue	Green	103.69	162.70	0.650	0.0461
Od04g02560	Blue	Green	76.06	119.11	0.647	0.0081
Od10g00290	Blue	Green	795.84	1245.05	0.646	0.0095
Od06g01900	Blue	Green	70.18	109.76	0.645	0.0104
Od15g00860	Blue	Green	322.05	503.53	0.645	0.0086
Od10g02450	Blue	Green	1000.01	1562.88	0.644	0.0108
Od11g03230	Blue	Green	250.59	391.60	0.644	0.0062
Od16g00760	Blue	Green	110.68	172.92	0.644	0.0095
Od13g02150	Blue	Green	126.20	196.82	0.641	0.0278
Od13g01950	Blue	Green	384.98	600.31	0.641	0.0130
Od09g01900	Blue	Green	564.99	879.93	0.639	0.0154
Od14g03300	Blue	Green	50.54	78.68	0.639	0.0287
Od01g06380	Blue	Green	108.72	169.07	0.637	0.0122
Od01g01040	Blue	Green	90.06	140.04	0.637	0.0154
Od08g02110	Blue	Green	36.34	56.49	0.636	0.0090
Od18g00380	Blue	Green	55.95	86.85	0.634	0.0117
Od19g00510	Blue	Green	59.49	92.32	0.634	0.0117
Od17g01140	Blue	Green	41.53	64.45	0.634	0.0122
Od11g00960	Blue	Green	59.60	92.40	0.633	0.0210
Od08g00030	Blue	Green	9.58	14.86	0.633	0.0184
Od12g02760	Blue	Green	88.59	137.34	0.633	0.0130
Od13g01670	Blue	Green	154.94	240.06	0.632	0.0108
Od20g03110	Blue	Green	129.43	200.41	0.631	0.0162
Od12g01230	Blue	Green	199.65	309.10	0.631	0.0138
Od08g01170	Blue	Green	90.58	140.13	0.630	0.0108
Od12g01510	Blue	Green	62.63	96.76	0.628	0.0192
Od03g01720	Blue	Green	38.01	58.68	0.627	0.0166
Od12g01570	Blue	Green	67.02	103.46	0.626	0.0113
Od20g03370	Blue	Green	116.16	179.18	0.625	0.0150
Od06g05740	Blue	Green	663.36	1023.07	0.625	0.0130
Od06g04680	Blue	Green	393.27	606.20	0.624	0.0146
Od06g02680	Blue	Green	58.41	90.01	0.624	0.0142
Od11g00770	Blue	Green	42.79	65.92	0.624	0.0146
Od01g06780	Blue	Green	50.49	77.75	0.623	0.0108
Od16g02230	Blue	Green	64.23	98.90	0.623	0.0166
Od20g03120	Blue	Green	52.06	80.05	0.621	0.0126

Od17g00300	Blue	Green	63.79	98.06	0.620	0.0162
Od13g00610	Blue	Green	75.50	116.04	0.620	0.0188
Od14g02160	Blue	Green	424.31	651.99	0.620	0.0138
Od03g02820	Blue	Green	111.38	171.07	0.619	0.0117
Od08g01520	Blue	Green	74.29	114.10	0.619	0.0126
Od13g02710	Blue	Green	451.10	692.76	0.619	0.0174
Od11g02470	Blue	Green	18077.70	27747.00	0.618	0.0057
Od01g01520	Blue	Green	783.74	1202.87	0.618	0.0130
Od02g00410	Blue	Green	50.02	76.70	0.617	0.0162
Od07g02520	Blue	Green	123.95	189.73	0.614	0.0150
Od10g00440	Blue	Green	496.90	760.58	0.614	0.0188
Od13g02650	Blue	Green	47.49	72.64	0.613	0.0341
Od01g01530	Blue	Green	145.20	221.91	0.612	0.0177
Od02g02250	Blue	Green	590.97	902.84	0.611	0.0142
Od16g01100	Blue	Green	92.67	141.56	0.611	0.0180
Od06g04510	Blue	Green	129.16	197.28	0.611	0.0122
Od06g01630	Blue	Green	175.08	267.39	0.611	0.0138
Od08g03020	Blue	Green	102.41	156.35	0.610	0.0180
Od11g00830	Blue	Green	82.57	126.05	0.610	0.0130
Od08g00080	Blue	Green	190.57	290.86	0.610	0.0170
Od09g05010	Blue	Green	384.40	586.52	0.610	0.0174
Od07g02050	Blue	Green	1582.54	2413.53	0.609	0.0184
Od11g01930	Blue	Green	69.39	105.81	0.609	0.0122
Od05g01030	Blue	Green	25.69	39.17	0.609	0.0463
Od13g00730	Blue	Green	405.57	618.17	0.608	0.0177
Od15g00090	Blue	Green	243.19	370.61	0.608	0.0188
Od02g01730	Blue	Green	401.25	611.36	0.608	0.0142
Od18g00220	Blue	Green	44.90	68.39	0.607	0.0341
Od05g04680	Blue	Green	108.76	165.65	0.607	0.0142
Od19g01200	Blue	Green	346.33	526.89	0.605	0.0199
Od03g01930	Blue	Green	37.68	57.29	0.605	0.0177
Od09g06000	Blue	Green	86.58	131.56	0.604	0.0402
Od14g03220	Blue	Green	213.81	324.62	0.602	0.0130
Od20g00300	Blue	Green	405.08	614.92	0.602	0.0195
Od05g00570	Blue	Green	54.56	82.81	0.602	0.0202
Od06g02640	Blue	Green	1204.25	1827.77	0.602	0.0213
Od01g05820	Blue	Green	322.48	488.88	0.600	0.0184
Od20g00850	Blue	Green	46.56	70.56	0.600	0.0184
Od06g03270	Blue	Green	86.94	131.73	0.600	0.0234
Od20g02670	Blue	Green	308.71	467.66	0.599	0.0227
Od10g00200	Blue	Green	102.78	155.69	0.599	0.0195
Od04g00690	Blue	Green	409.08	619.47	0.599	0.0217
Od08g00810	Blue	Green	286.50	433.50	0.598	0.0245

Od03g01000	Blue	Green	61.22	92.63	0.597	0.0268
Od05g01130	Blue	Green	61.53	93.08	0.597	0.0174
Od12g00990	Blue	Green	131.08	198.31	0.597	0.0188
Od03g00760	Blue	Green	905.41	1369.52	0.597	0.0234
Od07g02150	Blue	Green	155.49	235.18	0.597	0.0227
Od20g02130	Blue	Green	1143.52	1728.62	0.596	0.0366
Od03g00380	Blue	Green	36.80	55.63	0.596	0.0255
Od04g04520	Blue	Green	53.69	81.15	0.596	0.0142
Od04g03390	Blue	Green	65.85	99.49	0.595	0.0411
Od16g00600	Blue	Green	56.86	85.86	0.595	0.0213
Od01g01400	Blue	Green	211.59	319.42	0.594	0.0210
Od19g01150	Blue	Green	115.53	174.39	0.594	0.0241
Od03g02930	Blue	Green	83.76	126.39	0.594	0.0177
Od20g00350	Blue	Green	539.00	812.60	0.592	0.0202
Od07g00970	Blue	Green	48.87	73.67	0.592	0.0177
Od12g03440	Blue	Green	138.32	208.49	0.592	0.0177
Od01g04990	Blue	Green	122.64	184.79	0.592	0.0258
Od02g01760	Blue	Green	104.48	157.40	0.591	0.0231
Od09g05370	Blue	Green	974.81	1467.84	0.591	0.0331
Od13g00240	Blue	Green	59.36	89.35	0.590	0.0170
Od01g02380	Blue	Green	54.23	81.63	0.590	0.0405
Od06g06410	Blue	Green	67.66	101.83	0.590	0.0177
Od06g00080	Blue	Green	85.70	128.95	0.589	0.0217
Od09g05360	Blue	Green	190.64	286.69	0.589	0.0234
Od09g04960	Blue	Green	43.52	65.44	0.588	0.0227
Od11g02250	Blue	Green	35.28	53.01	0.587	0.0220
Od12g03290	Blue	Green	70.84	106.28	0.585	0.0213
Od05g00090	Blue	Green	173.22	259.60	0.584	0.0265
Od02g00100	Blue	Green	27.13	40.65	0.583	0.0227
Od09g02040	Blue	Green	268.66	402.38	0.583	0.0224
Od10g00080	Blue	Green	236.71	354.39	0.582	0.0248
Od02g04330	Blue	Green	48.29	72.28	0.582	0.0265
Od03g02030	Blue	Green	110.06	164.61	0.581	0.0206
Od09g00980	Blue	Green	120.40	179.95	0.580	0.0217
Od05g01680	Blue	Green	89.56	133.83	0.580	0.0224
Od20g02410	Blue	Green	129.53	193.49	0.579	0.0245
Od09g04130	Blue	Green	92.21	137.71	0.579	0.0248
Od08g02460	Blue	Green	114.85	171.52	0.579	0.0213
Od06g03540	Blue	Green	62.67	93.59	0.579	0.0220
Od10g00030	Blue	Green	401.95	600.12	0.578	0.0297
Od12g03310	Blue	Green	115.61	172.58	0.578	0.0170
Od03g01170	Blue	Green	270.23	403.30	0.578	0.0297
Od04g02820	Blue	Green	3417.15	5098.57	0.577	0.0206

Od12g03770	Blue	Green	135.11	201.50	0.577	0.0224
Od16g00470	Blue	Green	1930.41	2878.48	0.576	0.0199
Od07g02590	Blue	Green	379.18	565.27	0.576	0.0262
Od12g03280	Blue	Green	154.50	230.23	0.575	0.0202
Od03g01970	Blue	Green	48.19	71.79	0.575	0.0321
Od13g01560	Blue	Green	104.04	154.94	0.575	0.0278
Od01g02310	Blue	Green	54.41	80.90	0.572	0.0327
Od07g01750	Blue	Green	637.46	947.71	0.572	0.0268
Od06g06540	Blue	Green	26.07	38.74	0.572	0.0431
Od01g00110	Blue	Green	740.99	1101.18	0.572	0.0312
Od14g01870	Blue	Green	222.02	329.74	0.571	0.0271
Od02g04030	Blue	Green	120.18	178.36	0.570	0.0384
Od01g04910	Blue	Green	525.88	780.07	0.569	0.0300
Od12g01950	Blue	Green	275.77	409.06	0.569	0.0343
Od05g04450	Blue	Green	531.01	787.47	0.568	0.0297
Od06g02890	Blue	Green	153.71	227.86	0.568	0.0224
Od10g01060	Blue	Green	105.21	155.93	0.568	0.0262
Od02g00650	Blue	Green	129.63	191.89	0.566	0.0252
Od14g02940	Blue	Green	32.45	48.03	0.566	0.0357
Od07g01970	Blue	Green	242.39	358.73	0.566	0.0255
Od05g01070	Blue	Green	1232.73	1824.28	0.565	0.0369
Od06g04500	Blue	Green	107.26	158.73	0.565	0.0300
Od08g00820	Blue	Green	51.72	76.52	0.565	0.0294
Od01g02470	Blue	Green	172.76	255.46	0.564	0.0329
Od05g05070	Blue	Green	176.94	261.64	0.564	0.0331
Od06g01160	Blue	Green	762.03	1126.08	0.563	0.0329
Od16g01600	Blue	Green	104.82	154.82	0.563	0.0294
Od16g02270	Blue	Green	60.74	89.65	0.562	0.0321
Od04g01780	Blue	Green	116.56	172.04	0.562	0.0392
Od01g04450	Blue	Green	24.48	36.13	0.561	0.0387
Od13g02700	Blue	Green	335.31	494.76	0.561	0.0343
Od01g00540	Blue	Green	365.67	539.06	0.560	0.0302
Od14g01630	Blue	Green	93.18	137.25	0.559	0.0470
Od06g01910	Blue	Green	71.59	105.44	0.558	0.0324
Od11g00900	Blue	Green	34.61	50.96	0.558	0.0366
Od10g01370	Blue	Green	92.70	136.43	0.557	0.0363
Od13g02060	Blue	Green	69.95	102.94	0.557	0.0312
Od14g00630	Blue	Green	217.17	319.58	0.557	0.0312
Od01g04940	Blue	Green	59.41	87.39	0.557	0.0297
Od13g02920	Blue	Green	208.54	306.75	0.557	0.0315
Od08g03360	Blue	Green	38.43	56.50	0.556	0.0463
Od07g01260	Blue	Green	73.75	108.39	0.556	0.0355
Od06g02290	Blue	Green	55.00	80.80	0.555	0.0302

Od05g05150	Blue	Green	2729.04	4007.66	0.554	0.0170
Od06g01110	Blue	Green	156.23	229.36	0.554	0.0337
Od09g02790	Blue	Green	636.72	934.56	0.554	0.0327
Od08g00350	Blue	Green	54.86	80.45	0.552	0.0258
Od14g01920	Blue	Green	52.37	76.78	0.552	0.0387
Od01g00160	Blue	Green	61.34	89.93	0.552	0.0439
Od13g02490	Blue	Green	40.00	58.64	0.552	0.0331
Od01g04550	Blue	Green	255.36	374.21	0.551	0.0390
Od08g02100	Blue	Green	142.08	208.20	0.551	0.0271
Od06g04140	Blue	Green	238.48	349.35	0.551	0.0329
Od06g01000	Blue	Green	582.13	852.72	0.551	0.0420
Od03g02470	Blue	Green	113.46	166.17	0.550	0.0268
Od09g02940	Blue	Green	70.59	103.37	0.550	0.0306
Od13g01770	Blue	Green	100.85	147.65	0.550	0.0327
Od05g04560	Blue	Green	138.33	202.52	0.550	0.0265
Od03g03040	Blue	Green	21.83	31.95	0.550	0.0426
Od03g00550	Blue	Green	91.80	134.37	0.550	0.0476
Od04g03380	Blue	Green	22.32	32.67	0.550	0.0355
Od09g04720	Blue	Green	108.18	158.30	0.549	0.0384
Od16g00160	Blue	Green	127.98	187.25	0.549	0.0372
Od13g02880	Blue	Green	63.48	92.84	0.549	0.0363
Od08g02750	Blue	Green	27.10	39.63	0.548	0.0355
Od12g01860	Blue	Green	268.36	392.13	0.547	0.0268
Od12g02480	Blue	Green	58.77	85.88	0.547	0.0423
Od20g01230	Blue	Green	2456.74	3589.42	0.547	0.0329
Od04g02890	Blue	Green	105.37	153.93	0.547	0.0417
Od11g03300	Blue	Green	236.86	345.98	0.547	0.0439
Od04g04860	Blue	Green	114.31	166.87	0.546	0.0349
Od03g02850	Blue	Green	303.32	442.73	0.546	0.0408
Od16g01930	Blue	Green	87.69	127.93	0.545	0.0495
Od17g01080	Blue	Green	44.35	64.69	0.545	0.0399
Od01g06170	Blue	Green	133.98	195.37	0.544	0.0360
Od04g02960	Blue	Green	121.58	177.06	0.542	0.0329
Od06g00590	Blue	Green	171.05	249.08	0.542	0.0392
Od14g02330	Blue	Green	324.22	472.03	0.542	0.0360
Od13g00660	Blue	Green	57.79	84.10	0.541	0.0465
Od11g02320	Blue	Green	52.71	76.67	0.541	0.0378
Od12g02900	Blue	Green	263.31	382.90	0.540	0.0378
Od02g02800	Blue	Green	185.95	270.37	0.540	0.0449
Od16g00420	Blue	Green	259.52	377.33	0.540	0.0492
Od05g02220	Blue	Green	78.28	113.61	0.537	0.0392
Od02g03950	Blue	Green	25.72	37.32	0.537	0.0390
Od06g06090	Blue	Green	455.59	660.90	0.537	0.0381

Od18g00310	Blue	Green	52.95	76.79	0.536	0.0497
Od16g01620	Blue	Green	56.80	82.33	0.536	0.0465
Od01g03400	Blue	Green	293.71	425.74	0.536	0.0500
Od01g05190	Blue	Green	66.73	96.71	0.535	0.0408
Od20g02720	Blue	Green	278.75	403.76	0.535	0.0490
Od09g02710	Blue	Green	184.79	267.57	0.534	0.0390
Od09g02920	Blue	Green	279.06	403.87	0.533	0.0473
Od08g00770	Blue	Green	182.67	263.94	0.531	0.0390
Od04g00520	Blue	Green	151.87	219.34	0.530	0.0431
Od16g00430	Blue	Green	62.79	90.63	0.529	0.0378
Od05g00240	Blue	Green	96.08	138.64	0.529	0.0387
Od02g04760	Blue	Green	63.42	91.48	0.529	0.0337
Od07g02540	Blue	Green	55.11	79.44	0.528	0.0495
Od04g03370	Blue	Green	55.29	79.65	0.527	0.0434
Od04g02450	Blue	Green	2457.39	3539.75	0.527	0.0408
Od06g06890	Blue	Green	69.98	100.76	0.526	0.0449
Od04g04650	Blue	Green	11.37	16.36	0.526	0.0492
Od10g01550	Blue	Green	247.35	356.05	0.526	0.0417
Od06g04590	Blue	Green	82.67	118.98	0.525	0.0473
Od07g01270	Blue	Green	122.87	176.84	0.525	0.0492
Od01g00550	Blue	Green	74.69	107.38	0.524	0.0484
Od08g02170	Blue	Green	116.37	167.28	0.524	0.0387
Od09g01000	Blue	Green	73.49	105.60	0.523	0.0490
Od08g03480	Blue	Green	193.75	278.37	0.523	0.0484
Od01g06000	Blue	Green	557.02	800.10	0.522	0.0492
Od16g00010	Blue	Green	205.39	294.98	0.522	0.0458
Od05g04570	Blue	Green	124.99	179.49	0.522	0.0465
Od06g00310	Blue	Green	39.66	56.93	0.521	0.0465
Od16g01660	Blue	Green	145.47	208.50	0.519	0.0443
Od02g01230	Blue	Green	81.50	116.81	0.519	0.0417
Od04g03220	Blue	Green	253.96	363.80	0.519	0.0452
Od16g01820	Blue	Green	55.30	79.21	0.518	0.0443
Od04g05330	Blue	Green	62.46	89.44	0.518	0.0470
Od08g01810	Blue	Green	132.20	189.12	0.517	0.0443
Od09g01390	Blue	Green	88.03	125.91	0.516	0.0458
Od14g02750	Blue	Green	23.48	33.58	0.516	0.0497
Od06g05060	Blue	Green	35.70	51.02	0.515	0.0463
Od01g01470	Blue	Green	58.48	83.57	0.515	0.0484
Od16g00460	Blue	Green	111.99	160.02	0.515	0.0495
Od02g04440	Blue	Green	25.23	36.03	0.514	0.0458
Od01g00380	Blue	Green	44.34	31.05	-0.514	0.0487
Od16g00710	Blue	Green	91.28	63.64	-0.520	0.0443
Od08g00070	Blue	Green	80.31	55.94	-0.522	0.0487

Od03g00050	Blue	Green	38.95	27.10	-0.524	0.0465
Od07g04240	Blue	Green	33.79	23.49	-0.525	0.0439
Od20g03400	Blue	Green	91.23	63.10	-0.532	0.0443
Od05g00350	Blue	Green	186.29	128.73	-0.533	0.0372
Od01g01640	Blue	Green	282.82	195.15	-0.535	0.0402
Od08g00890	Blue	Green	66.84	46.12	-0.535	0.0439
Od20g01210	Blue	Green	95.28	65.72	-0.536	0.0363
Od09g00250	Blue	Green	26.78	18.45	-0.537	0.0408
Od02g04890	Blue	Green	87.30	60.10	-0.539	0.0436
Od03g00650	Blue	Green	62.34	42.88	-0.540	0.0357
Od06g04930	Blue	Green	238.56	164.06	-0.540	0.0405
Od12g01990	Blue	Green	428.37	294.49	-0.541	0.0392
Od10g01260	Blue	Green	38.66	26.56	-0.541	0.0315
Od07g03950	Blue	Green	28.04	19.26	-0.542	0.0341
Od17g00370	Blue	Green	90.82	62.33	-0.543	0.0408
Od04g02080	Blue	Green	105.06	72.10	-0.543	0.0436
Od14g02580	Blue	Green	143.91	98.71	-0.544	0.0375
Od05g03900	Blue	Green	30.93	21.22	-0.544	0.0420
Od01g04880	Blue	Green	115.13	78.94	-0.544	0.0426
Od05g00610	Blue	Green	116.59	79.91	-0.545	0.0372
Od13g02110	Blue	Green	617.62	423.18	-0.545	0.0324
Od01g00730	Blue	Green	276.26	189.09	-0.547	0.0352
Od04g04610	Blue	Green	128.46	87.91	-0.547	0.0366
Od02g02550	Blue	Green	59.24	40.51	-0.548	0.0312
Od06g01820	Blue	Green	117.70	80.48	-0.548	0.0360
Od08g01740	Blue	Green	77.49	52.96	-0.549	0.0390
Od01g04340	Blue	Green	111.90	76.46	-0.549	0.0302
Od17g00490	Blue	Green	42.39	28.95	-0.550	0.0381
Od01g05650	Blue	Green	29.72	20.29	-0.551	0.0297
Od04g02440	Blue	Green	22.40	15.27	-0.552	0.0366
Od12g03610	Blue	Green	43.24	29.48	-0.553	0.0387
Od09g04770	Blue	Green	316.04	215.23	-0.554	0.0287
Od14g02670	Blue	Green	68.32	46.49	-0.555	0.0309
Od01g02960	Blue	Green	46.50	31.65	-0.555	0.0329
Od04g05070	Blue	Green	38.01	25.84	-0.557	0.0372
Od07g03080	Blue	Green	443.20	300.79	-0.559	0.0319
Od19g01160	Blue	Green	93.49	63.45	-0.559	0.0255
Od14g00050	Blue	Green	195.49	132.65	-0.560	0.0324
Od04g02770	Blue	Green	55.45	37.62	-0.560	0.0449
Od12g02600	Blue	Green	16.29	11.04	-0.560	0.0278
Od08g03580	Blue	Green	237.79	160.92	-0.563	0.0297
Od02g00040	Blue	Green	112.48	76.11	-0.564	0.0258
Od10g02440	Blue	Green	103.21	69.78	-0.565	0.0284

Od01g03120	Blue	Green	54.42	36.78	-0.565	0.0468
Od04g04940	Blue	Green	20.29	13.70	-0.566	0.0337
Od11g00410	Blue	Green	115.91	78.27	-0.566	0.0411
Od20g00540	Blue	Green	61.16	41.30	-0.567	0.0248
Od16g00730	Blue	Green	138.93	93.79	-0.567	0.0271
Od01g06580	Blue	Green	1439.11	971.54	-0.567	0.0321
Od14g00470	Blue	Green	135.48	91.41	-0.568	0.0324
Od10g01220	Blue	Green	70.05	47.22	-0.569	0.0335
Od14g01340	Blue	Green	140.76	94.86	-0.569	0.0329
Od08g02240	Blue	Green	79.18	53.36	-0.569	0.0224
Od07g02180	Blue	Green	128.58	86.59	-0.570	0.0455
Od10g02380	Blue	Green	277.01	186.54	-0.570	0.0231
Od07g04460	Blue	Green	70.47	47.38	-0.573	0.0265
Od01g00840	Blue	Green	29.64	19.93	-0.573	0.0302
Od04g01850	Blue	Green	30.59	20.56	-0.573	0.0349
Od09g02400	Blue	Green	36.69	24.59	-0.577	0.0395
Od06g04960	Blue	Green	39.03	26.09	-0.581	0.0275
Od05g02950	Blue	Green	107.45	71.80	-0.581	0.0300
Od14g01210	Blue	Green	346.30	231.26	-0.583	0.0237
Od08g02210	Blue	Green	87.21	58.17	-0.584	0.0199
Od14g00810	Blue	Green	19.94	13.28	-0.586	0.0426
Od12g03190	Blue	Green	186.91	124.52	-0.586	0.0281
Od06g02210	Blue	Green	30.11	20.02	-0.589	0.0461
Od06g06050	Blue	Green	24.96	16.59	-0.589	0.0202
Od06g07330	Blue	Green	26.87	17.86	-0.589	0.0290
Od06g05280	Blue	Green	104.52	69.45	-0.590	0.0195
Od04g04980	Blue	Green	62.17	41.27	-0.591	0.0170
Od11g00160	Blue	Green	411.93	273.22	-0.592	0.0174
Od13g00080	Blue	Green	33.03	21.90	-0.593	0.0202
Od04g05310	Blue	Green	192.52	127.67	-0.593	0.0199
Od20g01710	Blue	Green	162.46	107.74	-0.593	0.0177
Od08g02960	Blue	Green	58.32	38.68	-0.593	0.0284
Od01g05680	Blue	Green	79.08	52.42	-0.593	0.0210
Od20g01930	Blue	Green	7.02	4.65	-0.594	0.0284
Od05g03190	Blue	Green	41.61	27.57	-0.594	0.0465
Od07g01500	Blue	Green	37.54	24.86	-0.594	0.0290
Od03g02690	Blue	Green	24.11	15.96	-0.595	0.0234
Od07g01740	Blue	Green	156.97	103.86	-0.596	0.0217
Od20g00290	Blue	Green	83.42	55.15	-0.597	0.0202
Od03g01220	Blue	Green	119.42	78.90	-0.598	0.0206
Od13g02330	Blue	Green	33.62	22.20	-0.599	0.0220
Od02g00430	Blue	Green	22.59	14.92	-0.599	0.0381
Od09g06110	Blue	Green	52.86	34.90	-0.599	0.0294

Od12g01750	Blue	Green	96.64	63.79	-0.599	0.0180
Od15g00100	Blue	Green	92.69	61.18	-0.599	0.0130
Od13g02140	Blue	Green	133.90	88.33	-0.600	0.0170
Od13g01580	Blue	Green	521.01	343.20	-0.602	0.0138
Od04g00430	Blue	Green	22.41	14.75	-0.604	0.0224
Od06g00390	Blue	Green	44.81	29.47	-0.604	0.0134
Od12g00800	Blue	Green	31.22	20.53	-0.605	0.0231
Od13g00300	Blue	Green	63.24	41.58	-0.605	0.0355
Od03g00540	Blue	Green	11.13	7.31	-0.606	0.0426
Od09g04070	Blue	Green	48.74	32.01	-0.607	0.0146
Od16g01790	Blue	Green	382.35	251.02	-0.607	0.0337
Od04g00060	Blue	Green	92.68	60.85	-0.607	0.0177
Od13g01800	Blue	Green	59.75	39.21	-0.608	0.0265
Od14g02410	Blue	Green	115.52	75.79	-0.608	0.0154
Od01g03870	Blue	Green	45.61	29.91	-0.609	0.0275
Od09g04670	Blue	Green	26.61	17.42	-0.611	0.0202
Od13g00590	Blue	Green	29.09	19.05	-0.611	0.0195
Od14g00390	Blue	Green	35.96	23.52	-0.612	0.0166
Od01g04230	Blue	Green	17.34	11.33	-0.614	0.0237
Od15g01180	Blue	Green	37.39	24.42	-0.615	0.0463
Od14g01660	Blue	Green	86.60	56.53	-0.615	0.0184
Od07g01860	Blue	Green	96.95	63.24	-0.616	0.0327
Od08g01820	Blue	Green	93.03	60.67	-0.617	0.0195
Od07g01630	Blue	Green	58.70	38.24	-0.618	0.0177
Od13g01310	Blue	Green	79.54	51.78	-0.619	0.0174
Od06g06480	Blue	Green	51.47	33.48	-0.620	0.0177
Od06g03700	Blue	Green	42.68	27.76	-0.620	0.0297
Od10g02090	Blue	Green	950.99	618.26	-0.621	0.0158
Od05g02560	Blue	Green	36.39	23.64	-0.622	0.0352
Od05g04620	Blue	Green	32.41	21.05	-0.622	0.0492
Od19g00150	Blue	Green	49.56	32.17	-0.624	0.0306
Od17g01100	Blue	Green	119.35	77.44	-0.624	0.0162
Od02g01580	Blue	Green	88.27	57.25	-0.625	0.0146
Od19g00730	Blue	Green	111.84	72.49	-0.626	0.0206
Od20g00930	Blue	Green	244.51	158.42	-0.626	0.0100
Od01g01260	Blue	Green	39.34	25.46	-0.628	0.0130
Od11g02070	Blue	Green	213.93	138.30	-0.629	0.0100
Od16g01910	Blue	Green	34.24	22.10	-0.631	0.0384
Od01g01700	Blue	Green	67.22	43.38	-0.632	0.0184
Od11g01470	Blue	Green	36.03	23.15	-0.638	0.0192
Od09g01560	Blue	Green	30.04	19.27	-0.640	0.0255
Od02g00160	Blue	Green	76.17	48.87	-0.640	0.0138
Od06g05140	Blue	Green	47.74	30.59	-0.642	0.0231

Od13g01210	Blue	Green	30.79	19.73	-0.643	0.0126
Od03g02740	Blue	Green	69.74	44.66	-0.643	0.0174
Od14g03150	Blue	Green	258.59	165.60	-0.643	0.0062
Od14g01310	Blue	Green	95.89	61.35	-0.644	0.0100
Od06g02910	Blue	Green	112.75	72.12	-0.645	0.0095
Od16g01730	Blue	Green	112.43	71.88	-0.645	0.0081
Od14g02010	Blue	Green	32.59	20.83	-0.646	0.0324
Od04g05040	Blue	Green	42.25	27.01	-0.646	0.0390
Od02g00880	Blue	Green	53.91	34.46	-0.646	0.0287
Od08g00090	Blue	Green	18.12	11.58	-0.646	0.0287
Od09g05910	Blue	Green	59.12	37.78	-0.646	0.0202
Od09g05320	Blue	Green	20.33	12.97	-0.648	0.0349
Od01g04300	Blue	Green	34.87	22.25	-0.648	0.0090
Od11g00080	Blue	Green	24.89	15.88	-0.649	0.0262
Od02g02740	Blue	Green	61.23	39.04	-0.649	0.0142
Od09g00260	Blue	Green	166.75	106.25	-0.650	0.0146
Od07g02670	Blue	Green	48.78	31.08	-0.650	0.0076
Od05g01260	Blue	Green	261.38	166.27	-0.653	0.0081
Od06g00520	Blue	Green	30.48	19.39	-0.653	0.0431
Od08g02400	Blue	Green	62.18	39.55	-0.653	0.0122
Od04g00970	Blue	Green	24.62	15.65	-0.654	0.0476
Od11g03070	Blue	Green	39.10	24.84	-0.655	0.0076
Od02g03880	Blue	Green	19.43	12.34	-0.655	0.0100
Od12g00010	Blue	Green	17.98	11.41	-0.656	0.0138
Od09g00310	Blue	Green	277.92	176.35	-0.656	0.0095
Od12g03470	Blue	Green	40.34	25.53	-0.660	0.0278
Od01g00800	Blue	Green	44.03	27.82	-0.662	0.0281
Od11g03270	Blue	Green	67.03	42.36	-0.662	0.0158
Od06g06390	Blue	Green	17.86	11.28	-0.663	0.0417
Od04g05090	Blue	Green	58.93	37.22	-0.663	0.0255
Od09g02740	Blue	Green	29.61	18.69	-0.664	0.0067
Od05g01180	Blue	Green	24.46	15.42	-0.665	0.0327
Od01g06790	Blue	Green	86.16	54.34	-0.665	0.0287
Od02g01150	Blue	Green	705.64	444.37	-0.667	0.0500
Od03g02120	Blue	Green	10.16	6.40	-0.667	0.0170
Od06g03060	Blue	Green	56.96	35.87	-0.667	0.0213
Od15g00490	Blue	Green	24.05	15.14	-0.667	0.0195
Od13g02570	Blue	Green	65.08	40.97	-0.667	0.0052
Od04g02750	Blue	Green	45.15	28.42	-0.668	0.0081
Od04g00250	Blue	Green	24.12	15.18	-0.668	0.0180
Od19g00570	Blue	Green	237.77	149.58	-0.669	0.0076
Od01g07020	Blue	Green	169.55	106.61	-0.669	0.0046
Od16g00890	Blue	Green	59.38	37.32	-0.670	0.0057

Od06g00830	Blue	Green	58.29	36.60	-0.671	0.0086
Od11g00620	Blue	Green	75.45	47.35	-0.672	0.0052
Od06g07420	Blue	Green	128.35	80.40	-0.675	0.0062
Od01g05110	Blue	Green	84.06	52.63	-0.676	0.0192
Od09g01220	Blue	Green	10.00	6.23	-0.682	0.0315
Od12g03130	Blue	Green	8.37	5.21	-0.683	0.0248
Od09g06210	Blue	Green	28.53	17.76	-0.684	0.0108
Od16g02520	Blue	Green	25.90	16.12	-0.684	0.0352
Od20g02900	Blue	Green	169.29	105.28	-0.685	0.0057
Od06g04370	Blue	Green	62.36	38.77	-0.686	0.0029
Od02g03700	Blue	Green	60.85	37.81	-0.687	0.0046
Od09g03070	Blue	Green	42.47	26.36	-0.688	0.0100
Od17g03060	Blue	Green	29.02	18.00	-0.689	0.0271
Od01g04140	Blue	Green	85.60	52.96	-0.693	0.0071
Od03g02830	Blue	Green	1629.82	1007.75	-0.694	0.0041
Od12g00850	Blue	Green	44.87	27.74	-0.694	0.0439
Od20g01260	Blue	Green	140.68	86.88	-0.695	0.0046
Od15g00810	Blue	Green	44.74	27.62	-0.695	0.0023
Od13g01110	Blue	Green	18.60	11.47	-0.698	0.0117
Od14g02720	Blue	Green	27.22	16.77	-0.699	0.0071
Od09g03960	Blue	Green	30.31	18.66	-0.699	0.0360
Od01g06620	Blue	Green	8.89	5.47	-0.700	0.0158
Od10g00340	Blue	Green	109.81	67.50	-0.702	0.0035
Od01g01190	Blue	Green	56.83	34.89	-0.704	0.0057
Od12g00060	Blue	Green	26.12	16.03	-0.705	0.0331
Od02g01330	Blue	Green	387.77	237.80	-0.705	0.0041
Od02g02310	Blue	Green	113.61	69.65	-0.706	0.0052
Od06g05360	Blue	Green	37.65	23.08	-0.706	0.0067
Od06g03190	Blue	Green	34.10	20.89	-0.707	0.0067
Od06g06580	Blue	Green	36.08	22.10	-0.707	0.0041
Od20g02420	Blue	Green	35.13	21.52	-0.707	0.0302
Od12g02800	Blue	Green	80.62	49.37	-0.708	0.0029
Od02g01320	Blue	Green	203.47	124.56	-0.708	0.0035
Od05g04810	Blue	Green	38.11	23.29	-0.710	0.0104
Od14g00700	Blue	Green	102.54	62.59	-0.712	0.0035
Od14g01350	Blue	Green	29.84	18.21	-0.713	0.0134
Od08g03250	Blue	Green	52.39	31.96	-0.713	0.0041
Od05g03180	Blue	Green	36.88	22.49	-0.713	0.0331
Od06g03710	Blue	Green	98.44	59.91	-0.717	0.0067
Od14g02450	Blue	Green	36.17	21.99	-0.718	0.0046
Od09g03510	Blue	Green	609.60	370.64	-0.718	0.0067
Od07g01660	Blue	Green	47.90	29.12	-0.718	0.0023
Od01g05270	Blue	Green	28.98	17.57	-0.722	0.0294

Od06g04690	Blue	Green	106.20	64.32	-0.723	0.0029
Od07g00310	Blue	Green	53.86	32.60	-0.724	0.0202
Od10g01480	Blue	Green	17.46	10.56	-0.725	0.0023
Od17g00920	Blue	Green	62.32	37.64	-0.727	0.0076
Od09g01350	Blue	Green	38.52	23.25	-0.728	0.0195
Od02g04230	Blue	Green	333.97	201.14	-0.731	0.0076
Od20g01020	Blue	Green	47.46	28.58	-0.732	0.0029
Od12g03840	Blue	Green	188.81	113.65	-0.732	0.0052
Od10g02290	Blue	Green	10.24	6.16	-0.733	0.0023
Od02g03200	Blue	Green	65.39	39.29	-0.735	0.0041
Od11g04050	Blue	Green	59.09	35.49	-0.735	0.0366
Od17g01360	Blue	Green	30.33	18.21	-0.736	0.0188
Od11g00490	Blue	Green	30.00	18.01	-0.736	0.0046
Od03g01590	Blue	Green	78.88	47.33	-0.737	0.0041
Od07g04070	Blue	Green	31.70	19.01	-0.738	0.0046
Od06g02230	Blue	Green	144.64	86.68	-0.739	0.0029
Od07g00510	Blue	Green	32.35	19.38	-0.739	0.0023
Od09g05240	Blue	Green	92.68	55.49	-0.740	0.0023
Od12g01640	Blue	Green	598.71	358.43	-0.740	0.0016
Od10g01700	Blue	Green	11.07	6.63	-0.740	0.0052
Od12g01220	Blue	Green	48.16	28.82	-0.741	0.0046
Od07g02950	Blue	Green	21.16	12.64	-0.743	0.0265
Od11g01550	Blue	Green	49.59	29.60	-0.744	0.0029
Od01g06230	Blue	Green	38.01	22.66	-0.747	0.0095
Od20g03360	Blue	Green	20.86	12.39	-0.751	0.0180
Od20g01910	Blue	Green	42.44	25.20	-0.752	0.0100
Od04g02090	Blue	Green	86.89	51.54	-0.754	0.0035
Od03g00890	Blue	Green	114.86	67.91	-0.758	0.0202
Od07g02460	Blue	Green	131.91	77.93	-0.759	0.0023
Od19g00380	Blue	Green	37.02	21.84	-0.761	0.0154
Od17g00420	Blue	Green	49.72	29.32	-0.762	0.0009
Od19g00920	Blue	Green	19.82	11.68	-0.763	0.0029
Od05g01850	Blue	Green	75.32	44.33	-0.765	0.0035
Od06g05680	Blue	Green	38.18	22.46	-0.765	0.0104
Od16g01550	Blue	Green	369.74	217.47	-0.766	0.0016
Od03g01070	Blue	Green	31.92	18.76	-0.767	0.0035
Od02g02010	Blue	Green	85.61	50.30	-0.767	0.0016
Od06g01640	Blue	Green	55.02	32.26	-0.770	0.0023
Od03g02240	Blue	Green	153.74	89.92	-0.774	0.0009
Od10g00830	Blue	Green	329.78	192.86	-0.774	0.0009
Od14g02680	Blue	Green	106.81	62.44	-0.774	0.0016
Od06g00190	Blue	Green	148.89	87.00	-0.775	0.0009
Od12g02690	Blue	Green	31.95	18.64	-0.777	0.0146

Od14g01990	Blue	Green	57.13	33.31	-0.779	0.0029
Od06g03940	Blue	Green	34.33	19.99	-0.780	0.0199
Od20g01820	Blue	Green	55.73	32.44	-0.781	0.0071
Od11g01050	Blue	Green	101.50	59.06	-0.781	0.0009
Od16g01970	Blue	Green	24.33	14.14	-0.783	0.0009
Od05g03090	Blue	Green	12.23	7.10	-0.783	0.0029
Od09g06310	Blue	Green	31.96	18.57	-0.783	0.0057
Od11g03980	Blue	Green	19.07	11.07	-0.785	0.0275
Od20g01580	Blue	Green	264.37	153.44	-0.785	0.0009
Od03g03210	Blue	Green	268.20	155.61	-0.785	0.0009
Od16g00380	Blue	Green	68.95	39.95	-0.788	0.0046
Od06g06640	Blue	Green	166.44	96.10	-0.792	0.0016
Od17g00750	Blue	Green	10.00	5.76	-0.795	0.0315
Od05g00600	Blue	Green	49.68	28.61	-0.796	0.0009
Od02g04740	Blue	Green	159.51	91.86	-0.796	0.0016
Od02g03890	Blue	Green	51.60	29.71	-0.797	0.0009
Od05g04790	Blue	Green	11.20	6.45	-0.797	0.0009
Od12g01680	Blue	Green	33.20	19.10	-0.798	0.0009
Od05g00700	Blue	Green	49.77	28.61	-0.799	0.0023
Od11g02720	Blue	Green	147.99	84.98	-0.800	0.0023
Od06g07000	Blue	Green	27.84	15.98	-0.801	0.0126
Od13g02190	Blue	Green	25.90	14.85	-0.802	0.0041
Od06g06240	Blue	Green	87.36	50.09	-0.802	0.0126
Od04g03140	Blue	Green	118.52	67.96	-0.802	0.0009
Od09g06080	Blue	Green	61.14	35.05	-0.802	0.0009
Od16g02570	Blue	Green	107.93	61.84	-0.803	0.0029
Od01g04010	Blue	Green	33.89	19.38	-0.806	0.0009
Od11g02930	Blue	Green	45.32	25.91	-0.807	0.0062
Od20g00280	Blue	Green	109.69	62.68	-0.807	0.0009
Od05g04770	Blue	Green	65.92	37.66	-0.808	0.0117
Od03g02590	Blue	Green	75.97	43.30	-0.811	0.0113
Od12g03830	Blue	Green	9.65	5.50	-0.812	0.0016
Od06g01710	Blue	Green	82.18	46.77	-0.813	0.0029
Od10g00890	Blue	Green	87.08	49.56	-0.813	0.0052
Od08g03120	Blue	Green	26.19	14.90	-0.814	0.0150
Od09g02900	Blue	Green	12.39	7.04	-0.815	0.0052
Od02g02480	Blue	Green	29.09	16.53	-0.815	0.0023
Od01g05760	Blue	Green	15.88	9.02	-0.816	0.0009
Od14g03010	Blue	Green	53.04	30.11	-0.817	0.0009
Od08g00910	Blue	Green	111.33	63.20	-0.817	0.0009
Od06g00250	Blue	Green	108.63	61.65	-0.817	0.0009
Od05g03270	Blue	Green	18.06	10.24	-0.819	0.0104
Od10g00110	Blue	Green	52.71	29.87	-0.819	0.0009

Od01g01310	Blue	Green	91.36	51.66	-0.823	0.0009
Od01g01160	Blue	Green	15.15	8.56	-0.823	0.0395
Od01g06040	Blue	Green	40.45	22.81	-0.826	0.0009
Od07g02940	Blue	Green	73.86	41.61	-0.828	0.0009
Od01g00970	Blue	Green	41.56	23.38	-0.830	0.0052
Od04g01730	Blue	Green	57.27	32.20	-0.831	0.0369
Od14g00870	Blue	Green	2.41	1.36	-0.831	0.0231
Od05g04960	Blue	Green	138.22	77.67	-0.831	0.0016
Od01g04280	Blue	Green	38.02	21.35	-0.833	0.0009
Od10g00130	Blue	Green	131.46	73.74	-0.834	0.0035
Od10g02460	Blue	Green	12.50	7.00	-0.835	0.0009
Od08g03230	Blue	Green	40.00	22.40	-0.836	0.0081
Od06g04290	Blue	Green	214.31	120.03	-0.836	0.0009
Od04g04790	Blue	Green	29.99	16.77	-0.838	0.0016
Od14g01750	Blue	Green	25.08	14.01	-0.840	0.0057
Od06g03070	Blue	Green	71.29	39.71	-0.844	0.0046
Od19g00930	Blue	Green	91.00	50.66	-0.845	0.0057
Od08g01280	Blue	Green	284.20	157.93	-0.848	0.0009
Od07g03870	Blue	Green	11.07	6.15	-0.848	0.0227
Od02g00970	Blue	Green	49.09	27.26	-0.849	0.0035
Od02g03110	Blue	Green	77.43	42.98	-0.849	0.0009
Od14g02920	Blue	Green	48.94	27.17	-0.849	0.0016
Od12g02460	Blue	Green	44.25	24.55	-0.850	0.0108
Od14g02460	Blue	Green	85.27	47.27	-0.851	0.0009
Od11g01460	Blue	Green	17.71	9.80	-0.853	0.0158
Od17g01280	Blue	Green	23.97	13.26	-0.854	0.0035
Od14g00170	Blue	Green	130.53	72.20	-0.854	0.0009
Od11g01950	Blue	Green	260.78	144.15	-0.855	0.0009
Od19g00090	Blue	Green	207.89	114.89	-0.856	0.0009
Od19g01060	Blue	Green	782.92	432.54	-0.856	0.0009
Od06g07410	Blue	Green	93.26	51.50	-0.857	0.0009
Od15g00160	Blue	Green	21.63	11.94	-0.858	0.0029
Od17g00980	Blue	Green	16.45	9.08	-0.858	0.0255
Od14g01240	Blue	Green	42.61	23.48	-0.860	0.0009
Od08g02120	Blue	Green	12.49	6.87	-0.862	0.0335
Od13g01540	Blue	Green	47.66	26.21	-0.863	0.0315
Od13g02610	Blue	Green	43.54	23.89	-0.866	0.0009
Od12g00690	Blue	Green	326.95	179.34	-0.866	0.0009
Od05g00470	Blue	Green	32.95	18.07	-0.866	0.0016
Od01g05260	Blue	Green	186.20	102.11	-0.867	0.0009
Od04g03500	Blue	Green	31.54	17.26	-0.870	0.0009
Od07g03500	Blue	Green	120.55	65.93	-0.871	0.0009
Od04g00500	Blue	Green	42.63	23.30	-0.872	0.0029

Od12g03250	Blue	Green	27.25	14.88	-0.873	0.0009
Od02g03690	Blue	Green	13.43	7.33	-0.874	0.0100
Od10g00780	Blue	Green	15.78	8.61	-0.875	0.0184
Od01g04120	Blue	Green	59.84	32.63	-0.875	0.0009
Od17g03020	Blue	Green	72.11	39.27	-0.877	0.0009
Od10g00450	Blue	Green	281.85	153.45	-0.877	0.0029
Od06g02880	Blue	Green	106.88	58.13	-0.879	0.0009
Od10g00880	Blue	Green	106.05	57.67	-0.879	0.0023
Od09g02310	Blue	Green	32.18	17.49	-0.880	0.0271
Od09g03580	Blue	Green	16.55	8.99	-0.881	0.0057
Od13g02590	Blue	Green	70.06	38.00	-0.883	0.0086
Od10g00720	Blue	Green	89.75	48.62	-0.885	0.0009
Od04g04960	Blue	Green	12.33	6.67	-0.885	0.0009
Od03g02610	Blue	Green	241.06	130.49	-0.885	0.0009
Od12g02090	Blue	Green	65.02	35.19	-0.886	0.0009
Od20g02320	Blue	Green	23.42	12.68	-0.886	0.0067
Od05g01880	Blue	Green	27.79	15.04	-0.886	0.0023
Od01g02820	Blue	Green	32.42	17.53	-0.887	0.0009
Od01g00810	Blue	Green	43.10	23.28	-0.889	0.0009
Od08g03280	Blue	Green	33.76	18.23	-0.889	0.0023
Od11g02190	Blue	Green	110.98	59.83	-0.891	0.0009
Od04g00930	Blue	Green	29.57	15.94	-0.891	0.0016
Od16g00170	Blue	Green	115.15	62.03	-0.892	0.0009
Od09g06130	Blue	Green	843.75	454.51	-0.892	0.0009
Od12g02330	Blue	Green	19.25	10.37	-0.893	0.0442
Od01g04930	Blue	Green	11.69	6.29	-0.894	0.0227
Od01g01950	Blue	Green	75.08	40.33	-0.896	0.0009
Od03g01380	Blue	Green	22.19	11.92	-0.897	0.0009
Od03g02870	Blue	Green	15.90	8.54	-0.897	0.0113
Od06g02430	Blue	Green	116.76	62.66	-0.898	0.0009
Od09g01260	Blue	Green	107.80	57.74	-0.901	0.0009
Od11g01590	Blue	Green	6.49	3.47	-0.901	0.0363
Od01g02230	Blue	Green	11.07	5.93	-0.901	0.0177
Od05g00150	Blue	Green	89.79	48.04	-0.902	0.0009
Od06g01230	Blue	Green	13.39	7.16	-0.903	0.0162
Od12g03660	Blue	Green	22.34	11.94	-0.904	0.0392
Od06g03090	Blue	Green	74.12	39.57	-0.906	0.0009
Od05g02890	Blue	Green	137.13	73.19	-0.906	0.0009
Od04g04750	Blue	Green	69.43	36.98	-0.909	0.0009
Od20g02460	Blue	Green	65.20	34.67	-0.911	0.0016
Od09g05630	Blue	Green	37.47	19.91	-0.912	0.0009
Od01g05600	Blue	Green	55.93	29.72	-0.912	0.0009
Od12g00130	Blue	Green	119.20	63.31	-0.913	0.0009

Od09g04910	Blue	Green	139.84	74.21	-0.914	0.0009
Od11g01910	Blue	Green	24.10	12.78	-0.915	0.0009
Od04g01720	Blue	Green	20.25	10.73	-0.916	0.0046
Od12g03340	Blue	Green	25.79	13.66	-0.917	0.0041
Od11g02130	Blue	Green	8.33	4.41	-0.917	0.0476
Od05g01480	Blue	Green	18.56	9.83	-0.918	0.0009
Od09g05870	Blue	Green	125.57	66.40	-0.919	0.0009
Od11g02370	Blue	Green	31.06	16.42	-0.920	0.0009
Od13g00120	Blue	Green	27.73	14.65	-0.920	0.0009
Od20g00380	Blue	Green	78.22	41.28	-0.922	0.0016
Od07g02720	Blue	Green	45.88	24.21	-0.922	0.0009
Od12g00150	Blue	Green	121.01	63.84	-0.923	0.0009
Od08g00490	Blue	Green	20.54	10.83	-0.923	0.0009
Od07g04510	Blue	Green	110.52	58.12	-0.927	0.0009
Od12g00030	Blue	Green	58.32	30.63	-0.929	0.0009
Od09g00890	Blue	Green	18.74	9.80	-0.935	0.0355
Od06g05210	Blue	Green	21.15	11.04	-0.938	0.0090
Od06g02660	Blue	Green	25.61	13.37	-0.938	0.0009
Od10g02550	Blue	Green	9.29	4.85	-0.939	0.0009
Od12g02860	Blue	Green	159.18	82.93	-0.941	0.0009
Od12g00040	Blue	Green	37.71	19.62	-0.943	0.0009
Od02g03580	Blue	Green	81.15	42.14	-0.945	0.0009
Od15g00210	Blue	Green	92.28	47.89	-0.946	0.0009
Od04g05220	Blue	Green	141.83	73.51	-0.948	0.0009
Od20g02080	Blue	Green	90.53	46.79	-0.952	0.0009
Od16g01770	Blue	Green	24.10	12.44	-0.954	0.0117
Od09g03330	Blue	Green	78.87	40.65	-0.956	0.0009
Od04g04730	Blue	Green	18.53	9.54	-0.957	0.0016
Od03g02600	Blue	Green	23.84	12.26	-0.960	0.0262
Od05g02520	Blue	Green	19.56	10.03	-0.963	0.0009
Od17g01120	Blue	Green	45.77	23.45	-0.965	0.0009
Od08g00450	Blue	Green	27.33	13.98	-0.967	0.0009
Od17g01290	Blue	Green	9.82	5.02	-0.967	0.0035
Od11g04450	Blue	Green	85.21	43.58	-0.968	0.0041
Od01g02860	Blue	Green	279.13	142.43	-0.971	0.0009
Od20g02870	Blue	Green	79.82	40.72	-0.971	0.0009
Od05g04730	Blue	Green	127.31	64.70	-0.977	0.0009
Od02g00150	Blue	Green	19.64	9.97	-0.978	0.0009
Od17g00030	Blue	Green	50.78	25.74	-0.980	0.0009
Od03g01460	Blue	Green	66.28	33.60	-0.980	0.0095
Od09g00610	Blue	Green	21.00	10.64	-0.980	0.0009
Od07g02340	Blue	Green	46.04	23.28	-0.984	0.0009
Od13g01020	Blue	Green	1094.84	553.22	-0.985	0.0009

Od04g03830	Blue	Green	19.29	9.73	-0.987	0.0052
Od05g03450	Blue	Green	24.87	12.54	-0.989	0.0343
Od03g01440	Blue	Green	16.79	8.46	-0.989	0.0009
Od11g01100	Blue	Green	5.45	2.74	-0.990	0.0009
Od11g03080	Blue	Green	201.23	101.10	-0.993	0.0009
Od05g03260	Blue	Green	13.28	6.65	-0.997	0.0268
Od12g02990	Blue	Green	43.77	21.91	-0.998	0.0016
Od10g01130	Blue	Green	30.36	15.19	-0.999	0.0009
Od05g03580	Blue	Green	24.88	12.43	-1.001	0.0134
Od20g00250	Blue	Green	42.02	20.96	-1.003	0.0009
Od12g03740	Blue	Green	26.89	13.41	-1.004	0.0009
Od04g02130	Blue	Green	29.15	14.51	-1.007	0.0009
Od09g00850	Blue	Green	19.08	9.49	-1.007	0.0009
Od13g02790	Blue	Green	34.40	17.11	-1.008	0.0009
Od20g02350	Blue	Green	6.46	3.20	-1.011	0.0245
Od07g00910	Blue	Green	36.05	17.88	-1.012	0.0041
Od04g01690	Blue	Green	59.58	29.54	-1.012	0.0016
Od09g02820	Blue	Green	17.75	8.79	-1.013	0.0090
Od06g00290	Blue	Green	20.49	10.15	-1.013	0.0009
Od06g07570	Blue	Green	19.05	9.44	-1.013	0.0016
Od10g02330	Blue	Green	12.38	6.13	-1.014	0.0009
Od05g00160	Blue	Green	10.99	5.43	-1.016	0.0009
Od06g00130	Blue	Green	165.51	81.83	-1.016	0.0009
Od12g02080	Blue	Green	38.73	19.06	-1.023	0.0016
Od01g00580	Blue	Green	28.44	14.00	-1.023	0.0009
Od07g00980	Blue	Green	36.32	17.86	-1.024	0.0009
Od05g04200	Blue	Green	18.28	8.98	-1.025	0.0009
Od04g00270	Blue	Green	24.57	12.06	-1.027	0.0023
Od17g00760	Blue	Green	11.99	5.87	-1.031	0.0162
Od08g01500	Blue	Green	20.85	10.17	-1.035	0.0009
Od08g02850	Blue	Green	51.35	25.04	-1.036	0.0009
Od04g00110	Blue	Green	5.91	2.88	-1.037	0.0009
Od07g04150	Blue	Green	43.63	21.26	-1.037	0.0046
Od19g00100	Blue	Green	289.99	140.98	-1.040	0.0142
Od10g00970	Blue	Green	31.98	15.54	-1.041	0.0009
Od05g04110	Blue	Green	15.11	7.34	-1.042	0.0217
Od16g01410	Blue	Green	36.08	17.51	-1.043	0.0009
Od01g03470	Blue	Green	101.11	49.07	-1.043	0.0009
Od11g03700	Blue	Green	26.84	13.02	-1.043	0.0130
Od13g01890	Blue	Green	12.68	6.15	-1.043	0.0009
Od04g04740	Blue	Green	21.26	10.31	-1.045	0.0217
Od19g00140	Blue	Green	96.15	46.60	-1.045	0.0177
Od14g00920	Blue	Green	55.06	26.68	-1.045	0.0009

Od01g06400	Blue	Green	32.36	15.66	-1.047	0.0009
Od16g01850	Blue	Green	54.11	26.19	-1.047	0.0009
Od14g00130	Blue	Green	162.67	78.61	-1.049	0.0009
Od09g05670	Blue	Green	8.00	3.86	-1.050	0.0461
Od02g01450	Blue	Green	81.01	39.07	-1.052	0.0009
Od07g02850	Blue	Green	50.16	24.13	-1.056	0.0009
Od06g01410	Blue	Green	15.20	7.31	-1.057	0.0095
Od04g03550	Blue	Green	101.73	48.84	-1.059	0.0009
Od03g00470	Blue	Green	7.33	3.50	-1.066	0.0134
Od19g00810	Blue	Green	10.02	4.75	-1.076	0.0217
Od17g00780	Blue	Green	60.97	28.83	-1.081	0.0009
Od20g01600	Blue	Green	17.73	8.37	-1.083	0.0009
Od04g01430	Blue	Green	20.44	9.65	-1.083	0.0009
Od16g00290	Blue	Green	151.62	71.54	-1.084	0.0275
Od19g01100	Blue	Green	137.62	64.92	-1.084	0.0009
Od09g01440	Blue	Green	128.42	60.51	-1.086	0.0009
Od10g01280	Blue	Green	5.56	2.62	-1.086	0.0405
Od04g03180	Blue	Green	64.88	30.52	-1.088	0.0009
Od03g00260	Blue	Green	62.71	29.47	-1.089	0.0009
Od17g00240	Blue	Green	49.98	23.46	-1.091	0.0009
Od16g02280	Blue	Green	16.89	7.92	-1.092	0.0108
Od02g03870	Blue	Green	122.04	57.11	-1.095	0.0009
Od13g01980	Blue	Green	12.31	5.76	-1.096	0.0177
Od11g00340	Blue	Green	21.25	9.93	-1.098	0.0016
Od10g01230	Blue	Green	25.19	11.76	-1.099	0.0029
Od16g02450	Blue	Green	34.53	16.12	-1.099	0.0023
Od19g01210	Blue	Green	6.03	2.81	-1.101	0.0150
Od01g06940	Blue	Green	7.33	3.42	-1.101	0.0455
Od07g03710	Blue	Green	17.87	8.32	-1.103	0.0016
Od05g01080	Blue	Green	38.23	17.71	-1.110	0.0009
Od15g00200	Blue	Green	25.26	11.68	-1.113	0.0199
Od07g04770	Blue	Green	6.70	3.09	-1.115	0.0100
Od11g02480	Blue	Green	64.90	29.96	-1.115	0.0009
Od09g00390	Blue	Green	41.22	19.01	-1.117	0.0009
Od10g02310	Blue	Green	34.36	15.79	-1.122	0.0009
Od04g04360	Blue	Green	34.22	15.72	-1.123	0.0009
Od12g01050	Blue	Green	28.92	13.27	-1.123	0.0016
Od16g01870	Blue	Green	105.37	48.36	-1.124	0.0009
Od14g02600	Blue	Green	27.25	12.46	-1.130	0.0009
Od01g01440	Blue	Green	68.84	31.45	-1.130	0.0009
Od17g03010	Blue	Green	178.61	81.58	-1.131	0.0009
Od14g02480	Blue	Green	101.10	46.16	-1.131	0.0009
Od17g02090	Blue	Green	102.08	46.58	-1.132	0.0090

Od17g01560	Blue	Green	185.83	84.78	-1.132	0.0009
Od13g01900	Blue	Green	22.85	10.42	-1.132	0.0009
Od06g04750	Blue	Green	170.43	77.54	-1.136	0.0009
Od02g03930	Blue	Green	17.78	8.09	-1.137	0.0095
Od07g02890	Blue	Green	26.43	12.01	-1.138	0.0009
Od02g03320	Blue	Green	29.83	13.52	-1.142	0.0009
Od02g04450	Blue	Green	6.45	2.91	-1.147	0.0100
Od19g01270	Blue	Green	31.39	14.17	-1.147	0.0009
Od17g01240	Blue	Green	4.58	2.06	-1.152	0.0452
Od14g00990	Blue	Green	9.37	4.22	-1.152	0.0016
Od17g01170	Blue	Green	28.86	12.96	-1.155	0.0009
Od14g00290	Blue	Green	3.06	1.37	-1.158	0.0217
Od14g00640	Blue	Green	14.76	6.61	-1.159	0.0009
Od01g01560	Blue	Green	11.57	5.17	-1.162	0.0057
Od16g00130	Blue	Green	5.88	2.62	-1.167	0.0248
Od07g03210	Blue	Green	22.29	9.89	-1.172	0.0023
Od19g00750	Blue	Green	26.66	11.82	-1.173	0.0009
Od01g05400	Blue	Green	28.62	12.67	-1.176	0.0009
Od09g01340	Blue	Green	25.01	11.06	-1.177	0.0009
Od10g02190	Blue	Green	8.51	3.76	-1.179	0.0086
Od12g00110	Blue	Green	18.11	7.99	-1.180	0.0009
Od09g05820	Blue	Green	43.53	19.14	-1.186	0.0009
Od12g00160	Blue	Green	110.67	48.59	-1.187	0.0009
Od06g02150	Blue	Green	16.32	7.15	-1.190	0.0258
Od10g02340	Blue	Green	45.78	19.98	-1.196	0.0009
Od05g01230	Blue	Green	59.71	26.04	-1.197	0.0046
Od17g00090	Blue	Green	83.30	36.19	-1.203	0.0009
Od06g04890	Blue	Green	203.82	88.47	-1.204	0.0009
Od02g03670	Blue	Green	121.80	52.84	-1.205	0.0009
Od07g02920	Blue	Green	159.28	68.76	-1.212	0.0009
Od11g00130	Blue	Green	143.09	61.60	-1.216	0.0009
Od05g00940	Blue	Green	2.49	1.07	-1.216	0.0497
Od11g04240	Blue	Green	328.77	141.38	-1.218	0.0009
Od04g00670	Blue	Green	130.46	56.09	-1.218	0.0009
Od13g02310	Blue	Green	11.93	5.09	-1.230	0.0100
Od02g04830	Blue	Green	28.18	12.00	-1.232	0.0009
Od08g03860	Blue	Green	86.82	36.96	-1.232	0.0009
Od08g01990	Blue	Green	10.72	4.56	-1.234	0.0016
Od01g02880	Blue	Green	20.62	8.75	-1.237	0.0009
Od19g00990	Blue	Green	4.15	1.76	-1.237	0.0009
Od12g02100	Blue	Green	48.04	20.38	-1.237	0.0009
Od08g00650	Blue	Green	50.61	21.41	-1.241	0.0009
Od01g04130	Blue	Green	101.97	43.13	-1.241	0.0009

Od13g02290	Blue	Green	161.19	67.51	-1.256	0.0009
Od03g03160	Blue	Green	183.75	76.95	-1.256	0.0009
Od06g06590	Blue	Green	47.44	19.86	-1.256	0.0009
Od11g00680	Blue	Green	25.96	10.86	-1.258	0.0016
Od09g06120	Blue	Green	50.12	20.96	-1.258	0.0009
Od17g02150	Blue	Green	9.17	3.80	-1.272	0.0023
Od03g03030	Blue	Green	17.81	7.37	-1.273	0.0009
Od01g03680	Blue	Green	24.40	10.09	-1.274	0.0029
Od15g00840	Blue	Green	9.53	3.93	-1.277	0.0035
Od17g01040	Blue	Green	108.45	44.74	-1.277	0.0009
Od11g02550	Blue	Green	2.94	1.21	-1.278	0.0434
Od16g01060	Blue	Green	23.08	9.51	-1.279	0.0009
Od11g01290	Blue	Green	20.71	8.53	-1.279	0.0009
Od12g00910	Blue	Green	6.21	2.55	-1.284	0.0195
Od09g05840	Blue	Green	13.22	5.42	-1.287	0.0009
Od10g01390	Blue	Green	35.09	14.37	-1.288	0.0009
Od10g01020	Blue	Green	73.72	30.15	-1.290	0.0009
Od07g00100	Blue	Green	210.40	86.01	-1.291	0.0009
Od10g00840	Blue	Green	303.20	123.87	-1.291	0.0009
Od01g04830	Blue	Green	21.22	8.66	-1.293	0.0009
Od12g00140	Blue	Green	495.77	202.09	-1.295	0.0009
Od06g04390	Blue	Green	15.97	6.49	-1.299	0.0009
Od01g04670	Blue	Green	20.34	8.25	-1.302	0.0009
Od13g00360	Blue	Green	24.39	9.88	-1.303	0.0016
Od01g01690	Blue	Green	275.49	111.51	-1.305	0.0009
Od06g04320	Blue	Green	30.30	12.23	-1.308	0.0009
Od19g00740	Blue	Green	505.52	203.97	-1.309	0.0009
Od06g07370	Blue	Green	94.20	37.97	-1.311	0.0009
Od01g00210	Blue	Green	54.69	22.03	-1.312	0.0009
Od20g02360	Blue	Green	13.20	5.31	-1.314	0.0009
Od01g06100	Blue	Green	2.55	1.03	-1.316	0.0217
Od01g04460	Blue	Green	53.87	21.59	-1.319	0.0009
Od02g04150	Blue	Green	5.65	2.26	-1.319	0.0009
Od14g01200	Blue	Green	6.17	2.47	-1.320	0.0081
Od04g04880	Blue	Green	47.65	19.03	-1.324	0.0009
Od01g05590	Blue	Green	23.61	9.42	-1.325	0.0009
Od06g03670	Blue	Green	31.07	12.38	-1.328	0.0009
Od16g00280	Blue	Green	122.12	48.63	-1.328	0.0009
Od15g00150	Blue	Green	21.59	8.55	-1.336	0.0009
Od20g00470	Blue	Green	19.92	7.84	-1.345	0.0265
Od07g00010	Blue	Green	10.98	4.31	-1.349	0.0009
Od15g00790	Blue	Green	43.78	17.18	-1.350	0.0009
Od12g00100	Blue	Green	35.24	13.78	-1.355	0.0009

Od16g01220	Blue	Green	31.89	12.45	-1.356	0.0009
Od11g00060	Blue	Green	76.97	30.05	-1.357	0.0009
Od10g01870	Blue	Green	218.38	85.01	-1.361	0.0009
Od02g00310	Blue	Green	1735.42	672.34	-1.368	0.0009
Od06g02450	Blue	Green	24.26	9.39	-1.370	0.0117
Od20g02780	Blue	Green	13.96	5.39	-1.373	0.0009
Od13g03140	Blue	Green	6.86	2.64	-1.378	0.0071
Od09g01150	Blue	Green	35.96	13.80	-1.382	0.0009
Od01g03970	Blue	Green	59.00	22.56	-1.387	0.0009
Od08g00250	Blue	Green	26.94	10.30	-1.387	0.0035
Od06g04940	Blue	Green	122.21	46.69	-1.388	0.0009
Od20g01140	Blue	Green	76.62	29.19	-1.392	0.0009
Od02g04950	Blue	Green	93.22	35.44	-1.395	0.0009
Od14g01000	Blue	Green	44.44	16.89	-1.396	0.0009
Od12g02680	Blue	Green	32.70	12.43	-1.396	0.0009
Od12g03330	Blue	Green	5.32	2.02	-1.397	0.0035
Od10g02430	Blue	Green	108.90	41.26	-1.400	0.0076
Od02g03170	Blue	Green	23.71	8.91	-1.411	0.0009
Od16g02500	Blue	Green	71.93	27.00	-1.414	0.0009
Od05g01170	Blue	Green	918.57	344.45	-1.415	0.0009
Od01g03690	Blue	Green	24.68	9.22	-1.421	0.0009
Od16g01180	Blue	Green	24.20	9.02	-1.424	0.0009
Od04g00790	Blue	Green	29.40	10.93	-1.428	0.0009
Od02g04350	Blue	Green	536.13	199.27	-1.428	0.0009
Od09g00660	Blue	Green	22.38	8.32	-1.428	0.0009
Od02g00280	Blue	Green	66.54	24.67	-1.432	0.0009
Od05g01200	Blue	Green	6.84	2.52	-1.439	0.0076
Od11g00170	Blue	Green	113.95	41.95	-1.442	0.0009
Od05g00890	Blue	Green	106.18	38.94	-1.447	0.0009
Od16g02460	Blue	Green	172.46	63.13	-1.450	0.0009
Od11g03030	Blue	Green	74.08	27.11	-1.450	0.0009
Od10g02150	Blue	Green	253.01	92.49	-1.452	0.0009
Od15g01490	Blue	Green	6.05	2.21	-1.455	0.0287
Od04g04460	Blue	Green	49.01	17.88	-1.455	0.0009
Od01g05320	Blue	Green	46.92	17.06	-1.460	0.0009
Od11g01110	Blue	Green	16.04	5.80	-1.467	0.0009
Od09g05100	Blue	Green	65.13	23.56	-1.467	0.0016
Od01g02300	Blue	Green	57.19	20.62	-1.472	0.0009
Od04g03210	Blue	Green	19.21	6.91	-1.475	0.0009
Od06g00540	Blue	Green	18.50	6.65	-1.476	0.0009
Od04g03740	Blue	Green	35.58	12.78	-1.477	0.0009
Od09g02830	Blue	Green	14.83	5.32	-1.480	0.0009
Od17g00270	Blue	Green	29.18	10.41	-1.487	0.0009

Od02g05030	Blue	Green	30.96	11.04	-1.488	0.0029
Od04g00100	Blue	Green	3.77	1.34	-1.491	0.0100
Od01g01650	Blue	Green	40.32	14.23	-1.503	0.0009
Od17g02170	Blue	Green	49.89	17.52	-1.510	0.0009
Od12g00180	Blue	Green	21.56	7.57	-1.511	0.0009
Od10g00330	Blue	Green	29.36	10.29	-1.513	0.0009
Od11g00700	Blue	Green	45.29	15.81	-1.518	0.0009
Od14g02910	Blue	Green	11.36	3.96	-1.520	0.0076
Od11g00400	Blue	Green	16.48	5.70	-1.532	0.0009
Od13g01180	Blue	Green	78.99	27.32	-1.532	0.0009
Od11g03280	Blue	Green	26.65	9.19	-1.537	0.0009
Od05g03390	Blue	Green	7.99	2.75	-1.539	0.0009
Od08g00520	Blue	Green	157.67	54.25	-1.539	0.0009
Od08g01830	Blue	Green	16.67	5.72	-1.542	0.0016
Od04g05020	Blue	Green	43.42	14.91	-1.543	0.0009
Od17g02180	Blue	Green	19.04	6.53	-1.545	0.0009
Od02g04480	Blue	Green	71.34	24.40	-1.548	0.0009
Od05g03930	Blue	Green	44.35	15.16	-1.548	0.0009
Od01g07040	Blue	Green	3.27	1.11	-1.552	0.0090
Od05g01470	Blue	Green	24.18	8.24	-1.553	0.0009
Od15g00350	Blue	Green	28.28	9.64	-1.553	0.0009
Od04g00310	Blue	Green	13.61	4.63	-1.556	0.0306
Od07g00210	Blue	Green	7.30	2.48	-1.559	0.0146
Od11g02410	Blue	Green	9.96	3.36	-1.567	0.0258
Od09g00120	Blue	Green	4.81	1.62	-1.569	0.0162
Od19g01120	Blue	Green	9.48	3.17	-1.578	0.0117
Od01g02570	Blue	Green	26.11	8.74	-1.579	0.0009
Od20g01510	Blue	Green	8.68	2.90	-1.581	0.0009
Od07g00340	Blue	Green	14.56	4.82	-1.594	0.0188
Od06g02440	Blue	Green	8.25	2.73	-1.595	0.0255
Od09g05920	Blue	Green	39.02	12.81	-1.607	0.0009
Od10g01930	Blue	Green	3.40	1.10	-1.627	0.0009
Od04g05300	Blue	Green	82.96	26.81	-1.630	0.0009
Od01g01230	Blue	Green	130.38	41.98	-1.635	0.0009
Od06g01250	Blue	Green	68.68	22.11	-1.635	0.0009
Od15g00900	Blue	Green	18.63	5.99	-1.638	0.0009
Od06g01240	Blue	Green	50.35	16.17	-1.638	0.0009
Od06g01420	Blue	Green	9.89	3.17	-1.641	0.0052
Od16g00900	Blue	Green	14.86	4.76	-1.642	0.0009
Od08g02180	Blue	Green	34.29	10.98	-1.643	0.0009
Od13g00190	Blue	Green	107.42	34.24	-1.649	0.0009
Od04g00320	Blue	Green	6.08	1.93	-1.655	0.0324
Od10g01650	Blue	Green	27.04	8.58	-1.657	0.0009

Od06g01270	Blue	Green	16.03	5.03	-1.670	0.0009
Od01g03480	Blue	Green	30.52	9.52	-1.680	0.0009
Od15g01260	Blue	Green	9.25	2.87	-1.690	0.0009
Od11g01890	Blue	Green	70.42	21.80	-1.691	0.0009
Od08g01720	Blue	Green	11.44	3.52	-1.702	0.0009
Od04g00640	Blue	Green	3.04	0.93	-1.708	0.0337
Od11g02950	Blue	Green	18.21	5.56	-1.713	0.0268
Od09g00150	Blue	Green	105.66	32.09	-1.719	0.0009
Od08g00830	Blue	Green	10.71	3.24	-1.725	0.0113
Od09g03260	Blue	Green	14.85	4.47	-1.732	0.0029
Od07g02910	Blue	Green	37.85	11.37	-1.735	0.0009
Od03g00630	Blue	Green	23.47	7.04	-1.738	0.0009
Od01g04760	Blue	Green	75.50	22.60	-1.740	0.0009
Od13g03060	Blue	Green	16.08	4.72	-1.768	0.0081
Od11g04460	Blue	Green	207.26	60.85	-1.768	0.0009
Od06g05070	Blue	Green	15.44	4.53	-1.770	0.0009
Od06g06820	Blue	Green	46.15	13.53	-1.770	0.0009
Od10g00820	Blue	Green	316.61	92.77	-1.771	0.0009
Od02g00320	Blue	Green	46.61	13.65	-1.771	0.0009
Od01g05390	Blue	Green	8.03	2.35	-1.775	0.0237
Od03g03200	Blue	Green	4.09	1.19	-1.779	0.0076
Od01g05030	Blue	Green	183.89	52.45	-1.810	0.0009
Od13g00760	Blue	Green	15.40	4.37	-1.817	0.0009
Od03g01340	Blue	Green	68.92	19.39	-1.829	0.0009
Od08g01230	Blue	Green	17.00	4.74	-1.843	0.0009
Od20g01170	Blue	Green	35.95	9.89	-1.862	0.0009
Od12g00470	Blue	Green	22.55	6.20	-1.863	0.0009
Od10g00760	Blue	Green	243.53	66.90	-1.864	0.0009
Od04g00010	Blue	Green	19.02	5.22	-1.865	0.0009
Od01g03410	Blue	Green	41.05	11.22	-1.871	0.0009
Od01g06980	Blue	Green	33.08	9.04	-1.871	0.0009
Od08g01730	Blue	Green	62.70	17.11	-1.874	0.0009
Od20g00040	Blue	Green	43.46	11.85	-1.874	0.0009
Od06g01470	Blue	Green	20.51	5.58	-1.879	0.0009
Od01g04620	Blue	Green	3.02	0.82	-1.886	0.0162
Od01g06640	Blue	Green	22.21	6.00	-1.887	0.0009
Od04g05390	Blue	Green	3.20	0.86	-1.896	0.0321
Od14g03310	Blue	Green	125.26	33.48	-1.903	0.0009
Od09g02120	Blue	Green	19.65	5.25	-1.904	0.0009
Od06g00230	Blue	Green	17.86	4.76	-1.909	0.0009
Od14g02780	Blue	Green	23.81	6.27	-1.926	0.0009
Od06g02850	Blue	Green	345.45	90.30	-1.936	0.0009
Od05g00920	Blue	Green	9.51	2.44	-1.961	0.0009

Od14g03320	Blue	Green	73.39	18.70	-1.973	0.0009
Od19g00370	Blue	Green	76.82	19.46	-1.981	0.0009
Od12g01040	Blue	Green	72.47	18.35	-1.981	0.0009
Od17g00150	Blue	Green	8.83	2.22	-1.991	0.0122
Od06g04270	Blue	Green	8.04	2.01	-1.997	0.0287
Od12g00120	Blue	Green	22.32	5.56	-2.005	0.0009
Od14g00740	Blue	Green	45.32	11.15	-2.023	0.0009
Od16g00040	Blue	Green	5.43	1.33	-2.026	0.0009
Od12g00290	Blue	Green	40.58	9.89	-2.037	0.0009
Od15g00850	Blue	Green	15.17	3.56	-2.090	0.0009
Od16g02330	Blue	Green	28.09	6.49	-2.115	0.0146
Od16g02320	Blue	Green	28.36	6.53	-2.118	0.0130
Od13g01790	Blue	Green	24.75	5.69	-2.121	0.0009
Od16g01980	Blue	Green	12.19	2.80	-2.122	0.0009
Od02g02690	Blue	Green	1779.39	406.16	-2.131	0.0009
Od03g01650	Blue	Green	49.66	11.26	-2.141	0.0009
Od04g00830	Blue	Green	26.95	6.09	-2.145	0.0009
Od04g05000	Blue	Green	4.87	1.07	-2.184	0.0009
Od08g02560	Blue	Green	9.33	2.03	-2.199	0.0009
Od09g02770	Blue	Green	2.04	0.44	-2.215	0.0210
Od19g01000	Blue	Green	24.50	5.24	-2.224	0.0009
Od20g00710	Blue	Green	4.64	0.96	-2.273	0.0041
Od06g04090	Blue	Green	79.02	16.34	-2.274	0.0009
Od17g01800	Blue	Green	84.66	17.51	-2.274	0.0009
Od20g02070	Blue	Green	62.06	12.82	-2.275	0.0009
Od07g00170	Blue	Green	6.78	1.40	-2.277	0.0009
Od04g00260	Blue	Green	31.04	6.35	-2.289	0.0009
Od15g00940	Blue	Green	6.05	1.24	-2.290	0.0071
Od07g04620	Blue	Green	101.21	19.99	-2.340	0.0009
Od05g01450	Blue	Green	29.36	5.73	-2.357	0.0009
Od14g01080	Blue	Green	106.93	20.79	-2.363	0.0009
Od07g03640	Blue	Green	27.62	5.33	-2.375	0.0104
Od11g01790	Blue	Green	2.52	0.48	-2.380	0.0029
Od14g00930	Blue	Green	33.04	6.27	-2.398	0.0009
Od07g00480	Blue	Green	41.29	7.74	-2.415	0.0009
Od19g00350	Blue	Green	13.26	2.47	-2.426	0.0009
Od07g00820	Blue	Green	7.89	1.46	-2.437	0.0184
Od05g03110	Blue	Green	34.31	6.32	-2.440	0.0009
Od20g00270	Blue	Green	82.85	14.23	-2.542	0.0009
Od01g06650	Blue	Green	66.16	11.28	-2.552	0.0009
Od07g02550	Blue	Green	17.75	3.01	-2.560	0.0009
Od06g07360	Blue	Green	42.75	7.21	-2.568	0.0009
Od20g00460	Blue	Green	33.60	5.66	-2.569	0.0009

Od08g03260	Blue	Green	14.96	2.51	-2.574	0.0009
Od05g00220	Blue	Green	60.18	9.80	-2.618	0.0009
Od11g01330	Blue	Green	30.29	4.90	-2.627	0.0009
Od12g01020	Blue	Green	17.07	2.70	-2.659	0.0009
Od13g01990	Blue	Green	42.22	6.12	-2.787	0.0009
Od07g00400	Blue	Green	64.09	9.23	-2.796	0.0009
Od07g03850	Blue	Green	41.90	5.91	-2.825	0.0016
Od06g02030	Blue	Green	12.34	1.73	-2.838	0.0067
Od13g01200	Blue	Green	33.81	4.73	-2.839	0.0009
Od15g00600	Blue	Green	24.87	3.35	-2.892	0.0009
Od02g03540	Blue	Green	45.17	5.98	-2.917	0.0009
Od09g05770	Blue	Green	12.18	1.59	-2.934	0.0009
Od11g03720	Blue	Green	12.13	1.58	-2.937	0.0076
Od16g00070	Blue	Green	58.64	7.63	-2.942	0.0126
Od07g00180	Blue	Green	225.13	28.19	-2.997	0.0009
Od11g00070	Blue	Green	252.45	31.23	-3.015	0.0009
Od02g00200	Blue	Green	44.41	5.47	-3.023	0.0009
Od07g02560	Blue	Green	32.56	3.94	-3.047	0.0009
Od09g02300	Blue	Green	200.61	24.08	-3.059	0.0009
Od04g04760	Blue	Green	13.81	1.57	-3.138	0.0009
Od01g00560	Blue	Green	77.56	8.64	-3.166	0.0009
Od09g01360	Blue	Green	22.42	2.40	-3.222	0.0009
Od04g03190	Blue	Green	50.03	5.30	-3.239	0.0009
Od19g00300	Blue	Green	20.90	2.07	-3.336	0.0009
Od07g03280	Blue	Green	20.40	1.84	-3.468	0.0009
Od08g02000	Blue	Green	46.84	3.43	-3.770	0.0009
Od03g03140	Blue	Green	14.04	0.97	-3.856	0.0009
Od08g00870	Blue	Green	151.85	9.05	-4.069	0.0009
Od01g06420	Blue	Green	78.19	4.21	-4.213	0.0023
Od15g01270	Blue	Green	281.66	13.97	-4.334	0.0009
Od07g00840	Red	Green	6.21	19.70	1.665	0.0095
Od10g02190	Red	Green	1.63	3.76	1.206	0.0352
Od05g00120	Red	Green	18.22	37.15	1.028	0.0213
Od17g03230	Red	Green	1.38	2.79	1.009	0.0009
Od14g01850	Red	Green	54.49	108.81	0.998	0.0113
Od03g02510	Red	Green	4.93	9.79	0.990	0.0252
Od11g02910	Red	Green	18.69	36.44	0.963	0.0052
Od04g03630	Red	Green	57.68	111.96	0.957	0.0009
Od17g00960	Red	Green	15.92	30.72	0.949	0.0009
Od14g01410	Red	Green	13.26	25.59	0.948	0.0337
Od14g01420	Red	Green	80.02	152.29	0.928	0.0009
Od14g00130	Red	Green	41.62	78.61	0.918	0.0009
Od05g03170	Red	Green	70.55	132.67	0.911	0.0009

Od12g00240	Red	Green	300.54	564.33	0.909	0.0009
Od13g00090	Red	Green	32.36	59.65	0.882	0.0312
Od05g03600	Red	Green	1.63	2.97	0.866	0.0372
Od20g01770	Red	Green	192.20	347.84	0.856	0.0009
Od02g04650	Red	Green	143.65	258.73	0.849	0.0009
Od05g01040	Red	Green	47.46	85.41	0.848	0.0009
Od13g02150	Red	Green	109.74	196.82	0.843	0.0009
Od05g01840	Red	Green	967.03	1710.00	0.822	0.0009
Od01g06390	Red	Green	3.25	5.73	0.821	0.0046
Od06g02650	Red	Green	51.19	88.70	0.793	0.0009
Od06g00340	Red	Green	16.70	28.54	0.773	0.0138
Od11g02310	Red	Green	89.21	152.05	0.769	0.0009
Od20g01670	Red	Green	26.23	44.29	0.756	0.0090
Od09g04040	Red	Green	15.30	25.62	0.744	0.0463
Od06g00920	Red	Green	116.06	193.61	0.738	0.0009
Od09g02940	Red	Green	62.57	103.37	0.724	0.0016
Od09g02220	Red	Green	703.00	1160.78	0.723	0.0029
Od09g03610	Red	Green	38.07	62.82	0.723	0.0199
Od09g05470	Red	Green	163.15	267.68	0.714	0.0188
Od09g05930	Red	Green	18.47	30.02	0.701	0.0177
Od09g00560	Red	Green	25.90	41.75	0.689	0.0174
Od03g03060	Red	Green	179.96	289.30	0.685	0.0035
Od10g00310	Red	Green	53.07	85.25	0.684	0.0016
Od09g00990	Red	Green	517.66	830.72	0.682	0.0029
Od01g02350	Red	Green	13.01	20.82	0.678	0.0095
Od09g01600	Red	Green	204.88	327.42	0.676	0.0023
Od17g00110	Red	Green	74.57	119.05	0.675	0.0046
Od06g07490	Red	Green	270.21	431.08	0.674	0.0041
Od16g01360	Red	Green	40.05	63.51	0.665	0.0062
Od01g03130	Red	Green	812.94	1286.28	0.662	0.0029
Od06g02120	Red	Green	65.98	104.36	0.661	0.0067
Od03g00090	Red	Green	109.97	173.81	0.660	0.0029
Od09g01820	Red	Green	42.60	67.18	0.657	0.0315
Od20g02620	Red	Green	245.54	380.96	0.634	0.0081
Od04g01520	Red	Green	48.97	75.89	0.632	0.0195
Od06g04740	Red	Green	62.54	96.77	0.630	0.0321
Od15g00340	Red	Green	177.81	273.90	0.623	0.0067
Od05g01340	Red	Green	11.75	18.07	0.620	0.0023
Od11g00240	Red	Green	80.27	123.08	0.617	0.0057
Od07g04340	Red	Green	116.14	177.93	0.616	0.0443
Od05g04090	Red	Green	71.13	108.98	0.616	0.0035
Od19g00590	Red	Green	28.21	43.16	0.613	0.0343
Od02g00410	Red	Green	50.22	76.70	0.611	0.0067

Od01g02070	Red	Green	299.36	454.49	0.602	0.0138
Od01g06180	Red	Green	154.24	234.16	0.602	0.0108
Od06g03250	Red	Green	667.97	1010.57	0.597	0.0067
Od09g04590	Red	Green	62.99	95.16	0.595	0.0134
Od09g00980	Red	Green	119.38	179.95	0.592	0.0062
Od10g00260	Red	Green	81.30	122.54	0.592	0.0158
Od03g00550	Red	Green	89.60	134.37	0.585	0.0130
Od07g02000	Red	Green	136.57	204.74	0.584	0.0090
Od04g01050	Red	Green	2636.43	3931.59	0.577	0.0177
Od12g01550	Red	Green	109.61	162.87	0.571	0.0423
Od08g01460	Red	Green	88.94	132.04	0.570	0.0343
Od01g02490	Red	Green	159.61	236.94	0.570	0.0122
Od14g01220	Red	Green	70.31	104.34	0.570	0.0166
Od04g02760	Red	Green	319.82	474.42	0.569	0.0150
Od07g02030	Red	Green	37.58	55.73	0.568	0.0268
Od09g00050	Red	Green	105.26	155.91	0.567	0.0142
Od11g03710	Red	Green	48.74	72.10	0.565	0.0213
Od01g01040	Red	Green	94.88	140.04	0.562	0.0297
Od13g00740	Red	Green	124.50	183.69	0.561	0.0174
Od06g06180	Red	Green	37.93	55.83	0.557	0.0384
Od09g03870	Red	Green	203.05	298.34	0.555	0.0177
Od07g02150	Red	Green	160.14	235.18	0.554	0.0199
Od06g06700	Red	Green	18.59	27.28	0.554	0.0306
Od05g03780	Red	Green	7.02	10.30	0.553	0.0343
Od02g03460	Red	Green	72.34	106.08	0.552	0.0470
Od09g06200	Red	Green	146.91	215.37	0.552	0.0327
Od13g02960	Red	Green	63.14	92.54	0.551	0.0206
Od13g02670	Red	Green	51.67	75.60	0.549	0.0420
Od01g05470	Red	Green	167.16	244.49	0.549	0.0234
Od01g06720	Red	Green	41.44	60.54	0.547	0.0195
Od11g04020	Red	Green	40.82	59.46	0.543	0.0335
Od08g00630	Red	Green	100.15	145.31	0.537	0.0177
Od13g00600	Red	Green	17.07	24.73	0.535	0.0224
Od12g03860	Red	Green	1281.24	1854.85	0.534	0.0315
Od20g00320	Red	Green	75.09	108.11	0.526	0.0278
Od09g00300	Red	Green	77.41	111.27	0.523	0.0278
Od15g01360	Red	Green	68.31	97.93	0.520	0.0237
Od03g02370	Red	Green	40.58	58.11	0.518	0.0275
Od07g02970	Red	Green	216.61	310.20	0.518	0.0268
Od16g01540	Red	Green	1216.36	1740.69	0.517	0.0278
Od06g00510	Red	Green	126.48	180.49	0.513	0.0319
Od07g02520	Red	Green	133.25	189.73	0.510	0.0294
Od01g01390	Red	Green	250.58	356.35	0.508	0.0324

Od11g01750	Red	Green	19.97	28.39	0.508	0.0395
Od08g00510	Red	Green	81.53	115.90	0.507	0.0337
Od10g02380	Red	Green	131.33	186.54	0.506	0.0329
Od12g01140	Red	Green	329.09	467.43	0.506	0.0369
Od09g01870	Red	Green	88.75	125.88	0.504	0.0492
Od16g00400	Red	Green	383.84	544.08	0.503	0.0346
Od06g05050	Red	Green	64.95	92.03	0.503	0.0355
Od02g04320	Red	Green	142.67	200.60	0.492	0.0392
Od05g04680	Red	Green	117.92	165.65	0.490	0.0375
Od06g05830	Red	Green	243.93	341.87	0.487	0.0390
Od15g00730	Red	Green	154.97	216.92	0.485	0.0452
Od17g01780	Red	Green	59.33	82.93	0.483	0.0436
Od12g00650	Red	Green	179.12	249.30	0.477	0.0458
Od07g00790	Red	Green	61.77	85.54	0.470	0.0484
Od10g00340	Red	Green	93.90	67.50	-0.476	0.0497
Od17g01560	Red	Green	118.64	84.78	-0.485	0.0423
Od11g01480	Red	Green	73.00	52.12	-0.486	0.0363
Od16g00280	Red	Green	68.14	48.63	-0.487	0.0463
Od09g02330	Red	Green	710.30	506.27	-0.489	0.0442
Od17g00370	Red	Green	87.47	62.33	-0.489	0.0395
Od10g01480	Red	Green	14.87	10.56	-0.494	0.0476
Od11g01850	Red	Green	69.20	49.07	-0.496	0.0331
Od08g03860	Red	Green	52.22	36.96	-0.499	0.0384
Od03g03160	Red	Green	108.76	76.95	-0.499	0.0346
Od02g01320	Red	Green	176.25	124.56	-0.501	0.0302
Od01g04040	Red	Green	46.01	32.46	-0.503	0.0431
Od06g04690	Red	Green	91.22	64.32	-0.504	0.0302
Od02g00680	Red	Green	77.12	54.25	-0.507	0.0329
Od01g04280	Red	Green	30.35	21.35	-0.507	0.0255
Od02g02850	Red	Green	448.05	315.17	-0.508	0.0231
Od02g02300	Red	Green	122.88	86.33	-0.509	0.0275
Od09g03220	Red	Green	67.02	47.01	-0.512	0.0300
Od13g03030	Red	Green	28601.40	20040.40	-0.513	0.0130
Od02g03070	Red	Green	545.91	382.39	-0.514	0.0321
Od11g02480	Red	Green	42.86	29.96	-0.516	0.0329
Od06g01080	Red	Green	587.70	410.71	-0.517	0.0300
Od05g00150	Red	Green	69.01	48.04	-0.523	0.0331
Od13g01510	Red	Green	236.00	164.08	-0.524	0.0234
Od02g00040	Red	Green	109.67	76.11	-0.527	0.0227
Od02g00280	Red	Green	35.63	24.67	-0.530	0.0202
Od05g01800	Red	Green	143.89	99.61	-0.531	0.0248
Od02g01490	Red	Green	723.61	500.92	-0.531	0.0255
Od10g01680	Red	Green	28.15	19.48	-0.531	0.0470

Od09g04300	Red	Green	143.92	99.41	-0.534	0.0241
Od12g03180	Red	Green	164.74	113.77	-0.534	0.0294
Od07g02850	Red	Green	34.97	24.13	-0.535	0.0327
Od07g04250	Red	Green	269.14	185.69	-0.535	0.0241
Od07g01600	Red	Green	107.38	74.03	-0.536	0.0284
Od09g02200	Red	Green	26.70	18.39	-0.538	0.0479
Od10g02460	Red	Green	10.19	7.00	-0.540	0.0180
Od17g01460	Red	Green	464.88	318.39	-0.546	0.0177
Od17g00640	Red	Green	293.29	200.79	-0.547	0.0234
Od02g02740	Red	Green	57.07	39.04	-0.548	0.0290
Od07g02940	Red	Green	60.89	41.61	-0.549	0.0188
Od02g02440	Red	Green	206.50	141.04	-0.550	0.0192
Od14g01990	Red	Green	48.83	33.31	-0.552	0.0312
Od07g02890	Red	Green	17.62	12.01	-0.553	0.0463
Od03g02850	Red	Green	649.95	442.73	-0.554	0.0174
Od17g00240	Red	Green	34.45	23.46	-0.554	0.0174
Od16g02720	Red	Green	62.57	42.61	-0.554	0.0300
Od11g00060	Red	Green	44.20	30.05	-0.557	0.0335
Od02g02110	Red	Green	398.89	270.32	-0.561	0.0234
Od14g00170	Red	Green	106.75	72.20	-0.564	0.0220
Od10g01390	Red	Green	21.25	14.37	-0.564	0.0281
Od13g01000	Red	Green	49.40	33.37	-0.566	0.0290
Od02g02420	Red	Green	109.71	74.04	-0.567	0.0166
Od04g04960	Red	Green	9.89	6.67	-0.567	0.0431
Od07g02260	Red	Green	32.23	21.73	-0.569	0.0346
Od12g02680	Red	Green	18.44	12.43	-0.569	0.0234
Od06g03170	Red	Green	145.62	98.04	-0.571	0.0306
Od02g02380	Red	Green	261.83	176.23	-0.571	0.0142
Od04g04480	Red	Green	60.32	40.59	-0.572	0.0268
Od20g01140	Red	Green	43.44	29.19	-0.573	0.0122
Od01g03690	Red	Green	13.75	9.22	-0.577	0.0206
Od05g03090	Red	Green	10.60	7.10	-0.578	0.0195
Od11g01950	Red	Green	215.59	144.15	-0.581	0.0117
Od04g01430	Red	Green	14.43	9.65	-0.581	0.0166
Od04g05270	Red	Green	22.66	15.14	-0.582	0.0206
Od04g04360	Red	Green	23.54	15.72	-0.583	0.0146
Od02g01330	Red	Green	357.60	237.80	-0.589	0.0095
Od02g02310	Red	Green	104.78	69.65	-0.589	0.0117
Od07g02180	Red	Green	130.28	86.59	-0.589	0.0202
Od17g01800	Red	Green	26.36	17.51	-0.590	0.0381
Od13g01890	Red	Green	9.29	6.15	-0.593	0.0343
Od08g00650	Red	Green	32.35	21.41	-0.595	0.0090
Od02g01920	Red	Green	77.10	50.97	-0.597	0.0134

Od01g00740	Red	Green	33.64	22.22	-0.598	0.0113
Od09g06120	Red	Green	31.73	20.96	-0.598	0.0343
Od15g00920	Red	Green	39.64	26.17	-0.599	0.0180
Od06g01240	Red	Green	24.53	16.17	-0.601	0.0071
Od09g03960	Red	Green	28.32	18.66	-0.602	0.0452
Od02g02130	Red	Green	312.56	205.60	-0.604	0.0062
Od06g06930	Red	Green	183.12	120.45	-0.604	0.0126
Od04g00670	Red	Green	85.46	56.09	-0.608	0.0086
Od17g03010	Red	Green	124.45	81.58	-0.609	0.0067
Od03g01440	Red	Green	12.91	8.46	-0.610	0.0248
Od07g01660	Red	Green	44.58	29.12	-0.614	0.0062
Od06g01470	Red	Green	8.55	5.58	-0.615	0.0490
Od02g02540	Red	Green	161.46	105.35	-0.616	0.0052
Od14g01310	Red	Green	94.30	61.35	-0.620	0.0057
Od02g01670	Red	Green	12.92	8.39	-0.623	0.0248
Od11g01290	Red	Green	13.17	8.53	-0.626	0.0113
Od17g01040	Red	Green	69.06	44.74	-0.626	0.0029
Od06g04370	Red	Green	59.90	38.77	-0.628	0.0041
Od06g06100	Red	Green	218.66	140.99	-0.633	0.0067
Od14g03310	Red	Green	51.99	33.48	-0.635	0.0016
Od02g03000	Red	Green	554.47	356.72	-0.636	0.0108
Od17g00040	Red	Green	106.35	68.36	-0.638	0.0090
Od06g02380	Red	Green	39.39	25.28	-0.640	0.0278
Od05g04650	Red	Green	141.50	90.52	-0.645	0.0052
Od06g03710	Red	Green	93.84	59.91	-0.648	0.0076
Od04g03180	Red	Green	47.82	30.52	-0.648	0.0046
Od03g00560	Red	Green	66.60	42.44	-0.650	0.0057
Od07g04620	Red	Green	31.45	19.99	-0.654	0.0224
Od02g01450	Red	Green	61.48	39.07	-0.654	0.0142
Od01g04270	Red	Green	53.47	33.97	-0.654	0.0076
Od06g02800	Red	Green	110.92	70.31	-0.658	0.0029
Od01g01440	Red	Green	49.66	31.45	-0.659	0.0081
Od16g02460	Red	Green	100.05	63.13	-0.664	0.0067
Od06g06590	Red	Green	31.54	19.86	-0.667	0.0199
Od13g01310	Red	Green	82.45	51.78	-0.671	0.0067
Od19g00150	Red	Green	51.24	32.17	-0.672	0.0086
Od13g01900	Red	Green	16.63	10.42	-0.674	0.0067
Od09g00150	Red	Green	51.37	32.09	-0.679	0.0150
Od14g02580	Red	Green	158.01	98.71	-0.679	0.0023
Od05g02890	Red	Green	117.50	73.19	-0.683	0.0035
Od06g03670	Red	Green	19.92	12.38	-0.686	0.0016
Od01g04190	Red	Green	23.23	14.43	-0.687	0.0465
Od01g04120	Red	Green	52.63	32.63	-0.690	0.0122

Od12g00470	Red	Green	10.02	6.20	-0.693	0.0081
Od04g02610	Red	Green	177.26	109.41	-0.696	0.0009
Od08g00090	Red	Green	18.78	11.58	-0.697	0.0052
Od06g05360	Red	Green	37.45	23.08	-0.698	0.0009
Od04g04790	Red	Green	27.24	16.77	-0.700	0.0081
Od12g00100	Red	Green	22.39	13.78	-0.700	0.0071
Od01g03410	Red	Green	18.24	11.22	-0.700	0.0100
Od14g02940	Red	Green	78.19	48.03	-0.703	0.0009
Od10g00860	Red	Green	656.49	402.76	-0.705	0.0016
Od06g01250	Red	Green	36.04	22.11	-0.705	0.0041
Od14g02780	Red	Green	10.25	6.27	-0.710	0.0090
Od10g00870	Red	Green	418.74	255.85	-0.711	0.0009
Od08g03600	Red	Green	177.34	107.73	-0.719	0.0009
Od17g02010	Red	Green	42.29	25.65	-0.721	0.0174
Od02g04870	Red	Green	11.82	7.17	-0.722	0.0482
Od02g03110	Red	Green	70.96	42.98	-0.723	0.0009
Od10g01970	Red	Green	132.01	79.96	-0.723	0.0016
Od07g04720	Red	Green	1294.55	779.66	-0.732	0.0016
Od02g01660	Red	Green	187.33	112.74	-0.733	0.0009
Od06g01270	Red	Green	8.43	5.03	-0.744	0.0357
Od10g02070	Red	Green	31.27	18.67	-0.744	0.0009
Od04g00980	Red	Green	41.68	24.85	-0.746	0.0023
Od13g02290	Red	Green	113.29	67.51	-0.747	0.0126
Od02g02010	Red	Green	84.49	50.30	-0.748	0.0009
Od07g04000	Red	Green	44.42	26.43	-0.749	0.0067
Od20g00270	Red	Green	23.94	14.23	-0.750	0.0035
Od09g00180	Red	Green	793.20	469.83	-0.756	0.0023
Od01g06400	Red	Green	26.58	15.66	-0.763	0.0009
Od09g03890	Red	Green	4693.28	2747.81	-0.772	0.0009
Od17g00010	Red	Green	117.35	68.33	-0.780	0.0016
Od17g02180	Red	Green	11.22	6.53	-0.782	0.0487
Od07g02910	Red	Green	19.58	11.37	-0.784	0.0009
Od11g01330	Red	Green	8.48	4.90	-0.789	0.0287
Od20g01510	Red	Green	5.02	2.90	-0.792	0.0237
Od06g05560	Red	Green	24.50	14.11	-0.796	0.0174
Od02g04950	Red	Green	61.59	35.44	-0.797	0.0035
Od17g00030	Red	Green	44.92	25.74	-0.803	0.0052
Od05g00470	Red	Green	31.57	18.07	-0.805	0.0009
Od03g01650	Red	Green	19.69	11.26	-0.807	0.0009
Od07g02920	Red	Green	120.62	68.76	-0.811	0.0009
Od01g01560	Red	Green	9.13	5.17	-0.820	0.0372
Od12g03190	Red	Green	220.33	124.52	-0.823	0.0009
Od09g04310	Red	Green	56.58	31.90	-0.827	0.0009

Od03g02610	Red	Green	231.91	130.49	-0.830	0.0009
Od02g02640	Red	Green	117.51	65.70	-0.839	0.0366
Od02g02690	Red	Green	727.30	406.16	-0.840	0.0009
Od12g00290	Red	Green	17.75	9.89	-0.844	0.0076
Od01g04130	Red	Green	77.70	43.13	-0.849	0.0009
Od08g03040	Red	Green	885.41	491.44	-0.849	0.0016
Od13g01200	Red	Green	8.56	4.73	-0.858	0.0234
Od11g01890	Red	Green	39.53	21.80	-0.858	0.0009
Od19g00370	Red	Green	35.40	19.46	-0.863	0.0029
Od01g04460	Red	Green	39.66	21.59	-0.877	0.0009
Od06g06820	Red	Green	24.89	13.53	-0.879	0.0009
Od02g05030	Red	Green	20.31	11.04	-0.880	0.0346
Od13g01180	Red	Green	50.46	27.32	-0.885	0.0009
Od09g03000	Red	Green	4.62	2.50	-0.886	0.0461
Od02g04480	Red	Green	45.22	24.40	-0.890	0.0009
Od04g00830	Red	Green	11.33	6.09	-0.895	0.0067
Od09g02300	Red	Green	44.82	24.08	-0.896	0.0009
Od09g05820	Red	Green	35.79	19.14	-0.903	0.0009
Od08g01820	Red	Green	113.53	60.67	-0.904	0.0009
Od05g03110	Red	Green	11.89	6.32	-0.910	0.0029
Od08g00450	Red	Green	26.33	13.98	-0.913	0.0009
Od03g01340	Red	Green	36.63	19.39	-0.917	0.0009
Od03g01220	Red	Green	149.30	78.90	-0.920	0.0009
Od02g02480	Red	Green	31.41	16.53	-0.926	0.0009
Od08g01500	Red	Green	19.42	10.17	-0.933	0.0009
Od01g01690	Red	Green	212.84	111.51	-0.933	0.0009
Od07g00400	Red	Green	17.63	9.23	-0.934	0.0041
Od16g01770	Red	Green	23.80	12.44	-0.936	0.0029
Od02g04150	Red	Green	4.35	2.26	-0.941	0.0150
Od15g01060	Red	Green	10.66	5.53	-0.948	0.0062
Od06g05070	Red	Green	8.76	4.53	-0.952	0.0009
Od03g01640	Red	Green	73.11	37.49	-0.964	0.0041
Od06g02850	Red	Green	176.55	90.30	-0.967	0.0009
Od03g00630	Red	Green	13.76	7.04	-0.968	0.0100
Od08g01810	Red	Green	369.95	189.12	-0.968	0.0009
Od16g00900	Red	Green	9.43	4.76	-0.986	0.0271
Od05g01450	Red	Green	11.39	5.73	-0.991	0.0016
Od04g00110	Red	Green	5.80	2.88	-1.009	0.0009
Od04g00260	Red	Green	12.84	6.35	-1.016	0.0009
Od04g03190	Red	Green	10.72	5.30	-1.016	0.0071
Od10g02310	Red	Green	31.93	15.79	-1.016	0.0009
Od07g02720	Red	Green	48.99	24.21	-1.017	0.0009
Od12g00120	Red	Green	11.35	5.56	-1.030	0.0071

Od09g02120	Red	Green	10.81	5.25	-1.042	0.0009
Od06g05500	Red	Green	58.56	28.39	-1.045	0.0375
Od11g00070	Red	Green	66.62	31.23	-1.093	0.0009
Od09g03210	Red	Green	76.88	36.04	-1.093	0.0009
Od17g03020	Red	Green	84.48	39.27	-1.105	0.0009
Od11g01110	Red	Green	12.50	5.80	-1.107	0.0009
Od10g00830	Red	Green	423.53	192.86	-1.135	0.0009
Od14g01080	Red	Green	45.84	20.79	-1.141	0.0009
Od10g00760	Red	Green	150.50	66.90	-1.170	0.0009
Od07g00480	Red	Green	17.48	7.74	-1.174	0.0009
Od19g00350	Red	Green	5.57	2.47	-1.175	0.0346
Od04g02130	Red	Green	33.47	14.51	-1.206	0.0009
Od12g00050	Red	Green	216.28	92.66	-1.223	0.0009
Od10g00330	Red	Green	24.06	10.29	-1.226	0.0009
Od06g04490	Red	Green	25.39	10.71	-1.246	0.0009
Od01g00560	Red	Green	20.56	8.64	-1.251	0.0009
Od05g00220	Red	Green	23.40	9.80	-1.255	0.0009
Od10g00840	Red	Green	296.95	123.87	-1.261	0.0009
Od16g01980	Red	Green	6.94	2.80	-1.309	0.0195
Od07g02560	Red	Green	9.83	3.94	-1.320	0.0035
Od02g03540	Red	Green	15.19	5.98	-1.345	0.0009
Od19g01000	Red	Green	13.38	5.24	-1.351	0.0009
Od07g00180	Red	Green	72.06	28.19	-1.354	0.0009
Od15g00600	Red	Green	8.63	3.35	-1.365	0.0029
Od08g01830	Red	Green	14.83	5.72	-1.373	0.0009
Od20g00460	Red	Green	14.94	5.66	-1.399	0.0180
Od10g02430	Red	Green	109.54	41.26	-1.408	0.0041
Od07g03280	Red	Green	4.97	1.84	-1.431	0.0035
Od13g01990	Red	Green	17.05	6.12	-1.479	0.0104
Od20g02070	Red	Green	36.24	12.82	-1.499	0.0009
Od10g00820	Red	Green	279.17	92.77	-1.589	0.0009
Od15g01270	Red	Green	43.60	13.97	-1.642	0.0009
Od05g01200	Red	Green	8.26	2.52	-1.711	0.0009
Od06g02030	Red	Green	5.76	1.73	-1.738	0.0449
Od14g01360	Red	Green	2.52	0.72	-1.800	0.0195
Od08g00870	Red	Green	36.19	9.05	-2.000	0.0016

Appendix 2 Significantly differentially expressed genes separated by light condition

OTH95 genes which increased expression in green compared to both red and blue light
ostta15g01710 ostta08g04240 ostta05g04970

OTH95 genes which decreased expression in red compared to both green and blue light
ostta15g01710 ostta08g04240 ostta05g04970

OTH95 genes which decreased expression in green compared to both red and blue light
ostta01g00150 ostta01g00530 ostta01g00570 ostta01g00720 ostta01g03480 ostta01g04380 ostta01g04840 ostta01g05470 ostta01g06010 ostta01g06120 ostta02g02790 ostta02g04010 ostta02g04930 ostta02g05290 ostta03g00060 ostta03g01070 ostta03g01170 ostta03g02220 ostta03g02650 ostta03g04380 ostta03g04840 ostta03g04970 ostta03g05040 ostta03g05370 ostta03g05760 ostta04g00340 ostta04g00770 ostta04g00970 ostta04g01120 ostta04g02770 ostta04g02880 ostta04g04050 ostta04g04310 ostta04g04930 ostta05g00190 ostta05g00360 ostta05g00450 ostta05g00690 ostta05g01080 ostta05g01450 ostta05g02690 ostta05g02870 ostta05g02880 ostta05g03090 ostta05g03410 ostta05g03560 ostta05g03750 ostta05g03820 ostta05g04180 ostta05g04940 ostta06g00670 ostta06g00860 ostta06g01030 ostta06g01120 ostta06g01550 ostta06g01610 ostta06g01640 ostta06g01960 ostta06g02410 ostta06g02970 ostta06g03980 ostta06g04000 ostta06g04610 ostta07g00710 ostta07g00750 ostta07g00780 ostta07g01760 ostta07g01810 ostta07g02060 ostta07g02070 ostta07g03200 ostta07g03260 ostta07g03380 ostta07g04020 ostta07g04430 ostta07g04450 ostta07g04660 ostta08g01000 ostta08g02420 ostta08g02930 ostta08g03170 ostta08g04210 ostta09g00290 ostta09g00785 ostta09g00890 ostta09g01190 ostta09g01210 ostta09g01960 ostta09g03130 ostta09g03580 ostta10g00150 ostta10g00320 ostta10g00565 ostta10g01740 ostta10g01900 ostta10g02520 ostta11g00160 ostta11g01100 ostta11g02020 ostta11g02120 ostta11g03220 ostta12g00070 ostta12g00590 ostta12g03000 ostta13g00130 ostta13g00720 ostta13g01100 ostta13g01240

RCC809 genes which increased expression in red light compared to both green and blue light	
Gene	Description
Od01g00740	Phytoene Desaturase, carotenoid biosynthesis
Od02g02380	Phosphatidic Acid Phosphatase-Related Protein
Od02g02850	Chloroplast Envelope Protein Translocase Family
Od03g00560	Membrane Component
Od03g02850	Fructose-1,6-Bisphosphatase
Od04g00980	Fructose-bisphosphate aldolase activity
Od04g02610	Predicted Protein
Od04g04480	Histone methyltransferase activity
Od04g05270	DNA binding, regulation of transcription
Od05g04650	Thylakoid
Od06g02800	Fad-Dependent Oxidoreductase
Od06g03170	Putative 2Fe-2S ferredoxin
Od06g04490	Translation elongation
Od06g06100	Methionine Synthase

Od07g04250	Predicted Protein, fatty acid biosynthesis
Od07g04720	Transketolase, Chloroplastic-Like
Od08g01810	Zinc Finger CCCH Domain-Containing Protein 28
Od08g03040	Predicted Protein
Od09g00180	Predicted Protein, glucose metabolism
Od09g02200	Membrane Component
Od09g03890	Adenosylhomocysteinase, cellular methylation
Od09g04300	LOV-HK
Od09g04310	LOV-HK
Od10g00860	Formate/Nitrite Transporter
Od10g00870	Nitrite Transporter Nar1
Od10g02070	DNA Replication Protein
Od11g01480	Predicted Protein, protein binding
Od12g00050	Urea-Proton Symporter Dur3
Od13g03030	Fasciclin Domain-Containing Protein
Od14g02940	Phosphoglucomutase, Chloroplastic
Od17g01460	Mitochondrial Phosphate Carrier Protein
Od17g02010	Chloroplast ribulose bisphosphate carboxylase complex

RCC809 genes which increased expression in green light compared to both red and blue light	
Gene	Description
Od01g01040	Unknown product
Od01g02070	RNA polymerase II-associated protein
Od01g02350	Lectin Domain-Containing Binding Protein
Od01g02490	Glutaredoxin, electron transport, RNA synthesis
Od01g03130	Peptidase containing nucleoporin and zinc finger CCCH
Od01g06180	Predicted Protein
Od02g00410	Major facilitator superfamily (MFS), transport of small solutes
Od02g04320	Nucleic acid binding, spliceosome
Od02g04650	Protein binding molecular chaperone, DNAJ domain, heat shock
Od03g00550	Ribonuclease inhibition, methyltransferase
Od03g02370	Translational activator GCN1-related
Od03g03060	Membrane component
Od04g01050	Hydrolase activity
Od04g02760	Predicted Protein, binding
Od05g01040	Heat Shock Protein Sti1, binding
Od05g01340	Protein binding, p-loop and WD40 repeat-containing
Od05g01840	Predicted Protein
Od05g04680	Predicted Protein
Od06g00510	mRNA splicing factor motif
Od06g00920	Arm Repeat Superfamily Protein, binding
Od06g02650	Ultraviolet-B Receptor Uvr8-Like Isoform X1
Od06g03250	Protein dephosphorylation
Od06g05830	Cellular protein modification process
Od06g06180	Protein binding, tetratricopeptide repeat
Od06g07490	Predicted Protein
Od07g00790	Protein binding

Od07g02000	Probable Inactive Shikimate Kinase Like 2, Chloroplastic
Od07g02150	Zinc Finger CCHC Domain-Containing Protein
Od07g02520	Predicted Protein
Od08g00510	Peptidase
Od08g00630	Unnamed Product
Od09g00050	Predicted Protein
Od09g00560	Sulfite Oxidase-Like Oxidoreductase
Od09g00980	Predicted Protein
Od09g01600	Predicted Protein
Od09g01870	Predicted Protein
Od09g02220	Membrane component
Od09g02940	U5 Small Nuclear Ribonucleoprotein
Od09g03610	Unnamed Product
Od09g03870	Pantoate-beta-alanine ligase, amino acid synthesis
Od09g06200	Unnamed Product
Od10g00310	Predicted Protein
Od11g02310	Serine-threonine/tyrosine-protein kinase catalytic domain
Od11g02910	Unnamed Product
Od12g01140	Unnamed Product
Od12g03860	Unnamed Product
Od13g00600	RNA binding domain containing protein
Od13g00740	Protein serine/threonine phosphatase activity
Od13g02150	Unnamed Product, membrane
Od14g01420	Protein folding, armadillo/beta-catenin-like repeat containing
Od15g00340	Fatty acyl-CoA-binding domain
Od15g00730	Tyrosine/serine/threonine phosphatase
Od15g01360	Unnamed Product
Od16g00400	Tetrahydrobiopterin biosynthetic process
Od16g01360	Membrane component
Od16g01540	Predicted Protein
Od17g00960	RNA binding
Od20g01670	Predicted Protein, nucleic acid binding
Od20g01770	Ankyrin Repeat, protein binding
Od20g02620	Predicted Protein, ribosome component

RCC809 genes which increased expression in blue light compared to both red and green light	
Gene	Description
Od01g00210	DNA Photolyase Activity
Od15g01260	5'-3' Exonuclease Family, DNA Repair
Od16g01180	Acetylhydrolase, Lipid Catabolic Process
Od17g00090	Amino Acid Transmembrane Transport, Tryptophan/Tyrosine
Od01g06580	Aminoacyl-TRNASynthetase, Protein Synthesis
Od19g00920	ATPase, Plasma-Membrane Proton-Efflux P-Type
Od01g03480	Calcium Binding Protein, Transmembrane Import
Od10g00970	Calcium Transport Mitochondrial, Wd40 Repeat
Od06g01820	Carbohydrate-Binding Family, Glucan 1,4-Alpha-Glucosidase
Od12g01220	Carboxylic Ester Hydrolase Domain

Od14g01080	Cell Cycle Dependent Kinase B, Cell Division (Serine/Threonine-Protein Kinase, Active Site)
Od02g03200	Chloramphenicol Acetyltransferase Domain
Od01g01950	Chromatin Binding Domain
Od20g01170	Cobalamin Adenosyltransferase-Like Superfamily
Od14g03010	Condensin Complex, Mitotic Chromosome Condensation
Od14g00920	Cysteine Protease
Od11g01050	Dehydrogenase, Nucleobase Biosynthesis
Od15g00900	DNA Base Excision Repair
Od02g00320	DNA Methylation, Methyltransferase
Od06g06580	DNA Mismatch Repair Protein, Muts-Like
Od11g01550	DNA Recombination Domain
Od04g03210	DNA Repair Protein, Mitotic Recombination, Helicase
Od01g06420	Fatty Acid Hydrolase, Acyl-Coa Thioesterase
Od12g03130	Glycoside Hydrolase, Carbohydrate Catabolism
Od11g02930	Had-Ib Family Hydrolase, Phosphatase Activity
Od11g00130	Histone Acetyltransferase, Chromatin Organization
Od09g06110	Histone Deacetylase, Transcription Regulation
Od01g02860	Histone H3, DNABinding
Od17g00420	Kh Domain, mRNA-Binding, Regulation Of Gene Expression
Od17g01120	Kinesin-Like, Microtubule Motor Activity
Od09g01340	Kinesin, Microtubule Activity P-Loop Containing
Od06g02230	Malate Dehydrogenase, Mitochondrial, Tca Cycle
Od14g02600	Microtubule Binding Protein Involved In Cell Cycle Control
Od09g00660	Microtubule Binding, Prc-Barrel-Like
Od19g00750	Mitochondrial Carrier, Ion Transport, Glycine Predicted
Od20g02780	mRNASplicing, Luc7-Related
Od04g05220	Mscs Family Transport, Ion Channel
Od13g02570	Myosin Class Ii Heavy Chain, Likely Cell Division Related
Od05g02520	Myosin Class Ii Heavy Chain, Membrane Transport
Od03g02690	Nitrogen Compound Transport, BCCT
Od11g01460	Nucleotide Binding, D-Amino Acid Oxidase
Od12g00150	Oxoglutarate/Iron-Dependent Dioxygenase, DNA Repair
Od06g00540	P-Loop Nucleoside Hydrolase, Possible Replication Factor
Od13g01200	Peptidase, Calcium-Dependent Cysteine-Type
Od06g04940	Peptidyl-Prolyl Cis-Trans Isomerase, Protein Folding
Od02g03320	Phosphatase, Positive Cell Cycle Regulation G2/M Phase
Od07g02950	Phosphatidyltransferase, Phospholipid Biosynthetic Process
Od13g02790	Potassium Ion Transmembrane Transport
Od11g01890	Primase, Large Subunit, DNA Replication
Od08g03230	Protein Binding, Ankyrin Repeat
Od12g00120	Protein Kinase
Od20g02320	Protein Modification, Peptide:N-Glycanase
Od02g00970	Protein Modifying Enzyme, Ion Channel Domain, Oxioreductase
Od01g01190	Pyruvate Dehydrogenase (Acetyl-Transferring)
Od16g00890	Rhodopsin-Like Gpcr (G Protein-Coupled Receptor)

Od03g01070	Ribonuclease H-Like Domain
Od12g02990	Ribonuclease HII
Od06g01410	Ribosomal RNA Methyltransferase
Od11g02410	RNA-Binding Protein
Od16g00280	Serine Hydroxymethyltransferase
Od04g04760	Serine/Threonine Protein Kinase, Phosphorylation
Od02g03690	Serine/Threonine-Protein Kinase 24
Od06g05210	Shugoshin, C-Terminal, Meiotic Chromosome Segregation
Od03g01340	Solute Membrane Transport
Od11g00340	Start Domain-Containing Protein, Lipid Binding
Od19g00730	Superoxide Dismutase Cu-Zn, Ion Binding
Od19g00740	Superoxide Dismutase Cu-Zn, Ion Binding
Od19g00350	Tesmin/Tso1-Like Domain, Transcription Regulation, May Be Negative Regulation
Od06g02440	Transcription Factor IIb, Recruits RNA Pol II
Od05g04810	Transmembrane Protein, Ion Channel
Od05g01080	tRNA Modification (Guanine-N(7)-)-Methyltransferase
Od01g06640	Voltage-Dependent Potassium Channel, Transmembrane
Od14g03150	Wd40 Repeat-Containing, Chromatin Binding, Regulatory
Od17g00150	Zinc Finger CCCH-Type, RNA Binding, Regulation of Expression
Od01g00560	Predicted Protein
Od01g00580	Predicted Protein, Protein Binding
Od01g00800	WD Repeat Domain-Containing Protein 83
Od01g00810	Kr Domain-Containing Protein
Od01g00970	Unnamed Product
Od01g01160	Predicted Protein
Od01g01230	Predicted Protein
Od01g01310	Predicted Protein
Od01g01640	Putative Peptide Methionine Sulfoxide Reductase Msrb
Od01g01650	Predicted Protein, Chitin Binding
Od01g02300	Thymidine Kinase, Cytosolic
Od01g02570	Predicted Protein
Od01g02820	Sister Chromatid Cohesion 1 Protein 1
Od01g02880	Predicted Protein, Proteolysis
Od01g03410	Predicted Protein, Ion Binding
Od01g03470	Membrane Component
Od01g03680	Predicted Protein, Hydrolase
Od01g03690	Glycoside Hydrolase Family 13 Protein
Od01g03970	Unnamed Product
Od01g04620	Membrane Component
Od01g04670	Membrane Component
Od01g04760	Unnamed Product
Od01g04830	Unnamed Product
Od01g04880	ATP-Dependent Clp Protease Proteolytic Subunit
Od01g04930	Predicted Protein, RNA Binding
Od01g05030	Membrane Component
Od01g05260	Unnamed Product

Od01g05270	Unnamed Product
Od01g05320	RNA Binding
Od01g05390	Otu Family Cysteine Protease
Od01g05400	Predicted Protein, Acetyl-CoA Transport
Od01g05590	Predicted Protein, tRNA Methylation
Od01g05600	Uncharacterized Calcium-Binding Protein
Od01g05760	DNA Repair Protein Rad50
Od01g06230	Predicted Protein, DNA Damage Checkpoint
Od01g06620	Denn Domain and WD Repeat-Containing Protein Scd1
Od01g06650	Unnamed Product
Od01g06790	Membrane Component
Od01g06980	Malic Enzyme
Od01g07020	Potassium Ion Transporter
Od02g00150	Predicted Protein
Od02g00160	Membrane Component
Od02g00200	Predicted Protein
Od02g00280	Predicted Protein, Microtubule
Od02g00310	Nucleosome
Od02g00430	Peptidyl-Prolyl Cis-Trans Isomerase Pasticcino1
Od02g00880	Unnamed Product
Od02g02690	Probable Histone H2A Variant 3
Od02g03170	Membrane Component
Od02g03540	Predicted Protein
Od02g03580	Unnamed Product
Od02g03670	Predicted Protein, Ferroxidase Activity
Od02g03870	Predicted Protein
Od02g03890	Condensin Complex Component, Non-Smc Subunit
Od02g04230	Chloroplast Thylakoid Membrane
Od02g04350	Membrane Component
Od02g04480	Ribosome Recycling Factor
Od02g04740	Predicted Protein
Od02g04830	Predicted Protein, Hydrolase
Od02g04950	50S Ribosomal Protein L9
Od03g00260	Predicted Protein
Od03g00630	Predicted Protein, tRNA Binding
Od03g01380	Predicted Protein, DNA Replication
Od03g01590	Membrane Component
Od03g01650	Predicted Protein, Protein Binding
Od03g02120	Protein Gfs12 Isoform X3
Od03g02830	Predicted Protein
Od03g02870	DNA Helicase Activity
Od03g03030	Membrane Component
Od03g03140	Predicted Protein
Od03g03160	Predicted Protein, Carbohydrate Metabolism
Od03g03210	Membrane Component
Od04g00010	Predicted Protein, Methyltransferase Activity

Od04g00100	Membrane Component
Od04g00260	Predicted Protein, Chromatin Binding
Od04g00270	Predicted Protein, Nuclease Activity
Od04g00500	Faa Hydrolase Family Protein
Od04g00640	Membrane Component
Od04g00670	Predicted Protein, Microtubule
Od04g00790	Predicted Protein, Spindle
Od04g00830	Predicted Protein, DNAReplication
Od04g01430	Predicted Protein, Kinase Activity
Od04g01690	Prenylated Rab Acceptor Pra1
Od04g01720	Predicted Protein, Gpi Anchor Attachment
Od04g01850	NADP-Dependent Malic Enzyme
Od04g02090	Predicted Protein, Fad Binding
Od04g02770	Glycerophosphodiester Phosphodiesterase Gdpd4
Od04g03140	Pgr5-Like Protein 1B, Chloroplastic
Od04g03190	Membrane Component
Od04g03500	Membrane Component
Od04g03550	Ras-Related Protein Rab7
Od04g03740	Unnamed Product
Od04g03830	Ultraviolet-B Receptor Uvr8 Isoform X2
Od04g04360	Predicted Protein, Cell Division
Od04g04460	Putative Kinesin K39
Od04g04730	Protein Ecdysoneless Homolog, Transcription
Od04g04740	Predicted Protein, RNA Modification
Od04g04750	Fanconi Anemia Group J -Like Protein
Od04g04880	Structural Maintenance of Chromosomes Protein 2-1-Like
Od04g05000	Membrane Component
Od04g05020	Glycogen Synthase Kinase 3
Od04g05040	Membrane Component
Od04g05090	Thioredoxin Domain-Containing Protein 5
Od04g05300	Predicted Protein, Protein Binding
Od04g05310	Predicted Protein, PSII Related
Od04g05390	Membrane Component
Od05g00160	Predicted Protein
Od05g00220	Predicted Protein, Protein Binding
Od05g00350	Predicted Protein
Od05g00600	Inner Centromere Protein, Ark-Binding Domain
Od05g00700	Predicted Protein
Od05g00890	Predicted Protein
Od05g00920	Membrane Component
Od05g01170	Membrane Component
Od05g01230	Membrane Component
Od05g01450	Predicted Protein, Kinase Activity
Od05g01470	Predicted Protein
Od05g01480	Protein Ros1-Like
Od05g01850	Probable Citrate Synthase 2, Mitochondrial

Od05g01880	Unnamed Product
Od05g03110	DNA Topoisomerase 6 Subunit B Isoform X1
Od05g03260	Membrane Component
Od05g03390	Membrane Component
Od05g03930	Protein Serine/Threonine Kinase Activity
Od05g04200	Guanine Nucleotide Exchange Factor Spike 1
Od05g04620	Predicted Protein, dsDNA Binding
Od05g04730	Predicted Protein, Glucose Metabolism
Od05g04770	Unnamed Product
Od05g04960	Predicted Protein, DNA Repair
Od06g00130	Predicted Protein
Od06g00230	Membrane Component
Od06g00250	Predicted Protein, Heme Binding
Od06g00290	Predicted Protein, Cell Division
Od06g00520	Membrane Component
Od06g00830	Membrane Component
Od06g01240	Structural Maintenance of Chromosomes Protein 4
Od06g01250	Predicted Protein, Methyltransferase Activity
Od06g01270	Unnamed Product, Transferase Activity
Od06g01470	Membrane Component
Od06g01640	Predicted Protein
Od06g01710	Ribulose-Phosphate 3-Epimerase
Od06g02030	Peptide-Methionine (S)-S-Oxide Reductase
Od06g02210	Membrane Component
Od06g02430	Predicted Protein
Od06g02450	Predicted Protein
Od06g02660	Predicted Protein, Hydrolase
Od06g02850	Proliferating Cell Nuclear Antigen, DNA Replication
Od06g02880	Predicted Protein
Od06g03060	Pyrimidine 5'-Nucleotidase
Od06g03090	Predicted Protein, Kinase Activity
Od06g03190	Predicted Protein
Od06g03670	Snf2 Super Family
Od06g03940	Acyltransferase
Od06g04090	Predicted Protein, Protein Binding
Od06g04270	Predicted Protein
Od06g04290	Polyphosphate Kinase 2
Od06g04320	Predicted Protein, DNA Replication
Od06g04390	Predicted Protein, Oxidoreductase Activity
Od06g04750	Phosphoserine Aminotransferase
Od06g04890	Membrane Component
Od06g04960	Membrane Component
Od06g05070	Predicted Protein
Od06g05680	Actin-Related Protein 2/3 Complex Subunit 2A
Od06g06240	Predicted Protein, Ion Binding
Od06g06390	Histone-Lysine N-Methyltransferase

Od06g06590	Predicted Protein, Mismatch Repair
Od06g06640	Peptidase Family M3 Protein
Od06g06820	Predicted Protein, Ion Binding
Od06g07000	Predicted Protein
Od06g07360	Predicted Protein
Od06g07370	Membrane Component
Od06g07410	Aldehyde Dehydrogenase
Od06g07420	Predicted Protein
Od06g07570	Predicted Protein
Od07g00010	Predicted Protein
Od07g00100	Photosystem II 22 Kda Protein, Chloroplastic
Od07g00170	BCCT Transporter Family
Od07g00180	BCCT Transporter Family
Od07g00310	Membrane Component
Od07g00400	Predicted Protein
Od07g00480	Beta-Propeller Repeat Tecpr
Od07g00510	Predicted Protein
Od07g00820	Ion Binding
Od07g00980	Duf1565 Domain-Containing Protein
Od07g01740	Predicted Protein, Phosphorylation
Od07g01860	Predicted Protein, Ion Binding
Od07g02340	Membrane Component
Od07g02550	Predicted Protein, Starch Metabolism
Od07g02560	Probable Alpha-Amylase 2
Od07g02670	Ribonuclease E/G
Od07g02850	Membrane Component
Od07g02890	Predicted Protein, Cell Division
Od07g02910	Predicted Protein, Ion Binding
Od07g03210	Membrane Component
Od07g03280	Predicted Protein, Ion Binding
Od07g03500	Predicted Protein, Starch Metabolism
Od07g03640	Unnamed Product
Od07g03710	E3 Ubiquitin-Protein Ligase Trim13 Isoform X1
Od07g03850	Predicted Protein
Od07g03870	Drug/Metabolite Transporter Superfamily
Od07g04070	Growth Hormone-Regulated Tbc Protein 1-A
Od07g04150	Maoc Family Dehydratase
Od07g04240	Ankyrin Repeat Protein
Od07g04510	Predicted Protein, Kinase Activity
Od07g04620	Predicted Protein
Od08g00070	Malate Dehydrogenase, Glyoxysomal
Od08g00250	Unnamed Product
Od08g00490	Ankyrin Repeat Protein, Protein Binding
Od08g00520	Ribonucleoside-Diphosphate Reductase Small Chain
Od08g00650	DNA Polymerase Alpha Catalytic Subunit
Od08g00870	Predicted Protein

Od08g01230	Predicted Protein
Od08g01280	Predicted Protein, DNA Binding
Od08g01720	Queuine tRNA-Ribosyltransferase
Od08g01730	DNA Repair Protein Rad51 Homolog
Od08g01740	Predicted Protein, Nucleic Acid Binding
Od08g01990	Molecular Chaperone Dnaj
Od08g02000	Predicted Protein, Signal Transduction
Od08g02120	WRKY Transcription Factor 20 Isoform X3
Od08g02180	Membrane Component
Od08g02560	Predicted Protein, DNA Recombination
Od08g02850	Predicted Protein, Microtubule
Od08g03260	Mitotic Spindle Checkpoint Protein Bubr1
Od08g03280	Predicted Protein
Od08g03580	Membrane Component
Od08g03860	Predicted Protein, Protein Binding
Od09g00150	Peptidyl-Prolyl Cis-Trans Isomerase B
Od09g00260	Predicted Protein
Od09g00310	Predicted Protein
Od09g00390	Glycosyl Transferase
Od09g00610	Predicted Protein, Nucleic Acid Binding
Od09g00850	Zinc Finger C2H2-Type/Integrase DNA Binding Domain
Od09g01150	Unnamed Product
Od09g01260	Membrane Component, Signal Transduction
Od09g01350	Nadh:Ubiquinone Oxidoreductase
Od09g01360	Predicted Protein
Od09g01440	Predicted Protein, Centromeric, Cell Cycle
Od09g02120	Predicted Protein
Od09g02300	Membrane Component
Od09g02310	Domain Of Unknown Function Duf4050
Od09g02770	Growth Hormone-Regulated Tbc Protein 1
Od09g02820	Predicted Protein, Transport
Od09g02830	Golgi Membrane Protein, Transport
Od09g03260	Predicted Protein, Cell Cycle
Od09g03330	Predicted Protein
Od09g03510	Predicted Protein, Transport
Od09g04670	Predicted Protein, Hydrolase
Od09g04910	Cytochrome C Peroxidase
Od09g05100	Predicted Protein
Od09g05630	Membrane Component
Od09g05770	Predicted Protein, Protein Binding
Od09g05840	Predicted Protein, Lipid Binding
Od09g05870	Predicted Protein, RNA Polymerase II Transcription Factor Activity
Od09g05920	Predicted Protein, Serine/Threonine Kinase Activity
Od09g06080	Predicted Protein
Od09g06120	Predicted Protein
Od09g06130	Peroxiredoxin, Bacteria-Like Protein

Od09g06210	Predicted Protein
Od10g00450	Predicted Protein, Oxidoreductase Activity
Od10g00720	Abc-2 Type Transporter
Od10g00760	Nitrate Reductase
Od10g00780	Adenylyltransferase And Sulfurtransferase Mocs3
Od10g00880	Predicted Protein
Od10g00890	Unnamed Product
Od10g01020	Adp-Sugar Pyrophosphatase
Od10g01130	Predicted Protein, Kinase Activity
Od10g01260	Predicted Protein, Peptidase
Od10g01390	Molecular Chaperone Htpg
Od10g01650	Hypoxia-Inducible Factor 1-Alpha Inhibitor
Od10g01870	Membrane Component
Od10g01930	Membrane Component
Od10g02090	Membrane Component
Od10g02150	Unnamed Product
Od10g02190	Bspa Family Leucine-Rich Repeat Surface Protein
Od10g02330	Transmembrane Protein, Serine/Threonine Kinase Activity
Od10g02340	Unnamed Product
Od10g02380	Unnamed Product
Od10g02550	Predicted Protein, Ion Binding
Od11g00060	Aspartate Carbamoyltransferase
Od11g00070	Mip Family Transporter: Water Channel
Od11g00080	Predicted Protein, Transferase Activity
Od11g00170	Violaxanthin De-Epoxidase
Od11g00400	Predicted Protein, Biosynthetic Process
Od11g00410	Predicted Protein, Ion Binding
Od11g00490	Predicted Protein
Od11g00680	17.8 Kda Class I Heat Shock Protein-Like
Od11g00700	Membrane Component
Od11g01100	Putative Kinesin K39
Od11g01290	Kinesin-Like Calmodulin-Binding Protein
Od11g01330	Predicted Protein
Od11g01470	Predicted Protein
Od11g01790	Voltage-Gated Ion Channel Superfamily
Od11g01910	Glycogen Phosphorylase 1
Od11g02480	DNA Polymerase Alpha Subunit B
Od11g02550	Membrane Component
Od11g02720	Predicted Protein, Protein Binding
Od11g03030	Predicted Protein, Kinase Activity
Od11g03070	Predicted Protein, Proteolysis
Od11g03080	Type 1 Glutamine Amidotransferase Domain-Containing Protein
Od11g03270	Nuclear Movement Protein, Putative
Od11g03280	Membrane Component
Od11g03720	Predicted Protein, Ion Binding
Od11g03980	Tubby Like Protein 3

Od11g04240	Predicted Protein
Od11g04450	Predicted Protein
Od11g04460	Unnamed Product
Od12g00030	Urease Accessory Protein G
Od12g00040	Urease
Od12g00100	Glutamate-Gated Ion Channel Neurotransmitter Receptor Family
Od12g00110	Abc Transporter Type 1, Transmembrane Domain
Od12g00130	Predicted Protein, Hydrolase
Od12g00140	Membrane Component
Od12g00160	Predicted Protein
Od12g00180	Unnamed Product
Od12g00290	Predicted Protein
Od12g00470	DNA Repair And Recombination Protein Rad54
Od12g00690	Predicted Protein, Methyltransferase Activity
Od12g00850	Protein Fmp32, Mitochondrial-Like
Od12g01020	Predicted Protein, Nucleic Acid Binding
Od12g01040	Membrane Component
Od12g01050	Unnamed Product
Od12g01640	Histone H2A
Od12g01680	Probable DNA Helicase Mcm8
Od12g01750	Predicted Protein, Transferase Activity
Od12g02080	Unnamed Product
Od12g02090	Predicted Protein, Catalytic
Od12g02100	Predicted Protein, Protein Binding
Od12g02460	Glutathione S-Transferase, Putative
Od12g02680	DNA Topoisomerase 1 Beta
Od12g02690	Methyltransferase-Like Protein 16
Od12g02800	Predicted Protein
Od12g02860	Membrane Component
Od12g03250	Serine/Threonine-Protein Kinase Edr1
Od12g03340	Predicted Protein
Od12g03470	Membrane Component
Od12g03660	Predicted Protein
Od12g03740	Predicted Protein, Transport
Od12g03830	Predicted Protein, Ion Binding
Od12g03840	Doxx Family Protein
Od13g00080	ATP-Dependent Protease La
Od13g00120	Predicted Protein, Methyltransferase Activity
Od13g00190	Isocitrate Dehydrogenase
Od13g00360	Predicted Protein, Nucleus
Od13g00760	Mitochondrial Thiamine Pyrophosphate Carrier-Like
Od13g01020	Carotene Biosynthesis Related or Early Light Induced-Like Protein, Chloroplast Precursor. Oth95 Homologue Is Chlorophyll A/B Binding Protein
Od13g01110	Predicted Protein
Od13g01180	DNAPrimase Small Subunit Isoform X2
Od13g01210	Predicted Protein

Od13g01540	Membrane Component
Od13g01790	Predicted Protein
Od13g01980	Yhyh Protein
Od13g01990	Predicted Protein
Od13g02310	Membrane Component
Od13g02330	Predicted Protein
Od13g02590	rRNA Processing
Od13g02610	2-Isopropylmalate Synthase
Od13g03060	Membrane Component
Od14g00130	Unnamed Product
Od14g00290	Membrane Component
Od14g00390	Predicted Protein, Carbon Utilisation
Od14g00640	Predicted Protein
Od14g00700	Chlorophyllide A Oxygenase
Od14g00740	Predicted Protein, DNA Binding Transcription Factor Activity
Od14g00810	Unnamed Product
Od14g00870	Predicted Protein
Od14g00930	Predicted Protein
Od14g00990	Tnf Receptor-Associated Factor 4
Od14g01000	Predicted Protein, Serine/Threonine Kinase Activity
Od14g01210	O-Acetylhomoserine Aminocarboxypropyltransferase/Cysteine Synthase
Od14g01240	Unnamed Product
Od14g01660	Predicted Protein, Serine/Threonine Kinase Activity
Od14g02010	Predicted Protein, Actin Binding
Od14g02450	Luxr Family Transcriptional Regulator
Od14g02480	Predicted Protein, Methyltransferase Activity
Od14g02670	Vacuolar Protein Sorting-Associated Protein 9A-Like
Od14g02680	Thylakoid Membrane Protein Terc, Chloroplastic
Od14g02780	Predicted Protein
Od14g02910	Predicted Protein
Od14g02920	Predicted Protein, Transferase Activity
Od14g03310	Membrane Component
Od14g03320	Unnamed Product
Od15g00100	Predicted Protein
Od15g00150	Predicted Protein
Od15g00200	Unnamed Product
Od15g00210	Alpha-Ketoglutarate-Dependent Dioxygenase Alkb Homolog 6
Od15g00350	Transmembrane and Coiled-Coil Domain-Containing Protein 4-Like
Od15g00600	Zinc Transporter Zip3
Od15g00790	Predicted Protein, Cell Division
Od15g00840	Predicted Protein
Od15g00850	Predicted Protein
Od15g00940	Udp-Glycosyltransferase Turan-Like
Od15g01180	Predicted Protein, Hydrolase
Od15g01270	Membrane Component
Od16g00040	Membrane Component

Od16g00070	Membrane Component
Od16g00130	Predicted Protein, Nuclease Activity
Od16g00170	Deoxyuridine 5'-Triphosphate Nucleotidohydrolase
Od16g00290	Serine Hydroxymethyltransferase
Od16g00380	2,5-Didehydrogluconate Reductase
Od16g00730	Membrane Component
Od16g01060	Dead/Deah Box Helicase
Od16g01220	Predicted Protein, Kinase Activity
Od16g01550	Membrane Component
Od16g01850	Non-Histone Chromosomal Protein 6
Od16g01870	Predicted Protein, Transport
Od16g01980	Membrane Component
Od16g02330	Predicted Protein
Od16g02450	Predicted Protein
Od16g02460	14-3-3 Protein Epsilon Isoform X2
Od16g02500	Predicted Protein
Od16g02570	Type Iii Effector
Od17g00240	Predicted Protein
Od17g00270	Chromosome Transmission Fidelity Protein 18 Homolog
Od17g00780	Predicted Protein, Ion Binding
Od17g00920	Exodeoxyribonuclease III
Od17g00980	Predicted Protein, Transferase Activity
Od17g01040	Formate--Tetrahydrofolate Ligase
Od17g01170	Voltage-Gated Ion Channel Superfamily
Od17g01280	Predicted Protein, Histone Acetyltransferase Activity
Od17g01290	Serine/Threonine-Protein Kinase Ctr1-Like Isoform X1
Od17g01360	Predicted Protein, Transcription Factor Complex
Od17g01560	Replication Protein A 70 Kda DNABinding Subunit B
Od17g01800	Predicted Protein
Od17g02170	Unnamed Product
Od17g02180	Ribulose-Phosphate 3-Epimerase
Od17g03010	Membrane Component
Od19g00090	ATP-Binding Cassette Superfamily
Od19g00300	Unnamed Product
Od19g00370	Predicted Protein
Od19g00380	Membrane Component
Od19g00570	Arp2/3 Complex, 21Kda Subunit (P21-Arc)
Od19g00930	Pentapeptide Repeat-Containing Protein
Od19g00990	Membrane Component
Od19g01000	Membrane Component
Od19g01100	Predicted Protein, Cell Division
Od19g01210	Predicted Protein, Protein Binding
Od19g01270	Predicted Protein
Od20g00040	Predicted Protein, Hydrolase
Od20g00250	Predicted Protein
Od20g00270	Small Conductance Mechanosensitive Ion Channel Family

Od20g00280	Predicted Protein
Od20g00290	Predicted Protein, Starch Metabolism
Od20g00380	Peptidyl-Prolyl Cis-Trans Isomerase
Od20g00460	7,8-Dihydro-8-Oxoguanine Triphosphatase-Like, DNA Repair
Od20g00470	Predicted Protein
Od20g00710	Predicted Protein, Ion Binding
Od20g00930	Predicted Protein, Electron Transport
Od20g01140	Predicted Protein, DNA Replication
Od20g01260	Tkl Protein Kinase
Od20g01510	Synaptotagmin-8
Od20g01580	Unnamed Product
Od20g01710	Predicted Protein, Transferase Activity
Od20g01820	Predicted Protein, Replication Fork
Od20g01910	Predicted Protein
Od20g01930	Laminin-Type Egf-Like Protein
Od20g02070	Protein Rkd5-Like Isoform X1
Od20g02080	Membrane Component
Od20g02360	Wash Complex Subunit 7
Od20g02460	Predicted Protein
Od20g02870	Predicted Protein
Od20g02900	Predicted Protein, Nuclear
Od20g03400	Predicted Protein

RCC809 genes which decreased expression in red light compared to both green and blue light	
Gene	Description
Od03g00090	Predicted protein, nucleoside catabolism
Od04g01520	Predicted protein, histone acetyltransferase complex
Od05g04090	Cupin
Od06g00340	Unnamed product
Od09g00990	Membrane component
Od09g04040	Abi-domain-containing protein
Od09g05470	Membrane component
Od10g02190	BspA family leucine-rich repeat surface protein
Od10g02380	Unnamed product
Od12g00240	Predicted protein, phosphorelay signal transduction system
Od14g00130	Unnamed product
Od14g01220	Membrane component
Od17g00110	Membrane component
Od17g03230	Membrane component

RCC809 genes which decreased expression in green light compared to both red and blue light	
Gene	Description

Od01g00560	Predicted Protein, Nucleus
Od01g01440	Predicted Protein, Glucose Metabolism
Od01g01560	RNA Polymerase II Regulatory Region Sequence-Specific DNA binding
Od01g01690	Glutamine Synthetase, Catalytic Domain Protein
Od01g03410	Predicted Protein, Ion Binding
Od01g03690	Glycoside Hydrolase Family 13 Protein
Od01g04120	Predicted Protein, Protein Binding
Od01g04130	Predicted Protein, DNA Ligase
Od01g04280	Predicted Protein, Lipid Binding
Od01g04460	DNA Replication Licensing Factor Mcm6
Od01g06400	Predicted Protein
Od02g00040	Fatty Acid Desaturase
Od02g00280	Predicted Protein, Microtubule
Od02g01320	DNA Replication Licensing Factor Mcm7
Od02g01330	DNA Replication Licensing Factor Mcm7
Od02g01450	DNA Excision Repair Protein Ercc-1
Od02g02010	Arginyl-TRNA Synthetase
Od02g02310	DNA Replication Licensing Factor Mcm3
Od02g02480	Predicted Protein, Protein Binding
Od02g02690	Probable Histone H2A Variant 3
Od02g02740	WD Repeat-Containing Protein 5
Od02g03110	Predicted Protein, Iron Binding
Od02g03540	Predicted Protein
Od02g04150	Predicted Protein, Transferase
Od02g04480	Ribosome Recycling Factor
Od02g04950	50S Ribosomal Protein L9
Od02g05030	Predicted Protein
Od03g00630	Predicted Protein, TRNA Binding
Od03g01220	Predicted Protein
Od03g01340	Xylulose 5-Phosphate/Phosphate Translocator, Chloroplastic-Like
Od03g01440	Abc Transporter ATP-Binding Protein
Od03g01650	Predicted Protein, Protein Binding
Od03g02610	Predicted Protein
Od03g03160	Predicted Protein, Carbohydrate Metabolism
Od04g00110	Putative Sac Domain-Containing Inositol Phosphatase 3
Od04g00260	Predicted Protein, Chromatin Binding
Od04g00670	Predicted Protein, Microtubule Binding
Od04g00830	DNA Replication Initiation
Od04g01430	Predicted Protein, Kinase Activity
Od04g02130	Predicted Protein, Terpenoid Biosynthesis
Od04g03180	Membrane Component
Od04g03190	Membrane Component
Od04g04360	DNA Binding, Cell Division
Od04g04790	Predicted Protein, Iron Binding
Od04g04960	Predicted Protein, DNA Recombination
Od05g00150	Replication Factor C Subunit 3
Od05g00220	Predicted Protein, Protein Binding
Od05g00470	Peptidyl-Prolyl Cis-Trans Isomerase, Chloroplastic
Od05g01200	Uroporphyrinogen Decarboxylase Isoform 1
Od05g01450	Predicted Protein, Kinase Activity
Od05g02890	Bifunctional Dihydrofolate Reductase, Tetrahydrofolate Biosynthetic Process
Od05g03090	Membrane Component
Od05g03110	DNA Topoisomerase 6 Subunit B Isoform X1

Od06g01240	Structural Maintenance of Chromosomes Protein 4
Od06g01250	Predicted Protein, Methyltransferase
Od06g01270	Membrane Component
Od06g01470	Membrane Component, Protein Binding
Od06g02030	Peptide-Methionine (S)-S-Oxide Reductase
Od06g02850	Proliferating Cell Nuclear Antigen, Regulation of DNA Replication
Od06g03670	Snf2 Super Family
Od06g03710	Predicted Protein, Chloroplast Thylakoid Membrane
Od06g04370	Nit2-Like Protein 1, Translation Initiation Factor Activity
Od06g04690	Nucleobase:Cation Symporter-1 Family
Od06g05070	Predicted Protein
Od06g05360	Dihydroxy-Acid Dehydratase
Od06g06590	Predicted Protein, DNA Mismatch Repair
Od06g06820	Predicted Protein, Ion Binding
Od07g00180	BCCT Transporter Family
Od07g00400	Predicted Protein
Od07g00480	Beta-Propeller Repeat Tecpr
Od07g01660	Predicted Protein, Electron Transport
Od07g02180	50S Ribosomal Protein L21
Od07g02560	Probable Alpha-Amylase 2
Od07g02720	Rubisco Binding Protein Subunit Beta
Od07g02850	Membrane Component
Od07g02890	Predicted Protein, Cell Division
Od07g02910	Predicted Protein, Ion Binding
Od07g02920	Myb Family Protein
Od07g02940	Predicted Protein, Double Strand Break Repair
Od07g03280	Predicted Protein, Ion Binding
Od07g04620	Predicted Protein
Od08g00090	Membrane Component
Od08g00450	Predicted Protein, RRNA Modification
Od08g00650	DNA Polymerase Alpha Catalytic Subunit
Od08g00870	Predicted Protein
Od08g01500	Ap-3 Complex Subunit Mu-1
Od08g01820	50S Ribosomal Protein L1
Od08g01830	Predicted Protein
Od08g03860	Predicted Protein, Protein Binding
Od09g00150	Peptidyl-Prolyl Cis-Trans Isomerase B
Od09g02120	Predicted Protein
Od09g02300	Membrane Component
Od09g03960	Predicted Protein, Fatty Acid Biosynthesis
Od09g05820	Predicted Protein, Heme Binding
Od09g06120	Predicted Protein
Od10g00330	Predicted Protein, Membrane Transport
Od10g00340	Predicted Protein, Oxidoreductase
Od10g00760	Nitrate Reductase
Od10g00820	Nitrate Transporter
Od10g00830	Predicted Protein, Nitrate Transport
Od10g00840	Ferredoxin--Nitrite Reductase, Chloroplastic
Od10g01390	Molecular Chaperone Htpg
Od10g01480	DNA Replication ATP-Dependent Helicase/Nuclease Dna2 Isoform X1
Od10g02310	Membrane Component
Od10g02430	Unnamed Product
Od10g02460	Predicted Protein, Endonucleolytic
Od11g00060	Aspartate Carbamoyltransferase
Od11g00070	Mip Family Transporter: Water Channel

Od11g01110	Predicted Protein
Od11g01290	Kinesin-Like Calmodulin-Binding Protein, Microtubule Activity
Od11g01330	Predicted Protein
Od11g01890	DNA Primase Large Subunit
Od11g01950	Unnamed Product
Od11g02480	DNA Polymerase Alpha Subunit B
Od12g00100	Glutamate-Gated Ion Channel Neurotransmitter Receptor Family
Od12g00120	Predicted Protein, Kinase Activity
Od12g00290	Predicted Protein
Od12g00470	DNA Repair and Recombination Protein Rad54
Od12g02680	DNA Topoisomerase 1 Beta
Od12g03190	K(+) Efflux Antiporter 2, Chloroplastic-Like
Od13g01180	DNA Primase Small Subunit Isoform X2
Od13g01200	Predicted Protein, Cysteine-Type Endopeptidase Activity
Od13g01310	Membrane Component
Od13g01890	Predicted Protein, Protein Peptidyl-Prolyl Isomerization
Od13g01900	Predicted Protein, Protein Peptidyl-Prolyl Isomerization
Od13g01990	Predicted Protein
Od13g02290	Predicted Protein, Electron Transport
Od14g00170	50S Ribosomal Protein L4
Od14g01080	Predicted Protein, Cell Division
Od14g01310	Predicted Protein
Od14g01990	Membrane Component
Od14g02580	50S Ribosomal Protein L6, Chloroplastic
Od14g02780	Predicted Protein
Od14g03310	Membrane Component
Od15g00600	Zinc Transporter Zip3
Od15g01270	Membrane Component
Od16g00280	Serine Hydroxymethyltransferase 3, Chloroplastic
Od16g00900	Predicted Protein, Hydrolase
Od16g01770	39S Ribosomal Protein L46, Mitochondrial
Od16g01980	Membrane Component
Od16g02460	14-3-3 Protein Epsilon Isoform X2
Od17g00030	Elmo Domain-Containing Protein A
Od17g00240	Predicted Protein
Od17g00370	Duf262 Domain-Containing Protein
Od17g01040	Formate--Tetrahydrofolate Ligase
Od17g01560	Replication Protein A 70 Kda DNA Binding Subunit B
Od17g01800	Predicted Protein
Od17g02180	Ribulose-Phosphate 3-Epimerase
Od17g03010	Membrane Component
Od17g03020	DNA Replication, Helicase Activity
Od19g00150	Membrane Component
Od19g00350	Tesmin/Tso1-Like Cxc Domain-Containing Protein
Od19g00370	Predicted Protein
Od19g01000	Membrane Component
Od20g00270	Small Conductance Mechanosensitive Ion Channel Family
Od20g00460	7,8-Dihydro-8-Oxoguanine Triphosphatase-Like, DNA Repair
Od20g01140	Predicted Protein, DNA Replication Initiation
Od20g01510	Synaptotagmin-8
Od20g02070	Protein Rkd5-Like Isoform X1, Regulation Of Transcription

RCC809 genes which decreased expression in blue light compared to both red and green light	
Gene	Description

Od01g00470	Predicted Protein, Protein Binding
Od01g00600	Transferase
Od01g00700	Predicted Protein
Od01g00710	Predicted Protein
Od01g00820	Vacuolar Transport
Od01g00910	MRNA Binding
Od01g01020	Porphyrin chlorophyll biosynthesis
Od01g01080	Predicted Protein, Protein Binding
Od01g01210	Cytochrome P450
Od01g01400	Predicted Protein
Od01g01520	Single-Stranded DNA Binding Protein, DNA Replication
Od01g01970	Protein Lsd1-Like Isoform X1
Od01g02120	Transcription factor activity, DNA binding AP2/ERF domain
Od01g02310	Alpha/Beta Hydrolase
Od01g02410	Membrane Component
Od01g02970	Dynamin, membrane remodelling
Od01g03140	Aspartate family amino acid biosynthetic process
Od01g03200	Mitochondrial Carrier Family
Od01g03210	Prasinophyte-specific protein, likely transport related
Od01g03260	Unnamed Product
Od01g03440	Acetyl-COA Carboxylase
Od01g03660	Predicted Protein
Od01g04550	Amino Acid Metabolism
Od01g04650	Porphobilinogen synthase
Od01g04970	Unnamed Product
Od01g04990	Mfs Transporter
Od01g05070	Membrane Component
Od01g05190	Predicted Protein, Acyl Transferase
Od01g05230	Heme Binding
Od01g05480	Enolase
Od01g05730	Chloroplast Stroma
Od01g06140	Ankyrin Repeat Protein, Protein Binding
Od01g06170	Predicted Protein
Od01g06190	H+-Or Na+-Translocating F-Type, V-Type And A-Type Atpase, Chloroplast Membrane
Od01g06380	3-Isopropylmalate Dehydratase
Od01g06560	Predicted Protein
Od01g07060	Predicted Protein
Od02g00070	Mfs Transporter
Od02g00080	Mfs Transporter
Od02g00190	Predicted Protein
Od02g00480	Predicted Protein
Od02g00530	Molecular Chaperone DNAJ
Od02g00710	Predicted Protein, Chloroplast Membrane
Od02g01370	Monogalactosyldiacylglycerol transferase, glycolipid biosynthesis
Od02g01610	Tubulin Gamma-1 Chain
Od02g01640	1-Deoxy-D-Xylulose-5-Phosphate Synthase, Terpenoid Biosynthesis
Od02g01720	Unnamed Product
Od02g01730	Bifunctional Aconitate Hydratase 2/2-Methylisocitrate Dehydratase
Od02g01760	Unnamed Product
Od02g01840	Luminal-Binding Protein
Od02g02250	Redox-Regulated ATPase Ychf
Od02g02530	Magnesium-protoporphyrin IX chelatase, porphyrin biosynthesis
Od02g02590	DNA directed RNA polymerase, zinc finger, TFIIS-type
Od02g02800	Predicted Protein, Transferase

Od02g02880	Clp protease
Od02g02890	ATP-Dependent Clp Protease Proteolytic Subunit-Related Protein 3, Chloroplastic
Od02g02950	Clp protease
Od02g02960	ATP-Dependent Clp Protease Proteolytic Subunit-Related Protein 4, Chloroplastic
Od02g03030	Protein Binding, Chloroplast Import, Response To Light
Od02g03130	9-Cis-Epoxycarotenoid Dioxygenase
Od02g03280	Predicted Protein
Od02g03500	Predicted Protein
Od02g03840	Predicted Protein, NADP Biosynthetic Process
Od02g03960	Unnamed Product
Od02g04020	Protein Serine/Threonine Kinase Activity
Od02g04030	Predicted Protein
Od02g04110	Aminoacyl TRNA Synthase Complex-Interacting
Od02g04200	50S Ribosomal Protein L24
Od03g00700	Predicted Protein
Od03g00760	Predicted Protein
Od03g01080	Light Induced Like Protein, Chloroplast Membrane
Od03g01170	Phosphatidylinositol Phosphorylation
Od03g01260	Aquaporin Aqpae.A
Od03g01290	Predicted Protein
Od03g01710	Predicted Protein
Od03g01850	Unnamed Product
Od03g01930	F0F1 Atp Synthase Subunit Alpha
Od03g02030	Dihydrolipoyllysine-Residue Acetyltransferase, Chloroplastic
Od03g02190	Cycloartenol Synthase
Od03g02200	1,4-Alpha-Glucan-Branching Enzyme 2-2, Chloroplastic/Amyloplastic Isoform X1
Od03g02230	Predicted Protein, DNA Binding
Od03g02310	Myb Transcription Factor
Od03g02360	Predicted Protein, Proteasome Complex
Od03g02370	Proteasome-Associated Protein Ecm29 Homolog Isoform X1
Od03g02850	Fructose-1,6-bisphosphatase
Od03g02930	Splicing Factor 3B Subunit 1-Like
Od03g03040	Predicted Protein, rRNA Binding
Od03g03050	Unnamed Product
Od04g00140	Predicted Protein
Od04g00330	Predicted Protein
Od04g00340	T9Ss C-Terminal Target Domain-Containing Protein
Od04g00460	Predicted Protein, DNA Binding Transcription Factor Activity
Od04g00520	Predicted Protein, RNA Splicing
Od04g00660	Dihydrolipoyl Dehydrogenase
Od04g00690	Predicted Protein
Od04g00700	DNA Binding
Od04g00720	Predicted Protein, Branched-Chain Amino Acid Biosynthetic Process
Od04g00730	Alanyl-tRNA Synthetase
Od04g01170	Unnamed Product
Od04g01340	Dicarboxylate Transporter 2.1, Chloroplastic-Like
Od04g01470	Ornithine Decarboxylase
Od04g01620	Predicted Protein
Od04g01630	Membrane protein, ion channel
Od04g01770	Predicted Protein
Od04g01800	CCT (CONSTANS, CO-like, and TOC1) domain, often involved in light signalling
Od04g01890	Predicted Protein, Fatty Acid Metabolism
Od04g01900	Predicted Protein, Lipid Metabolism
Od04g01950	Histone Acetyltransferase

Od04g02010	Predicted Protein
Od04g02180	Npl4-Like Protein 1
Od04g02270	Predicted Protein
Od04g02360	Predicted Protein
Od04g02450	Proline Dehydrogenase
Od04g02510	Dof-Like Transcription Factor
Od04g02530	Predicted Protein
Od04g02650	Predicted Protein
Od04g02810	Predicted Protein
Od04g02820	Rubisco Activase
Od04g02890	Glycoside Hydrolase Family 31 Protein
Od04g02910	Predicted Protein
Od04g02960	Ycf3-Interacting Protein 1, Chloroplastic
Od04g03220	Magnesium Chelatase Subunit H
Od04g03290	Predicted Protein
Od04g03380	Predicted Protein
Od04g03730	Unnamed Product
Od04g03820	Sugar Phosphate Exchanger 3
Od04g05010	Predicted Protein
Od04g05170	Ankyrin Repeat, Protein Binding
Od04g05330	Predicted Protein, Translation
Od04g05340	Predicted Protein, Translation
Od05g00090	GTP cyclohydrolase, tetrahydrofolate biosynthetic process
Od05g00580	Ammonium Transporter
Od05g00590	Ammonium Transporter
Od05g00680	Psbb MRNA Maturation Factor Mbb1, Chloroplast Precursor
Od05g00710	Membrane Component
Od05g01030	Membrane Component
Od05g01130	Predicted Protein
Od05g01280	Inner Membrane Protein Ppf-1, Chloroplastic
Od05g01350	Porphobilinogen deaminase, tetrapyrrole biosynthesis
Od05g01370	Predicted Protein, Nucleic Acid Binding
Od05g01720	Dmt Family Transporter: Phosphate/Phosphoenolpyruvate
Od05g01780	DNA Replication Licensing Factor, MCM5 Component (Iss)
Od05g01890	Membrane Component
Od05g01900	3-dehydroquinate synthase, aromatic amino acid biosynthesis
Od05g01980	DNA RNA-Binding Protein Alba-Like
Od05g02220	RNA Binding
Od05g02290	DNA Binding Transcription Factor
Od05g02490	Kinase Activity
Od05g02660	Glycylpeptide N-Tetradecanoyltransferase 1
Od05g02670	Transmembrane Protein 184A-Like
Od05g03200	Glycoside Hydrolase Family 31 Protein
Od05g03380	Negative Regulation Of Transcription By RNA Polymerase III
Od05g03520	Predicted Protein
Od05g03740	Membrin-11-Like
Od05g04140	Predicted Protein, Protein Binding
Od05g04230	Predicted Protein
Od05g04450	Probable Trehalose
Od05g04570	Predicted Protein, Protein Binding
Od05g04600	DNAJ Homolog Subfamily B Member 13
Od05g04640	Membrane Component
Od05g04700	Bromodomain-Containing Protein
Od05g04710	Predicted Protein
Od05g04740	Electron Transport

Od05g05070	Predicted Protein
Od05g05120	Magnesium protoporphyrin chelatase, chlorophyll biosynthesis
Od06g00580	DNA Binding
Od06g00660	Phosphoglycerate Kinase
Od06g00980	Membrane Component
Od06g00990	Membrane Component
Od06g01000	RNA Polymerase Sigma Factor Rpod
Od06g01010	Predicted Protein, Protein Binding
Od06g01110	Predicted Protein, Nucleotide Metabolism
Od06g01290	Ferredoxin, chloroplast precursor
Od06g01630	Predicted Protein
Od06g01660	Nucleobase biosynthesis
Od06g01900	WD40 repeat containing, actin cytoskeleton, TOR signalling
Od06g01910	Chaperone DNAJ homologue, Myb-like domain
Od06g02270	Transcription Factor
Od06g02790	Integral Membrane Protein
Od06g03120	Predicted Protein, Protein Binding
Od06g03250	Divergent Pap2 Family Protein
Od06g03260	Membrane Component
Od06g03270	Predicted Protein, Actin Binding
Od06g03340	Aminoacyl-tRNA synthetase, tRNA aminoacylation
Od06g03440	Protoporphyrinogen oxidase, porphyrin biosynthesis
Od06g03460	Photosystem I assembly protein Ycf4
Od06g03610	Dual Specificity Protein Phosphatase 1-Like
Od06g03790	NADP-Dependent Malic Enzyme
Od06g03820	Elongation Factor 4
Od06g04450	Transcription Factor Divaricata
Od06g04460	Unnamed Product
Od06g04530	Fatty acid desaturase, lipid metabolism
Od06g04580	Translation Elongation
Od06g04640	Porphyrin, chlorophyll biosynthesis
Od06g04660	Glycoside Hydrolase Family 14 Protein
Od06g04670	Unnamed Product
Od06g04680	Proteolysis
Od06g04800	Predicted Protein
Od06g04820	Membrane Component
Od06g06090	Predicted Protein
Od06g06110	B12 (cobalamin) dependent methionine synthase
Od06g06190	Abc Transporter I Family Member 6, Chloroplastic
Od06g06880	Protein Serine/Threonine Kinase Activity
Od06g06980	Fructose-1,6-bisphosphatase, gluconeogenesis
Od06g07010	Bah-Phd Domain-Containing Protein
Od06g07490	Predicted Protein
Od06g07510	La-Related Protein 1C-Like
Od07g00130	Cysteine Synthase 2
Od07g00140	Predicted Protein
Od07g00470	Predicted Protein, Proteolysis
Od07g00560	Predicted Protein
Od07g00720	Unnamed Product
Od07g00730	Short-Chain Dehydrogenase
Od07g00770	Membrane Component
Od07g00800	Unnamed Product
Od07g01230	Predicted Protein, Protein Binding
Od07g01310	Protein Chromatin Remodelling 4-Like Isoform X1
Od07g01350	DNA Binding Transcription Factor Activity

Od07g01360	Predicted Protein
Od07g01440	Malate Dehydrogenase (Oxaloacetate-Decarboxylating)(Nadp+)
Od07g01730	Lysine-Specific Demethylase 8, Cell Cycle
Od07g01750	Chloroplast ATP Synthase Subunit Delta Precursor
Od07g01970	50S ribosomal protein L27
Od07g02050	Predicted Protein, Microtubule
Od07g02100	Membrane Component
Od07g02380	Predicted Protein, Protein Serine/Threonine Kinase Activity
Od07g02800	Hypothetical Protein Micpucdraft_57447
Od07g02830	(2Fe-2S)-binding protein, chlorophyllide a oxygenase
Od07g02870	Predicted Protein
Od07g03190	Tryptophan Synthase Beta Chain 1
Od07g03230	T9Ss C-Terminal Target Domain-Containing Protein
Od07g03240	Bet1-Like Protein At4G14600
Od07g03350	Predicted Protein
Od07g03480	Predicted Protein, Nucleic Acid Binding
Od07g03510	Chromosome-Associated Kinesin Kif4A
Od07g03670	Predicted Protein
Od07g03760	Phospholipid biosynthetic process
Od07g03780	Membrane Component
Od07g03790	Coiled-Coil Domain-Containing Protein 25
Od07g03830	DNA Binding Transcription Factor
Od07g03910	Phosphoribosyltransferase, nucleotide synthesis and salvage
Od07g03920	Cytidylyltransferase, isoprenoid biosynthesis
Od07g04200	Predicted Protein
Od07g04230	Probable Serine Incorporator
Od07g04640	Sulp Family Inorganic Anion Transporter
Od07g04740	Chloroplast SRP receptor, signal recognition
Od07g04840	Ubiquinone/Menaquinone Biosynthesis Methyltransferase
Od08g00180	Histone H3
Od08g00340	Protein Lhcp Translocation
Od08g00380	Anaphase-Promoting Complex Subunit
Od08g01040	Chlorophyll Synthetase
Od08g01130	Predicted Protein
Od08g01380	Unnamed Product
Od08g01520	Predicted Protein, Nucleotide Metabolism
Od08g01560	Predicted Protein
Od08g01810	Zinc Finger CCCH Domain-Containing Protein 28
Od08g02040	Predicted Protein
Od08g02100	Predicted Protein
Od08g02170	Branched-Chain Amino Acid Aminotransferase
Od08g02490	Predicted Protein
Od08g02690	Predicted Protein, Protein Binding
Od08g02950	Predicted Protein
Od08g03020	Predicted Protein
Od08g03040	Hypothetical Protein, Partial
Od08g03150	Predicted Protein
Od09g00820	Phytoene desaturase, carotenoid biosynthesis
Od09g01000	(2Fe-2S)-binding protein, chlorophyllide a oxygenase
Od09g01170	Fatty acid desaturase, cytochrome b5 domain, unknown function
Od09g01770	Unnamed Product
Od09g02190	Predicted Protein
Od09g02220	Membrane Component
Od09g02460	Predicted Protein, Transport
Od09g02470	Predicted Protein

Od09g02650	Predicted Protein, Histone Methylation
Od09g02790	Probable Protein Phosphatase 2C 60 Isoform X1
Od09g03050	Predicted Protein
Od09g03380	Ribulose-1,5 bisphosphate carboxylase, methyltransferase
Od09g03480	Malonyl-Coa:Acp Transacylase
Od09g03710	Mfs Family Transporter: Glycerol-3-Phosphate
Od09g03950	Predicted Protein, Heme Binding
Od09g04020	Membrane Component
Od09g04370	Membrane Component
Od09g04740	Endonuclease
Od09g04760	Protein Kinase
Od09g04780	Predicted Protein, Protein Binding
Od09g04790	Predicted Protein, Protein Modification
Od09g05010	Constans-Like 1 Protein
Od09g05080	Predicted Protein, RNA Binding, Psi Related
Od09g05360	Terpenoid biosynthesis
Od09g05650	Predicted Protein
Od09g05690	Predicted Protein, Protein Serine/Threonine Kinase Activity
Od09g06000	Membrane Component
Od09g06240	Predicted Protein
Od09g06250	Fructose-1,6-Bisphosphatase, Cytosolic
Od10g00160	Predicted Protein, DNA Binding
Od10g00290	E3 Ubiquitin-Protein Ligase Rnf126-B
Od10g00380	Predicted Protein, Hydrolase
Od10g01170	Endosome Organisation
Od10g01180	NADH Dehydrogenase [Ubiquinone] 1 Beta Subcomplex Mitochondrial
Od10g01350	Patched Domain-Containing Protein 2
Od10g01360	Resistance-Nodulation-Cell Division Superfamily
Od10g01560	Translation Initiation Factor
Od10g01610	Predicted Protein
Od10g01620	Thiol-Disulfide Oxidoreductase Lto1-Like
Od10g01780	Unnamed Product
Od10g01790	Predicted Protein, Hydrolase
Od10g02060	Bacterial Surface Protein, Nucleic Acid Binding
Od10g02140	Unnamed Product
Od10g02230	Unnamed Product
Od10g02270	Morn Repeat Protein, Ion Transport
Od10g02420	Predicted Protein Hydrolase
Od10g02450	Unnamed Product
Od11g00560	ATP-binding cassette translation elongation factor
Od11g00650	Unnamed Product
Od11g00770	Predicted Protein
Od11g00830	Phosphatidylinositol 4-kinase mediated signalling
Od11g00840	Unnamed Product
Od11g00860	Negative Regulation of Transcription Elongation From RNA Polymerase II
Od11g00900	Starch synthase, glycosyltransferase
Od11g00960	MECDP synthase, terpenoid biosynthesis
Od11g01480	Predicted Protein, Protein Binding
Od11g01930	Predicted Protein, Nucleic Acid Binding
Od11g02010	Predicted Protein
Od11g02320	Arsenite-Antimonite Efflux Family
Od11g02450	Glycosyltransferase Family 4 Protein
Od11g02470	Membrane Component
Od11g04000	ATP-Binding Cassette Superfamily
Od11g04110	Predicted Protein, Proteolytic

Od11g04210	Sulp Family Inorganic Anion Transporter
Od11g04260	Nucleotide-Diphospho-Sugar Transferase
Od12g00050	Urea-Proton Symporter Dur3
Od12g00420	Membrane Component
Od12g00820	Membrane Component
Od12g00990	Predicted Protein, RNA Processing
Od12g01140	Unnamed Product, Protein Binding
Od12g01230	Membrane Component
Od12g01380	Predicted Protein, Hydrolase
Od12g01710	Predicted Protein, Protein Binding
Od12g01760	Predicted Protein, DNA Binding
Od12g01770	Predicted Protein, Fatty Acid Metabolism
Od12g01860	Predicted Protein
Od12g01950	Geranylgeranyl Diphosphate Synthase, Terpenoid Biosynthesis
Od12g02640	Putative Snf7-Like Protein
Od12g02660	Prasinophyte-Specific Protein-4
Od12g02670	Dsba Oxidoreductase
Od12g03120	Uroporphyrinogen decarboxylase, porphyrin biosynthesis
Od12g03300	Predicted Protein, Methyltransferase
Od12g03770	Predicted Protein, Protein Serine/Threonine Kinase Activity
Od13g00240	Predicted Protein, Protein Binding
Od13g00610	Peptidyl-Prolyl Cis-Trans Isomerase, Fkbp-Type
Od13g00740	Predicted Protein, Serine/Threonine Phosphatase Activity
Od13g00750	Cytochrome P450, heme binding, function undefined
Od13g00880	RNA Demethylase Alkbh5-Like
Od13g00890	Predicted Protein, TRNA Modification
Od13g00950	Predicted Protein
Od13g01560	Protein Binding
Od13g01670	Predicted Protein, Tetrahydrofolylpolyglutamate Biosynthetic Process
Od13g01760	Predicted Protein
Od13g01850	Predicted Protein, Lipid Metabolism
Od13g02060	Glycosyltransferase, starch/glycogen synthase
Od13g02090	Predicted Protein, Transport
Od13g02710	Predicted Protein
Od13g02780	Membrane Component
Od13g02920	Ankyrin repeat, protein binding
Od13g03160	RNA Polymerase II Transcription Factor Activity
Od13g03190	Duf1295 Domain-Containing Protein
Od14g00300	Predicted Protein, Glucose Metabolism
Od14g00760	Translation Initiation Factor Activity
Od14g01100	Predicted Protein, DNA Binding
Od14g01250	Predicted Protein, RNA Polymerase Activity
Od14g01500	DNA Binding Transcription Factor Activity
Od14g01690	Predicted Protein, PSII Related
Od14g01880	Basic-Leucine Zipper Domain
Od14g01920	Predicted Protein, Fatty Acid Synthase Complex
Od14g02160	Drug/Metabolite Transporter Superfamily
Od14g02210	pre-rRNA-processing
Od14g02230	Divinyl Chlorophyllide A 8-Vinyl-Reductase, Chloroplastic
Od14g02240	Unnamed Product
Od14g02280	Glutamine-Rich Tetratricopeptide Repeat-Containing Protein, Actin Related
Od14g02540	DNA Binding Protein Reb1-Like
Od14g02610	Probable Prolyl 4-Hydroxylase 4
Od14g02940	Phosphoglucomutase, carbohydrate metabolism
Od14g03220	Unnamed Product

Od14g03280	Methyltransferase Activity
Od14g03300	Glutaredoxin 2
Od15g00140	(2Fe-2S)-Binding Protein
Od15g00340	Acyl-COA-Binding Domain-Containing Protein 4 Isoform X1
Od15g00560	Predicted Protein
Od15g00670	Predicted Protein
Od15g00860	Vacuolar Protein Sorting-Associated Protein 41 Homolog Isoform X2
Od15g01050	GHMP kinase, terpenoid biosynthetic process
Od15g01150	Predicted Protein, Spliceosome
Od16g00010	Antibiotic Biosynthesis Monooxygenase
Od16g00350	Dead-Box ATP-Dependent RNA Helicase
Od16g00450	Predicted Protein, Transport
Od16g00460	Predicted Protein
Od16g00470	Probable Mediator Of RNA Polymerase II Transcription Subunit 37C
Od16g00500	Dmt Family Transporter: Udp-Galactose/Udp-Glucose
Od16g00600	Fatty acid desaturase, lipid metabolism
Od16g00750	Peptidyl-Prolyl Cis-Trans Isomerase Fkbp16-4, Chloroplastic
Od16g00770	Membrane Component
Od16g01250	Predicted Protein
Od16g01280	Protein Detoxification
Od16g01340	Predicted Protein
Od16g01370	Predicted Protein
Od16g01420	Drug/Metabolite Transporter Superfamily
Od16g01600	Predicted Protein
Od16g01660	Predicted Protein
Od16g01820	Drug/Metabolite Transporter Superfamily
Od16g01860	Predicted Protein, Kinase
Od16g02100	Pkinase-Domain-Containing Protein
Od16g02230	Membrane Component
Od16g02240	Predicted Protein
Od16g02340	DNA Binding Transcription Factor
Od16g02550	Multidrug/Oligosaccharidyl-Lipid/Polysaccharide Flippase
Od16g02600	Uroporphyrinogen decarboxylase, porphyrin biosynthesis
Od16g02630	Predicted Protein, Binding
Od16g02690	Translation Initiation Factor Activity
Od16g02700	Predicted Protein, Transport
Od17g00080	Predicted Protein
Od17g00180	Post-Set Domain
Od17g00300	Predicted Protein, Kinase
Od17g00310	Predicted Protein
Od17g00340	Divalent Anion:Na+ Symporter Family
Od17g00580	Predicted Protein, Methyltransferase Activity
Od17g00860	Membrane Component
Od17g00910	Predicted Protein, Electron Transport
Od17g00960	Polyadenylate-Binding Protein Rbp47B'
Od17g01480	Predicted Protein
Od17g01680	Unnamed Product
Od17g01690	Unnamed Product
Od17g01920	Predicted Protein
Od17g01930	Predicted Protein
Od17g01990	Chloroplast Ribulose Bisphosphate Carboxylase Complex
Od17g02000	Chloroplast Ribulose Bisphosphate Carboxylase Complex
Od17g02080	Mg2+ Transporter-E Family
Od17g02560	Unnamed Product
Od17g02960	Membrane Component

Od17g03100	Predicted Protein, DNA Metabolism
Od17g03170	Predicted Protein, Hydrolase
Od18g00230	Predicted Protein
Od18g00250	Unnamed Product
Od18g00260	Predicted Protein
Od18g00270	Predicted Protein
Od18g00310	Membrane Component
Od18g00380	Predicted Protein, Transferase
Od18g00470	Predicted Protein, Transferase
Od19g00040	Light Harvesting Complex Protein
Od19g00250	Sec14P-Like Phosphatidylinositol Transfer Family Protein
Od19g00430	Predicted Protein
Od19g00510	Predicted Protein, Hydrolase
Od19g00640	ATP-Dependent RNA Helicase Rhle
Od19g00660	Unnamed Product
Od19g01010	Predicted Protein
Od19g01200	Glutamate-1-Semialdehyde Aminotransferase, Chlorophyll Biosynthetic Process
Od19g01230	Heat Stress Transcription Factor A-8
Od20g00600	Auxin Efflux Carrier Family
Od20g00610	Membrane Component
Od20g00760	Lycopene beta cyclase, contains chlorophyll a/b binding domain
Od20g00770	Tho Complex Subunit 4, Nucleic Acid Binding
Od20g00950	Predicted Protein, Spliceosome
Od20g01100	Fructose-1,6-Bisphosphatase
Od20g01230	Chlorophyll A/B-Binding Protein Cp26, Chloroplast Precursor
Od20g01770	Ankyrin Repeat, Protein Binding
Od20g02020	Predicted Protein, Methyltransferase Activity
Od20g02230	Predicted Protein, RNA Binding
Od20g02410	Unnamed Product
Od20g02440	Predicted Protein, Electron Transport
Od20g02470	Isoamylase 1, Chloroplastic
Od20g02670	Predicted Protein, PSII Related
Od20g02980	Predicted Protein, Lipid Binding
Od20g03120	Niemann-Pick C1 Protein

Appendix 3 Overexpressed functional categories for GO enrichment

Overrepresented functional terms of RCC809 genes with increased expression in blue light compared to red and green							
Gene Ontology ID	FDR corrected q value	Genes with GO term in test set	Genes with GO term in genome	Genes in test set	Total Bio Process genes in genome	Description	
6259	3.89E-04	36	242	262	4247	DNA metabolic process	
Genes in test set	OD17G00920 OD06G02850 OD07G03710 OD01G00210 OD08G00650 OD04G00270 OD12G01680 OD12G02990 OD12G00470 OD11G01550 OD20G01140 OD01G02880 OD11G01890 OD06G06580 OD11G02480 OD04G04360 OD05G01480 OD15G01260 OD06G04320 OD06G03670 OD08G00520 OD04G00260 OD17G01560 OD03G01380 OD13G01180 OD04G00830 OD08G02560 OD15G00900 OD12G02680 OD08G01730 OD20G00460 OD05G04620 OD06G06590 OD01G05760 OD05G04960 OD05G03110						
33554	7.30E-03	29	204	262	4247	Cellular response to stress	
Genes in test set	OD17G00920 OD06G02850 OD07G03710 OD01G00210 OD13G00080 OD04G00270 OD12G02990 OD12G00470 OD11G01550 OD11G00060 OD06G06580 OD19G00740 OD05G01480 OD10G00450 OD15G01260 OD06G03670 OD04G00260 OD17G01560 OD03G01380 OD02G03690 OD15G00900 OD08G01730 OD09G06210 OD20G00460 OD09G04910 OD06G06590 OD01G05760 OD05G04960 OD01G06230						
6260	7.36E-03	17	89	262	4247	DNA replication	
Genes in test set	OD06G02850 OD04G04360 OD06G04320 OD08G00520 OD08G00650 OD17G01560 OD03G01380 OD13G01180 OD12G01680 OD12G02990 OD04G00830 OD12G02680 OD20G01140 OD11G01890 OD05G04620 OD11G02480 OD05G03110						
6261	7.81E-03	11	42	262	4247	DNA-dependent DNA replication	
Genes in test set	OD12G01680 OD06G02850 OD12G02990 OD04G00830 OD04G04360 OD20G01140 OD08G00650 OD11G01890 OD13G01180 OD05G04620 OD05G03110						
6281	1.47E-02	21	138	262	4247	DNA repair	
	OD17G00920 OD06G02850 OD07G03710 OD05G01480 OD15G01260 OD06G03670 OD01G00210 OD04G00260 OD17G01560 OD03G01380 OD04G00270 OD12G02990 OD15G00900 OD12G00470 OD11G01550 OD08G01730 OD20G00460 OD06G06590 OD01G05760 OD05G04960 OD06G06580						
6950	1.95E-02	39	351	262	4247	Response to stress	
Genes in test set	OD17G00920 OD06G02850 OD06G00250 OD07G03710 OD01G00210 OD01G01640 OD10G01390 OD13G00080 OD04G00270 OD12G02990 OD12G00470 OD11G01550 OD20G03400 OD11G00060 OD06G03190 OD06G06580 OD19G00740 OD05G01480 OD10G00450 OD15G01260 OD06G03670 OD06G07410 OD04G00260 OD17G01560 OD03G01380 OD02G03690 OD02G04480 OD15G00900 OD02G03670 OD08G01730 OD09G06210 OD20G00460 OD09G05100 OD09G04910 OD06G06590 OD01G05760 OD11G00170 OD05G04960 OD01G06230						
7059	1.95E-02	7	21	262	4247	Chromosome segregation	
	OD02G00280 OD05G00600 OD14G03010 OD06G05210 OD12G02680 OD02G03890 OD01G02860						

51716	2.15E-02	31	259	262	4247	Cellular response to stimulus	
	OD17G00920 OD06G02850 OD07G03710 OD01G00210 OD13G00080 OD04G00270 OD12G02990 OD12G00470 OD11G01550 OD11G00060 OD06G06580 OD19G00740 OD05G01480 OD10G00450 OD15G01260 OD06G03670 OD04G00260 OD17G01560 OD03G01380 OD12G00040 OD02G03690 OD09G05920 OD15G00900 OD08G01730 OD09G06210 OD20G00460 OD09G04910 OD06G06590 OD01G05760 OD05G04960 OD01G06230						
71705	2.15E-02	3	3	262	4247	Nitrogen compound transport	
	OD07G00170 OD07G00180 OD03G02690						
71103	2.20E-02	11	53	262	4247	DNA conformation change	
	OD03G02870 OD20G01820 OD06G03670 OD14G03010 OD12G02680 OD02G03890 OD20G01140 OD02G00310 OD03G01380 OD01G02860 OD05G03110						
6099	2.20E-02	9	37	262	4247	Tricarboxylic acid cycle	
	OD08G00070 OD04G01850 OD02G03200 OD06G02230 OD05G01850 OD13G00190 OD06G07420 OD03G03160 OD01G06980						
50896	2.69E-02	51	523	262	4247	Response to stimulus	
	OD17G00920 OD06G02850 OD07G03710 OD01G00210 OD13G00080 OD02G04230 OD12G00470 OD11G01550 OD14G03310 OD16G00040 OD20G03400 OD11G00060 OD06G03190 OD06G06580 OD19G00740 OD05G01480 OD15G01260 OD06G03670 OD03G01380 OD03G03160 OD12G00040 OD02G03690 OD09G05100 OD06G06590 OD01G05760 OD11G00170 OD14G01080 OD06G00250 OD01G01640 OD16G00890 OD10G01390 OD04G00270 OD12G02990 OD17G01040 OD04G03210 OD11G01910 OD10G00450 OD06G07410 OD04G00260 OD17G01560 OD09G05920 OD02G04480 OD15G00900 OD02G03670 OD08G01730 OD09G06210 OD20G00460 OD09G04910 OD05G04960 OD05G03110 OD01G06230						
9263	2.69E-02	4	7	262	4247	Deoxyribonucleotide biosynthetic process	
	OD01G02300 OD08G00520 OD16G00170 OD07G01740						
6270	2.69E-02	5	12	262	4247	DNA-dependent DNA replication initiation	
	OD12G01680 OD04G00830 OD04G04360 OD20G01140 OD08G00650						
22402	4.80E-02	9	43	262	4247	Cell cycle process	
	OD14G01080 OD05G00600 OD14G03010 OD06G05210 OD04G00790 OD02G03890 OD01G02860 OD05G04620 OD05G03110						

Overrepresented functional terms of RCC809 genes with increased expression in green light compared to red and blue						
Gene Ontology ID	FDR corrected q value	Genes with GO term in test set	Genes with GO term in genome	Genes in test set	Total Bio Process genes in genome	Description
45454	3.03E-02	4	62	21	4247	Cell redox homeostasis
	OD05G04680 OD16G01540 OD01G02490 OD06G07490					

Overrepresented functional terms of RCC809 genes with increased expression in red light compared to green and blue						
Gene Ontology ID	FDR corrected q value	Genes with GO term in test set	Genes with GO term in genome	Genes in test set	Total Bio Process genes in genome	Description
6098	2.56E-03	4	28	25	4247	Pentose-phosphate shunt OD03G02850 OD04G00980 OD07G04720 OD14G02940
6740	2.56E-03	4	29	25	4247	NADPH regeneration OD03G02850 OD04G00980 OD07G04720 OD14G02940
15976	2.56E-03	4	34	25	4247	Carbon utilization OD04G02610 OD03G02850 OD04G00980 OD07G04720
44282	4.07E-03	5	87	25	4247	Small molecule catabolic process OD03G02850 OD04G00980 OD09G03890 OD07G04720 OD14G02940
6007	4.07E-03	4	49	25	4247	Glucose catabolic process OD03G02850 OD04G00980 OD07G04720 OD14G02940
6096	1.29E-02	3	33	25	4247	Glycolysis OD03G02850 OD04G00980 OD14G02940
55086	1.44E-02	6	211	25	4247	Nucleobase, nucleoside and nucleotide metabolic process OD04G02610 OD03G02850 OD04G00980 OD09G03890 OD07G04720 OD14G02940
6094	1.45E-02	3	37	25	4247	Gluconeogenesis OD03G02850 OD04G00980 OD14G02940
16138	1.81E-02	2	11	25	4247	Glycoside biosynthetic process OD03G02850 OD14G02940
46364	1.81E-02	3	42	25	4247	Monosaccharide biosynthetic process OD03G02850 OD04G00980 OD14G02940
9266	1.87E-02	3	43	25	4247	Response to temperature stimulus OD04G02610 OD09G00180 OD14G02940
46165	2.41E-02	3	48	25	4247	Alcohol biosynthetic process OD03G02850 OD04G00980 OD14G02940
160	3.20E-02	2	16	25	4247	Two-component signal transduction system (phosphorelay) OD09G04300 OD09G04310
43094	4.16E-02	2	19	25	4247	Cellular metabolic compound salvage OD04G02610 OD17G02010
9628	4.16E-02	4	126	25	4247	Response to abiotic stimulus OD04G02610 OD09G00180 OD14G02940 OD06G03170
98	4.16E-02	1	1	25	4247	Sulfur amino acid catabolic process OD09G03890
6090	4.16E-02	3	64	25	4247	Pyruvate metabolic process OD03G02850 OD04G00980 OD14G02940
6013	4.48E-02	2	21	25	4247	Mannose metabolic process OD03G02850 OD04G00980
6000	4.69E-02	2	22	25	4247	Fructose metabolic process OD03G02850 OD04G00980

Overrepresented functional terms of RCC809 genes with decreased expression in blue light compared to red and green						
Gene Ontology ID	FDR corrected q value	Genes with GO term in test set	Genes with GO term in genome	Genes in test set	Total Bio Process genes in genome	Description
46148	1.56E-07	18	47	273	4247	Pigment biosynthetic process
	OD16G02600 OD05G05120 OD11G00960 OD06G03440 OD14G02230 OD06G04640 OD04G03220 OD02G02530 OD19G01200 OD08G01040 OD13G00750 OD12G03120 OD01G01020 OD01G04650 OD09G00820 OD05G01350 OD20G00760 OD09G03950					
15995	9.29E-07	11	19	273	4247	Chlorophyll biosynthetic process
	OD19G01200 OD08G01040 OD05G05120 OD11G00960 OD14G02230 OD12G03120 OD04G03220 OD01G01020 OD01G04650 OD02G02530 OD05G01350					
6779	9.55E-06	14	39	273	4247	Porphyrin biosynthetic process
	OD16G02600 OD05G05120 OD11G00960 OD06G03440 OD14G02230 OD06G04640 OD04G03220 OD02G02530 OD19G01200 OD08G01040 OD12G03120 OD01G01020 OD01G04650 OD05G01350					
8299	4.72E-05	12	33	273	4247	Isoprenoid biosynthetic process
	OD07G03920 OD15G01050 OD13G00750 OD08G01130 OD11G00960 OD05G01900 OD09G05360 OD09G00820 OD02G01640 OD20G00760 OD12G01950 OD09G03950					
16114	9.98E-05	10	25	273	4247	Terpenoid biosynthetic process
	OD15G01050 OD13G00750 OD11G00960 OD05G01900 OD09G05360 OD09G00820 OD02G01640 OD20G00760 OD12G01950 OD09G03950					
6782	2.74E-04	6	9	273	4247	Protoporphyrinogen IX biosynthetic process
	OD19G01200 OD16G02600 OD06G03440 OD12G03120 OD01G04650 OD05G01350					
44271	5.77E-04	37	278	273	4247	Cellular nitrogen compound biosynthetic process
	OD06G01660 OD07G03910 OD06G03440 OD14G02230 OD04G03220 OD04G02450 OD07G01750 OD13G01670 OD04G00720 OD08G01040 OD01G06380 OD08G01560 OD05G01900 OD12G03120 OD06G01110 OD16G02600 OD05G05120 OD11G00960 OD11G01930 OD06G04640 OD05G00090 OD04G01470 OD07G00130 OD02G03840 OD02G02530 OD08G02170 OD01G05480 OD19G01200 OD07G03190 OD01G06190 OD03G01930 OD01G01020 OD06G06110 OD01G04650 OD11G00770 OD01G04550 OD05G01350					

6007	1.49E-03	12	49	273	4247	Glucose catabolic process
	OD05G04230 OD01G05480 OD03G02850 OD04G00660 OD09G06250 OD06G00660 OD06G06980 OD11G00770 OD20G01100 OD14G00300 OD16G01600 OD14G02940					
6783	2.85E-03	7	19	273	4247	Heme biosynthetic process
	OD19G01200 OD16G02600 OD06G03440 OD12G03120 OD06G04640 OD01G04650 OD05G01350					
6096	3.89E-03	9	33	273	4247	Glycolysis
	OD01G05480 OD03G02850 OD04G00660 OD09G06250 OD06G00660 OD06G06980 OD20G01100 OD14G00300 OD14G02940					
34637	6.26E-03	13	68	273	4247	Cellular carbohydrate biosynthetic process
	OD09G06250 OD06G00660 OD13G02060 OD03G02200 OD01G05480 OD12G01770 OD03G02850 OD04G00660 OD20G02470 OD06G06980 OD20G01100 OD14G00300 OD14G02940					
6740	6.88E-03	8	29	273	4247	NADPH regeneration
	OD05G04230 OD03G02850 OD09G06250 OD06G06980 OD11G00770 OD20G01100 OD16G01600 OD14G02940					
6094	7.91E-03	9	37	273	4247	Gluconeogenesis
	OD01G05480 OD03G02850 OD04G00660 OD09G06250 OD06G00660 OD06G06980 OD20G01100 OD14G00300 OD14G02940					
16117	1.04E-02	5	12	273	4247	Carotenoid biosynthetic process
	OD13G00750 OD11G00960 OD09G00820 OD20G00760 OD09G03950					
46165	1.28E-02	10	48	273	4247	Alcohol biosynthetic process
	OD01G05480 OD03G02850 OD08G01130 OD04G00660 OD09G06250 OD06G00660 OD06G06980 OD20G01100 OD14G00300 OD14G02940					
19319	1.28E-02	9	40	273	4247	Hexose biosynthetic process
	OD01G05480 OD03G02850 OD04G00660 OD09G06250 OD06G00660 OD06G06980 OD20G01100 OD14G00300 OD14G02940					
8610	1.58E-02	18	126	273	4247	Lipid biosynthetic process
	OD07G03920 OD15G01050 OD11G00960 OD09G05360 OD07G03760 OD02G01640 OD12G01950 OD02G01370 OD12G01770 OD13G00750 OD08G01130 OD05G01900 OD09G03480 OD01G03440 OD09G00820 OD20G00760 OD09G03950 OD14G01920					
15979	2.45E-02	15	101	273	4247	Photosynthesis
	OD09G05080 OD05G05120 OD14G01690 OD06G00660 OD05G05070 OD17G01990 OD17G02000 OD02G02530 OD03G02850 OD19G00040 OD20G02670 OD01G01020 OD20G01230 OD06G03460 OD20G01100					
7034	3.43E-02	4	10	273	4247	Vacuolar transport

	OD04G02810 OD01G00820 OD12G02640 OD16G00450					
9250	4.67E-02	4	11	273	4247	Glucan biosynthetic process
	OD03G02200 OD20G02470 OD13G02060 OD14G02940					
42372	4.67E-02	2	2	273	4247	Phylloquinone biosynthetic process
	OD20G02670 OD07G04840					
30388	4.67E-02	2	2	273	4247	Fructose 1,6-bisphosphate metabolic process
	OD03G02850 OD20G01100					

Overrepresented functional terms of RCC809 genes with decreased expression in green light compared to red and blue						
Gene Ontology ID	FDR corrected q value	Genes with GO term in test set	Genes with GO term in genome	Genes in test set	Total Bio Process genes in genome	Description
6260	5.75E-10	18	89	101	4247	DNA replication
	OD06G02850 OD05G00150 OD04G04360 OD10G01480 OD08G00650 OD17G01560 OD02G01320 OD13G01180 OD02G02310 OD04G00830 OD17G03020 OD02G01330 OD12G02680 OD20G01140 OD11G01890 OD11G02480 OD05G03110 OD01G04460					
6261	1.01E-09	13	42	101	4247	DNA-dependent DNA replication
	OD06G02850 OD04G04360 OD10G01480 OD08G00650 OD02G01320 OD13G01180 OD02G02310 OD04G00830 OD02G01330 OD20G01140 OD11G01890 OD05G03110 OD01G04460					
6270	5.24E-09	8	12	101	4247	DNA-dependent DNA replication initiation
	OD04G00830 OD04G04360 OD02G01330 OD08G00650 OD20G01140 OD02G01320 OD02G02310 OD01G04460					
34645	8.08E-05	29	470	101	4247	Cellular macromolecule biosynthetic process
	OD06G02850 OD14G00170 OD08G00650 OD20G02070 OD17G03020 OD03G00630 OD02G02010 OD20G01140 OD11G01890 OD11G02480 OD01G01690 OD01G04460 OD05G00150 OD04G04360 OD14G02580 OD10G01480 OD17G01560 OD02G01320 OD13G01180 OD02G02310 OD02G04950 OD07G01660 OD04G00830 OD02G04480 OD02G01330 OD07G02180 OD12G02680 OD06G04370 OD05G03110					
6269	9.32E-03	3	5	101	4247	DNA replication, synthesis of RNA primer
	OD08G00650 OD11G01890 OD13G01180					
32508	1.08E-02	5	24	101	4247	DNA duplex unwinding

	OD06G03670 OD02G01330 OD20G01140 OD02G01320 OD01G04460					
71103	1.08E-02	7	53	101	4247	DNA conformation change
	OD06G03670 OD02G01330 OD12G02680 OD20G01140 OD02G01320 OD05G03110 OD01G04460					
32392	1.14E-02	5	25	101	4247	DNA geometric change
	OD06G03670 OD02G01330 OD20G01140 OD02G01320 OD01G04460					
6271	1.57E-02	3	7	101	4247	DNA strand elongation involved in DNA replication
	OD06G02850 OD10G01480 OD08G00650					
15706	1.84E-02	2	2	101	4247	Nitrate transport OD10G00820 OD10G00830
10016	2.92E-02	3	9	101	4247	Shoot morphogenesis OD11G01290 OD08G00650 OD05G03110

Overrepresented functional terms of RCC809 genes with decreased expression in red light compared to green and blue

Gene Ontology ID	FDR corrected q value	Genes with GO term in test set	Genes with GO term in genome	Genes in test set	Total Bio Process genes in genome	Description
16337	2.61E-02	1	3	3	4247	Cell-cell adhesion OD17G03230
9143	2.61E-02	1	5	3	4247	Nucleoside triphosphate catabolic process OD03G00090
160	4.17E-02	1	16	3	4247	Two-component signal transduction system (phosphorelay) OD12G00240

Appendix 4 Light quality responsive enzymes in RCC809 mapped to metabolic pathways from the KEGG database

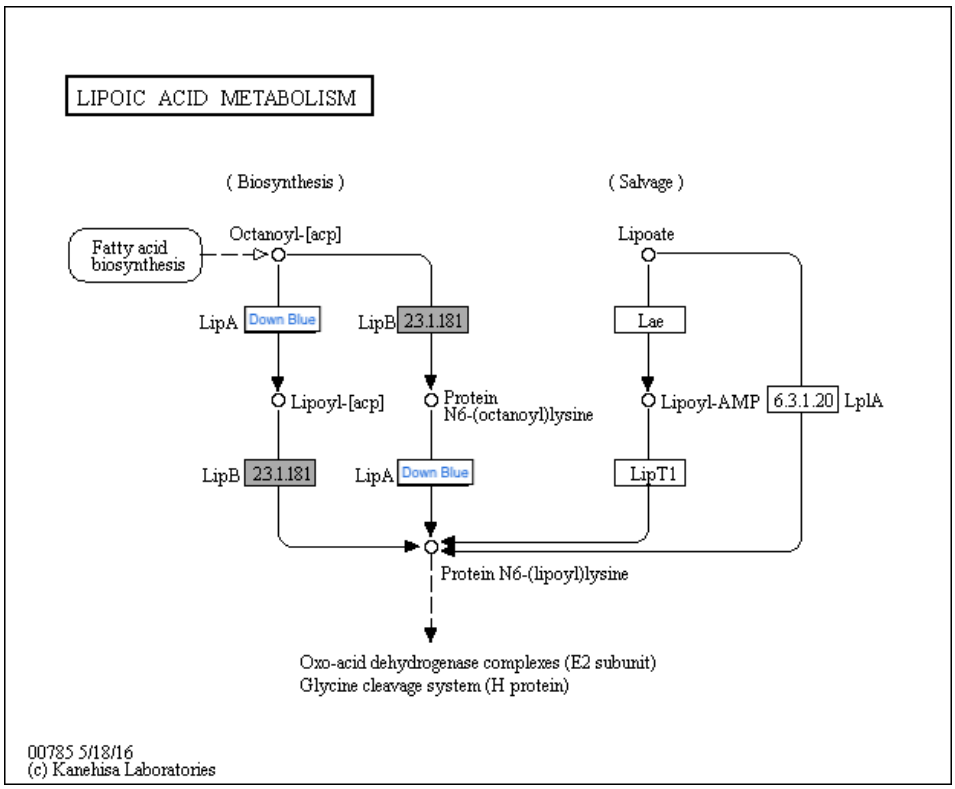

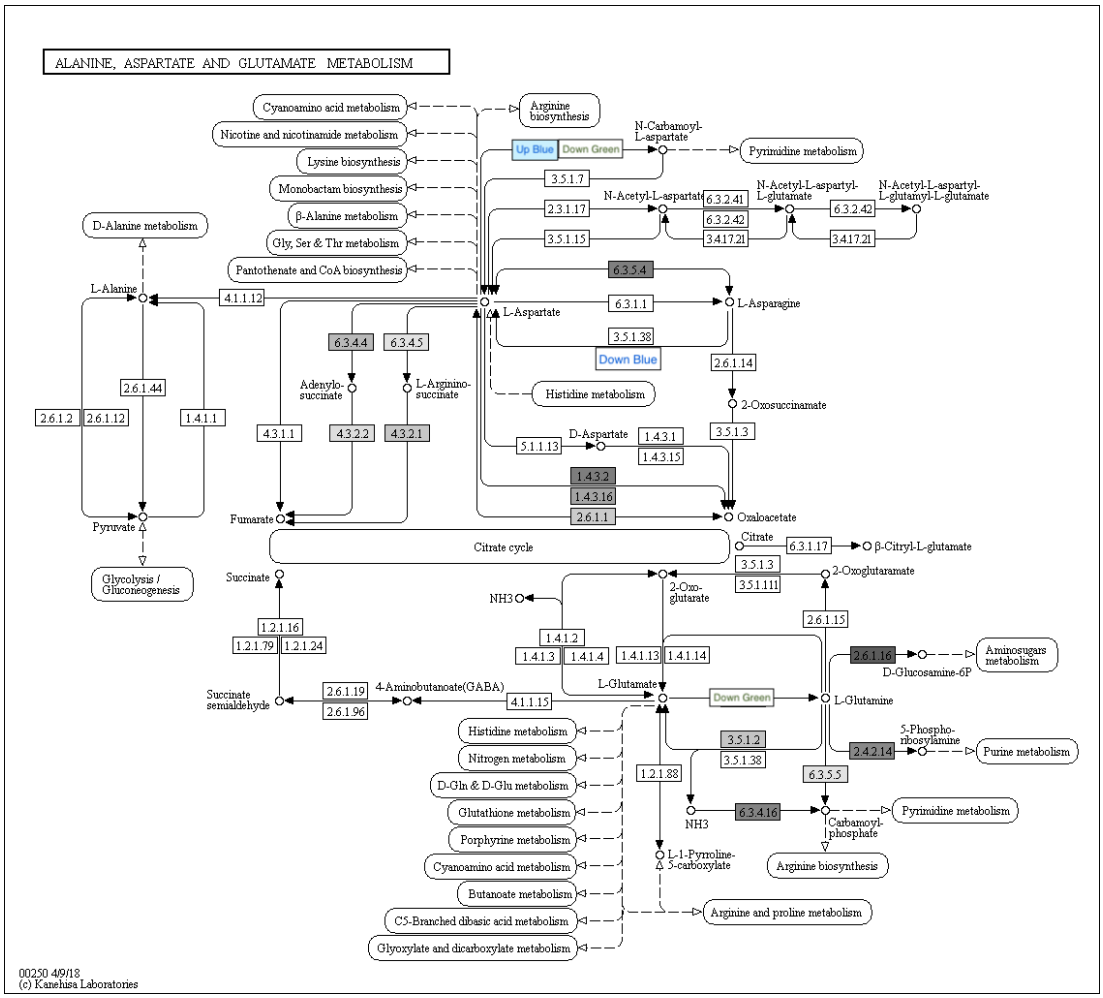
ALANINE, ASPARTATE AND GLUTAMATE METABOLISM
Cyanoamino acid metabolism
Nicotine and nicotinamide metabolism
Lysine biosynthesis
Monobactam biosynthesis
β-Alanine metabolism
Gly, Ser & Thr metabolism
Pantothenate and CoA biosynthesis
Arginine biosynthesis
Pyrimidine metabolism
Up Blue
Down Green
N-Carbamoyl-L-aspartate
3.5.1.7
N-Acetyl-L-aspartate
2.3.1.17
6.3.2.41
6.3.2.42
3.4.17.21
N-Acetyl-L-aspartyl-L-glutamate
N-Acetyl-L-aspartyl-L-glutamyl-L-glutamate
3.5.1.15
D-Alanine metabolism
L-Alanine
4.1.1.12
6.3.5.4
L-Aspartate
6.3.1.1
L-Asparagine
3.5.1.38
Down Blue
2.6.1.14
2-Oxosuccinamate
6.3.4.4
6.3.4.5
Adenylo-succinate
L-Arginino-succinate
Histidine metabolism
2.6.1.44
2.6.1.2
2.6.1.12
1.4.1.1
4.3.1.1
4.3.2.2
4.3.2.1
5.1.1.13
D-Aspartate
1.4.3.1
1.4.3.15
3.5.1.3
1.4.3.2
1.4.3.16
2.6.1.1
Pyruvate
Fumarate
Oxaloacetate
Citrate cycle
Citrate
6.3.1.17
β-Citryl-L-glutamate
Glycolysis / Gluconeogenesis
Succinate
3.5.1.3
3.5.1.111
2-Oxoglutaramate
NH3
2-Oxo-glutarate
2.6.1.15
1.2.1.16
1.2.1.79
1.2.1.24
1.4.1.2
1.4.1.3
1.4.1.4
1.4.1.13
1.4.1.14
2.6.1.16
Aminosugars metabolism
D-Glucosamine-6P
Succinate semialdehyde
2.6.1.19
2.6.1.96
4-Aminobutanoate(GABA)
4.1.1.15
L-Glutamate
Down Green
L-Glutamine
Histidine metabolism
Nitrogen metabolism
D-Gln & D-Glu metabolism
Glutathione metabolism
Porphyrine metabolism
Cyanoamino acid metabolism
Butanoate metabolism
C5-Branched dibasic acid metabolism
Glyoxylate and dicarboxylate metabolism
3.5.1.2
3.5.1.38
2.4.2.14
5-Phospho-ribosylamine
Purine metabolism
1.2.1.88
6.3.5.5
NH3
6.3.4.16
Carbamoyl-phosphate
Pyrimidine metabolism
L-1-Pyrroline-5-carboxylate
Arginine biosynthesis
Arginine and proline metabolism
00250 4/9/18
(c) Kanehisa Laboratories

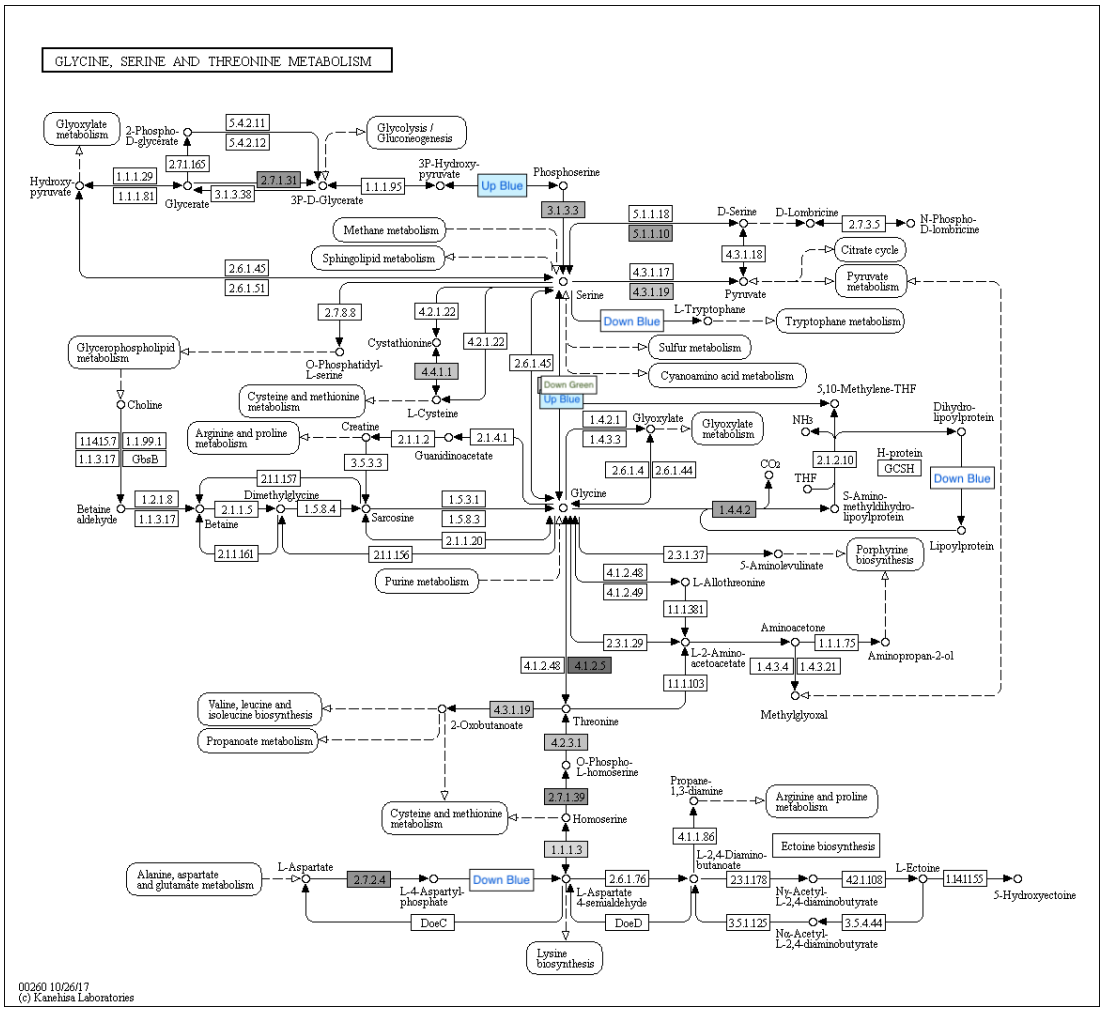
GLYCINE, SERINE AND THREONINE METABOLISM
Glyoxylate metabolism
2-Phospho-D-glycerate
5.4.2.11
5.4.2.12
Glycolysis / Gluconeogenesis
2.7.1.165
Hydroxy-pyruvate
1.1.1.29
1.1.1.81
Glycerate
3.1.3.38
2.7.1.31
3P-D-Glycerate
1.1.1.95
3P-Hydroxy-pyruvate
Up Blue
Phosphoserine
3.1.3.3
5.1.1.18
5.1.1.10
D-Serine
D-Lombricine
2.7.3.5
N-Phospho-D-lombricine
Methane metabolism
Sphingolipid metabolism
4.3.1.18
Citrate cycle
Pyruvate metabolism
2.6.1.45
2.6.1.51
4.3.1.17
4.3.1.19
Serine
Pyruvate
2.7.8.8
4.2.1.22
Down Blue
L-Tryptophane
Tryptophane metabolism
Glycerophospholipid metabolism
Cystathionine
4.2.1.22
Sulfur metabolism
O-Phosphatidyl-L-serine
4.4.1.1
2.6.1.45
Cyanoamino acid metabolism
Down Green
Up Blue
Cysteine and methionine metabolism
L-Cysteine
5,10-Methylene-THF
Choline
1.4.2.1
1.4.3.3
Glyoxylate
Glyoxylate metabolism
NH3
Dihydro-lipoylprotein
1.14.15.7
1.1.3.17
1.1.99.1
GbsB
Arginine and proline metabolism
Creatine
2.1.1.2
2.1.4.1
Guanidinoacetate
3.5.3.3
2.6.1.4
2.6.1.44
CO2
2.1.2.10
H-protein
GCSH
Down Blue
THF
2.1.1.157
Dimethylglycine
Glycine
1.4.4.2
S-Amino-methyldihydro-lipoylprotein
Betaine aldehyde
1.2.1.8
1.1.3.17
2.1.1.5
Betaine
1.5.8.4
Sarcosine
1.5.3.1
1.5.8.3
2.1.1.20
2.1.1.161
2.1.1.156
2.3.1.37
5-Aminolevulinate
Porphyrine biosynthesis
Lipoylprotein
Purine metabolism
4.1.2.48
4.1.2.49
L-Allothreonine
11.1.381
Aminoacetone
2.3.1.29
1.1.1.75
L-2-Amino-acetoacetate
Aminopropan-2-ol
4.1.2.48
4.1.2.5
1.4.3.4
1.4.3.21
11.1.103
Methylglyoxal
Valine, leucine and isoleucine biosynthesis
4.3.1.19
2-Oxobutanoate
Threonine
Propanoate metabolism
4.2.3.1
O-Phospho-L-homoserine
Propane-1,3-diamine
2.7.1.39
Arginine and proline metabolism
Cysteine and methionine metabolism
Homoserine
4.1.1.86
Ectoine biosynthesis
1.1.1.3
L-2,4-Diamino-butanoate
Alanine, aspartate and glutamate metabolism
L-Aspartate
2.7.2.4
Down Blue
2.6.1.76
2.3.1.178
4.2.1.108
L-Ectoine
1.14.11.55
5-Hydroxyectoine
L-4-Aspartyl-phosphate
L-Aspartate 4-semialdehyde
Nγ-Acetyl-L-2,4-diaminobutyrate
DoeC
DoeD
3.5.1.125
3.5.4.44
Nα-Acetyl-L-2,4-diaminobutyrate
Lysine biosynthesis
00260 10/26/17
(c) Kanehisa Laboratories

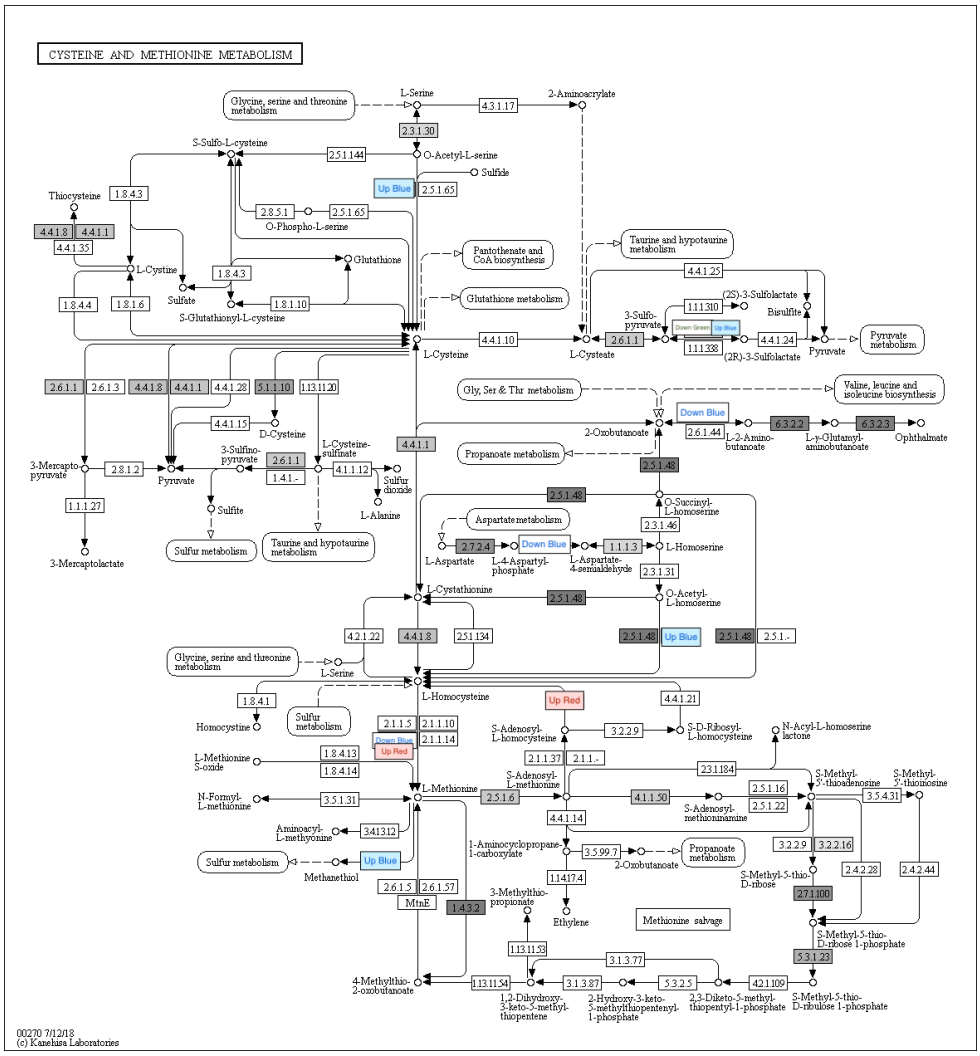
CYSTEINE AND METHIONINE METABOLISM
Glycine, serine and threonine metabolism
L-Serine
4.3.1.17
2-Aminoacrylate
2.3.1.30
S-Sulfo-L-cysteine
2.5.1.144
O-Acetyl-L-serine
Sulfide
Up Blue
2.5.1.65
Thiocysteine
1.8.4.3
2.8.5.1
2.5.1.65
O-Phospho-L-serine
4.4.1.8
4.4.1.1
4.4.1.35
L-Cystine
Glutathione
Pantothenate and CoA biosynthesis
Taurine and hypotaurine metabolism
1.8.4.3
4.4.1.25
Sulfate
1.8.1.6
1.8.1.10
S-Glutathionyl-L-cysteine
Glutathione metabolism
(2S)-3-Sulfolactate
1.1.1.310
Bisulfite
3-Sulfo-pyruvate
Down Green
Up Blue
1.1.1.338
(2R)-3-Sulfolactate
4.4.1.24
Pyruvate
Pyruvate metabolism
4.4.1.10
L-Cysteine
L-Cysteate
2.6.1.1
2.6.1.3
4.4.1.8
4.4.1.1
4.4.1.28
5.1.1.10
1.13.11.20
Gly, Ser & Thr metabolism
Valine, leucine and isoleucine biosynthesis
4.4.1.15
D-Cysteine
Down Blue
2-Oxobutanoate
2.6.1.44
L-2-Amino-butanoate
6.3.2.2
L-γ-Glutamyl-aminobutanoate
6.3.2.3
Ophthalmate
3-Mercapto-pyruvate
2.8.1.2
Pyruvate
3-Sulfino-pyruvate
2.6.1.1
1.4.1.-
L-Cysteine-sulfinate
4.1.1.12
Sulfur dioxide
4.4.1.1
Propanoate metabolism
2.5.1.48
1.1.1.27
Sulfite
L-Alanine
2.5.1.48
O-Succinyl-L-homoserine
3-Mercaptolactate
Sulfur metabolism
Taurine and hypotaurine metabolism
Aspartate metabolism
2.3.1.46
2.7.2.4
Down Blue
1.1.1.3
L-Homoserine
L-Aspartate
L-4-Aspartyl-phosphate
L-Aspartate-4-semialdehyde
2.3.1.31
L-Cystathionine
2.5.1.48
O-Acetyl-L-homoserine
4.2.1.22
4.4.1.8
2.5.1.134
2.5.1.48
Up Blue
2.5.1.48
2.5.1.-
Glycine, serine and threonine metabolism
L-Serine
1.8.4.1
L-Homocysteine
Up Red
4.4.1.21
Homocystine
Sulfur metabolism
2.1.1.5
2.1.1.10
Down Blue
Up Red
2.1.1.14
S-Adenosyl-L-homocysteine
3.2.2.9
S-D-Ribosyl-L-homocysteine
N-Acyl-L-homoserine lactone
L-Methionine S-oxide
1.8.4.13
1.8.4.14
2.1.1.37
2.1.1.-
23.1.184
S-Adenosyl-L-methionine
S-Methyl-5'-thioadenosine
S-Methyl-5'-thioinosine
N-Formyl-L-methionine
3.5.1.31
L-Methionine
2.5.1.6
4.1.1.50
S-Adenosyl-methioninamine
2.5.1.16
2.5.1.22
3.5.4.31
4.4.1.14
Aminoacyl-L-methionine
3.4.13.12
1-Aminocyclopropane-1-carboxylate
3.5.99.7
2-Oxobutanoate
Propanoate metabolism
3.2.2.9
3.2.2.16
Sulfur metabolism
Up Blue
Methanethiol
1.14.17.4
S-Methyl-5-thio-D-ribose
2.4.2.28
2.4.2.44
2.6.1.5
2.6.1.57
MtnE
1.4.3.2
3-Methylthio-propionate
Ethylene
Methionine salvage
27.1.100
S-Methyl-5-thio-D-ribose 1-phosphate
1.13.11.53
3.1.3.77
5.3.1.23
4-Methylthio-2-oxobutanoate
1.13.11.54
3.1.3.87
5.3.2.5
42.1.109
1,2-Dihydroxy-3-keto-5-methyl-thiopentene
2-Hydroxy-3-keto-5-methylthiopentenyl-1-phosphate
2,3-Diketo-5-methyl-thiopentyl-1-phosphate
S-Methyl-5-thio-D-ribulose 1-phosphate
00270 7/12/18
(c) Kanehisa Laboratories

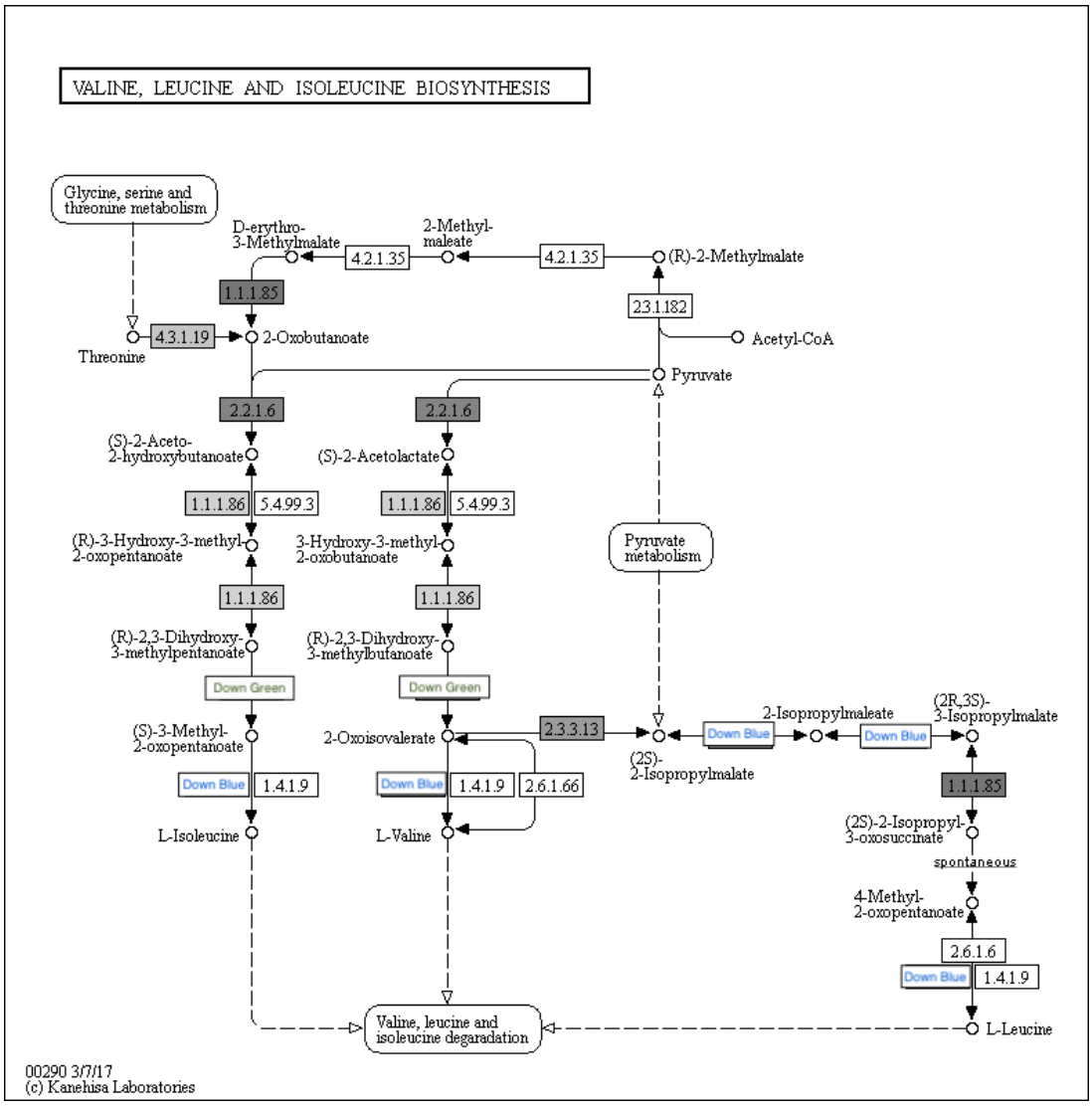
VALINE, LEUCINE AND ISOLEUCINE BIOSYNTHESIS
Glycine, serine and threonine metabolism
D-erythro-3-Methylmalate
2-Methyl-maleate
(R)-2-Methylmalate
4.2.1.35
4.2.1.35
1.1.1.85
2.3.1.182
Acetyl-CoA
4.3.1.19
Threonine
2-Oxobutanoate
Pyruvate
2.2.1.6
2.2.1.6
(S)-2-Aceto-2-hydroxybutanoate
(S)-2-Acetolactate
1.1.1.86
5.4.99.3
1.1.1.86
5.4.99.3
(R)-3-Hydroxy-3-methyl-2-oxopentanoate
3-Hydroxy-3-methyl-2-oxobutanoate
Pyruvate metabolism
1.1.1.86
1.1.1.86
(R)-2,3-Dihydroxy-3-methylpentanoate
(R)-2,3-Dihydroxy-3-methylbutanoate
Down Green
Down Green
2-Isopropylmaleate
(2R,3S)-3-Isopropylmalate
(S)-3-Methyl-2-oxopentanoate
2-Oxoisovalerate
2.3.3.13
Down Blue
Down Blue
(2S)-2-Isopropylmalate
Down Blue
1.4.1.9
Down Blue
1.4.1.9
2.6.1.66
1.1.1.85
L-Isoleucine
L-Valine
(2S)-2-Isopropyl-3-oxosuccinate
spontaneous
4-Methyl-2-oxopentanoate
2.6.1.6
Down Blue
1.4.1.9
Valine, leucine and isoleucine degaradation
L-Leucine
00290 3/7/17
(c) Kanehisa Laboratories

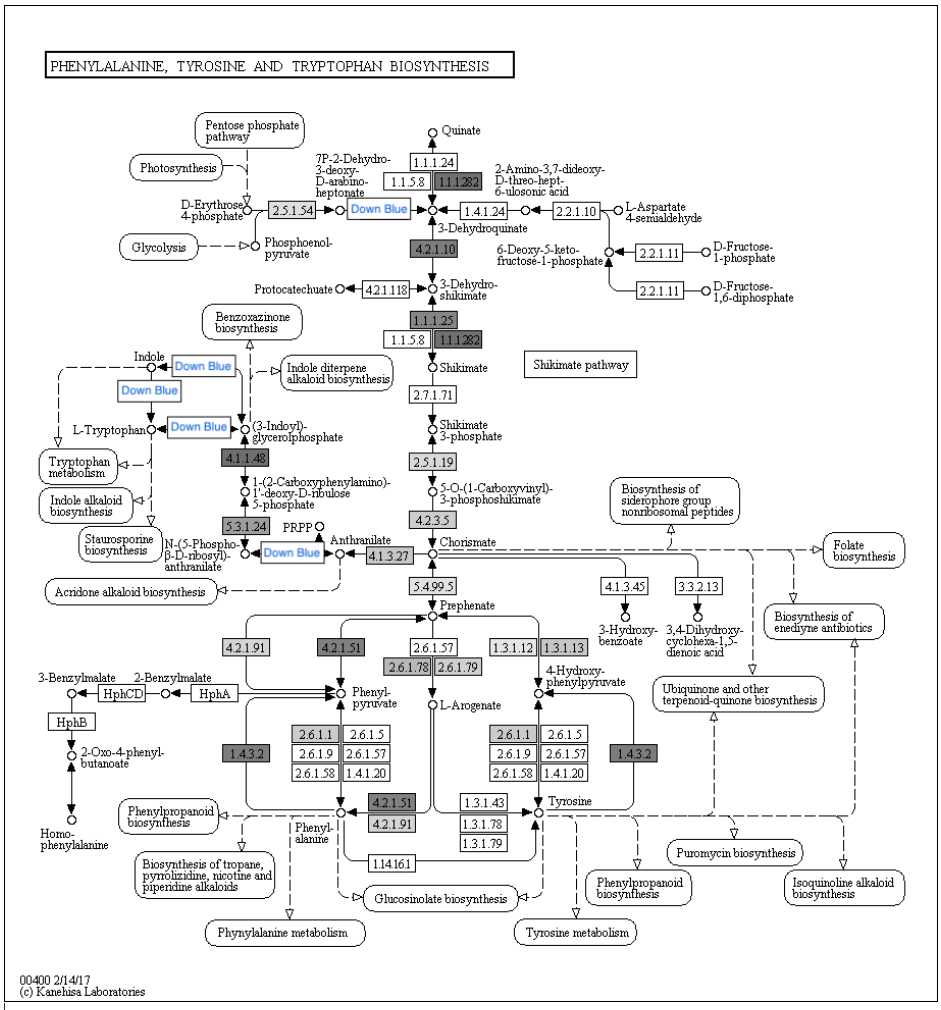
PHENYLALANINE, TYROSINE AND TRYPTOPHAN BIOSYNTHESIS
Pentose phosphate pathway
Photosynthesis
Glycolysis
Quinate
7P-2-Dehydro-3-deoxy-D-arabino-heptonate
2-Amino-3,7-dideoxy-D-threo-hept-6-ulosonic acid
D-Erythrose 4-phosphate
Phosphoenol-pyruvate
3-Dehydroquinate
L-Aspartate 4-semialdehyde
6-Deoxy-5-keto-fructose-1-phosphate
D-Fructose-1-phosphate
D-Fructose-1,6-diphosphate
Protocatechuate
3-Dehydro-shikimate
Benzoxazinone biosynthesis
Indole
Indole diterpene alkaloid biosynthesis
Shikimate
Shikimate pathway
L-Tryptophan
(3-Indoyl)-glycerolphosphate
Shikimate 3-phosphate
Tryptophan metabolism
Indole alkaloid biosynthesis
1-(2-Carboxyphenylamino)-1'-deoxy-D-ribulose 5-phosphate
5-O-(1-Carboxyvinyl)-3-phosphoshikimate
Biosynthesis of siderophore group nonribosomal peptides
Staurosporine biosynthesis
PRPP
N-(5-Phospho-β-D-ribosyl)-anthranilate
Anthranilate
Chorismate
Folate biosynthesis
Acridone alkaloid biosynthesis
Prephenate
3-Hydroxy-benzoate
3,4-Dihydroxy-cyclohexa-1,5-dienoic acid
Biosynthesis of enediyne antibiotics
3-Benzylmalate
2-Benzylmalate
HphCD
HphA
HphB
Phenyl-pyruvate
L-Arogenate
4-Hydroxy-phenylpyruvate
Ubiquinone and other terpenoid-quinone biosynthesis
2-Oxo-4-phenyl-butanoate
Homo-phenylalanine
Phenylpropanoid biosynthesis
Phenyl-alanine
Tyrosine
Puromycin biosynthesis
Biosynthesis of tropane, pyrrolizidine, nicotine and piperidine alkaloids
Glucosinolate biosynthesis
Phenylpropanoid biosynthesis
Isoquinoline alkaloid biosynthesis
Phynylalanine metabolism
Tyrosine metabolism
Down Blue
00400 2/14/17
(c) Kanehisa Laboratories

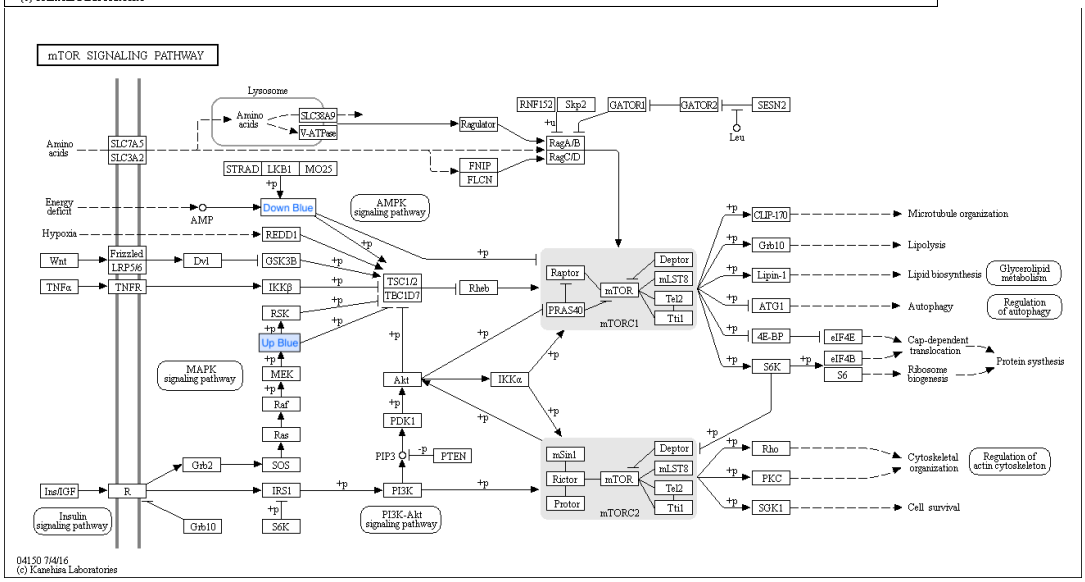
mTOR SIGNALING PATHWAY
Lysosome
Amino acids
SLC38A9
V-ATPase
Ragulator
RagA/B
RagC/D
RNF152
Skp2
GATOR1
GATOR2
SESN2
Leu
SLC7A5
SLC3A2
STRAD
LKB1
MO25
FNIP
FLCN
Energy deficit
AMP
Down Blue
AMPK signaling pathway
Hypoxia
REDD1
Wnt
Frizzled
LRP5/6
Dvl
GSK3B
TNFα
TNFR
IKKβ
TSC1/2
TBC1D7
Rheb
Raptor
mTOR
PRAS40
mTORC1
Deptor
mLST8
Tel2
Tti1
CLIP-170
Grb10
Lipin-1
ATG1
4E-BP
eIF4E
eIF4B
S6K
S6
Microtubule organization
Lipolysis
Lipid biosynthesis
Glycerolipid metabolism
Autophagy
Regulation of autophagy
Cap-dependent translocation
Ribosome biogenesis
Protein systhesis
RSK
Up Blue
MAPK signaling pathway
MEK
Raf
Ras
Akt
IKKα
PDK1
PIP3
PTEN
mSin1
Rictor
Protor
mTORC2
Rho
PKC
SGK1
Cytoskeletal organization
Regulation of actin cytoskeleton
Cell survival
Grb2
SOS
Ins/IGF
R
IRS1
PI3K
Insulin signaling pathway
PI3K-Akt signaling pathway
04150 7/4/16
(c) Kanehisa Laboratories

Appendix 5 Light quality responsive genes in RCC809 containing overrepresented promoted motifs

Selected genes with motif in promoter Up in red	
Gene	**Description**
Od03g02850	Fructose-1,6-bisphosphatase **Also contains down blue motif 1**
Od07g04250	Predicted glucose/ribitol dehydrogenase
Od04g02610	Phosphoribulokinase chloroplast precursor (carbohydrate metabolism)
Od03g00560	Mitochondrial substrate/solute carrier
Od17g01460	Mitochondrial phosphate carrier protein
Od04g05270	**DNA binding, regulation of transcription**
Od09g03890	Adenosylhomocysteinase, cellular methylation
Od06g03170	Putative 2Fe-2S ferredoxin

Selected genes with motif in promoter Down in blue 1	
GENE	**Description**
Od09g05360	Terpenoid biosynthesis
Od11g00960	MECDP synthase, terpenoid biosynthesis
Od15g01050	GHMP kinase, terpenoid biosynthetic process
Od06g04640	Porphyrin, chlorophyll biosynthesis
Od01g01020	Porphyrin chlorophyll biosynthesis

Od01g04650	Porphobilinogen synthase
Od05g05120	Magnesium protoporphyrin chelatase, chlorophyll biosynthesis
Od07g03920	Cytidylyltransferase, isoprenoid biosynthesis
Od05g01350	Porphobilinogen deaminase, tetrapyrrole biosynthesis
Od06g03440	Protoporphyrinogen oxidase, porphyrin biosynthesis
Od12g03120	Uroporphyrinogen decarboxylase, porphyrin biosynthesis
Od02g02530	Magnesium-protoporyphyrin IX chelatase, porphyrin biosynthesis
Od16g02600	Uroporphyrinogen decarboxylase, porphyrin biosynthesis
Od05g00090	GTP cyclohydrolase, tetrahydrofolate biosynthetic process
Od09g01000	(2Fe-2S)-binding protein, chlorophyllide a oxygenase
Od07g02830	(2Fe-2S)-binding protein, chlorophyllide a oxygenase
Od20g00760	Lycopene beta cyclase, contains chlorophyll *a/b* binding domain
Od06g01290	Ferredoxin, chloroplast precursor
Od09g00820	Phytoene desaturase, carotenoid biosynthesis
Od13g00750	Cytochrome P450, heme binding, function undefined
Od06g03460	Photosystem I assembly protein Ycf4
Od04g01800	**CCT (CONSTANS, CO-like, and TOC1) domain, often involved in light signalling**
Od07g04740	Chloroplast SRP receptor, signal recognition
Od03g02850	Fructose-1,6-bisphosphatase **Also contains up red motif**
Od09g03380	Ribulose-1,5 bisphosphate carboxylase, methyltransferase
Od06g06980	Fructose-1,6-bisphosphatase, gluconeogenesis

Od14g02940	Phosphoglucomutase, carbohydrate metabolism
Od11g00900	Starch synthase, glycosyltransferase
Od13g02060	Glycosyltransferase, starch/glycogen synthase
Od02g01370	Monogalactosyldiacylglycerol transferase, glycolipid biosynthesis
Od07g03760	Phospholipid biosynthetic process
Od06g04530	Fatty acid desaturase, lipid metabolism
Od16g00600	Fatty acid desaturase, lipid metabolism
Od09g01170	Fatty acid desaturase, cytochrome b5 domain, unknown function
Od02g02950	Clp protease
Od02g02880	Clp protease
Od07g03910	Phosphoribosyltransferase, nucleotide synthesis and salvage
Od06g01660	Nucleobase biosynthesis
Od05g01900	3-dehydroquinate synthase, aromatic amino acid biosynthesis
Od01g03140	Aspartate family amino acid biosynthetic process
Od06g03340	Aminoacyl-tRNA synthetase, tRNA aminoacylation
Od14g02210	pre-rRNA-processing
Od02g02590	DNA-directed RNA polymerase, zinc finger, TFIIS-type
Od01g02120	Transcription factor activity, DNA binding AP2/ERF domain
Od06g01910	Chaperone dnaJ homologue, Myb-like domain
Od11g00560	ATP-binding cassette translation elongation factor
Od13g02920	Ankyrin repeat, protein binding

Od06g06110	B12 (cobalamin) dependent methionine synthase
Od07g01970	50S ribosomal protein L27
Od01g02970	Dynamin, membrane remodelling
Od04g01630	Membrane protein, ion channel **Also contains other down blue motif**
Od06g01900	WD40 repeat containing, actin cytoskeleton, TOR signalling
Od01g03210	Prasinophyte-specific protein, likely transport related **Also contains other down blue motif**
Od11g00830	Phosphatidylinositol 4-kinase mediated signalling

Selected genes with motif in promoter Up in green	
Gene	**Description**
Od01g02490	Glutaredoxin, electron transport, RNA synthesis
Od03g00550	Ribonuclease inhibition, methyltransferase
Od13g00600	RNA binding domain containing protein
Od06g00510	mRNA splicing factor motif
Od17g00960	RNA binding
Od09g03870	Pantoate-beta-alanine ligase, amino acid synthesis
Od11g02310	Serine-threonine/tyrosine-protein kinase catalytic domain
Od15g00730	Tyrosine/serine/threonine phosphatase
Od06g03250	Protein dephosphorylation
Od03g02370	Translational activator GCN1-related
Od14g01420	Protein folding, armadillo/beta-catenin-like repeat containing
Od05g01340	Protein binding, p-loop and WD40 repeat-containing
Od02g04650	Protein binding molecular chaperone, DnaJ domain, heat shock
Od06g06180	Protein binding, tetratricopeptide repeat
Od15g00340	Fatty acyl-CoA-binding domain
Od08g00510	Peptidase
Od01g03130	Peptidase containing nucleoporin and zinc finger CCCH
Od02g00410	Major facilitator superfamily (MFS), transport of small solutes

Selected genes with motif in promoter Up in blue 1 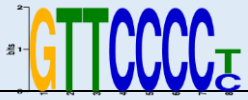	
GENE	**Description**
Od01g00560	Cyclin B
Od04g03210	DNA repair protein, mitotic recombination, helicase **Also contains other up in blue motif**
Od14g01080	Cell cycle dependent kinase B, cell division (Serine/threonine-protein kinase, active site) **Also contains other up in blue motif**
Od08g02850	Kinesin, microtubule
Od04g04460	Putative kinesin K39 myosin class II heavy chain, protein binding
Od13g02570	Myosin class II heavy chain, likely cell division related **Also contains other up in blue motif**
Od02g03890	Mitotic chromosome condensation
Od08g03260	Mitotic spindle checkpoint BUBR1, serine/threonine-protein
Od15g00790	Centromere DNA-binding domain
Od04g00790	Actin filament binding, microtubule associated
Od04g05300	Transcription factor, Zinc finger, plant homeodomain (PHD), chromatin binding
Od11g03720	Zinc finger, RING-H2-type
Od06g02440	Transcription factor IIB, recruits RNA pol II **Also contains other up in blue motif**
Od07g00400	DNA binding, SAP domain
Od14g00740	Transcription factor, ethylene responsive
Od04g05310	Rieske [2Fe-2S] iron-sulphur domain
Od04g05310	PSII assembly, rieske [2Fe-2S] iron-sulphur domain
Od08g03580	Chlorophyll *a-b* binding protein

Od16g01220	Serine threonine protein kinase, catalytic domain
Od03g01650	Protein binding, WD40 repeat

Selected genes with motif in promoter Up in blue 2	
GENE	**Description**
Od14g01080	Cell cycle dependent kinase B, cell division (Serine/threonine-protein kinase, active site) **Also contains other up blue motif**
Od04g03210	DNA repair protein, mitotic recombination, helicase **Also contains other up in blue motif**
Od13g02570	Myosin class II heavy chain, likely cell division related **Also contains other up in blue motif**
Od05g02520	Myosin class II heavy chain, membrane transport
Od02g03320	Phosphatase, positive cell cycle regulation G2/M phase
Od06g05210	Shugoshin, C-terminal, meiotic chromosome segregation
Od09g01340	Kinesin, microtubule activity P-loop containing
Od09g00660	Microtubule binding, PRC-barrel-like
Od17g01120	Kinesin-like, microtubule motor activity
Od14g03010	Condensin complex, mitotic chromosome condensation
Od14g02600	Microtubule binding protein involved in cell cycle control
Od01g01950	Chromatin binding domain
Od11g01550	DNA recombination domain
Od06g00540	P-loop nucleoside hydrolase, possible replication factor
Od11g01890	Primase, large subunit, DNA replication
Od11g01550	DNA recombination/repair protein domain

Od15g00900	DNA base excision repair
Od12g00150	Oxoglutarate/iron-dependent dioxygenase, DNA repair
Od06g06580	DNA mismatch repair protein, MutS-like
Od15g01260	5'-3' exonuclease family, DNA repair
Od11g01050	Dehydrogenase, nucleobase biosynthesis
Od11g00130	Histone acetyltransferase, chromatin organization
Od01g02860	Histone H3, DNA binding
Od09g06110	Histone deacetylase, transcription regulation
Od14g03150	WD40 repeat-containing, chromatin binding, regulatory
Od11g01460	Nucleotide binding, D-amino acid oxidase
Od02g00320	DNA methylation, methyltransferase
Od11g02410	RNA-binding protein
Od12g02990	Ribonuclease HII
Od03g01070	Ribonuclease H-like domain
Od06g01410	Ribosomal RNA methyltransferase
Od20g02780	mRNA splicing, LUC7-related
Od05g01080	tRNA modification (guanine-N(7)-)-methyltransferase
Od17g00150	**Zinc finger CCCH-type, RNA binding, regulation of expression**
Od06g02440	Transcription factor IIB, recruits RNA pol II **Also contains other up in blue motif**
Od19g00350	**Tesmin/TSO1-like domain, transcription regulation, may be negative regulation**
Od17g00420	KH domain, mRNA-binding, regulation of gene expression

Od04g04760	Serine/threonine protein kinase, phosphorylation
Od02g03690	Serine/threonine-protein kinase 24
Od12g00120	Protein kinase
Od01g06580	Aminoacyl-tRNA synthetase, protein synthesis
Od06g04940	Peptidyl-prolyl cis-trans isomerase, protein folding
Od02g00970	Protein modifying enzyme, ion channel domain, oxioreductase
Od20g02320	Protein modification, peptide:N-glycanase
Od14g00920	Cysteine protease
Od13g01200	Peptidase, calcium-dependent cysteine-type
Od08g03230	Protein binding, ankyrin repeat
Od16g00890	**Rhodopsin-like GPCR (G protein-coupled receptor)**
Od05g04810	Transmembrane protein, ion channel
Od13g02790	Potassium ion transmembrane transport
Od01g03480	Calcium binding protein, transmembrane import
Od03g01340	Solute membrane transport
Od04g05220	MscS family transport, ion channel
Od01g06640	Voltage-dependent potassium channel, transmembrane
Od19g00750	Mitochondrial carrier, ion transport, glycine predicted
Od17g00090	Amino acid transmembrane transport, tryptophan/tyrosine
Od19g00920	ATPase, plasma-membrane proton-efflux P-type
Od07g02950	Phosphatidyltransferase, phospholipid biosynthetic process

Od10g00970	Calcium transport mitochondrial, WD40 repeat
Od19g00740	Superoxide dismutase Cu-Zn, ion binding
Od19g00730	Superoxide dismutase Cu-Zn, ion binding
Od03g02690	Nitrogen compound transport, BCCT
Od16g00280	Serine hydroxymethyltransferase
Od11g00340	START domain-containing protein, lipid binding
Od02g03200	Chloramphenicol acetyltransferase domain
Od01g01190	Pyruvate dehydrogenase (acetyl-transferring)
Od11g02930	HAD-IB family hydrolase, phosphatase activity
Od06g01820	Carbohydrate-binding family, glucan 1,4-alpha-glucosidase
Od06g02230	Malate dehydrogenase, mitochondrial, TCA cycle
Od16g01180	Acetylhydrolase, lipid catabolic process
Od20g01170	Cobalamin adenosyltransferase-like superfamily
Od12g03130	Glycoside hydrolase, carbohydrate catabolism
Od01g06420	Fatty acid hydrolase, acyl-CoA thioesterase
Od12g01220	Carboxylic ester hydrolase domain

Key genes with motif in promoter Down in blue 2	
GENE	**Description**
Od16g00450	Vacuolar protein, membrane transport

Od04g02810	Vacuolar protein, membrane transport
Od07g04230	Serine incorporator, membrane protein
Od05g00590	Ammonium transmembrane transport
Od03g01260	Aquaporin-like, membrane transport
Od04g01630	Membrane protein, ion channel **Also contains other down blue motif**
Od01g06190	ATP synthesis coupled proton transport, transmembrane
Od07g01750	ATP synthesis coupled proton transport
Od09g02460	Intracellular protein transport
Od05g02670	Organic solute transporter
Od01g03210	Prasinophyte-specific protein, likely transport related **Also contains other down blue motif**
Od07g00140	Cysteine protease, calcium ion binding
Od14g02610	Prolyl 4-hydroxylase, protein modifying enzyme
Od01g06140	Ankyrin repeat, protein binding
Od17g03100	Helicase or endonuclease domain containing, DNA binding
Od08g01810	Zinc finger CCCH-type, zinc or nucleic acid binding
Od14g01500	**Transcription factor, basic-leucine zipper (bZIP) domain**
Od06g03790	NADP-dependent malic enzyme, pyruvate synthesis
Od18g00260	Carboxylesterase, alpha/beta hydrolase
Od10g01790	Carboxylesterase, alpha/beta hydrolase